AD-A126 004 REPORT ON RESEARCH AT AFGL JANUARY 1979-DECEMBER 1980 1/3
(U) AIR FORCE GEOPHYSICS LAB HANSCOM AFB MA
A B MCGINTY APR 82 AFGL-TR-82-0132

UNCLASSIFIED F/G 5/1 NL

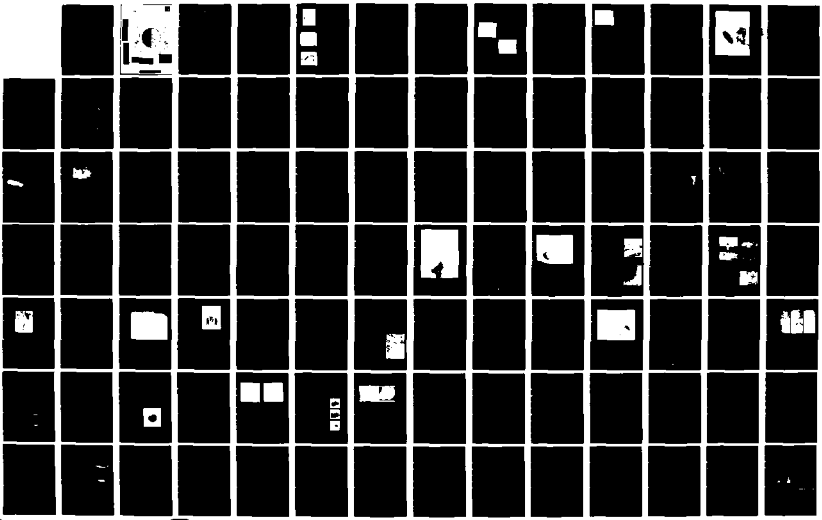

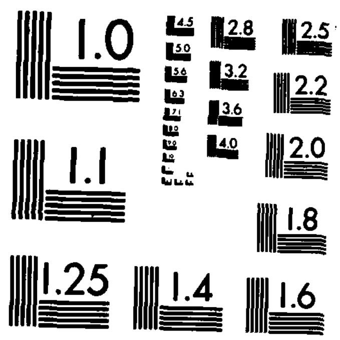

MICROCOPY RESOLUTION TEST CHART
NATIONAL BUREAU OF STANDARDS-1963-A

Unclassified

SECURITY CLASSIFICATION OF THIS PAGE (When Data Entered)

REPORT DOCUMENTATION PAGE		READ INSTRUCTIONS BEFORE COMPLETING FORM
1. REPORT NUMBER AFGL-TR-82-0132	2. GOVT ACCESSION NO. A126004	3. RECIPIENT'S CATALOG NUMBER
4. TITLE (and Subtitle) REPORT ON RESEARCH		5. TYPE OF REPORT & PERIOD COVERED Scientific, Interim, Jan 1979 - Dec 1980
		6. PERFORMING ORG. REPORT NUMBER Special Reports, No. 230
7. AUTHOR(s) Alice B. McGinty, Editor		8. CONTRACT OR GRANT NUMBER(s) N/A
9. PERFORMING ORGANIZATION NAME AND ADDRESS Air Force Geophysics Laboratory Hanscom AFB, MA 01731		10. PROGRAM ELEMENT, PROJECT, TASK AREA & WORK UNIT NUMBERS 9993XXXX
11. CONTROLLING OFFICE NAME AND ADDRESS Office of Research Services (SU) Air Force Geophysics Laboratory Hanscom AFB, MA 01731		12. REPORT DATE April 1982
		13. NUMBER OF PAGES 212
14. MONITORING AGENCY NAME & ADDRESS(if different from Controlling Office)		15. SECURITY CLASS. (of this report) Unclassified
		15a. DECLASSIFICATION/DOWNGRADING SCHEDULE N/A

16. DISTRIBUTION STATEMENT (of this Report)

Approved for public release; distribution unlimited.

17. DISTRIBUTION STATEMENT (of the abstract entered in Block 20, if different from Report)

18. SUPPLEMENTARY NOTES

Tech, other

19. KEY WORDS (Continue on reverse side if necessary and identify by block number)

Geokinetics	Solar Radiations	Trans-Ionospheric Signal Propagation
Geodesy	Balloon Technology	Rocket Instrumentation
Gravity	Optical Physics	Upper Atmosphere Physics
Seismology	Ionospheric Physics	Upper Atmosphere Chemistry
Meteorology	Magnetospheric Dynamics	

20. ABSTRACT (Continue on reverse side if necessary and identify by block number)

This report is the tenth Report on Research at the Air Force Geophysics Laboratory. It covers a two-year interval. Although written primarily for Air Force and DOD managers of research and development it is intended to interest an even broader audience. For this audience, the report relates the Laboratory's programs to the larger scientific field of which they are a part. The work of each of the Laboratory's six divisions is discussed in a separate chapter, followed by a listing of its publications. The report also includes an introductory chapter on AFGL management and logistic activities related to the reporting period.

DD FORM 1 JAN 73 1473 EDITION OF 1 NOV 65 IS OBSOLETE

Unclassified

SECURITY CLASSIFICATION OF THIS PAGE (When Data Entered)

AFGL-TR-82-0132

Report on Research at AFGL

January 1979—December 1980

SURVEY OF PROGRAMS AND PROGRESS

THE AIR FORCE GEOPHYSICS LABORATORY

AIR FORCE SYSTEMS COMMAND

HANSCOM AIR FORCE BASE

MASSACHUSETTS

April 1982

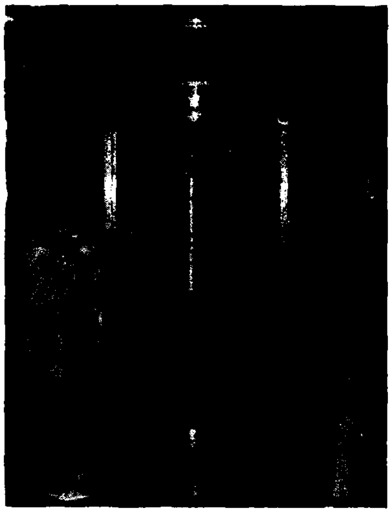

Foreword

This report summarizes the recent achievements and progress of on-going programs at the Air Force Geophysics Laboratory. It is the tenth in a series initiated by AFGL's predecessor, the Air Force Cambridge Research Laboratories (AFCRL). Written primarily for Air Force and DOD managers of research and development, it shows how AFGL met Air Force needs and extended our technology base in geophysics during the period from January, 1979, through December, 1980.

JOHN FRIEL
Colonel, USAF
Commander

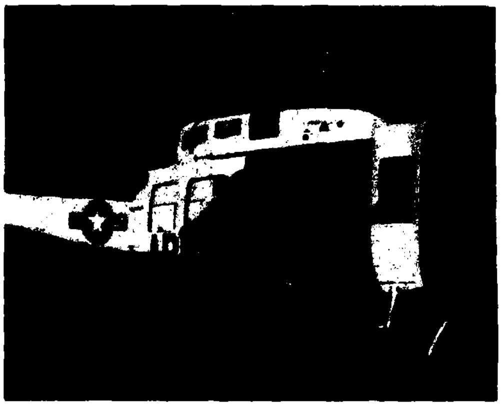

Contents

Appendices

I AIR FORCE GEOPHYSICS LABORATORY

The Air Force Geophysics Laboratory (AFGL), located at Hanscom AFB, Bedford, Massachusetts, is the Air Force Center for research in the environmental sciences. Its mission is to understand the earth's environment, to mitigate its effects on Air Force systems, and to exploit its advantages in defense of the United States and its allies. It is one of fourteen Air Force laboratory complexes. This report describes AFGL's research programs, activities, and achievements from January 1, 1979, through December 31, 1980.

AFGL's professional staff of 321 scientists and engineers is organized into six divisions: the Aeronomy Division, the Aerospace Instrumentation Division, the Meteorology Division, the Optical Physics Division, the Space Physics Division, and the Terrestrial Sciences Division. AFGL also maintains a small West Coast Office at El Segundo, California, to focus support to the Space Division.

From January to August, 1979, Colonel Bernard S. Morgan commanded AFGL. He was succeeded by Colonel James E. Baker. Colonel Chester G.R. Czepyha was the Vice Commander from January through August, 1979, when he was succeeded by Colonel Gerald P. D'Arcy.

Of the professional staff of 321, 93 held doctor's degrees (an increase of 12 over December, 1978), 98 held master's degrees (an increase of 5), and 130 held bachelor's degrees (an increase of 6).

AFGL scientists are widely recognized for their contributions to the Air Force and their respective fields. In 1979, Captain Henry B. Garrett, a physicist in AFGL's Space Physics Division, was named the

winner of the 1978 Harold Brown Award for developing a mathematical model of the earth's space environment at high altitudes. Don F. Smart and Margaret A. Shea, a husband and wife team in the Plasmas, Particles and Fields Branch, were awarded the Air Force Association Citation of Honor Award for their achievements in assessing and predicting the effects of solar events on Air Force communications by pioneering research in cosmic radiation. Eunice Cronin, Chief of AFGL's Computation Branch, was promoted to the GM-15 level of the Federal Civil Service in 1980. She is the second AFGL woman and the third of the more than 6,000 women in the Air Force Systems Command to attain this rank in the Federal Civil Service.

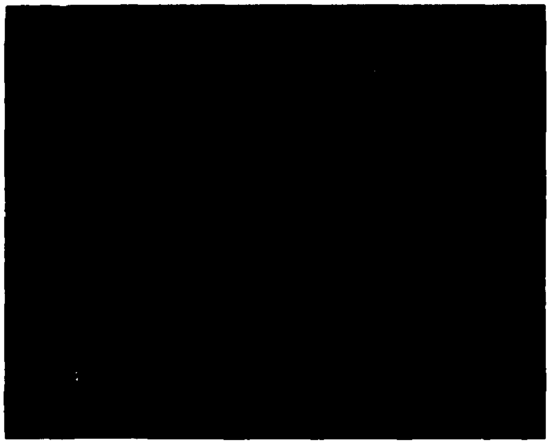

The AFGL Laboratory complex is located 17 miles west of Boston (seen against the skyline) at Hanscom AFB, where it is a tenant of the Electronic Systems Division of the Air Force Systems Command.

Many members of the AFGL staff serve on international commissions such as the International Association of Geomagnetism and Aeronomy, Committee on Space Research, International Committee for High Altitude Pollution, International Committee for Fourier Transform Spectroscopy, NATO Research Study Groups 8 and 14, and the International Standard Organizations Committee on Standard Atmosphere. In 1979, Laboratory scientists were chosen to be delegates to the Indo-U.S. Workshop on Solar-Terrestrial Physics, Udaipur, India, the STIP Symposium on Solar Radio Astronomy, Interplanetary Scintillation, and Co-ordination with Spacecraft, and the International Solar-Terrestrial Predictions Workshop, Boulder, Colorado.

Nationally, AFGL scientists serve on committees such as the Committee on Solar-Terrestrial Sciences of the U.S. National Academy of Science, the Committee on Extension to the Standard Atmosphere, the Air Force Subgroup on High Altitude Nuclear Effects, National Storm Program, U.S. Technical Advisory Group to the International Electrotechnical Commission, and the U.S. Gravity Standards Committee.

The editor of *Applied Optics* is an AFGL scientist, as is the associate editor of the *Journal of Atmospheric Sciences* and the *Journal of Applied Meteorology*. Another scientist serves on the Geophysical Monograph Board of the American Geophysical Union.

A third of AFGL's professional staff of 321 scientists and engineers hold the Ph.D. degree.

During the reporting period, AFGL scientists presented 335 papers and pub-

lished 159 journal articles and 111 technical reports.

Annual Budgets: The annual budgets for the 2 years covered in this report are shown in the accompanying table. The totals cover salaries, equipment, travel, supplies, computer rental, service contracts, and those funds going into contract research. The largest expenditure is for contract research and development.

Funds received from AFGL's higher headquarters, the AFSC Director of Science and Technology (DL), and to a lesser extent those received from AFSC organizations other than headquarters are used to conduct continuing programs.

AFGL receives support from the Electronic Systems Division, the host organization at Hanscom AFB, in accounting, personnel, procurement, security, civil engineering, and supply. Holloman AFB, New Mexico, provides services to the AFGL Balloon Detachment. AFGL supports RADC's Deputy for Electronic Technology (ET) in the areas of the Research Library, laboratory materials needed for the ET mission, computer, technical photography, mechanical and electrical engineering, laboratory layouts, electronic instrumentation, and woodworking.

AFGL contracts are monitored by scientists who are themselves active, participating researchers, and who plan the research, organize the program, interpret the results, and share the workload of the actual research.

Field Sites: AFGL operates several field sites, the largest of which is the Ground-Based Remote Sensing Facility in Sudbury, Massachusetts. During the reporting period, work began on a new dual-frequency Doppler weather radar system operating at a wavelength of 10 cm. It will be used to develop models for the automated interpretation of features of storms that affect Air Force operations. A separate Weather Test Facility is located at Otis AFB, Massachusetts.

In New Mexico, AFGL operates a balloon launch site at Holloman AFB and at Sunspot maintains the Solar Research Branch (nine scientists) of the Space Physics Division at the Sacramento Peak Solar Observatory.

At Goose Bay Station, Labrador, AFGL's Goose Bay Ionospheric Laboratory studies subarctic events, including the aurora and polar cap absorption of high-frequency radio waves.

AFGL carries out field tests at a number of military installations including the Fort Churchill, Canada, rocket range; Fort Wainwright and Eielson AFB, Alaska; Albrooke AFB, Canal Zone; Vandenberg

TABLE 1
SOURCES OF AFGL FUNDS
FISCAL YEARS 1980 - 81

	FY 80	FY 81
	(In millions)	
Air Force Systems Command-DL	$40,818	$46,698
Air Force Systems Command-Other than DL	8,453	13,367
Air Force	139	529
Defense Nuclear Agency	2,866	3,093
Defense Mapping Agency	1,234	783
Army	255	45
Navy	40	8
Defense Advanced Research Projects Agency	635	107
National Security Agency	50	0
Department of Energy	555	432
National Aeronautics and Space Administration	280	152
	$55,325	$65,214

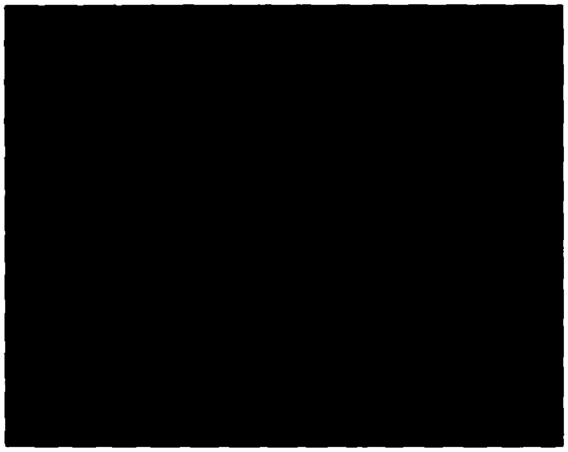

AFGL's Ground-Based Remote Sensing Facility, Sudbury, Massachusetts, is developing models for automated interpretation of storms that affect Air Force operations.

AFB, California; and the White Sands Missile Range, New Mexico. In addition, the Poker Flat Rocket Range, Alaska, and commercial airports are also used.

Research Vehicles: AFGL launched 103 research balloons during the reporting period from its permanent balloon launch site at Holloman AFB, New Mexico, and from several other temporary sites in the United States, Panama, and Germany. Of these, 19 were tethered flights. Between October 12 and November 12, 1979, the Balloon Research Branch conducted the first flights of two connected tethered balloons for the National Aeronautics and Space Administration (see Chapter III). For this work, the Branch received a NASA Group Achievement Award, given usually only to NASA employees.

AFGL balloons carried test and experimental payloads for the Space Division, the Defense Nuclear Agency, the National Aeronautics and Space Administration, the Department of Energy, the Army and a number of universities. The largest number of flights, however, were for AFGL projects.

AFGL launched its one-thousandth research sounding rocket from the White Sands Missile Range on May 21, 1980 (see Chapter III). In addition, eighteen other rocket systems were flown from launch sites within the United States, Canada, Peru, and Norway. These rockets carried experimental payloads to measure such events as a total solar eclipse, characteristic radiation patterns of rocket motors in flight, the mass and number density of positive and negative ions, the outgassing of solid-propellant rocket motors, and zodiacal light. The rockets used on these flights were modified Aries Talos-Castor, Taurus-Orion, Sergeant, and Minuteman I.

The Aerospace Instrumentation Division also played a major role in designing and launching Space Division's SCATHA satellite in January, 1979.

AFGL Computer Center: AFGL operates: (1) a large central-site scientific data processing facility consisting of two CDC 6600 computing systems which support AFGL, ESD, other government agencies and DOD contractors; and (2) a Telemetry Data Processing facility which processes analog or digital data from satellites, rockets, aircraft, balloons, and laboratory data collection systems.

The CDC 6600 systems consist of a modular-designed multi-processor operation with extensive input-output devices, peripheral equipment, and communications equipment. The systems provide remote batch, interactive graphics, and conversational capabilities through a network of approximately 50 remote stations located within the laboratory complex and at off-base locations.

The Center also provides analytical support in mathematical systems modeling; spectral, numerical, and statistical techniques; as well as space-probe data reduction and ephemeris determinations.

Action has been undertaken to establish a mini-computer support service, as well as to upgrade both the large scientific data processing and the Telemetry Data Processing facilities.

AFGL Research Library: The AFGL Research Library has the largest and most comprehensive scientific and technical research collection in the United States Air Force. This collection is international in scope and includes extensive holdings in mathematics, chemistry, physics, astrophysics, electronics, and geophysics. Each year the library adds more than 2,500 new titles to the book collection and 4,000 bound journal volumes. The library subscribes to approximately 1800 current periodical titles. In-house and contractor technical reports from AFGL and the Electronic Systems Division are also maintained, both in paper and microfiche.

In addition to its collection of publications, the library offers computer-aided literature searches. This service provides the patron with immediate access to millions of citations from journals, books, reports, proceedings and reviews published throughout the world. Online interactive searching of the Defense Technical Information Center's (DTIC) several files, as well as many commercially available data bases, gives the library user immediate access to much of the world's information.

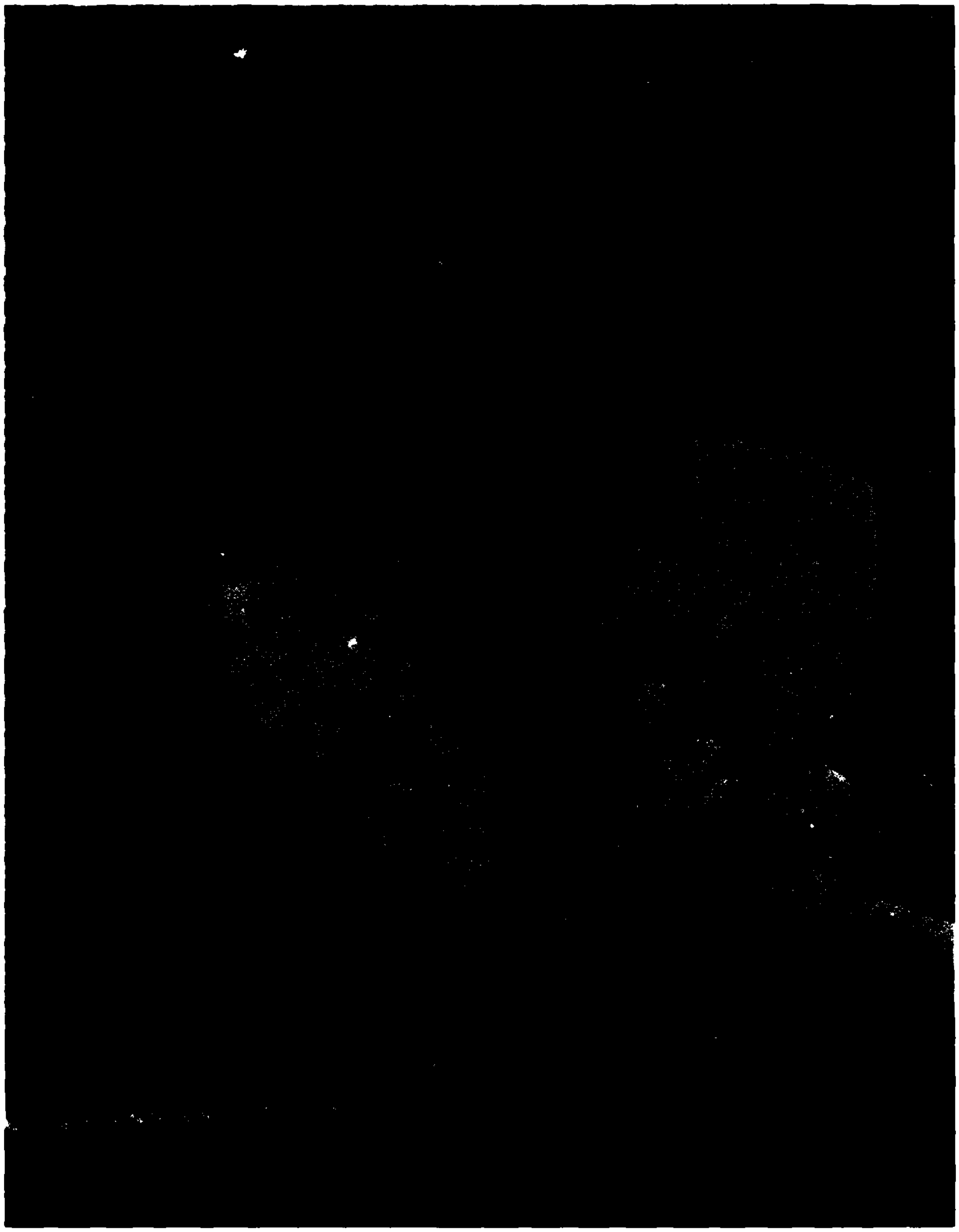

Cleaning the Mirror of AFGL's Ultraviolet Calibration Facility.

II AERONOMY DIVISION

Aeronomy is the study of the physical and chemical properties of the earth's upper atmosphere. It deals principally with the atomic, molecular, and ionic composition of the atmosphere and how energy sources such as solar radiation affect this composition. The Aeronomy Division's principal activities are in the altitude regions above about 15 km, which include the stratosphere, mesosphere, and thermosphere.

The principal energy source affecting the structure and properties of the earth's upper atmosphere is the ultraviolet radiation from the sun. This solar ultraviolet flux, its long-term variability, and its absorption in the atmosphere are measured by instrumented sounding rockets and satellites, such as the NASA Atmosphere Explorer satellites.

Atmospheric ultraviolet radiations can be used to help solve defense problems in the areas of missile surveillance and tracking, spacecraft horizon sensing, atmospheric/ionospheric sensing for communication and detection purposes, and technical intelligence. These radiations are measured principally by means of satellites, although rocket measurements are used in the definition of new concepts and in the development of instrumentation for satellite use.

A knowledge of the structure and properties of the upper atmosphere necessary to determine the trajectories of space vehicles is obtained by developing unique payloads which are flown on rockets and satellites. These measurements and analyses are supplemented by laboratory investigations and by the development of comprehensive models of the upper atmos-

phere. The Aeronomy Division has a major role in the definition of the U.S. Standard Atmosphere, a cooperative effort by the Air Force, the National Aeronautics and Space Administration, and the National Oceanic and Atmospheric Administration. The Division is developing atmospheric density models for use by the Aerospace Defense Command in tracking and predicting the orbits, including reentry, of more than 3500 space objects. Accelerometers are flown on Defense Mapping Agency satellites for obtaining atmospheric density data and improving satellite navigation. A LIDAR (Light Detection and Ranging) system, capable of remote sounding of density and other atmospheric properties, is being developed for use on the Space Shuttle.

In the upper atmosphere are regions of intense turbulence which cause fluctuations in the index of refraction and which, in turn, affect optical systems such as laser communications. The Division is measuring this turbulence by means of ground-based optical and radar techniques and by instrumented balloons to determine the intensity of the turbulence and its variation with time and location.

The National Environmental Policy Act of 1969 requires the Air Force to provide environmental impact statements for its flight operations. For this purpose, the Division measures the composition and dynamics of the stratosphere and the solar energy flux, from which appropriate environmental assessment models are developed.

The electrically charged particles in the upper atmosphere have a significant effect on the propagation of radio waves. The concentration of these particles varies significantly during disturbed conditions such as polar-cap absorption events, auroral events and ionospheric scintillation events and can degrade the performance of satellite communications systems. The Division is measuring the composition of these events by means of mass spectrometers on sounding rockets and on satellites.

The atoms, molecules, ions, and photons present in the upper atmosphere constantly interact. These interactions are investigated in the laboratory and the rates at which the reactions occur are measured. For this purpose the Division recently constructed a SIFT (Selected Ion Flow Tube) device, a very potent instrument for such investigations and one of the few now in existence.

UPPER ATMOSPHERE COMPOSITION

Research in the composition of the upper atmosphere included rocket field measurements, laboratory measurements and theoretical work. Atmospheric measurements were conducted in four different rocket programs to examine various natural and artificial disturbances in the D-, E- and F-regions of the ionosphere and to assess their effects on communication and navigation systems. Measurements were obtained in equatorial spread F conditions during periods of strong ionospheric irregularities in a Defense Nuclear Agency program. The D- and E-region responses to the 1979 solar eclipse were studied as part of an international effort. D-region perturbations generated by a strong geomagnetic storm were observed. Finally, rocket measurements were performed in a barium ion cloud as part of a Defense Nuclear Agency ionospheric modification/simulation test.

The laboratory effort consisted of studies of atmospheric dimers, or van der Waals molecules, meteoric sulfur chemistry, and the determination of nitric oxide variability with sunspot number, as well as an estimate of a mean nitric-oxide profile for the middle atmosphere. A code is being developed to describe the chemical distributions of meteoric compounds throughout the middle atmosphere. Laboratory measurements of several metal-hydroxide dissociation energies and ionization potentials were made.

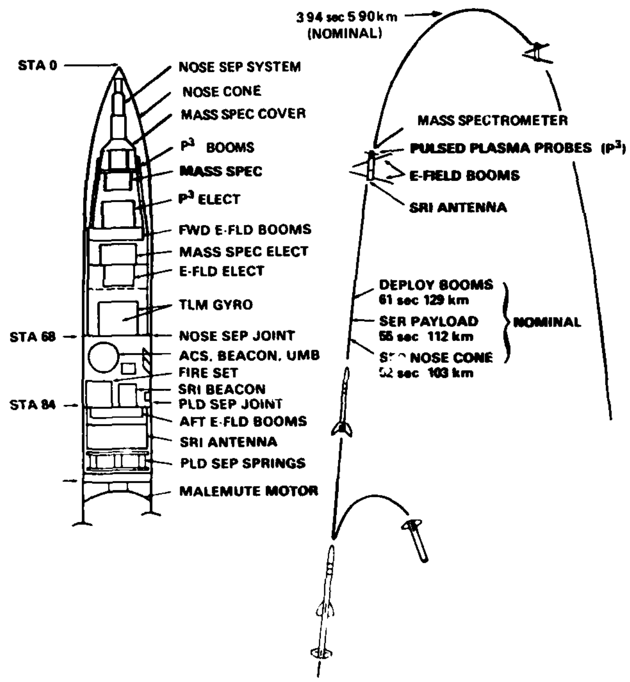

Plumex Payload Instrumentation and Flight Scenario.

Equatorial Ionospheric Irregularities Studies: Coordinated measurements of equatorial spread-F conducted at the Kwajalein Atoll have yielded the first definitive space- and time-coincident radar and rocket observations of small-scale irregularities and large-scale plasma depletions. As part of this Defense Nuclear Agency Program designated "PLUMEX," multi-instrumented Terrier Malemute rockets, including AFGL ion mass spectrometers, were launched on the nights of July 17 and 23, 1979, during equatorial spread-F events. The effort was designed to examine the causes of transionospheric radio-communication scintillations. The program provided the first vertical profile measurements of the detailed ion composition and structure in equatorial ionospheric irregularities.

The results have shown that:

1. During well-developed spread-F, the most intense in-situ irregularities occurred near the bottomside of the F-layer.

2. Within a large-scale topside F-layer depletion, radar backscatter and the rocket-measured irregularities were greatest near the depletion's upper wall, or at the positive plasma gradient.

3. Ion composition within a topside hole provided signatures showing that the origin for such holes was near the F-region bottomside ledge and that the signatures permit a determination of the altitude of the ledge at the time of hole formation.

4. Large-scale fluctuations of O^+ ions accompanied by nearly constant levels of molecular ions (NO^+ and O_2^+) adjacent to the F-layer ledge suggested that neutral atmospheric turbulence is not a major

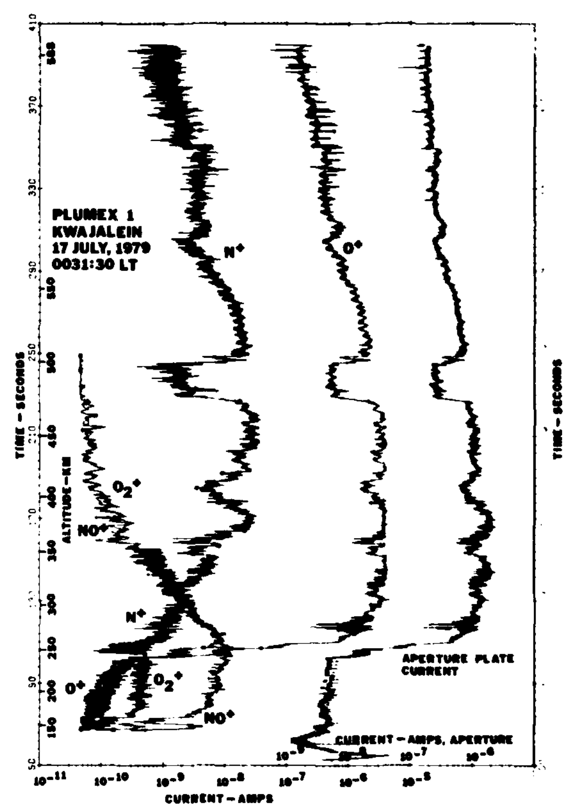

Measurements in Equatorial Ionospheric Irregularities Showing Strong Fluctuations and Holes. The currents are proportional to ionospheric densities. Aperture plate current corresponds to total ionospheric density. The remaining species currents relate to species concentrations.

source for triggering equatorial spread-F.

The measurements obtained during this program are the best data-set available on spread-F. Future theoretical treatment of the data will allow a detailed determination of the processes of ionospheric irregularities.

Eclipse 79 Program: The Eclipse 79 Program was primarily intended to study the ion chemistry processes in the D-region of the ionosphere. In particular, the response of the fast chemical reactions involving the positive and negative ions of the region were to be analyzed as the ionizing ultraviolet radiation from the sun was rapidly turned off and on again by the passage of the shadow of the moon. The eclipse on February 26, 1979, provided the last opportunity to study these effects in the Northern Hemisphere during this century.

On the day of the eclipse, an energetic electron precipitation event occurred, enhancing the D-region ionization well above its normal quiescent values. The normal eclipse effects due to solar radiation were masked. However, in the E-region of the ionosphere, where solar radiation was still the prevalent ionization source, the effects of the eclipse were observed. The measurement program was highly successful in providing an excellent set of coordinated measurements on the ionization produced by energetic particles, the chemistry of the neutral atmosphere and ionosphere, and the dynamical processes in the mesosphere and lower thermosphere.

The Eclipse 79 Program brought together scientists from the United States, Canada, and Switzerland in a cooperative investigation of the altitude region between 50 and 150 km. The campaign was conducted at Red Lake, Ontario, Canada, on February 26, 1979. Included in the program were 12 large sounding-rocket payloads and several small meteorological payloads, as well as ground-based and satellite measurements. A total of 82 experiments were included in the payloads and nearly all provided useful scientific results. The campaign was a cooperative effort of the National Research Council of Canada, NASA, the U.S. Army, USAF and DNA.

The launch site near Red Lake allowed the flight path of the rockets to intercept the path of the total eclipse as it swept across North America. The temporary field site was constructed during the summer of 1978. A few payloads were launched two days before the eclipse to obtain background measurements of the atmospheric properties and to check out the operational readiness of the launch complex, telemetry site and radar site. Most of the measurements for the program were planned for the two-hour interval centered about the four-minute period of eclipse totality.

The measurements in the program made by AFGL scientists included two payloads to measure the density, temperature, wind and dynamical processes in the neutral atmosphere, two payloads to

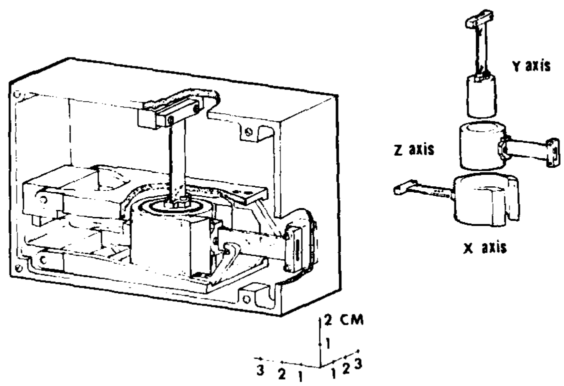

Three-Axis Piezoelectric Accelerometer. The three concentric proof masses are attached to the piezoelectric crystals of the accelerometer. The voltage generated by strain of the crystals under drag acceleration is measured and telemetered to the ground. The proof masses are positioned at the center of a 25 cm diameter sphere and are securely clamped during the powered portion of the rocket flight to prevent crystal breakage.

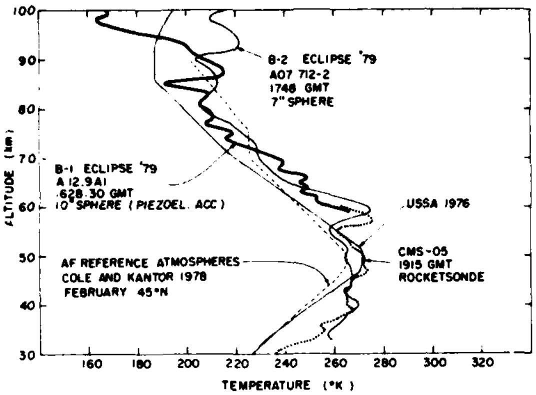

Comparison of Temperature Measurements Made by Piezoelectric Accelerometer, Fall-Time Accelerometer, and Meteorological Rocketsonde with US Standard Atmosphere 1976 and AF Reference Atmosphere 1978. The gravity wave structure present during the program is evident in the profiles.

measure the ion density and composition, one payload to measure the infrared emission at three wavelengths, and ground-based instruments to measure the total electron content of the ionosphere.

The measurements of the properties of the neutral atmosphere were made using two different types of accelerometer-instrumented falling sphere payloads. One of the measurements was obtained 25 minutes before totality using a recently modified piezoelectric accelerometer system in a 25 cm diameter sphere. This instrument provided measurements of the density and winds from the drag acceleration components, at altitudes between 50 and 150 km. The density results can be used to derive a temperature profile under the assumptions of hydrostatic equilibrium and the ideal gas law. Gravity wave structure is easily observed in the high resolution data obtained from the accelerometer. The atmospheric stability criteria can be examined using the density data to define regions which are statically unstable and using the wind data to describe regions that are dynamically unstable. The turbulence regions so defined have been found to correlate well with the regions of increased backscatter in the partial reflection radar measurements of the lower D-region during this campaign. A second set of density and temperature measurements were obtained using a fall-time accelerometer, which measures the drag acceleration on a 18 cm diameter sphere. This payload was launched 50 minutes after totality and provided measurements between 40 and 100 km.

The measurements of the density have provided inputs to the calculations of ionization rates for the energetic particle fluxes measured during the program. The temperature measurements have provided very important inputs to the calculations of the ion chemistry because of the strong dependence of many of the chemical reactions on temperature.

As part of the eclipse program, two AFGL Paiute Tomahawk rockets were launched with payloads containing a liquid-helium, cryopumped quadrupole mass spectrometer and two Gerdien condensers to measure positive and negative ion composition, ion densities, and mobilities between 50 and 120 km. The mass spectrometers utilized shock-attaching conical samplers to prevent the break-up of large cluster ions. Attitude control systems maintained the rockets at very low attack angles. The first rocket was launched during eclipse totality at 10:52:30 CST and the second was fired after totality in 75 percent solar illumination at 11:41 CST.

As previously noted, an energetic electron-deposition event was in progress. The ion composition signatures of the particle event were apparent: a significant enhancement of O_2^+ at lower altitudes and large amounts of $H_5O_2^+$ ions in the D-region, which are formed from an ion chemical clustering mechanism that begins with O_2^+.

Of particular interest were the large relative amounts of $H_7O_3^+$ and $H_9O_4^+$ ions measured. The AFGL model developed

earlier to calculate the D-region under natural or nuclear-disturbed conditions could not account for the large abundances of $H_7O_3^-$ and $H_9O_4^-$. This has led to a complete re-examination of the D-region ion processes. No clear explanations are available to date.

The negative ion situation is even more complicated. Both flights exhibited distributions with a distinct negative ion shelf about 83 ± 2 km, with concentrations dropping off by more than an order of magnitude by 90 km and with minima near 75 km. In the 75-90 km range a significant percentage of the negative ions had masses greater than 160 amu. An explanation for the formation of such massive ions does not exist. Heterogeneous reactions with atmospheric conglomerates have been hypothesized as a possible mechanism, but the exact processes are unknown.

Following this successful campaign, there have been two scientific workshops to exchange results and interpret the measurements. A special session of the American Geophysical Union meeting at Toronto in May, 1980, was devoted to presentation of the results. The final results of the program are planned for publication as a group in a scientific journal in 1982.

Disturbed Lower Ionosphere Rocket Program: Another rocket and ground-based program was conducted at Poker Flat, Alaska, to further study the disturbed lower ionosphere, which affects communications and radar systems. Two rockets were launched during a significant geomagnetic disturbance which produced a strong auroral-zone absorption event (the ionosonde records exhibited complete absorption). A Paiute Tomahawk rocket payload was launched at 1131 local time on October 22, 1980. It contained a liquid-helium cryopumped quadrupole mass spectrometer to measure positive and negative ion composition, a Gerdien condenser to determine positive and negative ion densities and mobilities, and a retarding potential analyzer to obtain positive ion and electron densities. A second rocket with an electron energy deposition scintillator for measuring the energetic electron flux and an impedance and dc probes for measuring the electron density distribution was launched at 1145 local time. Both rockets had apogees near 90 km. Ground measurements were also performed by the Chatanika radar and also by NOAA's MST and Hf radars. The data are presently being analyzed. An immediate observation was the elimination of the water-cluster oxonium ions between 74 and 82 km and their replacement by the simpler molecular ions of NO^- and O_2^- as a result of the energetic particle event.

PLACES Program: The Defense Nuclear Agency's PLACES (*P*osition *L*ocation *a*nd *C*ommunications *E*ffects *S*imulations) Program was conducted between December 4 and 12, 1980, at Eglin Air Force Base, Florida. The objective of the program was to demonstrate and investigate the effect of structured ionospheric plasmas on satellite communication and navigation systems. The structured plasma environment was created by four rockets' releasing barium at 185 km during four separate evenings. Signals from satellites passing through all the barium ion clouds were received by an airborne (AFAL) receiving station. During one event, signals from two rocket-borne transmitters passing through the drifting plasma cloud were received by ground stations. In the final event, a rocket carrying an AFGL ion mass spectrometer and NRL plasma probes was launched on December 12, 1980, into the barium ion cloud at 22:42:52 UT (5:42:52 CST), about 32 minutes after the barium release. The very first measurements of the ion composition and structure through a barium ion cloud were obtained. The results exhibited both interesting plasma chemistry and striations, which caused the observed electromagnetic absorption.

The rocket penetrated the barium cloud

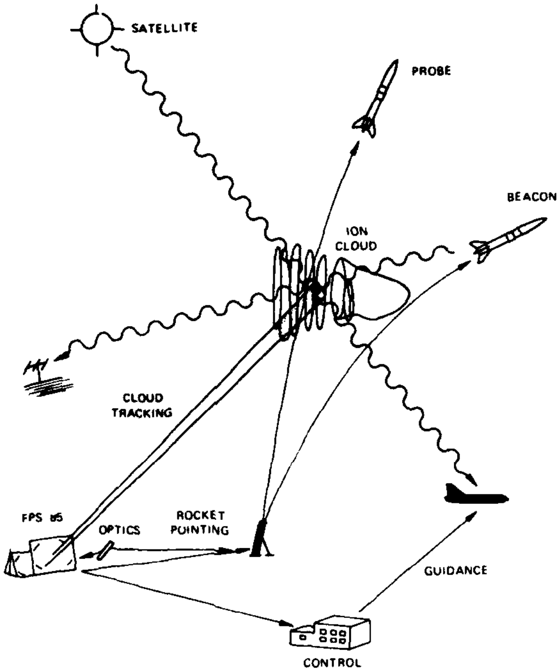

Schematic Diagram of the PLACES Program.

between 148 and 183 km. A maximum barium (and electron) density of 7.3×10^6 ions (electrons) per cc was measured in a broad peak near 155 km. The electron concentration was greater than two orders of magnitude over the normal ionosphere. The barium plasma caused an almost complete depletion of the NO^+ and O_2^+ ions normally dominating in this region. Doubly ionized barium ions were also detected; they were most likely produced by double solar-photon ionization. The barium plasma showed significant concentration fluctuations with structural disturbances propagating upward into the normal ionosphere where no barium ions were present. All elements of the program including ground-based radar and optical measurements were successful. The data are presently being reduced for analysis.

Van der Waals Molecules: Van der Waals molecules have been largely ignored in the natural atmosphere, primarily because the types and quantities of these molecules in the atmosphere were unknown. Atmospheric equilibrium number densities were calculated for the first time for the van der Waals molecules (or dimers) $N_2 \cdot N_2$, $N_2 \cdot O_2$, $O_2 \cdot O_2$, $N_2 \cdot CO_2$, $O_2 \cdot CO_2$, $N_2 \cdot H_2O$, $O_2 \cdot H_2O$, $CO_2 \cdot CO_2$, $H_2O \cdot H_2O$, $Ar \cdot Ar$, $Ar \cdot CO_2$ and $Ar \cdot H_2O$ for the altitude range from 5 to 90 km. Some of the dimer concentrations are significant, being of the same order as minor, rather than trace, species. It was shown that the van der Waals molecules play important roles in neutral and ionic reactions as well as infrared absorption and emission in the natural atmosphere. A paper published on these results is expected to generate interest in the study of van der Waals molecules in planetary atmospheres and their roles in various other processes like atmospheric nucleation.

Meteor Sulfur Chemistry: Meteors ablate in the lower ionosphere and give rise to a host of positive ion spectra, many of which have been properly identified to date. However, no clear evidence for sulfur in any form had been produced until a Swiss group recently reported an ion of mass 48 amu in the lower E-region. Although titanium ions do have a mass of 48 amu, AFGL demonstrated, in collaboration with the Swiss group in a theoretical study, that the 48 amu ions they measured represent SO^+, sulfur monoxide ions. It was argued that free sulfur undergoes rapid processes with molecular oxygen to produce, eventually, the stable compound sulfur dioxide, SO_2. Most of the sulfur finds its way into neutral compounds, particularly SO_2. However, in the lower E-region, oxidation is probably not yet complete as compared to lower altitudes, and hence a sulfur species hierarchy was suggested for the lower E-region: $[SO] >> [SO^+] > [S] >> [S^+]$. The quantity of SO^+ in the lower ionosphere is low, about 10 ions per cubic centimeter.

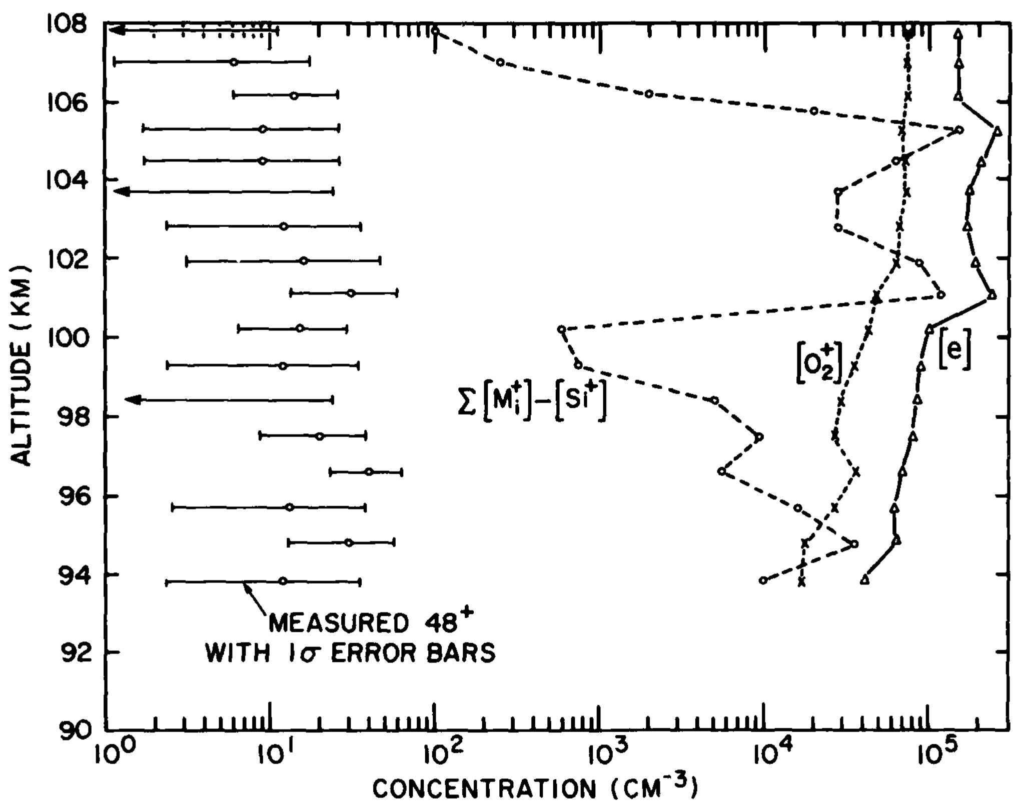

Upleg Concentration Profiles for SO^+ Ions (48^+ amu ions), O_2^+ Ions, Electrons and Total Metal Ions Less Si^+ Ions as Measured by Herrmann et al. (1978) August 12, 1976, at Wallops Island, VA.

The sulfur deposited by meteor ablation in the atmosphere may possibly contribute to the sulfur burden of the stratosphere, particularly the upper stratosphere. Most sulfur in the stratosphere, however, rises from the earth's surface.

Atmospheric Nitric Oxide Variations: Nitric oxide plays a major role in the aeronomy of the lower ionosphere, since it strongly influences the ionic ratio $[NO^+]/[O_2^+]$ because of the fast charge transfer process $O_2^+ + NO \rightarrow NO^+ + O_2$ and because ionization of NO by solar hydrogen Lyman alpha radiation is the main source of the quiet daytime D-region. Nitric oxide profiles derived from daytime ion-composition measurements of the lower ionosphere indicate that NO concentrations tend to increase by more than an order of magnitude with increasing solar activity or sunspot number.

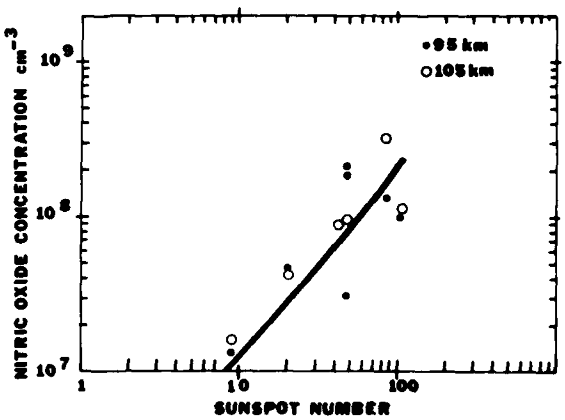

Variation of Nitric Oxide with Sunspot Number for Two Mid-latitude Altitudes

In the AFGL-Swiss study, a best-fit NO profile was derived for the middle atmosphere. This experimental mean profile is rather close to a theoretical study of Ogawa and Shimazaki. The experimental mean NO profile appears to provide for a quiet electron concentration profile in the upper D-region, which is in reasonable

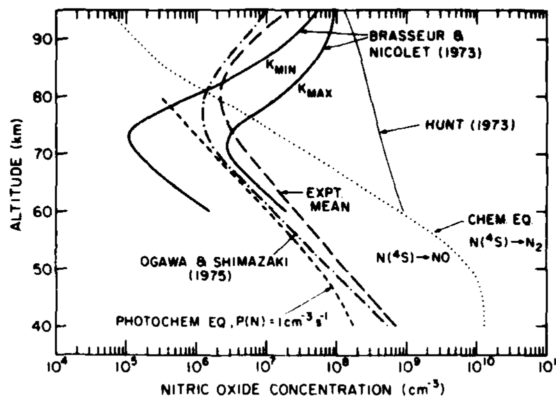

Comparison of Theoretical Nitric Oxide Profile with an Experimentally Determined Mean Profile for Mid-latitudes.

accord with the mass of observational evidence. However, it should be stressed that there are important variations in NO. Thus, as stated in the *Report on Research* for the period July 1976-December 1978 (p. 18), NO in the auroral E-region can be enhanced over an order of magnitude with respect to quiet conditions. This finding is in agreement with satellite-based evidence. The quantity of NO in the E-region near 105 km tends to increase with latitude for moderate to high solar activity. This behavior must influence the amount of NO in the D-region. Nitric oxide rises with decreasing altitude below about 70 km because there is a stratospheric source of NO, the destruction of nitrous oxide, N_2O.

Laboratory Measurements of Meteor Metal Chemistry: Meteor metals may play a role in maintaining certain chemical equilibria in the earth's ionosphere and stratosphere. A code is being developed which will describe the chemical reactions these metals undergo in their transport from the point of injection (ionosphere) to the ground. Likely metallic compound intermediates in the lower ionosphere and in the upper stratosphere are the monohydroxides of these metals, which are converted to chlorides in the stratosphere by reaction with odd chlorine compounds. In support of this model-making effort, the dissociation energies and ionization potentials of some monohydroxides (MgOH, FeOH, CaOH, BaOH, and AlOH) have been measured using a high temperature mass spectrometer. These measurements make it possible to assess the likelihood that these species will influence the ozone chlorine cycle.

MIDDLE ATMOSPHERE EFFECTS

The stratospheric environment has been broadened to include the middle atmosphere, the 15 to 85 km altitude region. This region was long excluded from systematic investigation because of a lack of appropriate observation techniques and the absence of an urgent need to answer unresolved questions. Concern has now, however, been focused on potential environmental impacts upon the stratosphere. Furthermore, the middle atmosphere is known to affect laser and vlf propagation. New measurement techniques now permit observation of trace gas constituents, aerosols, and the dynamic characteristics of the middle atmosphere.

The study of middle atmosphere effects is currently divided into three areas: electrical and aerosol properties, environmental impact assessments, and optical turbulence. The electrical properties of the middle atmosphere are determined by the number density of positive and negative ions, the ion mass, and the free electron density. These parameters will be directly measured at AFGL through the development of a balloonborne ion mass spectrometer.

Particulate Measurements: An experimental balloon flight of the high resolution AFGL/Epsilon aerosol spectrometer was conducted from Holloman AFB on May 27, 1980. Although the initial eruption of Mt. St. Helens occurred several days before this flight, the volcanic debris had not reached the measurement area, thereby permitting a last-chance, high-resolution measurement of the undisturbed aerosol background. A comparison of these data with data taken in May, 1973, a period of relatively undisturbed atmosphere, shows the concentration of particles having diameters below 0.35μ to be approximately the same as that above the tropopause. Such is not the case, however, for the particles greater than 0.4μ in diameter. The 1980 data show a virtual absence of particles greater than 0.4μ in diameter, whereas the 1973 flight indicated an appreciable quantity of aerosols in this size regime.

In sharp contrast to the foregoing measurements are data obtained on January 21, 1975, three months after the eruption of the Fuego volcano in Guatemala. The particle concentration plot shows the dramatic increase in the Junge layer, centered at 19 km, as the result of this volcanic eruption. An equivalent atmospheric disturbance is likely as a result of the Mt. St. Helens eruption, although no subsequent measurements have been made with the AFGL Epsilon instrument.

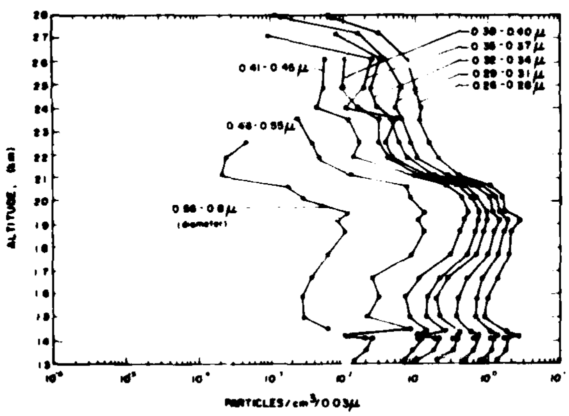

Particle Concentration Plot of Data Obtained Three Months After Eruption of Fuego Volcano, Guatemala, January 21, 1975.

Environmental Impact Assessments: Concern has been focused on the stratosphere during the last few years because it is becoming evident that man's activities can significantly change the environment. Chlorofluoromethanes have been banned in aerosol sprays because they may contribute to the destruction of the ozone layer in the stratosphere. Some Air Force weapons systems operate in the stratosphere, and careful evaluations must be made to avoid inadvertent modification of the environment.

The Middle-Atmospheric Effects Program predicts what environmental changes may occur from USAF missiles and aircraft operations in the stratosphere. In this program, minor stratospheric constitutents, aerosols, solar energy deposition, and pollution transport properties and residence times in the stratosphere are measured with unique state-of-the-art instruments flown on large balloon systems. Mathematical models are continually revised by incorporation of the newest determinations of reaction rate constants and data on density. A respected scientific technology base and predictive models exist to determine if changes occur in the atmosphere as a result of emissions from USAF flight operations. This capability has been used to provide environmental assessments on aircraft and missile systems.

Whole-Air Sampling Measurements: The primary method for measuring the composition of the stratosphere is to fly a cryogenic vessel on a high altitude balloon, collect a one mole sample, and return it to the laboratory for trace gas analysis. Cryogenic sampling provides large sample quantities and minimum potential for chemical changes in the stored sample, which is frozen. The first liquid-helium-cooled sampler used in this program col-

lected a single one-mole sample on each flight. A newer tri-sampler collects a one-mole sample at each of three altitudes on each flight, providing both more economical operation and same-day measurements of a large altitude range.

The tri-sampler contains three sample holders immersed in a single liquid-helium chamber which is thermally shielded by both liquid nitrogen and vacuum blankets. The sampling valves are remotely actuated in sequence. The air sample tubes are sized for the altitude at which they are used, so that the air molecules enter at a rate slow enough to freeze on their first contact with the cylinder wall. Samples are taken only while the balloon is descending, and a fan downstream from the sampling tube draws air across the sample tube inlet from a larger diameter tube, which extends 6 meters below the gondola. These precautions prevent contamination of the samples by the flight package.

Stratospheric composition studies based on in-situ whole-air sampling with a cryogenic sampler continued with six balloon flights during the reporting period. All were successful. Initial measurements at all five specified latitudes from 9° to 64°N and six altitudes from 12 to 30 km at all sites have been completed. Such a spectrum of altitudes and latitudes is required to establish a data base sufficient to permit conclusions to be drawn about the possible effects of Air Force operations on stratospheric trace gases. This data base will also facilitate development and testing of theoretical models for the chemical budget and transport within the stratosphere, both for the oxides of nitrogen and the fluorocarbons. The initial set of measurements from twenty-two balloon flights are considered baseline values against which future, potential changes can be compared. Oxides of nitrogen content have been shown to be quite variable and larger than generally predicted. They also exhibit considerable diurnal dependence but, at best, a marginal latitudinal dependence. Fluorocarbon concentrations have been shown to decrease from tropopause values (similar to tropospheric values) down to roughly 10 percent of these values at a 30 km altitude. Measurements have not, so far, indicated year-to-year variations in mixing ratios within the stratosphere. Occasionally, folded profiles have been obtained, indicating vertical air motion within the stratosphere.

Central to the ability to measure trace-gas concentrations down to the required parts per trillion range is the need to accurately calibrate the diagnostic equipment down to this range. The initial method involved successive dynamic dilutions of the five species of interest through titration tubes. Improved accuracy has been provided through addition of two other methods: precision electronic mass-flow controllers and permeation tubes. All three methods produce agreement to within a few percent.

Stratospheric Solar Ultraviolet Measurements: For accurate modeling of the stratosphere it is necessary to know the solar irradiance as a function of height in the absorbing region and the variability of the irradiance during the 11-year solar activity cycle. Previous estimates of the variability have ranged from a few percent to factors of three or four. AFGL has made measurements of the solar irradiance in the wavelength range up to 40 km in balloon flights of April 1977, April 1978, and April 1980, and an additional flight is planned for April 1981. These flights span a change from a minimum to maximum solar activity, as monitored by other indicators. The change in the 2000-3000 Å region of the spectrum will be investigated in the data from these four flights. On theoretical grounds, the change is expected to be only a few percent and difficult to detect. Therefore, the measuring instrument has been carefully calibrated against standards of irradiance before and after each flight.

The instrument used for these measurements is an ultraviolet spectrometer of the Ebert-Fastie type with a wavelength resolution of 0.12 Å. It is mounted on a balloon-borne biaxial solar-pointing control and carried to a float altitude of 40 km by an 11 million cu ft balloon. The spectrometer makes measurements during ascent and descent, as well as during a three-hour period at the float altitude.

Turbulence Studies: A critical value of the gradient Richardson number, determined from rawinsonde measurements of winds and temperatures, is used as an in-

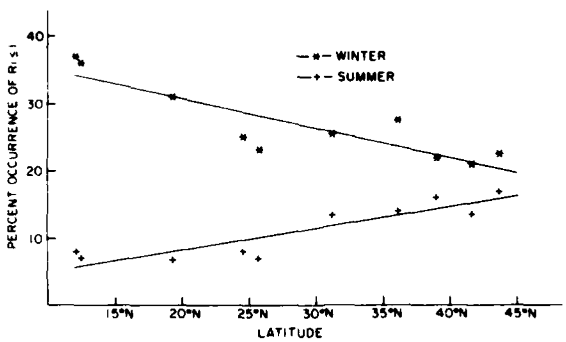

Latitudinal Variation in Five-Year Average Percent Occurrences of Ri ≤ 1 for Peak Layer at 10 km at Longitude 68°W to 82°W. Stations from left to right are: Willemstad, Curacao; San Andres, Col.; Grand Cayman, W.I.; Key West, FL; Miami, FL; Waycross, GA; Greensboro, NC; Washington, DC; Chatham, MA; and Portland, ME.

dicator of the presence of turbulence in the lower atmosphere. These twice daily sets of balloon measurements of temperature and winds are obtained from ground level to approximately 30 km at 144 stations located mainly in North and South America. Data from the years 1971-1975 have been used to determine the relative frequency of occurrence of turbulence as a function of season, location (latitude and longitude) and altitude.

Layers of high occurrences of turbulence are found near 10 km at low latitudes in the winter. This 10 km peak layer diminishes in amplitude with increasing latitude. The summer peak layer at 10 km is low in amplitude near the equator and increases in amplitude at nearly the same rate with latitude as the winter peak diminishes. The spring and fall peak layers

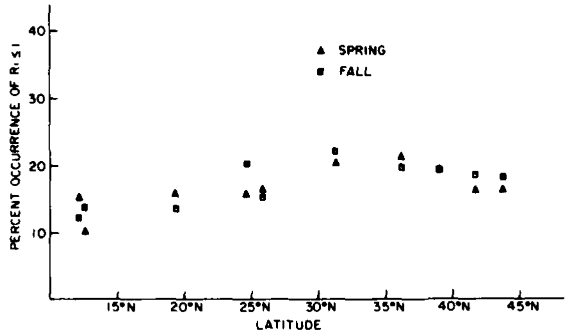

Spring and Fall Five-Year Average Percent Occurrence of Ri ≤ 1 as Function of Latitude at Longitude 68°W to 82°W.

fall between winter and summer values and are very nearly equal in amplitude. This seasonal and latitudinal effect is shown here. Each plotted point represents a five year average in the percent occurrences of turbulence at the 10 km level. Data from ten stations were used, ranging from the northern coast of South America, through the Caribbean, across the tip of Florida, and along the eastern coast of the United States.

A regression analysis has been performed on data from twenty-one stations located throughout the continental United States. It relates the turbulence indicator to location (latitude and longitude), altitude, season, and year. Results obtained from this statistical analysis indicate that consistent patterns of turbulence appear from year to year and can be predicted fairly well. The ability to model and predict layers of turbulence in the lower atmosphere is important in determining the nature and degree of dispersion of pollutants as well as the effects of pollution on communications, surveillance, and detection.

Theories of turbulence usually make the simplifying assumption that the turbulence is homogeneous. The stratosphere, however, is an unusually stable "fluid" which causes the turbulence to take on a very peculiar structure, namely, that of layers that spread out in the horizontal direction for miles but are relatively thin (200 meters) and have been compared to pancakes. These are separated by thick laminar layers that typically occupy a few percent of the fluid volume. It is hard to imagine how this turbulence could be more inhomogeneous.

This laboratory has developed a new turbulence transport parameter (in the vertical direction) which, for the first time, accurately reflects this physical situation. This new parameter takes the place of, but must not be confused with, the "eddy diffusion" coefficient. The validity of this concept was proved mathematically and will be published in 1981 as a cover story in *Science*. It is a breakthrough of general applicability (e.g., oceans, upper troposphere).

To connect the new parameter to observations and to older theories and to define its limits of applicability, a research study was conducted and published as an in-house report (790042). Another in-house report (800186) was devoted to a rather detailed display of computer simulations which demonstrated the self-consistency of the concept. One of the key assumptions for the valid application of the new approach is that the turbulent layers cause a high degree of mixing before they decay, and a study was made and then published (790091) which gave both theoretical and experimental evidence that this is a correct assumption.

The new turbulence parameter, when applied to existing data, gave ten times the vertical transport usually attributed to stratospheric turbulence. In view of this discrepancy, a critical review of the other work was performed. The conclusion was reached that, until certain key experimental observations are made, we will not know the significance of local turbulence in the transport of pollution in the stratosphere so far as "residence time" is concerned. As things now stand, one cannot even say whether it plays a dominant or insignificant role in comparison to global circulation.

Optical Turbulence: Turbulence effects on light transmission have been studied for decades, the twinkling of stars being the prime example of the observed turbulence effect. The advent of powerful lasers in many military applications, including weapons, communication and surveillance systems, has led to a study of turbulence effects on optical systems. It has become important to know the extent and characteristics of atmospheric turbulence. AFGL is currently involved in an optical turbulence program that brings together all the methods of measuring optical turbulence and is conducting a comparative measurement program. AFGL has modified the radiosonde to obtain higher resolution data. This high resolution data will permit interpretation and correlation of the different techniques of measuring optical turbulence. A large tutorial report (800030) was prepared and published, which not only describes in simple terms the physics of optical turbulence and its effects on systems, but also contains a comprehensive description of how one calculates the main parameters relating to system design. A field program has been started to determine atmospheric parameters and their connection (through models) with synoptic, geographical, and diurnal data.

SOLAR ULTRAVIOLET RADIATION

Only 2 percent of the solar energy radiated from the sun is emitted in the ultraviolet (uv) region of the solar spectrum, which extends from 30 to 3500 Å. Because this radiation is completely absorbed by

the upper atmospheric atoms and molecules, it is the principal source of energy in the earth's upper atmosphere. The absorption of solar uv radiation in the atmosphere controls the composition, temperature, and photochemistry of the atmosphere and is the principal source of production of the ionosphere and an important source for atmospheric airglow radiation.

To develop quantitative upper atmospheric and ionospheric models for predicting neutral and charged-particle distributions, accurate measurements of the absolute intensity and spectral distribution of solar uv radiation incident on the earth's atmosphere are needed. Data are also required on the variation of the radiation during periods of changing solar activity. Measurements of solar uv radiation are made with optical spectrometers mounted on solar-pointed platforms that are flown in rockets and satellites.

Rocket Measurements of Solar UV: A rocket experiment was flown from the White Sands Missile Range, NM, on August 14, 1979, to obtain simultaneous measurements of the solar ultraviolet flux, the energy distribution and density of atmospheric photoelectrons, and molecular nitrogen (N_2) airglow radiation. The parameters are interrelated. The photoionization of atmospheric gases by solar ultraviolet radiation at wavelengths shorter than 1026 Å produces electrons having an energy range from approximately 0 to 100 eV. These atmospheric photoelectrons then excite the N_2 second positive band as well as other emission lines and bands of various atomic and molecular species. The purpose of the rocket experiment was to measure these parameters within the atmosphere to verify a theoretical model developed to determine if atmospheric density profiles can be determined remotely from a satellite by observing optical emissions from the earth's upper atmosphere.

The rocket payload was instrumented with a grazing incidence spectrometer to measure solar uv flux between 50 and 1026 Å emitted from the full solar disk. The spectrometer was pointed at the center of the solar disk with a biaxial solar-pointing control. The energy distribution and density of the atmospheric photoelectrons in the energy range between 2.4 and 5.7 eV and between 14 and 34 eV were measured with an electron energy analyzer. This analyzer was mounted on the rear surface of the solar-pointed spectrometer so that the entrance aperture of the analyzer was pointed nearly in an anti-solar direction. This orientation shields the analyzer aperture from solar uv radiation that would produce extraneous photoelectrons and degrade the analyzer data. The electron analyzer could be adjusted to align its axis nearly parallel to the geomagnetic field lines. The experiment was successful and the rocket payloads were recovered. The data have been reduced and analyzed and are now being used to verify the theoretical model for obtaining atmospheric density profiles from optical emissions within the earth's atmosphere.

On September 18, 1980, an Ebert-Fastie spectrometer mounted on a solar-pointing control was flown in a rocket from the White Sands Missile Range, NM. Solar ultraviolet (uv) radiation incident on the top of the earth's atmosphere was measured for the wavelength range from 1750 to 3200 A with a spectral resolution of 0.1 A. The experiment was one of a series of five rocket flights that have been flown during the rising phase of the present 11-year solar cycle 21. The first experiment was flown in May, 1976, which is close to the minimum level of activity of cycle 21. Three experiments were flown during April and August, 1977, and September, 1978, while the level of solar activity was increasing. The flight of September 18, 1980, was close to the maximum level of activity for cycle 21. The data from the five rocket flights will allow a determination of

the variation of solar uv radiation between 1750 and 3200 Å from the minimum to the maximum level of activity for a solar cycle. This wavelength region is of importance to the study of photochemical processes occurring in the stratosphere and to the development of stratospheric models.

Four rocket payloads to be launched from Poker Flat Research Range, Alaska, during March, 1981, are being assembled. As part of the Auroral-E program, the objectives of the rocket experiments are to measure several interrelated auroral parameters, during steady-state auroral conditions, that are needed for correlating auroral optical emissions with electron density profiles. The rocket payloads will contain several instruments. Electron and proton analyzers will measure the energy distribution and density of electrons between 1 eV and 20 keV and protons between 50 eV and 60 keV. Optical spectrometers and photometers will measure auroral optical emissions of several emission lines and bands in the wavelength range from 1300 to 5700 Å. A switched positive ion and neutral mass spectrometer will measure auroral ions, and a pulsed plasma probe will provide data on electron density and temperature. Auroral electric fields will be measured with extended booms, and upper atmosphere winds will be determined by photographing, from the ground, vapor trails produced by a chemical (TMA) released from one of the rockets. The data will be used to verify theoretical models being developed for use in determining auroral electron-density profiles from a satellite.

Satellite Measurements of Solar UV: Satellite-borne optical spectrometers allow long-term variations of solar uv radiation associated with changing levels of solar activity to be measured. This Laboratory has flown three solar ultraviolet spectrometers on the NASA Atmosphere Explorer (AE) series of satellites. Twenty-four individual grazing-incidence units mounted on a solar-pointed platform obtain solar uv radiation measurements for the wavelength range from 140 to 1850 Å. The first satellite, AE-C, was launched during 1973. The second (AE-D) and third (AE-E) satellites were launched during 1975. The satellite AE-D became inoperative approximately one month after launch. However, AE-C was still operating when AE-E was launched so that continuous data were obtained with these two satellites. The satellite AE-E continues to provide data on solar uv radiation. These satellite flights have measured, for the first time, the long-term variations of solar uv radiation continuously from the minimum through the maximum level of activity of an 11-year solar cycle. The highest levels of flux measured near solar maximum between November, 1979, and January, 1980, were found to exceed the minimum levels of July, 1976, by significant amounts, depending upon the wavelength. At longer wavelengths, the increase in flux ranged from a factor of 1.2 near 1800 Å to 2.5 near 1400 Å. At shorter wavelengths, chromospheric solar lines increased by a factor of from 2 to 3.5 and coronal lines by as much as 100.

Absolute values of solar uv radiation and its variability are needed to allow accurate modeling of the composition and structure of the upper atmosphere and ionosphere and to predict the response of the atmosphere and ionosphere to temporal variations in the radiation.

ATMOSPHERIC UV RADIATION

Knowledge of the naturally-occurring ultraviolet emission from the earth's atmosphere is necessary before the ultraviolet can be used for such purposes as missile detection, auroral and ionospheric remote sensing, and horizon location. Since the atmosphere is opaque to the ultraviolet at wavelengths shorter than about 2900 Å, the ultraviolet is used in space-based observation systems taking advantage of the extremely low level of

natural background emission. While the emission background is known to be small, its exact value and wavelength distribution during both day and night have not been well characterized and have generally not been included in aeronomic models.

Ultraviolet Backgrounds Satellite Experiment: Measurements of the ultraviolet background were obtained on the Space Test Program flight S3-4 in 1978. The sensor package measured the background of the atmospheric radiance from space in the nadir, or earth-center, direction from the polar-orbiting satellite. The range from 1100 to 2900 A was covered by two one-quarter meter Ebert-Fastie spectrometers, and the range from 1100 to 1900 A was covered by any one of four filters in a photometer having a variable aperture.

Ebert-Fastie Spectrometer Flown in Auroral-E Payload.

Observations included the auroral zone seen both night and day, the night tropical uv airglow belts, and twilight effects, as well as the airglow and solar-scattering components of the day and night backgrounds. Spectral features measured included the oxygen atom (1356 and 1304 A lines), the nitrogen Lyman-Birge-Hopfield bands (about 1250-2200 A), the hydrogen Lyman alpha line (1216 A), the oxygen Herzberg bands (2500-2900 A), and the nitric oxide delta and gamma bands (about 1900-2400 A). In addition, a previously unrecognized nitrogen Lyman-Birge-Hopfield source in the night and day northern hemisphere was found. Initial publication has been made of these results.

The satellite experiment AFGL-101, Auroral/Ionospheric Mapper (AIM), was begun during this period. Based on S3-4 data, it is being designed to obtain global images of the aurora and the ionosphere from a polar-orbiting stabilized spacecraft. Any 30 A band in the 1100-2000 A region can be isolated by command of a spectrometer. A rotating mirror sweeps the nadir field of view from horizon to horizon with 25 km resolution. In this way, images are obtained similar to present visual wavelength images from the Defense Meteorological Satellite Program. Initial specifications were developed in this period.

An ultraviolet calibration facility has been built to calibrate and test the flight sensors, using calibrated detectors from the National Bureau of Standards. The AFGL digicon sensors for the Multispectral Measurement Program used on an Aries rocket payload have also been calibrated in this facility, as have a number of other sensors for Army, Navy, and Air Force programs.

Horizon Ultraviolet Program: The brightness of the horizon seen in the ultraviolet must be measured to develop spacecraft horizon or altitude sensors. Design and fabrication of prototype sensors were finished. A preliminary test flight of one sensor, AFGL 801A, is being prepared for an early shuttle flight. The full complement of six sensors, AFGL-801B or 801C, covering the range from 1100 to 4000 A, is being built. The one-eighth meter Ebert-Fastie spectrometer used as the key component in this sensor is shown here.

Auroral and Ionospheric Remote Sensing: The examination of the S3-4 data in

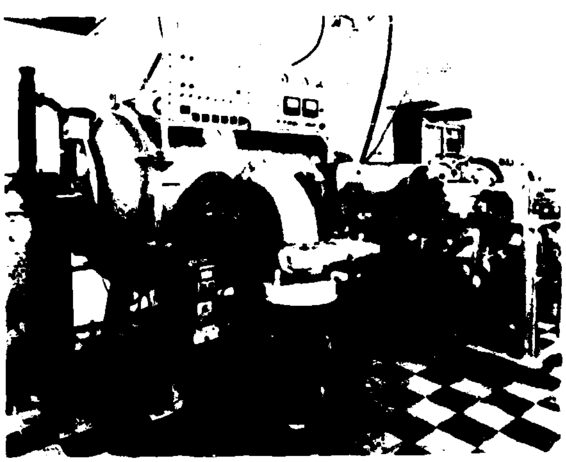

AFGL Ultraviolet Calibration Facility.

1979 demonstrated the great potential of the vacuum ultraviolet to detect auroral excitation regions both day and night. Auroras indicate disturbed ionospheric conditions adversely affecting communications and radar systems. The possibility of observing auroral and ionospheric regions from space has resulted in two types of effort: the Auroral E-program and the Auroral/Ionospheric Mapper (AIM) experiment. The Auroral E-program observes a diffuse (continuous) aurora with rockets, aircraft, and ground-based radar. AFGL provided ultraviolet and visible sensors for a Taurus-Orion payload. The field program is planned for February-March 1981 at Poker Flat Research Range, Alaska.

SATELLITE ACCELEROMETER DENSITY MEASUREMENTS

A major goal of the satellite accelerometer program has been the development of improved global empirical models for the lower thermosphere. In addition to being extremely useful for organizing and analyzing large data sets, models of this type can generate atmospheric density predictions required for Air Force operations. Using data from MESA (Miniature ElectroStatic Accelerometer) accelerometers on the four low-altitude satellites S3-1 and AE-C, -D and -E, we formulated an initial model to describe the quiescent atmosphere from 140-250 km. (The large density variations related to geomagnetic storms were not included in this model.) We selected data from 2000 orbits corresponding to periods of low geomagnetic activity. Ten terms were used in a linear regression analysis to describe density variations associated with local time, day of year, and a narrow range of solar and geomagnetic conditions. The following results, given at an altitude of 200 km, indicate the magnitude of the derived density variations. An increase of 40 solar flux units (from $F_{10.7} = 60$ to $F_{10.7} = 100$ units) results in a density increase of 20 percent. For the low range of geomagnetic activity represented by the range of a_p from 0 to 15, the density increase is 11 percent. The semiannual variation, derived by superimposing pure sine and cosine terms, each with periods of one-half year and one-third year, shows maxima on April 21 and October 13 and minima on January 6 and July 25. Peak-to-peak amplitude was 21 percent. The diurnal variation reached its maximum at 1430 hours and exhibited an amplitude of 9 percent.

This regression model was compared with three currently used atmospheric models J71, J77 and MSIS. Each of the models showed significant differences in specific representations of atmospheric variability. The J71 model was in closest agreement with the empirical model for the range of solar flux and geomagnetic activity variations. Local time variations were best represented by the MSIS model. All three models showed general agreement with the phase of the semiannual variation but predicted a larger amplitude. MSIS, with a 31 percent amplitude prediction, was closest to the empirical model. These comparisons demonstrate the requirement for continued theoretical and experimental effort to develop accurate atmospheric models.

Major features of the diurnal variation in atomic oxygen, molecular nitrogen, and total mass density below 250 km were elucidated by using a theoretical analysis and satellite accelerometer data. Seasonal, latitudinal, solar cycle, and altitudinal dependence were computed with a formalism using tidal winds and temperatures as external inputs. The input tidal fields were computed a priori by numerically solving the linearized tidal equations for a spherical, rotating viscous atmosphere with anisotropic ion drag and thermal excitation by in situ absorption of uv and euv radiation. These theoretical calculations showed that the diurnal tidal components of O, N_2, and total mass density should possess seasonal and latitudinal variations that are sufficiently large to be of interest to researchers involved in the modeling and interpretation of data in the thermosphere and ionosphere.

Only scant observational data are available to test these theoretical predictions. Using the extensive accelerometer data base, we could verify the manner in which the diurnal phase varied with latitude. Seasonal divisions of the data set were not possible. The empirical model terms were used to calculate density in 2-hour local time bins and 20° latitude bins at 10 km altitude intervals. A least-squares harmonic analysis was performed at each height and latitude to determine the tidal components. The results showed that below about 180 km there is a phase shift to later local times from the equator to midlatitudes. The magnitude of this shift is approximately seven hours from the equator to 50°N. These results were in good agreement with the theoretical values. The effect is basically a manifestation of the relative amplitudes and phases of O and N_2 variations at different latitudes, which are in turn controlled by the influences of tidal winds and temperature in determining tidal changes in composition.

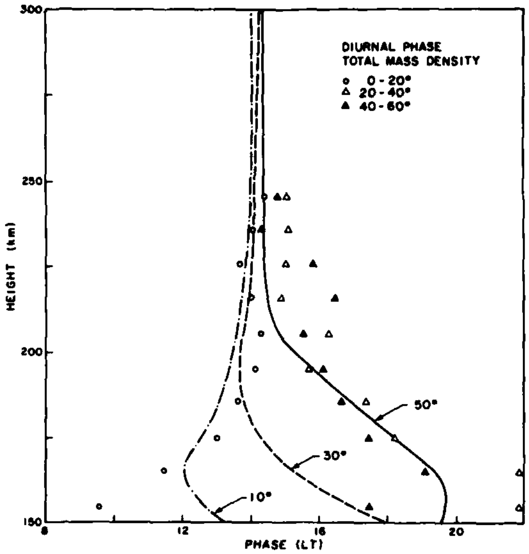

Comparison of Theoretical Diurnal Phases of Total Mass Density at Latitudes 10°, 30°, and 50° with Tidal Determinations from MESA Accelerometer Data over Corresponding Latitude Bands. The experimental data confirm the predicted shift of the diurnal phase to later local times with increasing latitude at altitudes below about 200 km.

The present empirical model is being extended to incorporate conditions of moderate and high geomagnetic activity. In this model, the amplitude of geomagnetic-activity variations in density is a function of both latitude and season. A latitude-dependent time delay has also been derived. It varies from three hours at the auroral zone to eight hours at the equator. A latitudinal dependence has also been included for terms associated with the local time and day-of-year variations. All 8000 orbits in the density data base are being used in this study. A total of twenty-four terms describe atmospheric variations. This new model is nearly completed. It will provide a more accurate description of the satellite-measured density results than other atmospheric models presently available. A preliminary result is shown in the contour plot.

A single proof-mass triaxial accelerometer was successfully flown during 1979 on

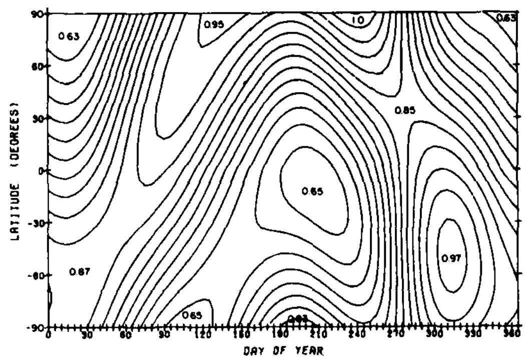

Typical Contour Plot of Density at 200 km as Function of Geographic Latitude and Day of Year. The data correspond to a solar flux of 75 units, a local time of 1400 hours, and low geomagnetic activity. The numbers signify relative density values scaled to the maximum value of 1.0 occurring at 90°N on day 240.

a three-axis stabilized low-altitude satellite in a near polar orbit. The instrument accurately measured accelerations in the satellite's in-track, cross-track and radial directions at altitudes ranging from 165 to 270 km. The in-track data provide direct determination of atmospheric density. These data, obtained during a period of high solar flux, supplement the extensive set of measurements obtained by previous accelerometer experiments during low solar-flux conditions. They will permit extension of present empirical models to include a more accurate representation of solar cycle variability of the neutral atmosphere. The cross-track data permit, for the first time, large scale measurements of the zonal component of horizontal neutral winds. Results obtained during a large geomagnetic storm are being studied. The data show eastward winds with speeds of the order of 100 m/sec at low and middle latitudes. At latitudes greater than about 65°N there is a sharp reversal in direction to westward and speeds as high as 800 m/sec are encountered. These observations reveal the influence on the neutral atmosphere of ionospheric motions driven by large-scale electric fields. The radial axis accelerations, which have been measured for the first time with a satellite, provide information on vertical atmospheric motions. These measurements are presently being analyzed. Atmospheric dynamic processes are extremely complex and variable. The combination of simultaneous accelerometer measurements of density and horizontal and vertical winds provides a unique opportunity to make fundamental progress toward development of more accurate global density models.

UPPER ATMOSPHERE DENSITY MEASUREMENTS

Neutral density measurements obtained on board the Air Force S3 satellites have been reduced, processed and merged into an extensive geophysical data base. Methods and data handling techniques developed during the reduction and processing phases were previously reported and will be used again for handling the experimental data obtained from on board the S3-4 satellite. These S3-4 measurements will be decommutated and digitized later this year and provided to AFGL, where computer processing into density results will begin. Presently the ionization gauge data base is comprised of over two hundred thousand values. A statistical and correlative analysis of the data base produced results indicative of atmospheric tidal effects displaying hemispherical asymmetry. These effects were more pronounced at higher altitudes (>200 km) than at lower (near perigee) altitudes. Initial results from this analysis have been reported, and additional study is planned to delineate the extent of these effects. Data are also being examined to extract semiannual density variations which are known to exist, although the causative mechanisms are not at all certain. The results from this study will also be reported if significant variations are derived.

A LIDAR (*L*ight *D*etection *a*nd *R*ang-

ing) engineering design for a ground-based system, utilizing a two-color neodymium-YAG laser at wavelengths 355 nm and 532 nm, was completed. This ground-based LIDAR system will be capable of determining upper atmosphere densities at altitudes from about 20 km to 100 km. Eventual applications of the system will include deployment as a mobile, portable station to be used in measuring atmospheric density variations in support of Air Force systems development. Further applications will include measurements of the seasonal and other systematic variations of atmospheric density and the aerosol content of the atmosphere as a function of altitude. Implementation of the LIDAR design has begun with initiation of the acquisition of long lead-time components, such as a suitable Dall-Kirkham receiving telescope and Nd-YAG laser.

The LIDAR system will be pulse-operated, transmitting simultaneously at both color wavelengths, 532 nm (green) and 355 nm (near uv). LIDAR backscattered signals will be acquired by the receiving telescope, with photon counting being accomplished with high sensitivity photomultiplier tubes. The dual wavelength transmission is required in order to discriminate between backscattered molecular (Rayleigh scatter) density signals and backscattered aerosol returns (Mie scatter).

THEORETICAL DENSITY STUDIES

The expected global distributions of exospheric temperature were studied for the period from December 1847 to September 1980, using sunspot numbers to specify solar activity and the U.S. Standard Atmosphere supplements (1966) to model variations in the spatial, solar flux and geomagnetic activity. This period corresponds to 12 solar cycles and was chosen so that accurate statistics could be obtained for long-term mean and median exospheric temperatures and the distributions about these values. The long-term average global distribution of exospheric temperature, including the effects of geomagnetic activity, is shown here. The contribution from geomagnetic activity was based on

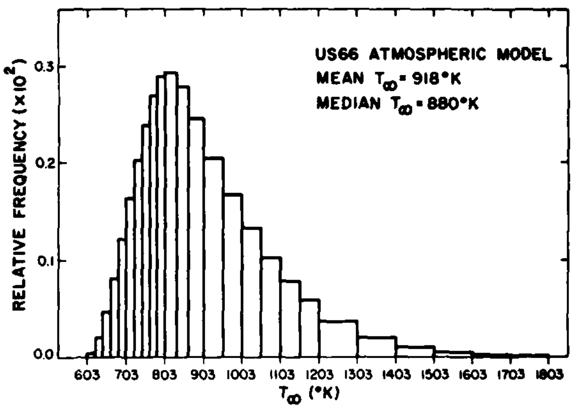

Global Distribution of Exospheric Temperature Including Geomagnetic Variation, US66 Model.

the distribution of geomagnetic activity for solar cycle 20. The long-term mean exospheric temperature was found to be about 10 percent lower than that for the past two solar cycles and about 40 percent lower than that for cycle 19.

The properties of the mesosphere and lower thermosphere were reviewed. The variability and systematic variations of the properties of the upper mesosphere and lower thermosphere are probably the least well-known aspects of the terrestrial atmosphere. Satellite measurements of these regions are very limited, and rocket and remote-sounding techniques do not provide comprehensive coverage. The review covered recent theoretical work and data on diurnal, semidiurnal and terdiurnal tides in total density and composition in the lower thermosphere. The predominant tide changes from semidiurnal below approximately 180 km to diurnal above this altitude; the semidiurnal tide has an important latitude dependence.

A significant amount of data from the

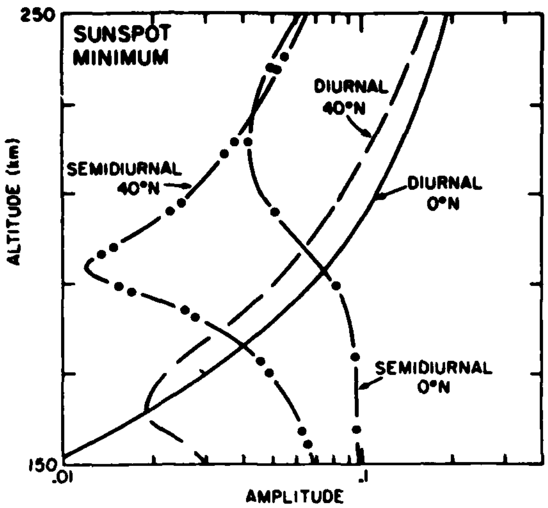

Theoretical Calculations for Amplitude of Diurnal and Semidiurnal Components of Total Mass Density at 0°N and 40°N under Equinox Conditions at Sunspot Minimum, using the Forbes 1978 Model with Tidal Winds and Temperatures from Garrett and Forbes, 1978, as Input.

mesosphere and lower thermosphere suggests that the occurrence and magnitude of turbulence, oxygen green-line intensity, median meridional and zonal winds, and temperatures are dependent on the solar cycle. The decrease in the temperature gradient of the lower thermosphere, observed at high latitudes during high solar activity, might be due to an increase in nitric oxide concentration produced by chemical reactions resulting from high fluxes of precipitating particles and subsequent cooling due to increased infrared radiation at 5.3 microns.

Progress has been made in the theoretical modeling of tidal variations in thermospheric composition and total mass density. The mathematical formulation and selection of model parameters for an atmospheric tidal model have been completed. Diurnal oscillations in wind, temperature, density and pressure fields from the surface to 400 km have been calculated. Thermospheric extensions of the westerly wind velocity, northerly velocity and vertical velocity have also been computed. For exospheric temperatures of 600, 800, 1000, 1200 and 1400 K, temperature fields associated with the (2,2), (2,3), (2,4), and (2,5) tidal modes have been calculated.

Work has continued on satellite orbital studies, which have been primarily aimed at deriving atmospheric densities from orbital decay, and developing and evaluating density models for use in predicting satellite ephemerides. The performance of the MSIS 1977 and 1979 (UT/Longitude) models was evaluated in orbit determination and ephemeris prediction for several low-altitude satellites. The difference in accuracy between these two models for these conditions was not statistically significant. A number of orbit determination/ephemeris prediction runs were made using observations for a low-altitude satellite to compare the accuracy of the 1971 and 1977 Jacchia models and the 1977 MSIS model. During high geomagnetic activity, the 24-hour prediction error for the 1977 Jacchia model was considerably larger than for the other two models. This indicates that the 1977 Jacchia model responds too strongly to geomagnetic activity. Research is underway to develop a modification to the 1977 Jacchia model to improve its response to geomagnetic activity.

An analytic representation of the 1977 Jacchia model atmosphere has been developed. This model, designated the Jacchia-Bass model, uses modified Jacchia-Walker temperature profiles to represent accurately the 1977 Jacchia temperature profiles above 125 km. The diffusive equilibrium equations are analytically integrable for these profiles, greatly reducing the need for tabular storage of solutions. The accuracy of the Jacchia-Bass model compares favorably with that of the 1977 Jacchia Model, and computer storage requirements are significantly reduced although the computer processing time is nearly the same for both models.

Another method for reducing the storage requirements for the 1977 Jacchia model was developed. The principle of this method is to simplify the tables for solutions of the diffusion equation. Instead of having tables for all the constituents, only a table of one major constituent is required, plus the temperature profile, number density ratios at the turbopause, and the scale heights for each species. A separate table is needed for hydrogen because it is not in diffusive equilibrium. This procedure has reduced computer storage requirements again, and gives accuracy comparable to the full Jacchia 1977 model.

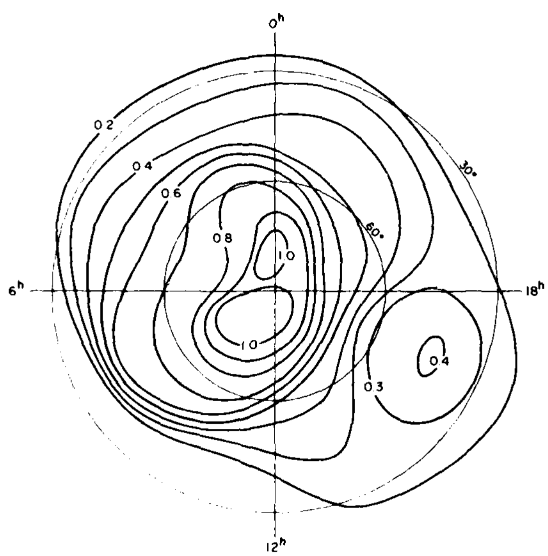

Isotherms of the Mean Normalized Temperature Increase Derived from N_2 Densities for K_p' in the Range 3-4.

Analysis of satellite mass spectrometer data from ESRO4 is being used in the development of a detailed global model of geomagnetic variation, including dependence on local time. The data for an altitude of 280 km were used to compute the global distributions of argon, helium, atomic oxygen, and molecular nitrogen under disturbed geomagnetic conditions. This study forms the basis for the previously mentioned improvement in the representation of geomagnetic disturbance in the 1977 Jacchia model. Isotherms of the mean normalized temperature increase are derived from molecular nitrogen densities for K_p' in the range 3-4, where K_p' is the time-lagged value for the geomagnetic index, K_p. The plot uses magnetic latitude and local time as coordinates and covers the region poleward of about 30° latitude. Two maxima are located near the pole. The larger of these is centered at about 9^h LMT at a latitude of about 80°, while the other near 0^h LMT occurs at a latitude of about 75°. These maxima seem to be related to heating resulting from particle precipitation. There is also evidence of Joule heating due to the auroral electrojets in the morning and evening auroral belts. Enhancement of the temperature response in middle latitudes can be observed throughout the night side and in a region centered in the late afternoon.

CHEMICAL TRANSPORT MODELS, TURBULENCE AND FORCING FUNCTIONS

The combined use of mass-spectrometer and chemical-trail observations of the turbopause (by determining, respectively, the altitude that marks the neutral species transition from mixed to diffusive equilibrium and the cessation of turbulent fluctuations in the chemical trail) shows that mid- and high-northern latitudes have similar turbopause altitudes in winter and a significant diurnal variation. The joint spring-summer results, with some latitude divergence, also demonstrate a diurnal variability. Further, they unambiguously show that the turbopause is significantly lower in the summer than in the winter. A comprehensive body of data at mid-latitude (30°N) measured around a fixed hour clearly shows a Gaussian-like distribution of the turbopause altitude,

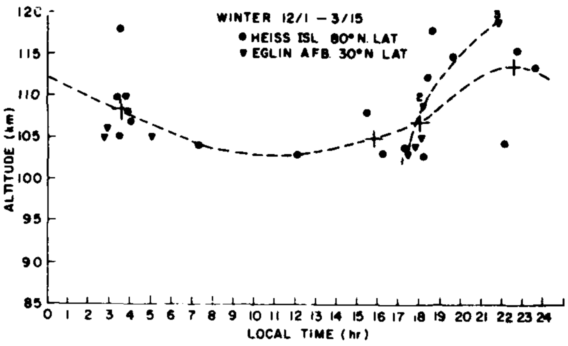

Winter Diurnal Variation of the Turbopause as Determined from Chemical Trail Release Analysis and Mass Spectrometer Analysis of Diffusive Separation. The dashed line connecting the crosses is the average of all the data. The dashed line connecting the numerals 1, 2, and 3 represents three time-sequential experiments that graphically show the nighttime rise of the turbopause.

from which is inferred the most probable turbopause altitude for this season, latitude, and hour.

To examine the role of metallic ions in the ionosphere we have incorporated sodium into the one-dimensional ion neutral model of the mesosphere and thermosphere (up to 400 km). We have also utilized the experimental results of the midlatitude turbopause diurnal variability in these calculations. We assume meteoric ablative mechanisms as the source of neutral free sodium, proceeding then via chemical reactions to the end product, sodium bicarbonate. The sodium bicarbonate then effectively transfers net sodium through the lower boundary into the stratosphere by turbulent transport. In these calculations neutral sodium [Na] is in ablative-chemical equilibrium, but the sodium ion [Na^+], having a fairly long chemical life, may be affected to a significant degree by transport. These results are seen in the noon and midnight profiles of neutral sodium and the sodium ion. [Na] is confined around the meteoric source region of 90 km, but does exhibit diurnal variability. [Na^+], on the other hand, is significantly modulated by turbulent transport. The midnight [Na^+] concentration is larger than the noon profile in the lower thermosphere at the same time that the [Na] concentration is significantly lower than the noon value below 100 km. The shape of the [Na^+] profile is indicative of a dynamically controlled species affected by the diurnal variability of the turbopause altitude and molecular diffusion. This then leaves more [Na^+] in the lower thermosphere, where the chemical

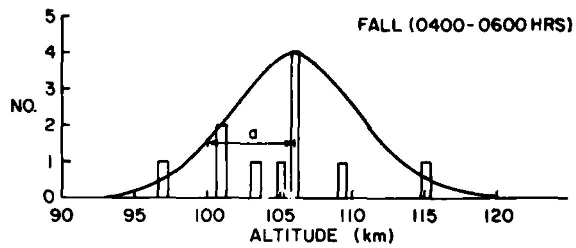

Histogram Showing the Number of Occurrences of the Turbopause at Each Kilometer for the Time Period 0400 to 0600 hr. The solid line is a Gaussian distribution, with a 6 km half-width drawn through the data points, and it roughly describes the observations.

reactions are less effective, and thus we have free [Na^+] ions migrating up into the thermosphere. As demonstrated by these preliminary results, this pumping mechanism may be the process whereby metallic ions, that have no local thermospheric source, are observed at high elevations in the thermosphere.

The study of turbulence in the mesosphere was conducted by using the Richardson number (R_i) as the criterion of turbulent motions and parameters. Richardson number normalized non-dimensional velocities $\frac{u'}{U}$ R_i (where u′ is the turbulent velocity and U the mean wind velocity) are shown to be altitude-invariant as functions of R_i in two extensive lower atmospheric experiments. Similarly, the non-dimensional source function $\frac{\overline{u'w'}}{U}R_i$ (where u′w′ is the correla-

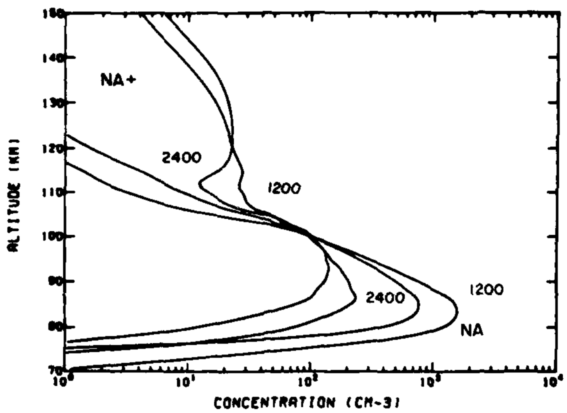

Preliminary Results of the Model Calculation Showing the Noon and Midnight Profiles of Neutral and Ionic Sodium ([Na] and [Na$^+$]). These results demonstrate the thermospheric penetration by [Na$^+$], due mainly to turbopause variability.

tion of the horizontal and vertical turbulent velocities) is also shown to be invariant and dependent only upon the Richardson number. Once these standardized Richardson number relations ratios are determined, they are then utilized in finding the turbulent parameters of the upper stratosphere and mesosphere.

The data base considered for this analysis was the rocket grenade data that supplies winds and temperatures from 30 to 90 km. These data are utilized in determining the Richardson number. Then, by application of the previously determined ratios as functions of R_i, we deduce the turbulent motions of this region of the atmosphere, such as the scalar temperature diffusivity, the resultant rate of local heating due both to dissipation and positive and negative heat transfer, and the momentum transfer to and from the mean motions by Reynolds stress. These analyses are compared to the results of the analysis of the Groves dynamic model atmosphere by Ebel (1974), where he determined the necessary amplitude of heat and momentum sources locally required to maintain the observed temperature and wind distributions. The Ebel results and those of this turbulence analysis are quite similar in phase and amplitude to both the heat and momentum production and loss mechanisms, as shown here for momentum. This is particularly so where these results predict a reversal of phase of both heating and momentum transfer at the altitude of ~ 70 km.

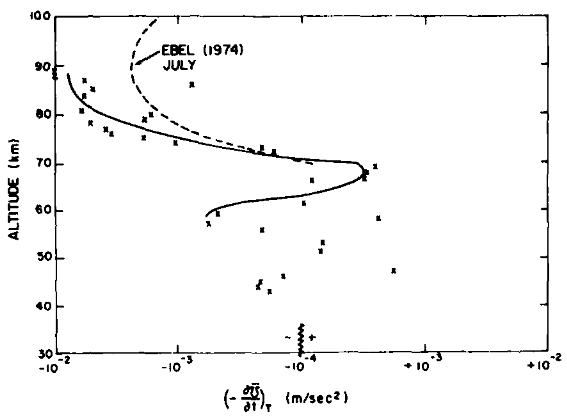

Annual Average of the Turbulent Acceleration and Deceleration of the Mean Mass Motion from 40 to 90 km. Also shown are the required source values from Ebel (1974). The crosses denote the analysis utilizing rocket grenade data.

ATMOSPHERIC ION CHEMISTRY

Experimental research on the chemistry of atmospheric positive and negative ions has included studies on reactions between several normal and pollutant atmospheric neutral species with such ions as N^+, O^+, N_2^+, H^-, CN^-, $OH^- \cdot nH_2O$, and NO_3^-. The objective of this research is to provide data on reaction cross sections, rate coefficients, bond dissociation energies, and electron affinities, and information on reaction mechanisms. Such data are required as inputs for the computer models used to predict the effects of natural and nuclear perturbations upon atmospheric composition and density.

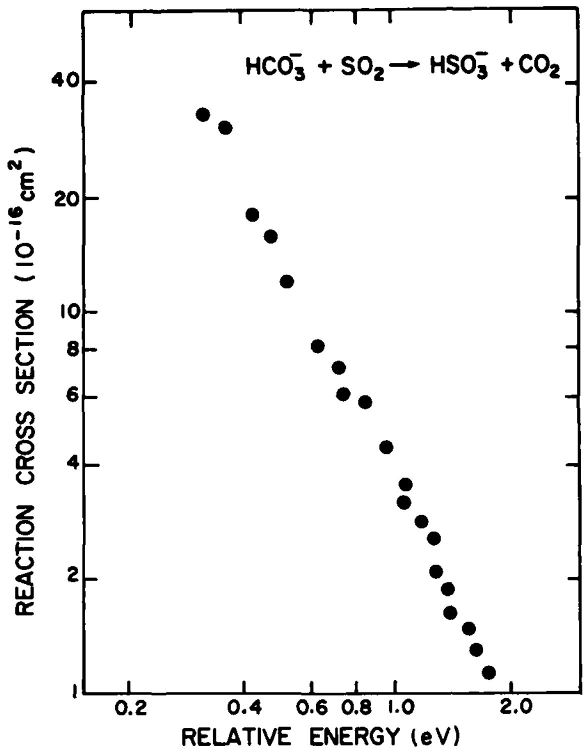

Cross Sections for the Reaction Converting the Bicarbonate Ion to the Bisulfite Ion in the Gas Phase as a Function of Energy.

The studies on ion-neutral reactions are performed both at suprathermal energies, for example 0.3 eV to 100 eV, and at thermal energies, about 0.03 eV. In the former case, a mass-analyzed beam of reactant ions reacts with neutral molecules in a thin collision chamber. Ions issuing from this chamber are mass-analyzed and counted. Velocity and/or energy analysis of these ions is also possible. The parameters measured are reaction cross sections as a function of interaction energy. A reaction cross section may be converted to a reaction rate coefficient, a quantity more generally useful in modeling atmospheric phenomena, if the energy dependence of the cross section and the energy distribution function are known. For example, in the figure the species HCO_3^-, the bicarbonate ion, familiar in solution chemistry but also present in the atmosphere, reacts in the gas phase with sulfur dioxide, producing the bisulfite ion, HSO_3^-, and carbon dioxide. At low interaction energies, this reaction is fast and thus provides a possible sink for pollutant sulfur dioxide in ionized regions of the atmosphere.

Studies of ion-neutral reactions at thermal energies are carried out using a recently constructed Selected Ion Flow Tube (SIFT) apparatus. Here mass-analyzed ions are injected into a fast flowing stream of helium. As the result of multiple collisions, the initially energetic ions quickly reach the temperature of the chemically inert helium carrier gas. A reactant neutral gas is then injected into the flowing gas further downstream. The ion composition of the gas stream is monitored with a mass spectrometer. Reaction rate coefficients are determined from the relative abundances of product ions and from the decay of the reactant-ion number density as the flow rate of the reactant neutral gas is varied.

Solvated ions are among the dominant charged species in the stratosphere and mesosphere. Rate coefficients have recently been measured for several reactions of these ion species with atmospheric neutral molecules. Typical ions are $OH^- \cdot nH_2O$ (n = 0 to 3) and $H_3O^+ \cdot H_2O$. The reactions studied include solvent switching, charge exchange, and collisional dissociation. Combining the results of the SIFT experiments with those from the ion beam apparatus has provided rate coefficients for several such reactions over the energy range from 0.03 to 100 eV.

The species NO^+ is a dominant ion in the ionosphere, where it is produced both by electron exchange reactions, e.g., $O_2^+ + NO \rightarrow NO^+ + O_2$, and by ion or atom exchange reactions, e.g., $O^+ + N_2 \rightarrow NO^+ + N$ and $N^+ + O_2 \rightarrow NO^+ + O$. The last of these reactions is highly exoergic (6.7 eV) and could result in products having high kinetic energy and/or high internal energy. If the energy is internal,

its distribution between the products and its presence as rotational, vibrational, or electronic excitation are of interest. In addition collisions between N^+ and O_2 produce not only $NO^+ + O$ but also $O_2^+ + N$ and $O^+ + NO$. Recent studies using our ion beam apparatus have shown that the excess energy (6.7 eV) in the reaction producing $NO^+ + O$ is contained entirely as internal energy in the NO^+ product. There is evidence from experiments carried out elsewhere that this NO^+ is not electronically excited. It is certain, then, that the NO^+ is vibrationally and rotationally excited and is thus a likely source of infrared radiation in the atmosphere.

Reaction rate coefficients and cross sections were also measured in these experiments as a function of interaction energy from 0.03 to 40 eV. At all energies, the reaction producing $O_2^+ + N$ is the most probable, although at low energies the production of $NO^+ + O$ is almost as rapid. The reaction producing $O^+ + NO$ is slow at all energies. With increasing interaction energy the internal energy of the NO^+ product increases and eventually becomes high enough for the ion to dissociate. Measurement of the interaction energy at which the dissociation occurs and of the ion product of the dissociation, i.e., whether O^+ or N^+, has provided information on the mechanism of this reaction and on the electronic state of the NO^+ ion.

ENERGY BUDGET CAMPAIGN

The Energy Budget of the Mesosphere and Thermosphere was a major campaign organized by West German scientists to study heating input and dissipation in the high latitude upper atmosphere. Scientists from ten countries participated in the campaign. The goal was to measure the energy input to the mesosphere and lower thermosphere, 60 to 180 km, during three levels of geomagnetic activity and to measure the effects produced by this input as it was dissipated in the atmosphere. The program represented the most comprehensive effort to date to study these effects. A total of 50 rocket payloads, 18 major multiply-instrumented rockets and 32 small meteorological rockets, carried a total of 99 scientific instruments. The program was considered to be highly successful, with 87 of the instruments providing useful scientific data.

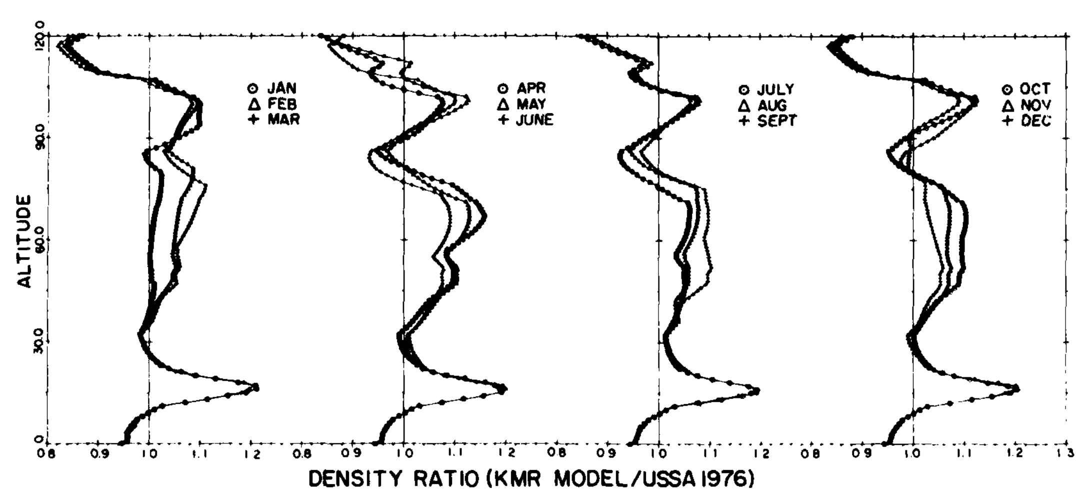

Kwajalein Reference Atmospheres, 1979, Density Models Shown as a Ratio to US Standard Atmosphere, 1976, for Each of the Months, from the Surface to 120 km.

The program was carried out in three parts, called "salvos." During Salvo C, measurements of the background, or "quiet" atmospheric conditions, were obtained on November 11, 1980. On November 16, in Salvo B, measurements were obtained during a moderate geomagnetic storm. The majority of the payloads were launched in Salvo A into major geomagnetic storms on November 28 and December 1. The rocket payloads were launched on a coordinated schedule from both Kiruna, Sweden, and Andoya, Norway. During the campaign approximately 80 ground stations with magnetometers, radars, cameras or photometers recorded data and four satellites measured various properties.

AFGL participation included two payloads to measure the neutral atmosphere density, temperature, wind, wave structure, and turbulence and one payload which measured the infrared radiation, electron density, particle energy, atomic oxygen density and optical emission. In addition, AFGL scientists were co-investigators in the 32 meteorological sensor measurements, provided support in executing the program, and performed ground-based measurements of infrared emission spectra. Data analysis and interpretation will be performed during 1981.

KWAJALEIN REFERENCE ATMOSPHERES, 1979

As a result of AFGL involvement in reentry measurement programs at the Kwajalein Missile Range (KMR) and consulting for the Ballistic Missiles Office (BMO, formerly SAMSO), AFGL was asked by the Army BMDSC, who are responsible for the operation of the Missile Range, to take responsibility for preparing new KMR atmospheric models. All the atmospheric measurements which had been made at Kwajalein Atoll and at several other low latitude sites were assembled to form a basis for the development of the models. Several programs in recent years have added significantly to the data base, particularly at the higher altitudes. Several studies were undertaken as part of the development of the models, including investigation of temporal and spatial variability, monthly

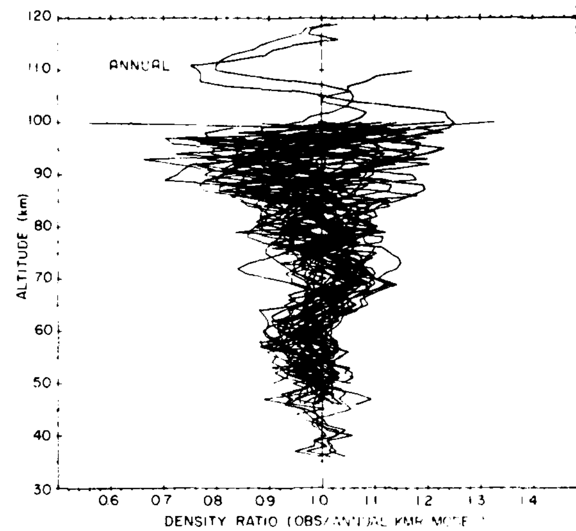

High-altitude Measurements of Atmospheric Density from Kwajalein Atoll Shown as a Ratio to the Mean Annual KMR Model. Part of the variation is that due to the seasonal changes, but a significant amount of wave structure and short time variability also contribute to the observed profiles.

models of index of refraction for radar and optics, and models for interlevel correlation of density, temperature and wind.

The models which were developed include the monthly and mean annual models for all the major properties of the atmosphere from the surface of the earth to 120 km altitude. The report on the models provides a relatively complete handbook on the atmospheric properties for the Kwajalein area. Since the models were prepared, several measurement cases have been compared with the model predictions and the results show excellent agreement. Use of the model allows the upper level calculations of reentry trajectories to be performed for those mis-

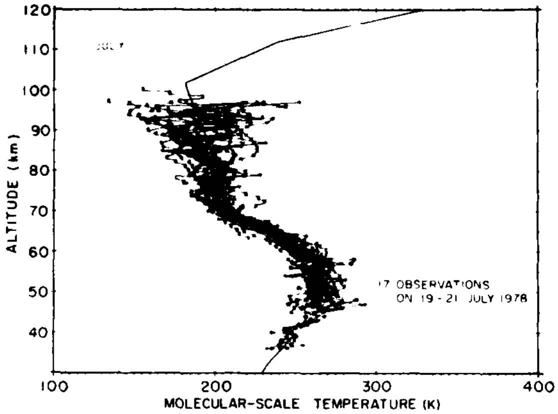

Set of 17 High Altitude Temperature Observations Taken during a Two Day Period in July 1978 Shown with the Kwajalein Reference Atmospheres, 1979, Model for July.

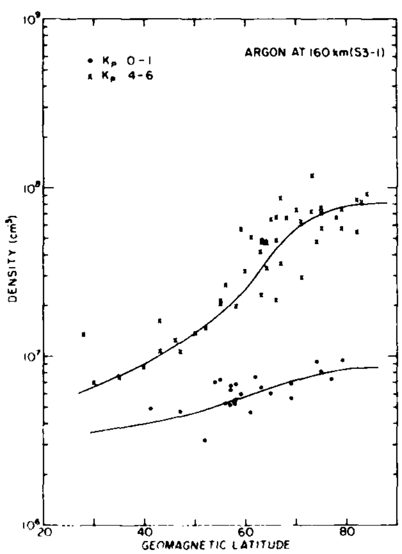

Measurements of Argon at 160 km from the S3-1 Satellite for Low (0 ≤ K_p ≤ 1) and Moderately High (4 ≤ K_p ≤ 6) Geomagnetic Activity. Each point represents the crossing at 160 km for an orbit. The large increase in density corresponding to high-latitude energy input in geomagnetic storm periods is evident.

sions where the detailed structure and accuracy of the individual high-altitude measuring techniques are not required.

SATELLITE STUDIES OF THE NEUTRAL ATMOSPHERE

The mass spectrometer instruments on the S3-1 and S3-2 satellites have provided the bases for several studies of atmospheric and ionospheric properties. One recent study involved analysis of the effects of heating in the atmosphere produced by geomagnetic storms. The latitude dependence of the heating can be easily observed in the argon distribution, which we refer to as the "thermometer of the upper atmosphere." Near 160 km altitude, the argon density may increase by more than a factor of 10 at high latitudes during geomagnetic storms. The response of the argon to the storm effects has also been used to infer the variation of CO_2, which cannot be measured at these altitudes by mass spectrometry. These satellite measurements have also been used for comparison with

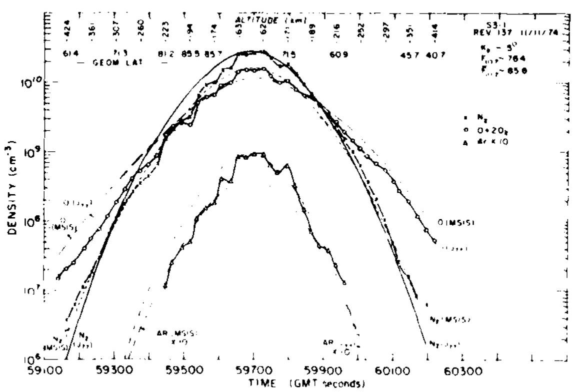

Measurements of One Orbit from the S3-1 Satellite Compared to the MSIS and Jacchia 77 Models. This case corresponds to quiet solar and geophysical conditions. The agreement appears to be reasonable at the lower latitudes, but the differences at high latitude are significant. Computer comparisons of the models and measurements suggest the improvements that should be considered in the next generation of model development.

the Jacchia 77 and MSIS models to find the weaknesses in currently used models and suggest improvements for the future.

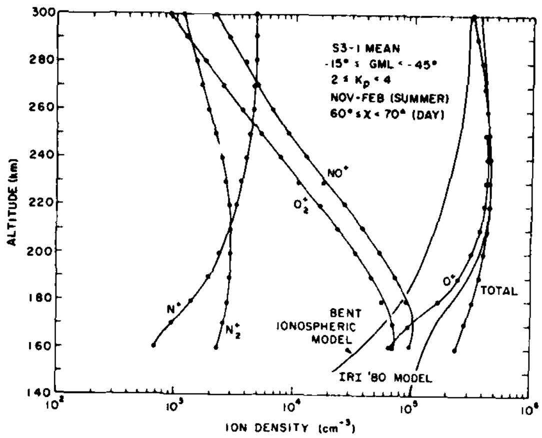

Comparison of Mean Profiles for the S3-1 Satellite Data for the Five Primary Ion Species (O^+, N^+, NO^+, O^+_2 and N^+_2) with the Total Density from IRI and Bent Models. This case shows the F-region profiles for summer daytime mid-latitude conditions in the southern hemisphere.

SATELLITE STUDIES OF THE IONOSPHERE

The measurements of the density of the five primary ions in the F-region have been used as the basis for the development of a model of the F-region and to test other models. These studies have shown that while the CCIR, IRI and other models provide reasonable predictions for the peak density in the F_2-region, much more attention must be given to the slope and density in the F_1-region. The IRI model of ion composition has been found inadequate, and the development based on the current satellite data should make a major improvement. From the studies of the data from S3-1 and the Aeros-B satellites, the high latitude region of the ionosphere was found to be represented best when the invariant latitude was used as the primary modeling parameter. As a result of current progress in the ionospheric modeling area, a useful reference model should be available for general use within the next two years. Changes in the ionosphere are so important that its variability should also be modeled to provide a useful tool.

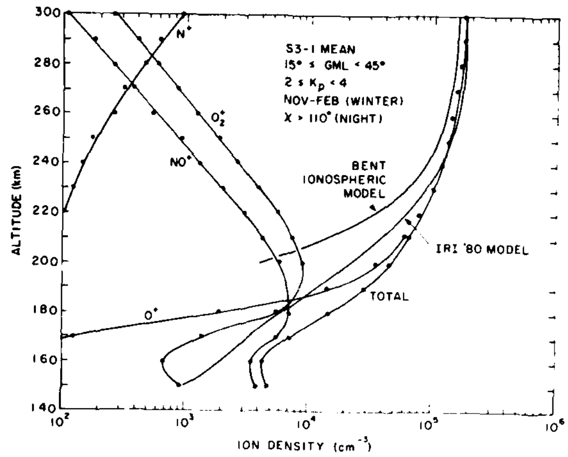

Mean profiles from the S3-1 Satellite Data. Each point is the mean value of several hundred independent measurements. This case shows the F-region profiles for winter night-time mid-latitude conditions in the northern hemisphere.

JOURNAL ARTICLES JANUARY 1979 - DECEMBER 1980

ADAMS, N.G., SMITH, D., and PAULSON, J.F.
An Experimental Survey of the Reactions of NH^+_n Ions (n = 0 to 4) with Several Diatomic and Polyatomic Molecules at 300°K
J. Chem. Phys. 72, No.1 (January 1980)

BLAKE, A.J.
An Atmospheric Absorption Model for the Schumann-Runge Bands of Oxygen
J. Geophys. Res. 84, No. A7 (July 1979)

CALO, J.M., and NARCISI, R.S.
Van Der Waals Molecules - Possible Roles in the Atmosphere
Geophys. Res. Lett. 7, No. 5 (May 1980)

GOOD, R.E., and CLEWELL, H.J.
Drop Formation and Evaporation of JP-4 Fuel Jettisoned from Aircraft
J. Aircraft 17, No.7 (July 1980)

GUBERMAN, S.L.
Potential Curves for Dissociative Recombination of O^+_2
Int. J. Quantum Chem., Symp. 13 (1979)

HEROUX, L.
Absolute Photon Counting in the Ultraviolet in Spectrometric Techniques 2
Academic Pr., N.Y. (1981)

HINTEREGGER, H.E.
Development of Solar Cycle 21 Observed in EUV Spectrum and Atmospheric Absorption
J. Geophys. Res. 84, No. A5 (May 1979)

HUFFMAN, R.E., LEBLANC, F.J., LARRABEE, J.C., and PAULSEN, D.E.
Vacuum Ultraviolet Backgrounds from Space
SPIE 197 (February 1980)
Vacuum Ultraviolet Airglow and Auroral Observations
J. Geophys. Res. 85, No. A5 (May 1980)

KATAYAMA, D.H.
New Vibrational Quantum Number Assignments for the UV Absorption Bands of Ozone Based on the Isotope Effect
J. Chem. Phys. 71 (2) (July 1979)

KATAYAMA, D.H., COOK, J.M., BONDYBEY, V.E., and MILLER, T.A.
Rydberg Series of Atomic He by Opto-Galvanic Spectroscopy
Chem. Phys. Lett. 62, No. 3 (April 1979)

KATAYAMA, D.H., MILLER, T.A., and BONDYBEY, V.E.
Radiative Decay and Radiationless Deactivation in Selectively Excited CN
J. Chem. Phys. 71 (4) (August 1979)
Collisional Deactivation of Selectively Excited N^+_2
J. Chem. Phys. 72 (10) (May 1980)

KENESHEA, T.J., ZIMMERMAN, S.P., and PHILBRICK, C.R.
A Dynamic Model of the Mesosphere and Lower Thermosphere
Planet. Space Sci. 27 (June 1979)

MARCOS, F.A.
Atmospheric Response to Geomagnetic Activity
Proc. Symp. Scientific Results Atmosphere Explorer 2 (April 1979)

MURAD, E.
Thermochemical Properties of Gaseous FeO and FeOH
J. Chem. Phys. 73 (3) (August 1980)
Mass Spectrometric Study of the Thermochemical Properties of Gaseous MgOH
Chem. Phys. Lett. 72, No.2 (June 1980)

MURAD, E., and SWIDER, W.
Chemistry of Meteor Metals in the Stratosphere
Geophys. Res. Lett. 6, No.12 (December 1979)

MURAD, E., and HILDENBRAND, D.L.
Dissociation Energies of GdO, HoO, ErO, TmO, and LuO
J. Chem Phys. 73, No. 8 (October 1980)

PALENIUS, H.P., HUFFMAN, R.E., LARRABEE, J.C., and TANAKA, Y.
The Absorption Spectrum of Flourine F I Observed with the Helium Continuum
J. Opt. Soc. Am. 68, No. 11 (November 1978)

PHILBRICK, C.R., MURPHY, E.A., ZIMMERMAN, S.P., FLETCHER, E.T., and OLSEN, R.O.
Mesospheric Density Variability
COSPAR Space Res. 20, Ed. by M.J. Rycroft, Pergamon Pr., N.Y. (1980)

PRICE, S.D., MURDOCK, T.L., MCINTYRE, A., HUFFMAN, R.E., and PAULSEN, D.E.
On the Diffuse Cosmic Ultraviolet Background Measured from Aries A-8
Astrophys. J. 240 (August 1980)

REES, D., ROUNCE, R.A., BEST, G.T., and QUESADA, A.F.
Midlatitude Measurements of the Thermospheric Neutral Wind During the Aladdin Programme
J. Atmos. Terr. Phys. 41 (1979)

ROSE, T.L., KATAYAMA, D.H., WELSH, J.A., and PAULSON, J.F.
Photodissociation of Vibrationally Excited AR^+_2 Formed by Associative Ionization
J. Chem. Phys. 70, No. 10 (May 1979)

SHERMAN, C.
Emission of Particles from a Charged Sphere into a Magnetic Field
J. Appl. Phys. 51, No. 3 (March 1980)

SWIDER, W.
Ion Production in the D-Region
Solar Terr. Proc. 2, Working Group Reports and Reviews (May 1980)

SWIDER, W.
Nitric Oxide in the Upper Stratosphere and Mesosphere
Proc. NATO Advanced Study Institute on Ozone
FAA-EE-80-20 (May 1980)

SWIDER, W., MURAD, E., and HERMANN, U.
Sulphur Chemistry in the E-Region
Geophys. Res. Lett. 6 (November 1979)

SZUSZCZEWICZ, E.P., TSUNODA, R.T., NARCISI, R., and HOLMES, J.C.
Coincident Radar and Rocket Observations of Equatorial Spread-F
Geophys. Res. Lett. 7, No. 7 (July 1980)

THOMAS, T.F., ROSE., T.L., and PAULSON, J.F.
On the Photochemical Stability of $H_3O^+ (H_2O)_n$
J. Chem. Phys. 71, No. 1 (July 1979)

TORR, M.R., TORR, D.G., ONG, R.A., and HINTEREGGER, H.E.
Ionization Frequencies for Major Thermospheric Constituents as a Function of Solar Cycle 21
Geophys. Res. Lett. 6, No. 10 (October 1979)

TORR, M.R., TORR, D.G., and HINTEREGGER, H.E.
Solar Flux Variability in the Schumann-Runge Continuum as a Function of Solar Cycle 21
J. Geophys. Res. 85, No. A11 (November 1980)

PAPERS PRESENTED AT MEETINGS JANUARY 1979 - DECEMBER 1980

CHAMPION, K.S.W.
Properties of the Mesosphere and Lower Thermosphere
COSPAR, Budapest, Hungary (2-14 June 1980)

DEARBORN, F.K.
In-Situ Chemical Analysis of Individual Aerosol Particles
Atmospheric Transmission and Particle Size Measurements Wkshp., Dayton, OH (23-25 October 1979)

DEWAN, E.M.
Waves and Turbulence in the Stratosphere
St. Univ. of New York, Albany, N.Y. (26 October 1979)
Turbulent Eddy Diffusion in the Stratosphere
Am. Geophys. Un. Mtg., Spring, Washington, D.C. (May 1979)
Stochastic Simulation of the Diffusion Equation by Turbulent Layers in Stratified Fluids, Vertical Bulk Eddy Diffusion in the Stratosphere and in Other Stratified Fluids
Am. Geophys. Un. Mtg., Toronto, Canada (22-27 May 1980)

FAIRE, A.C., and MICHAEL, I.
Falling Sphere Density Results During Total Solar Eclipse, Red Lake, 1979
Am. Geophys. Un. Mtg., Toronto, Canada (22-27 May 1980)

HANSON, W. (Univ. of Texas, Dallas, TX), MARCOS, F.A., and CHAMPION, K.S.W.
MESA Wind Data
AE Mtg., NASA Goddard Space Flight Ctr., Greenbelt, MD (1-3 October 1980)

HENCHMAN, M.J. (USAF - SCREE Summer Faculty), PAULSON, J.F., ADAMS, N., and SMITH, D. (Univ. of Birmingham, Birmingham, England)
The Reactivity of Water Cluster Ions with D_2O and NH_3
AFOSR/FJSRL Conf. on Molecular Dynamics, USAF Academy, Colorado Springs, CO (3-5 Oct 1979)
Proton-Transfer Reactions Involving $H_3O^+ n(H_2O)$ and $OH^- n(H_2O)$ in the Gas Phase: Reactivity as a Function of Solvation Number and the Relevance for Wet Chemistry
Int. Symp. on Phys. Organic Chemistry, Chemical Inst. of Canada, Toronto, Canada (6-9 August 1979)

HENCHMAN, M.J., and PAULSON, J.F.
Beam Studies of the Reaction of H_3O^+ and OH^- with H_2O at Energies of 0.3 – 1.0 ev
28th Ann. Conf. on Mass Spectrometry and Allied Topics, New York, NY (25-30 May 1980)

HERMANN, U. (Univ. of Bern, Bern, Switzerland), and PHILBRICK, C.R.
The Influence of Mesospheric Temperature Variation on the Positive Ion Composition During the 1979 Solar Eclipse
Am. Geophys. Un. Mtg., Toronto, Canada (22-27 May 1980)

HINTEREGGER, H.E.
Representations of Solar EUV Fluxes for Aeronomical Applications
XXIII COSPAR, Budapest, Hungary (2-14 June 1980)
AE-E Experiences of Irradiance Monitoring for 1200-1850A
Wksp. on Solar UV Irradiance Monitors, Boulder, CO (31 July - 1 August 1980)
Variation of Solar EUV Input from Past Solar Minimum to Spring of 1979

HINTEREGGER, H.E.
Bulgarian-United States Seminar, Stara Zagora, Bulgaria (3-8 September 1979)
Response of the Thermosphere to Solar Cycle Variations in the EUV and 10.7 CM Fluxes
I.A.G.A. Special Scientific Session, Canberra, Australia (1-16 December 1979)
The Solar Ultraviolet Source for the Ionosphere and its Variations
27th Panel Mtg. Electromagnetic Wave Propagation Panel AGARD, Naples, Italy (27-31 October 1980)

HUFFMAN, R.E.
Night Airglow, 1250 - 3000 A
10th Texas Symp. on Relativistic Astrophys., Baltimore, MD (15-19 December 1980)

HUFFMAN, R.E., LEBLANC, F.J., LARRABEE, J.C., and PAULSEN, D.E.
Satellite Vacuum Ultraviolet Airglow Backgrounds
Am. Geophys. Un. Mtg., San Francisco, CA (3-7 December 1979)
Nitrogen Vacuum Ultraviolet Airglow: Global Spectral Variability
Am. Geophys. Un. Mtg., San Francisco, CA (December 1980)
Atmospheric Vacuum Ultraviolet Radiance by Satellite Observations and by Digicon Spatial Sensors
VI Int. Conf. on Vacuum Ultraviolet Radiation Physics, Univ. of Virginia, Charlottesville, VA (2-6 June 1980)

HUFFMAN, R.E., LEBLANC, F.J., LARRABEE, J.C., and PAULSEN, D.E.
Satellite Measurement of Vacuum Ultraviolet Radiation from the Earth's Atmosphere
Int. Radiation Symp., Colorado St. Univ., CO (11-16 August 1980)
Vacuum Ultraviolet Backgrounds from Space
Soc. Photo-Opt. Instrumentation Engineers (SPIE), 23rd Ann. Int. Tech. Symp., San Diego, CA (27-30 August 1979)
Ultraviolet Calibration of Digicon Detectors and Satellite Sensors
5th Wkshp. on VUV Radiometric Calibration of Space Experiments, Nat'l. Ctr. Atmospheric Res., Boulder, CO (22-23 March 1979)

KATAYAMA, D.H., MILLER, T.A., and BONDYBEY, V.E. (of Bell Labs., Murray Hill, N.J.)
Laser Induced Fluorescence from the A$^2\pi u$ State of N^+_2
35th Symp. on Molecular Spectroscopy, Ohio St. Univ., Columbus, OH (16-20 June 1980)
Radiative Decay and Radiationless Deactivation in Selectively Excited CN
34th Symp. Molecular Spectroscopy, Ohio St. Univ., Columbus, OH (11-15 June 1979)
Radiative Quenching of a Selectively Excited Vibronic Level in the A$^2\pi u$ State of N^+_2
AFOSR FJSRL Molecular Dynamics Conf., USAF Academy, Colorado Springs, CO (3-5 October 1979)

KENESHEA, T.J., MURAD, E., SWIDER, W., and ZIMMERMAN, S.P.
Diurnal Model of Mesospheric Sodium
Am. Geophys. Un. Mtg., San Francisco, CA (December 1979)

KITTRELL, C. (MIT, Cambridge, MA), KATAYAMA, D.H., McDONALD, S.A., and FIELD, R.W. (of MIT)
Stimulated Emission Pumping of $I_2BO^+{}_u$ - $X^1\Sigma^+{}_g$ with Pulsed Dye Lasers
35th Symp. Molecular Spectroscopy, Ohio St. Univ., Columbus, OH (16-20 June 1980)

LARRABEE, J.C., and HUFFMAN, R.E.
Measurements of Threat Warning Sensors and Photomultiplier Tubes
9th Tri-Service Ultraviolet Tech. Mtg., Naval Ocean Syst. Ctr., San Diego, CA (15 January 1979)

LEBLANC, F.J., HUFFMAN, R.E., LARRABEE, J.C., PAULSEN, D.E., and WHALEN, J.A.
Auroral Structure from Satellite Vacuum Ultraviolet Data
Am. Geophys. Un. Mtg., Fall, San Francisco, CA (December 1980)

MARCOS, F.A.
Empirical Model of Neutral Atmospheric Density Based on Satellite Accelerometer Data
Am. Geophys. Un. Mtg., Spring, Toronto, Canada (22-27 May 1980)

MARCOS, F.A., and CHAMPION, K.S.W.
Empirical Model of Lower Thermosphere Density for Low Solar Flux and Geomagnetic Activity
22nd COSPAR Mtg., Bangalore, India (June 1979)
Empirical Model of Lower Thermosphere for Low Solar Flux and Quiet Geomagnetic Conditions
AE Mtg., NASA Goddard Space Flight Ctr., Greenbelt, MD (10-12 October 1979)

MICHELS, H.H. (United Technologies Res. Ctr., East Hartford, CT), and PAULSON, J.F.
Potential Energy Surface and Cross Sections for th $H(D^+) + H_2(D_2,HD)$ Ion-Molecule Reactions
2nd Chemical Congress of North Am. Continent, San Francisco, CA (24-30 August 1980)

MURAD, E.
Thermochemistry of Hydroxides of Some Meteor Metals
AFOSR Molecular Dynamics Conf., Hanscom AFB, MA (8-10 October 1980)
Thermochemical Studies of Meteor Metal Hydroxides
AFOSR Molecular Dynamics Contractor's Mtg., USAF Academy, Colorado Springs, CO (3-5 October 1979)

MURAD, E., and SWIDER, W.
Can Metallic Species Play a Role in the Atmospheric Chemistry of Cl and ClO?
Am. Geophys. Un. Mtg., San Francisco, CA (3-7 December 1979)

NARCISI, R.S.
Structure and Composition Measurements in Equatorial Ionospheric Bubbles; Positive and Negative Ion Composition Measurements in the D and E Regions During the 26 February 1979 Solar Eclipse
Am. Geophys. Un. Mtg., Spring, Toronto, Canada (22-27 May 1980)

PAULSEN, D.E., HUFFMAN, R.E., LARRABEE, J.C., and LEBLANC, F.J.
Vacuum Ultraviolet Auroral Observations by Satellite
Am. Geophys. Un. Mtg., San Francisco, CA (3-7 December 1979)
VUV/UV Rocket Exhaust Plume Data from the Multispectral Measurements Program TEM-2 Rocket Flight
7th Strategic Space Symp., Naval Postgraduate Schl., Monterey, CA (11-13 November 1980)

PAULSON, J.F., and MORGENTHALER, L.N.
Reactions of N^+ with O_2
DNA-AFGL Nuclear Weapons Effects Chemistry Conf., Bedford, MA (26 June 1980)
Tandem Mass Spectrometric Studies of the Reactions of N^+ and O_2
28th Conf. Mass Spectrometry and Allied Topics, New York, NY (25-30 May 1980)

PAULSON, J.F., HENCHMAN, M.J. (Brandeis Univ.), and HIERL, P.M.
Reactions of Solvated Ions with Neutral Molecules in the Collision Energy Range 0.3-10 eV
AFOSR Molecular Dynamics Conf., AFGL, Hanscom AFB, MA (8-10 October 1980)
Reactions of Some Solvated Ions
DNA-AFGL Nuclear Weapons Effects Chemistry Conf., Bedford, MA (26 June 1980)

PHILBRICK, C.R.
Low Altitude Satellite Measurements of Argon Densities
COSPAR, Bangalore, India (29 May - 9 June 1979)
Measurements of Mesospheric Species Concentrations
Middle Atmospheric Program, Univ. of Illinois, Urbana, IL (28 July - 1 August 1980)

PHILBRICK, C.R. and FRYKLUND, D.H. (Accumetrics Corp., Cambridge, MA)
Atmospheric Density and Temperature Structure - Eclipse '79 Program
Am. Geophys. Un. Mtg., Toronto, Canada (22-27 May 1980)

PHILBRICK, C.R.; LAMMERZAHL, P., and KRANKOWSKY, D. (both of Max-Planck Inst., Heidelberg, Germany)
Comparison of Mass Spectrometer Measurements from the S3-1 and AEROS-B Satellites
COSPAR, Bangalore, India (29 May - 9 June 1979)

PHILBRICK, C.R., MURPHY, E.A., ZIMMERMAN, S.P., FLETCHER, E.T. (Xonics, Inc., Los Angeles, CA), and OLSEN, R.O. (Army Atmos. Sci. Lab., White Sands Missile Range, NM)
Mesospheric Density Variability in the Presence of Turbulence Layers
COSPAR, Bangalore, India (30 May - 1 June 1979)

SWIDER, W.
Nitric Oxide in the Upper Stratosphere and Mesosphere
NATO Advanced Inst. on Atmospheric Ozone, Aldeia das Acoteias, Portugal (1-13 October 1979)
Electron Concentrations in the C-Region
Am. Geophys. Un. Mtg., Fall, San Francisco, CA (December 1979)
Neutral Concentrations Inferred from the 26 February 1979 Eclipse Ion-Composition Data
Am. Geophys. Un. Mtg., Spring, Toronto, Canada (22-27 May 1980)
The Background (Quiet) D-region
DNA-AFGL Nuclear Weapons Conference (26-27 June 1980) AFGL

ZIMMERMAN, S.P.
The Diurnal Variation of Turbopause Height
Am. Geophys. Un. Mtg., Washington, D.C. (28 May - 1 June 1979)
The Structure of the Equatorial Mesosphere - Mesoscale and Microscale
Wkshp. Equatorial Ionosphere, Cornell Univ., Ithaca, NY (22-23 October 1979)

ZIMMERMAN, S.P., and KENESHEA, T.J.
Turbulent Heating and Transfer in the Mesosphere and Upper Stratosphere
Int. Symp. on Middle Atmosphere Dynamics and Transport, Univ. of Illinois, Urbana, IL (28 July - 1 August 1979)

ZIMMERMAN, S.P., and MURPHY, E.A.
Stratospheric and Tropospheric Vertical Transfer
NATO Advanced Study Inst., Aldeia das Acoteias, Portugal (30 September - 13 October 1979)

TECHNICAL REPORTS JANUARY 1979 - DECEMBER 1980

CHAIKIN, L.M., and FUKUI, K.
Absorption Data Analysis for EUVS Experiment on the Satellites AE-C, D, and E, AFGL-TR-79-0191 (8 August 1979), ADA078663

DEWAN, E.M.
Mixing in Billow Turbulence and Stratospheric Eddy Diffusion
AFGL-TR-79-0091 (10 April 1979), ADA074466
Estimates of Vertical Eddy Diffusion Due to Turbulent Layers in the Atmosphere
AFGL-TR-79-0042 (1 February 1979), ADA069750
Optical Turbulence Forecasting: A Tutorial
AFGL-TR-80-0030 (22 January 1980), ADA086863
A One Dimensional Vertical Diffusion Parameter for Extremely Inhomogeneous, Layered Turbulence in Stratified Fluids
AFGL-TR-80-0186 (16 June 1980), ADA090340

GILSON, B.R., and FUKUI, K.
Solar EUV Flux-Data Analysis for EUVS Experiments on the AE-Satellites
AFGL-TR-79-0052 (23 February 1979), ADA074470

HUFFMAN, R.E., LEBLANC, F.J., LARRABEE, J.C., and PAULSEN, D.E.
Satellite Atmospheric Radiance Measurements in the Vacuum Ultraviolet
AFGL-TR-79-0151 (5 July 1979), ADA078628

HUFFMAN, R.E., PAULSEN, D.E., LARRABEE, J.C., BAISLEY, V.C., LEBLANC, F.J., FRANKEL, D.S., and GERSH, M.E.
Vacuum Ultraviolet Airglow and Stellar Observations on the MSMP TEM-1 Rocket Flight
AFGL-TR-80-0278 (15 September 1980), ADA099386

MARCOS, F.A., and CHAMPION, K.S.W.
Satellite Density Measurements with the Rotatable Calibration Accelerometer (ROCA)
AFGL-TR-79-0005 (4 January 1979), ADA069740

McISSAC, J.P.
Hemispheric Asymmetries Detected from Satellite Ionization Gauge Measurements
AFGL-TR-80-0066 (25 February 1980), ADA090339

NARCISI, R., TRZCINSKI, E., FEDERICO, G., WLODYKA, L., and BENCH, P.
Structure and Composition Measurements in Equatorial Ionospheric Bubbles
AFGL-TR-80-0222 (9 July 1980), ADA092448

RUSSAK, S.L., FLEMMING, J.C., HUFFMAN, R.E., PAULSEN, D.E., and LARRABEE, J.C.
Development of Proximity and Electrostatically Focused Diodes for UV Measurements from Sounding Rockets
AFGL-TR-79-0006 (4 January 1979), ADA068086

SHERMAN, C.
Emission of Particles from a Charged Sphere into a Magnetic Field
AFGL-TR-79-0211 (20 September 1979), ADA081781

TRZCINSKI, E.
Instrumentation Development for LASSII Equatorial Measurements
AFGL-TR-80-0150 (23 April 1980), ADA088880

ZIMMERMAN, S.P.
The Diurnal Variation of Turbopause Height
AFGL-TR-80-0332 (3 November 1980), ADA099340

ZIMMERMAN, S.P., and MURPHY, E.A.
Tropospheric Stratospheric Turbulence and Vertical Diffusivities
AFGL-TR-80-0020 (14 January 1980), ADA084809

CONTRACTOR JOURNAL ARTICLES JANUARY 1979 - DECEMBER 1980

FORBES, J.M., and MARCOS, F.A.
Seasonal-Latitudinal Tidal Structures of O, N_2, and Total Mass Density in the Thermosphere
J. Geophys. Res. 85, No. A7 (July 1980)
Tidal Variations in Total Mass Density as Derived from the AE-E Mesa Experiment
J. Geophys. Res. 84, No. A1 (January 1979)

GROVES, G.V. (Univ. Coll. London, London, England)
Seasonal and Diurnal Variations of Middle Atmosphere Winds
Phil. Trans. R. Soc. Lond., A 296 (1980)

ORVILLE, R.E. (St. Univ. of New York, Albany, NY)
Daylight Spectra of Individual Lightning Flashes in the 370-690 nm Region
J. Appl. Meteorology 19, No. 4 (April 1980)

SZE, N.D., and KO, M.K.W. (Atmospheric and Environmental Res., Inc., Cambridge, MA)
Is CS^2 A Precursor for Atmospheric COS?
Nature 278 (April 1979)
Photochemistry of COS, CS_2, CH_3SCH_3, and H_2S: Implications for the Atmospheric Sulfur Cycle
Atmospheric Environment, 14 (1980)
CS_2 and COS in the Stratospheric Sulphur Budget
Nature 280, 308 No. 5720 (August 1979)

CONTRACTOR TECHNICAL REPORTS JANUARY 1979 - DECEMBER 1980

ACCARDO, C.A., and DULCHINOS, J. (Epsilon Labs, Bedford, MA)
Satellite Density Gauge Program
AFGL-TR-80-0036 (January 1980), AD086809

BASS, J.N. (Logicon, Inc., Lexington, MA)
Analytic Representation of the Jacchia 1977 Model Atmosphere
AFGL-TR-80-0037 (15 January 1980), ADA085782

BIEN, F. (Aerodyne Res., Inc., Bedford, MA)
Nitric Oxide Ion and Uranium Oxide Ion Studies
AFGL-TR-79-0164 (June 1979), ADA077870

BREHM, W.F., and BUCKLEY, J.L. (General Electric Space Division, Philadelphia, PA)
Design Study of a Laser Radar System for Spaceflight Application
AFGL-TR-79-0264 (December 1979), ADA082332

DALGARNO, A. (Harvard Coll. Obs., Cambridge, MA)
AE Reaction Rate Data
AFGL-TR-79-0067 (27 March 1979), ADA067941

DUNBAR, R.C. (Case Western Reserve Univ., Cleveland, OH)
Positive Ion Photodissociation
AFGL-TR-80-0270 (8 September 1980), ADA096703

EBACHER, R.W. (Wentworth Inst. Tech., Boston, MA)
Instrumentation for Accelerometer Density Measurements
AFGL-TR-80-0026 (December 1979), ADA092905

FIELD, R.W. (Mass. Inst. Tech., Cambridge, MA)
Lowest Energy Electronic States of Rare Earth Monoxides
AFGL-TR-80-0328 (1 September 1980), ADA104039

FIORETTI, R.W., BARRY, E., and CIESZKA, S. (RDP, Inc., Waltham, MA)
Data Processing Systems for Accelerometer Experiments on Air Force Satellites
AFGL-TR-79-0237 (May 1979), ADA080460

FIORETTI, R.W., MAZZELLA, A.J., and LEONG, R.J. (RDP, Inc., Waltham, MA)
Satellite Data Processing Systems and Accelerometer Density Data Base
AFGL-TR-80-0247 (30 April 1980), ADA102229

FITE, W.L., and SIEGEL, M.W. (Extranuclear Labs., Inc., Pittsburgh, PA)
Metal Ion Reactions with Ozone and Atomic Oxygen
AFGL-TR-79-0092 (5 April 1979), ADA081516

FRANKLIN, R.L., BETHKE, G.W., and SPRINGER, L.W. (General Elec. Co., Philadelphia, PA)
Design Study for Ground-Based Atmospheric Lidar System
AFGL-TR-80-0264 (29 September 1980), ADA091955

FRYKLUND, D.H. (Accumetrics Corp., Cambridge, MA)
Applied Research & Development of Triaxial Piezoelectric (PZL) Accelerometer Systems of Improved Design
AFGL-TR-79-0101 (June 1979), ADA084762

GROVES, G.V. (Univ. Coll. London, London, England)
Tropospheric-Stratospheric Tidal Investigations: Diurnal and Semidiurnal Wind Oscillations in the Stratosphere
AFGL-TR-80-0348 (31 December 1979), ADA092628
Tropospheric-Stratospheric Tidal Investigations Through Components of Ozone Heating
AFGL-TR-80-0351 (30 June 1980), ADA092631
Tropospheric-Stratospheric Tidal Investigations: Notes on Obtaining the Eigenvalues of Laplace's Tidal Equation
AFGL-TR-80-0350 (31 December 1979), ADA092630

HALDEMAN, C.W. (MIT, Cambridge, MA)
Wind Tunnel Tests of a Gerdien Capacitor Vehicle Combination
AFGL-TR-80-0179 (May 1980), ADA091719

HANSON, W.B., COLEY, W.R., and HEELIS, R.A. (Univ. of Texas at Dallas, Richardson, TX)
Study of Upper Atmosphere Wind Motions
AFGL-TR-80-0307 (15 September 1980), ADA097733

HILLS, R.S. (Tri-Con Assoc., Inc., Cambridge, MA)
Electronic Sub-System for a Solar EUV Spectrometer
AFGL-TR-79-0258 (October 1979), ADA080560

HUBER, W.B. (Tri-Con Assoc., Inc., Cambridge, MA)
Design, Fabrication and Testing of a Satellite Electron Beam System
AFGL-TR-80-0161 (16 May 1980), ADA095362

KITROSSER, D.F. (Univ. Lowell, Lowell, MA)
Measurement of Neutral Temperature in the 120-180 KM Region of the Atmosphere Following TMA Releases from a Rocket
AFGL-TR-79-0120 (May 1979), ADA081445

LARSON, L.J. (HYCOR, Inc., Woburn, MA)
High Altitude Smoke Program (HASP-II)
AFGL-TR-79-0252 (26 October 1979), ADA080964

McDONALD, M. (Wentworth Inst. of Tech., Boston, MA)
Design and Fabrication of Quadrupole Ion Mass Spectrometer for Upper Atmosphere: Sci. Rpt. No. 2
AFGL-TR-80-0025 (December 1979), ADA083019
Design and Fabrication of Quadrupole Ion Mass Spectrometer for Upper Atmosphere: Sci. Rpt. No. 1
AFGL-TR-80-0024 (December 1979), ADA083022

McGREGOR, R.D., and SUGIMURA, T. (TRW Systems Group, Redondo Beach, CA)
Monte Carlo Simulation of Negative Ion Collection by a Rocket-Borne Mass Spectrometer
AFGL-TR-80-0206 (June 1980), ADA091721

MILLER, T.M., HICKMAN, A.P., SMITH, F.T., and PETERSON, J.R. (SRI Int. Molecular Physics Lab., Menlo Pk., CA)
Two-Body Positive Ion-Negative Ion Neutralization
AFGL-TR-79-0039 (30 January 1979), ADA073145

MIRANDA, H.A. (Epsilon Lab., Inc., Bedford, MA)
Stratospheric Aerosol Measurements
AFGL-TR-80-0366 (December, 1980), ADA097716
A Molecular Identification Device for Individual Sub-Micron Aerosols: Feasibility Study
AFGL-TR-80-0155 (May 1980), ADA090018

MURPHY, G.P. (Tri-Con Assoc., Inc., Cambridge, MA)
The Design of Mass Spectrometer Assemblies for Space Shuttle Launched Satellites
AFGL-TR-79-0233 (September 1979), ADA080439

PALASEK, T.A. (Northeastern Univ., Boston, MA)
An RF Oscillator for Rocket Borne and Balloon-Borne Quadrupole Mass Spectrometers
AFGL-TR-79-0226 (10 September 1979), ADA078797

ROE, J.M., and JASPERSON, W.H. (Control Data Corp., Minneapolis, MN)
A New Tropopause Definition from Simultaneous Ozone-Temperature
AFGL-TR-80-0289 (August 1980), ADA091718

SHEPHERD, O., AURILIO, G., BUCKNAM, R.D., BROOKE, R.W., HURD, A.G., and ZEHNPFENNIG, T.F. (Visidyne, Inc., Burlington, MA)
Balloonborne LIDAR Experiment
AFGL-TR-80-0373 (24 December 1980), ADA095366

SHEPHERD, O., HURD, A.G., SHEEHAN, W.H., and BUCKNAM, R.D. (Visidyne, Inc.)
Rocketborne Laser Backscatter Experiment
AFGL-TR-79-0081 (15 March 1979), ADA073853

SLOWEY, J.W. (Smithsonian Institution, Astrophysical Obs., Cambridge, MA)
Global Frequency Distribution of Exospheric Temperature
AFGL-TR-79-0143 (November 1979), ADA077293

SMITH, D., and ADAMS, N.G. (Univ. of Birmingham, Birmingham, England)
Ion-Ion Neutralization
AFGL-TR-80-0010 (November 1979), ADA080209

STOKES, C.S., MURPHY, W.J., and KERSHNER, A.D. (Germantown Labs. Inc., Philadelphia, PA)
Chemical Release Payloads: Stratospheric Wind Measurement
AFGL-TR-80-0073 (January 1980), ADA084100

SUGIMURA, T., and BIRD, G. (TRW, Inc., Redondo Beach, CA)
Direct Simulation Monte Carlo Description of Ionospheric Chemistry
AFGL-TR-79-0114 (May 1979), ADA073893

TROWBRIDGE, C.A. (PhotoMetrics, Inc., Lexington, MA)
Digitization and Analysis of Photographic Images of Stratospheric Smoke Trails
AFGL-TR-80-0230 (30 July 1980), ADA093926

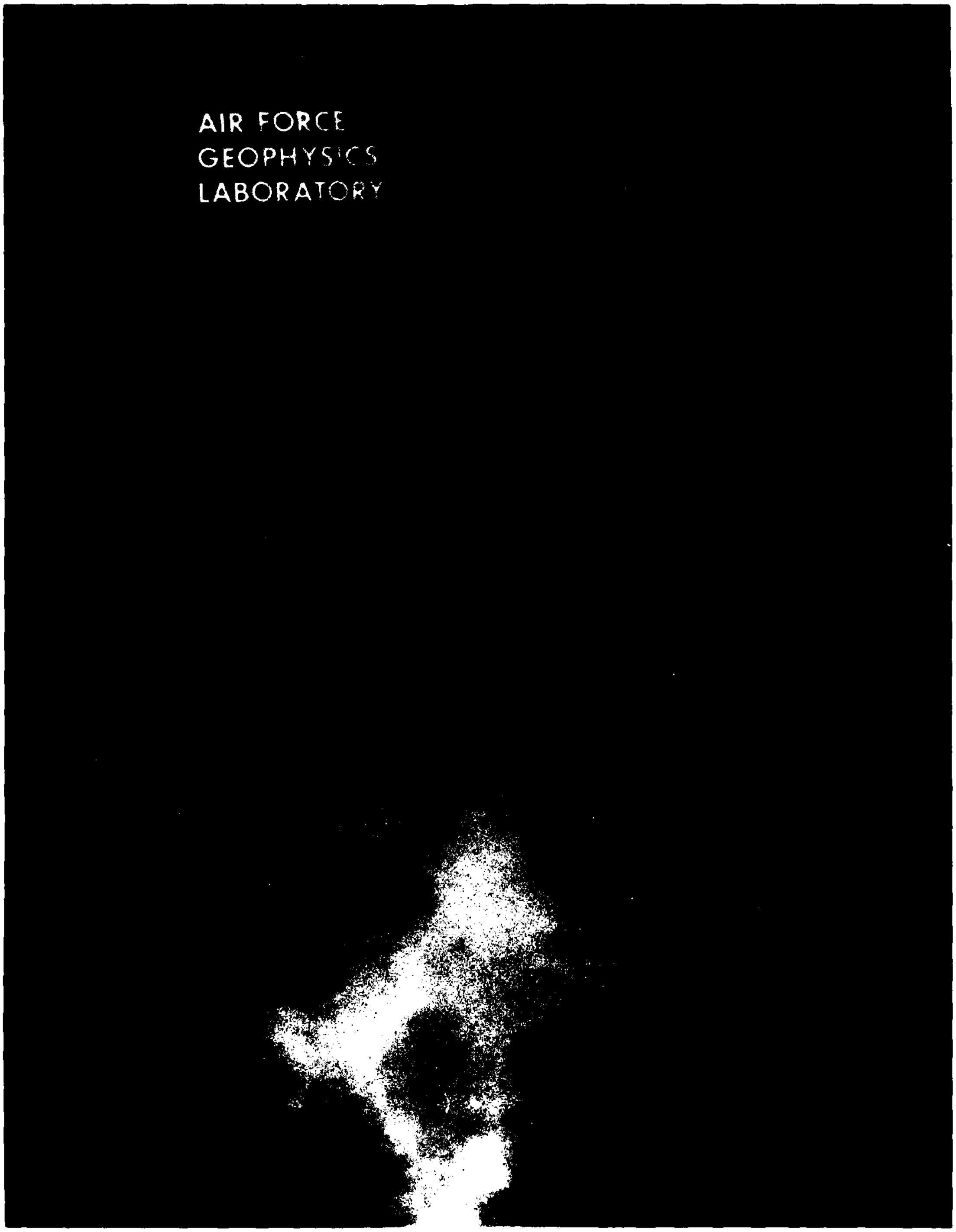

AFGL's One Thousandth Sounding Rocket Launch, A24.609-2 (TEM-2), from White Sands Missile Range, May 27, 1980.

III AEROSPACE INSTRUMENTATION DIVISION

The Aerospace Instrumentation Division supports the other divisions of AFGL by providing the probe vehicles—balloons, sounding rockets, and satellites—which gather data for scientists in their studies of the environment. Efficient, reliable, and economical probe systems require development over periods of months or years to meet ever-increasing Air Force mission requirements. Detailed planning, vehicle procurement, payload design, construction, system integration and testing precede each vehicle launch.

Most rocket and balloon flights are conducted from the White Sands Missile Range, New Mexico, where restricted air space, optical tracking, precision radar, and excellent conditions for payload recovery are available. AFGL mans Detachment 1, a permanent balloon-launch facility, located at Holloman AFB, within the White Sands Missile Range. A site at the Chico Municipal Airport, California, is activated when required for long-duration balloon flights. Fair Site, on the White Sands Missile Range, is permanently maintained for tethered balloon experiments. The Division also has mobile units for conducting rocket and balloon flights from almost any point in the world.

SOUNDING ROCKET PROGRAM

The Sounding Rocket Branch supports the in-house projects of AFGL scientists and other agencies, such as the Space Division and the Defense Nuclear Agency. Responsibilities include management of the rocket/payload system, vehicle procure-

Inflation of Zero-Pressure, Free Balloon, Fabricated from a Polyethylene Film 0.00075 inch Thick.

ment, payload design, fabrication, test, launch support, position tracking, and data acquisition. The Branch also provides engineering management of the experiment/spacecraft interface for satellites and for the shuttle (Space Transportation System). This involves interface management, starting with design and following through fabrication, integration, and prelaunch testing.

Engineering development is conducted in sounding rocket systems, instrumentation, tracking and data handling to improve existing techniques or advance the state of the art when required. Automatic telemetry trackers incorporating pulse-code-modulated ranging systems have been developed to the point where we can be independent of launch range support for these functions, enabling us to conduct expeditionary missions from remote sites.

In 1979-1980, half the vehicles flown could trace their ancestry to surplus military rocket motors. Some have been single-stage, such as the Sergeant, or the actively guided Minuteman I second stage. Others have been two-stage, developed from individual rockets, the Talos-Castor and the Taurus-Orion (Improved Honest John-Improved Hawk). The use of surplus rockets, which has significantly decreased the vehicle acquisition cost, is expected to increase in future years.

1000th Sounding Rocket Launch: The Sounding Rocket Branch launched its 1,000th research sounding rocket from the White Sands Missile Range on May 21, 1980. An Aries rocket carried a highly sophisticated payload for the Multi-Spectral Measurements Program (MSMP) to ascertain the characteristic radiation patterns of rocket motors in flight. The data are being used by the Space Division to design better surveillance systems.

This successful Aries payload development, launch, and recovery is the latest milestone in AFGL's history of research sounding-rocket operations that began in 1946 with a captured German V2 rocket. This history has included the launch of as many as 96 vehicles in a single year; the launch of payloads with weights exceeding 5800 lb; and the recovery of payloads with weights of 2000 lb. AFGL has also launched rockets from the deck of an aircraft carrier. The success rate has been better than 85 percent for vehicles and payloads.

During the past two years, the Sounding Rocket Branch provided state-of-the-art payload design and vehicle support for 18 sounding rocket systems flown from launch sites within and outside the United States. The rockets ranged from the 4.5 in. diameter Super Arcas to the 44 in. Aries. The overall vehicle and experiment success rate was 91 percent. Among the significant programs were the Solar Eclipse experiments at Red Lake, Ontario, Canada; EXCEDE II at Poker Flat, Alaska, the Rocket Post-Burnout Characteristics studies and the Zodiacal Infrared Program (ZIP) at White Sands Missile Range, New Mexico, and the Energy Budget Campaign at Andoya, Norway.

Solar Eclipse Experiments: In February 1979, AFGL participated with the National Research Council, Canada, the U.S. Army Atmospheric Sciences Laboratory, and the NASA Wallops Flight Center in a joint scientific effort in which 14 sounding rockets were launched. This program took advantage of the last total

Preparing Rocket Launchers for Solar Eclipse, Red Lake, Ontario, February 26, 1979.

Rocket Launched at Red Lake, Ontario, during Solar Eclipse, February 26, 1979.

eclipse of the sun visible from the North American continent during this century. Principal research interest centered upon the behavior of ionized regions at altitudes below 100 km. Since the sun provides the major source of ionization at altitudes above 70 km, except under disturbed conditions, significant ionizing source variations were produced by the solar eclipse. Measurements of the charging ionizing source strengths, coupled with measurements of atmospheric responses (both ionized and neutral constituents), provided data necessary for developing physical models of ion and neutral processes.

The five AFGL sounding rockets were launched on 26 February 1979 from a remote site erected for this joint program near Red Lake, Ontario, Canada. Two Paiute Tomahawk rockets carried cryopumped liquid helium quadrupole mass spectrometers to obtain the mass and number density of positive and negative ions. A Nike Orion rocket determined atmospheric density from a 10-in falling sphere. A Niro, in a similar experiment, used a 7-in sphere, and a Nike Orion measured long-wavelength infrared emission dynamics by a 3-channel radiometer cooled by liquid helium.

Post-Burnout Characteristics: A Black Brant VC payload, instrumented with performance diagnostic instruments, television and film cameras, an upleg command system, and an in-flight commandable attitude-control system, was flown in August, 1979, from the White Sands Missile Range. This flight was the first to measure the low-level, post-burnout thrust, outgassing, and particulate contamination by spent solid-propellant rocket motors. It satisfied a long-standing need, since contamination of experiment sensors by rocket outgassing has been evident to sounding rocket experimenters since the initial use of solid-propellant rocket motors. In addition, spent vehicles have been documented overtaking separated payloads and even colliding with them.

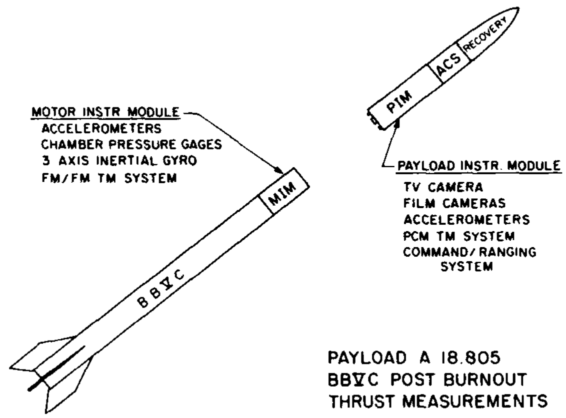

Makeup of Post-Burnout Thrust Measurements Payload.

Analysis of post-flight data showed that the payload separated cleanly from the vehicle at a relative separation velocity of 2.25 ft/sec (0.69 m/sec). However, the residual thrust of the spent motor overcame this differential and the motor caught up to the payload 37 sec after separation, continuing on a parallel velocity vector at about 3.37 ft/sec (1.03 m/sec). This experiment proved the necessity of developing a high-velocity payload-separation capability, and vehicle tumble systems, to achieve large spatial separations between payloads and motors.

EXCEDE II: A Talos-Castor rocket experiment, EXCEDE II, was instrumented and integrated by the Sounding Rocket Branch. It measured ultraviolet, visible, and infrared emissions induced in the night atmosphere by a rocket-borne 100-kW electron accelerator. We then successfully launched the system in October, 1979, from the Poker Flat Research Range, Alaska, carrying 5850 lb, the heaviest known payload ever flown on a sounding rocket.

Equatorial Smoke: In October, 1979, three Nike-Nike rocket systems lifted chemical payloads, consisting of titanium tetrachloride and water-methanol, to generate smoke releases. The smoke was observed by ground-based cameras to de-

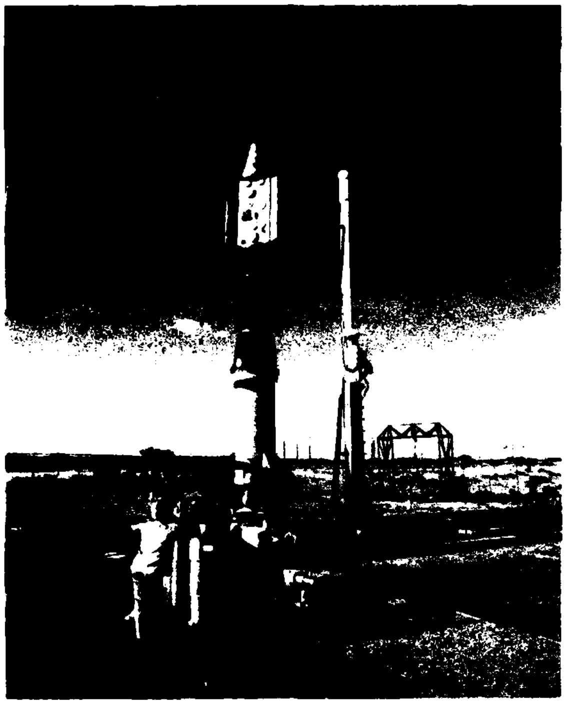

TEM-2 on Launch Pad at White Sands Missile Range with Payload Doors Open, Showing Scientific Instruments.

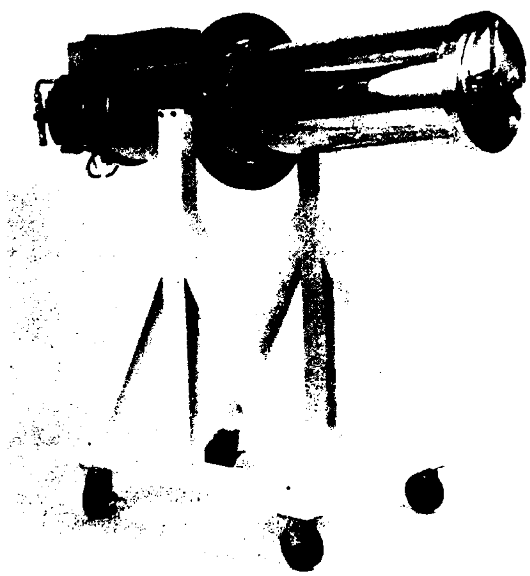

ZIP Sensor (Zodiacal Infrared Program). Advanced Cryogenic Sensor Designed and Built at AFGL to Measure Zodiacal Light.

termine the magnitude and direction of stratospheric winds and shears and the turbulence at an equatorial latitude. This program, conducted from Punta Lobos, Peru, was AFGL's first from that country.

Multispectral Measurements Program (MSMP): The second of three MSMP Aries rockets was launched from the White Sands Missile Range on May 21, 1980. It lifted the 3250 lb, two-part TEM-2 payload to an apogee of 232 km. A complex array of eleven experiments in the sensor module accurately tracked the target module, measuring its exhaust plume characteristics in the ultraviolet, visible, and infrared spectral regions. The sensor module was recovered in excellent condition after a flawless flight sequence. As previously mentioned, this highly successful mission marked the 1000th sounding rocket launch for AFGL.

Zodiacal Infrared Program (ZIP): The first ZIP mission was launched on August 18, 1980, from the White Sands Missile

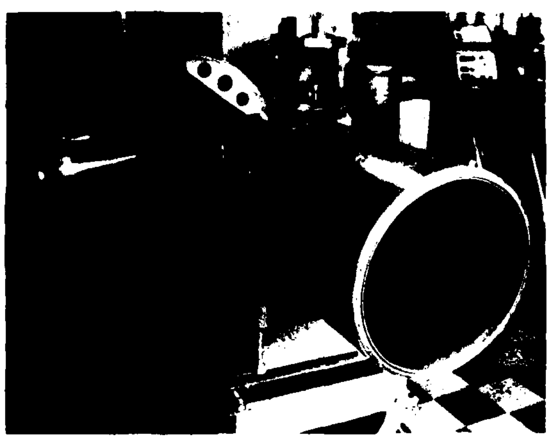

ZIP Sensor in Data Acquisition Position

Range. ZIP is one of several experiments associated with the Background Measurements Program. This complex experiment successfully measured thermal emissions from zodiacal dust near the ecliptic plane while looking at the night sky. The sensor is a state-of-the art, liquid-helium-cooled infrared telescope, designed jointly by the Optical Physics and Aerospace Instrumentation Divisions. The Sounding Rocket Branch was responsible for the design of the telescope's thermal-vacuum vessel, the liquid-helium dewar support, and the sensor calibration source.

Energy Budget Campaign: An instrumented military surplus Taurus-Orion rocket was flown from the Andoya Rocket Range, Norway, on November 11, 1980, to measure auroral, infrared and ultraviolet emissions, total electron energy deposition, and atomic oxygen concentrations. This was AFGL's first use of these low-cost (about $20,000), highly reliable motors in a sounding rocket configuration. (A comparable commercial system would cost approximately $50,000.) This flight, part of a large international program involving 50 rockets and 16 balloons, was designed as an integrated campaign of ground-based, balloon and rocket-borne measurements to study some aspects of the atmospheric energy budget in northern latitudes. Other countries represented in this effort were England, Russia, Austria, Sweden, Spain, and West Germany.

SATELLITE SUPPORT

The Aerospace Instrumentation Division played a major systems-engineering role in the design and launch of the SCATHA satellite, spacecraft S-78-1, launched in January, 1979. An experiment on this satellite measured electron energy in the auroral oval. On-going studies of the data from this highly successful program, which included critical solar-eclipse periods, are providing eagerly sought answers to spacecraft charging problems.

ROCKET AND SATELLITE INSTRUMENTATION

In supporting major AFGL rocket and satellite programs, the Division has advanced the state of the art in data acquisition, antenna development and tracking, and trajectory and command instrumentation. There were accomplishments in three important areas.

Telemetry Instrumentation: A microprocessor pulse-amplitude-modulation (PAM) decommutator was designed for field use. Its first important application occurred during prelaunch testing of the Balloon Altitude Mosaic Measurements program. The decommutator can display, in engineering units, such "housekeeping" data as voltages, pressures, temperatures and other critical parameters, and can flag the data if they have exceeded predetermined, limiting values.

Several state-of-the-art pulse-code-modulation (PCM) telemetry encoders were designed and flown on sounding rockets for the Background Measurement Program. These highly successful devices are part of a continuing effort which originated with the design of a PCM encoder for the Balloon Altitude Mosaic Measurements project. Each encoder was tailored for an individual research payload—the Zodiacal Infrared Project, the Infrared Background Experiment, the Multispectral Measurements Program, and the Far Infrared Sky Survey Experiment. As the first 14-bit analog-to-digital conversion unit designed and flown by AFGL, the encoder for the Zodiacal Infrared Program represented a quantum step in multiplex data-encoding technology.

A new, 10-bit PCM encoder with additional channels, a faster sampling rate, and a 430 MHz receiving ranging system was incorporated into a 10-in falling sphere experiment. This addition of a

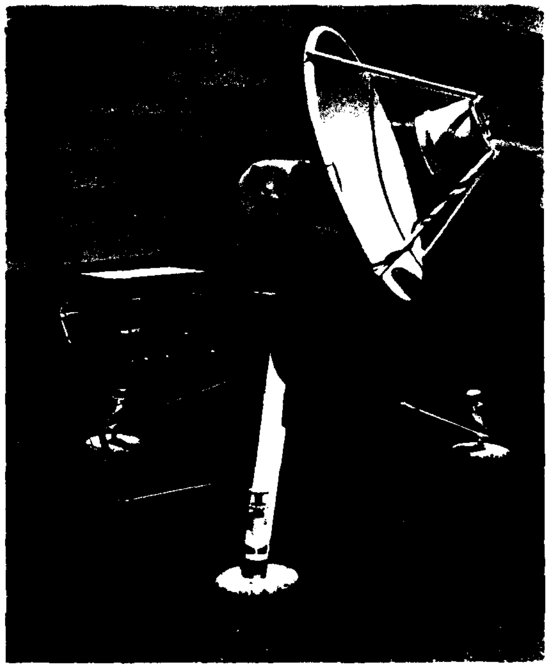

Minitracker Used at Remote Launch Sites.

ranging capability allows launching and tracking of the experiment from remote areas where radar support is not available.

Tracking, Trajectory and Command: Improvements were made in software design and real-time data display for the microcomputer trajectory system (Minitracker) used at remote launch sites. This new system can easily be adapted to any rf tracking ranging system. It provides the following information on visual displays and printer readouts: time, status indicators, computed ellipsoidal earth coordinate data (mean sea-level altitude, ground range, distance north and distance east, or, mean sea-level altitude, vehicle latitude and vehicle longitude), azimuth, elevation, and slant range—all referenced to one of three selectable data origin sites. In addition, an upleg command capability was added to the ranging/trajectory link to permit the transmission of up to 16 discrete signals to a rocket-borne payload. (Additional commands can be added if required.) A separate command link was thus eliminated. The command-through-ranging technique was successfully tested on the Post-Thrust Burnout experiment.

Antenna Development: There are continuing requirements for antennas configured specifically for payloads of different size, such as:

(1) An advanced design for a 10-in falling sphere. This was successfully flown during the Auroral E-Program. The significance of this antenna is that stripline technology is used to incorporate two widely separated frequencies. The antenna is capable of receiving signals from 430 to 550 MHz while simultaneously transmitting 2250 MHz telemetry signals. The physical constraints of the falling sphere added to the complexity of the design.

(2) A large 20.75-in diameter, flush-mounted antenna capable of handling two or more 20 W transmitters. This was successfully flown on the ZIP payload.

BALLOON PROGRAM

The Aerospace Instrumentation Division provides the only comprehensive Department of Defense in-house capability for research, design, development and test of envelopes, instrumentation, launch equipment and techniques for scientific balloons.

The focus of the development program has been changing in recent years from extremely high altitude, modest scientific payload flights to tethered balloons, heavier payloads to 100,000 ft, and controlled ascent/descent profile flights. Investigation of air-launched balloons, vertical-motion and descent-rate control of free balloons, and the upgrading and improving of the data telemetry system and balloon control instrumentation continue as part of the development program.

During the past two years, there has

been a measurable increase in the reliability of polyethylene plastic balloons. This is principally due to improved design and engineering production specifications coupled with better quality control processes for material extrusion and manufacturing. Requirements for a versatile, high-rate communication system for in-flight data recording and display and for uplink commands have also increased.

The use of tethered balloon platforms to lift scientific sensors and antenna systems to meet unique measurement requirements at remote locations has increased in importance. Techniques for positioning single and multiple tethered balloons over selected points for long periods have been successfully employed. The main advantages of tethered balloon systems, in addition to a "quick response" capability, are simple configuration, high reliability, and inexpensive costs for vehicles and operations.

The demand for balloon-flight support in both free and tethered balloons has remained steady but the requirements for individual flights have increased in complexity. Although balloon flight tests can be conducted in all seasons from Holloman AFB, during the past two years some scientific programs required measurements at extreme northern and southern latitudes (Alaska and Panama), or at test sites requiring flights over land and water masses. Additionally, specialized tethered balloon tests were conducted at Dugway Proving Grounds, Utah, and at two selected sites in the Federal Republic of Germany. The experiences have demonstrated a continuing need for modernizing our mobile launching and instrumenting capability for both free and tethered balloon systems.

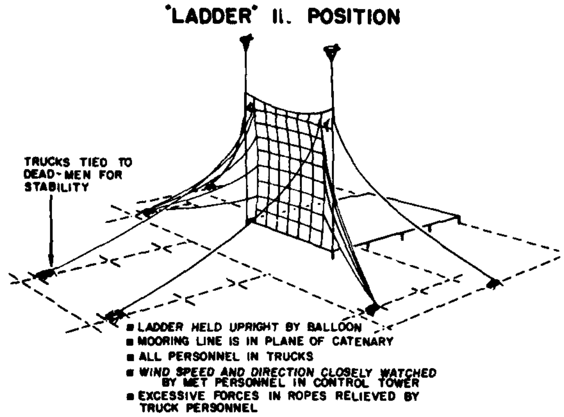

Diagram of Kevlar Cable Net (100 × 100 feet) Tied to Two Tethered Balloons, Used in Carbon Fiber Burn Tests, Dugway Proving Ground, Fall, 1979.

Carbon Fiber Risk Tests: The Division balloon groups conducted a series of five dual tethered-balloon flights during October and November, 1979, at the Dugway Proving Ground, Utah, to assess the distribution and size of carbon fibers released from burning carbon-fiber composite material. This investigation was organized by NASA at the request of the President's Office of Science and Technology Policy to evaluate hazards resulting from the crash and fire of aircraft containing parts fabricated from carbon-fiber composite materials.

A net of Kevlar cable, 1000 ft high by 1000 ft wide, was positioned vertically 500 ft downwind from a burning pool of JP-4 jet fuel and carbon fiber composite material. (Five hundred carbon-fiber collectors of various types were attached to the net.) Before each test, this net was positioned horizontally on a rope lattice 6 ft above the ground to protect the sensors. Two 45,000 cu ft tethered balloons, one at each end of the net, raised the unwieldy flexible net into the vertical position. After the burning, the net was lowered once more onto the horizontal supporting lattice without damage to the 500 samplers. The five completely successful operations enabled NASA and the Department of Defense to acquire a much more complete range of fiber release data than had been possible from previous methods of testing. AFGL's procedure for raising and lowering a large, flexible fragile payload, using an intercon-

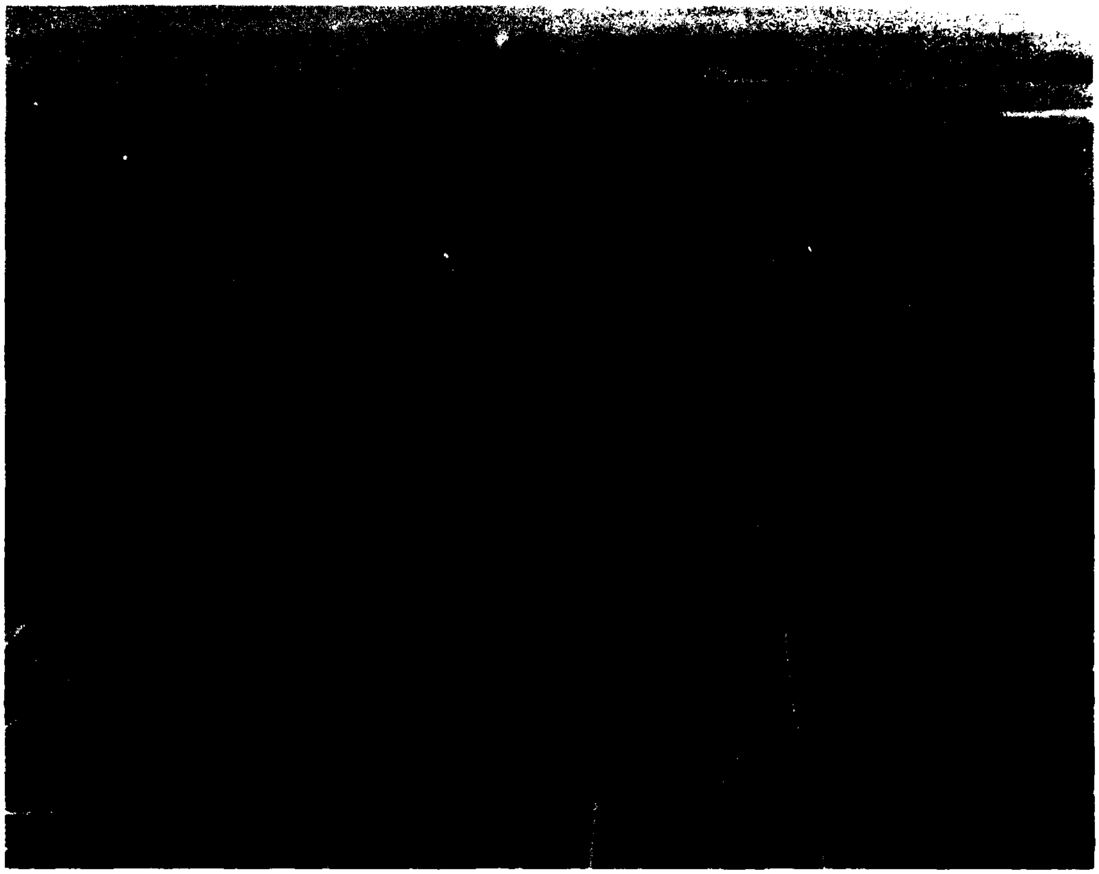

NASA/DOD Carbon Fiber Burn Tests. Two tethered balloons support the net, which collects specimens in the fire plume.

nected, widely separated, pair of balloons marks an extension in the state of the art for tethered balloon operations.

Stinger Winter Field Tests: During February-March 1980, a 6000 cu ft, aerodynamically shaped balloon system carrying a Knollenberg spectrometer was provided and operated for the U.S. Army/ NATO tests of the Stinger missile in West Germany.

Low Visibility Measurements: The Division also again supported the U.S. Army Atmospheric Sciences Laboratory field program to collect data at Meppen, West Germany, for modeling the effect of atmospheric fog and haze on the ability to see ground targets from aircraft. An AFGL launch crew operated the 6000 cu ft balloon system on a 24-hour schedule from 24 October to 10 December 1980.

Ash Can: The Division is responsible for a Department of Energy (DOE) program called "Ash Can" to provide measurements of man-made atmospheric constituents which could have an impact on health. Balloon flights are conducted to altitudes from 21 to 27 km. Operations occur on an annual basis from Panama, Alaska, and Holloman AFB. Frequently, AFGL atmospheric measurement programs are joined with Ash Can field efforts to reduce costs and compare data. During

the past 2 years, 48 successful flights were conducted and 88 samples obtained. The data were sent for analysis to the Argonne National Laboratory and the DOE's Health and Safety Laboratory.

Air-Launched Balloon System: The Air-Launched Balloon System (ALBS) development program proceeded through most of its second phase. The item requiring the greatest effort was the redesign of the liquid-helium dewar and heat-transfer system into a "hardened" configuration, capable of withstanding all extraction and deployment shocks. This effort was carried out successfully, as were refinements of the parachute subsystem design to eliminate a serious extraction line-recoil problem observed at the end of Phase One. Several other system components were also improved (inflation tubing, interface hardware, release devices, timing and control circuits). The culmination of these endeavors was the preparation of a flight-ready system which was to have been air-launched over the White Sands Missile Range in November, 1980. The last-minute cancellation of the arrangements for C-130 aircraft test support prevented the test from taking place until early 1981.

Balloon Altitude Mosaic Measurements Program (BAMM): The BAMM program continued during 1979 with the second data-gathering flight from Holloman AFB, N. Mex., and the third from Keesler AFB, Miss. The 5 million cu ft balloons carried a radiometer, TV camera, and interferometer mounted on a stabilized platform with command-controlled pointing. To obtain data above land/water terrain the third flight was over the Gulf of Mexico. The gondola was rigged with a special packed parachute so that the instrumentation could be snatched by helicopter in mid-air to prevent impact damage. This proved to be a highly satisfactory operation—the payload was lowered to the runway completely undamaged. In 1980, a successful test flight was made from Holloman AFB using a stabilized platform having much higher pointing accuracy.

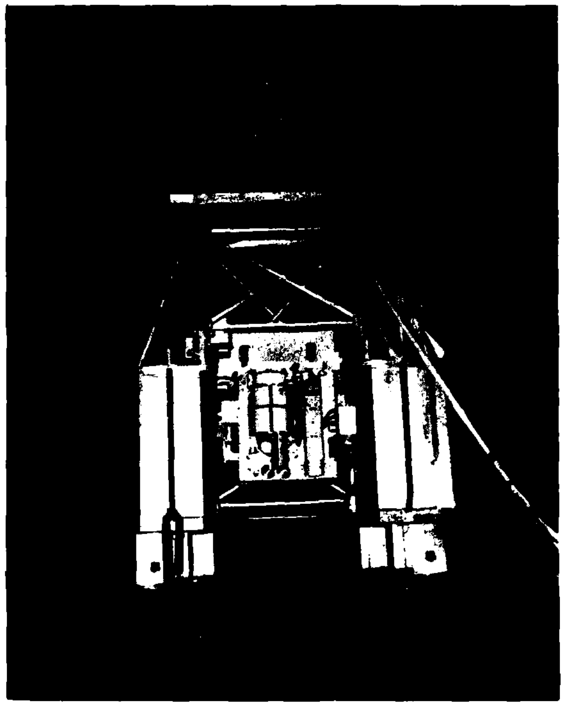

Payload of Balloon Altitude Mosaic Measurements Program (BAMM) Ready for Launch, 1979.

Balloon Vertical Motion Control: Since the first public demonstration of balloon flight in 1783, the control of the vertical motions of unpressurized balloons has been a continuing concern. Vertical motions result from an imbalance between the gravitational force, or system weight, and the buoyant force acting on the system. To control the vertical motions it is necessary to control these forces. System weight is controlled by deballasting. In practice, it is used effectively to initiate ascent or to increase ascent rate, and to arrest descent or decrease descent rate. Buoyant force control, on the other hand, is not simple in either practice or theory. It is achieved by reducing the volume displaced by the balloon by venting lifting gas, or valving. Buoyant force control is complicated for reasons related to the

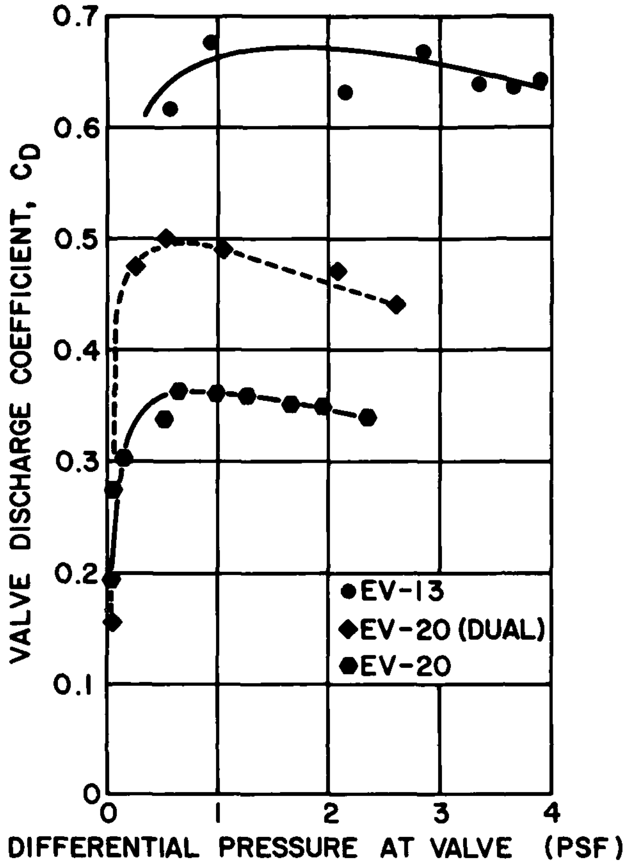

Apex Valve Performance Characteristics. Because most valving requirements occur at differential pressures in the neighborhood of 0.25 psf, apex valves are not an efficient means to initiate descent from high altitudes.

mechanics of the valve itself, the dynamics and thermodynamics of the lifting gas being valved, and the resultant vertical motion of the balloon. Its limited effects include initiation of descent, increase in descent rate, arrest of ascent, and decrease in ascent rate. Many atmospheric probe and sampling experiments using balloons require a controlled descent rate and, ideally, a constant descent rate. These problems were studied during the period covered by this report.

Quick Descent: The problem of promptly initiating descent from high altitudes (greater than 30 km) is not amenable to solutions involving a conventional apex valve, primarily because the pressure causing the flow is roughly proportional to the atmospheric pressure. The flow rate at low atmospheric pressures (high altitudes) is thus much too slow to be practical. The efficiency of the valve orifice depends upon the pressure differential and is extremely low for the differential pressures at the high altitudes. In addition, free flow is restricted by the formation of a negative pressure region at the balloon nadir in response to the flow. An alternative method to initiate descent was investigated in four flights under the in-house technology base program. Large ducts, 6 ft in diameter, located at selected distances above the balloon base were used instead of the standard apex valve. They functioned either alone or in conjunction with a comparably sized base-inlet duct intended to eliminate the formation of a negative pressure region. Used alone, the upper duct did produce a rapid response to the descent initiation command, but a negative pressure region formed and prematurely stopped the flow before the desired descent rate occurred. With both ducts in use, the negative pressure region did not form, but during descent the ingested air apparently either warmed compressively or maintained a temperature warmer than the decreasing ambient-air temperature and thus effectively counterbalanced the valving. The result of these experiments was a clearer definition of the problem and the accumulation of information on balloon thermodynamics and aerodynamic drag which is essential to the formulation of the next approach to this continuing balloon-control problem.

Descent Rate Control: Once descent has been initiated, continuous valving during descent through an orifice of fixed size has long been known to result in a continuously increasing descent rate. When the orifice is eventually shut, however, the system will experience an abrupt decelera-

tion. If the descent rate at the time of closing is slow enough (threshold unknown), the system can actually reverse direction and rise, before continuing down at a reduced rate. To operate between these extreme responses and achieve relatively constant, slow descent rates, the Aerospace Instrumentation Division has designed an apex valve to provide an orifice area that is continuously variable between fully open and fully closed. The valve setting is selectable by command during flight. The flight test results show that such a system is capable of achieving the stated objectives. Guidelines for its operation, however, must be derived from practical experience because of the uniqueness of each balloon system, the variability of the actual operating environment, and the complexities of aerodynamic drag and inflation gas thermodynamics.

Balloon Design: A procedure is being developed whereby a set of specified flight requirements—payload, altitude, duration and profile manipulation—will translate into engineering production specifications for balloons. As part of this effort, a computerized table-scanning procedure has been written to ascertain the suitability of proven balloon engineering designs. In addition to the yes/no suitability answer, for the acceptable designs in the tabulation, the output includes both the ballast weight and the parachute size and weight required for the system. Because each acceptable design is listed in the output, selection of the most suitable balloon design is then possible, based on unprogrammable or unaccounted operational considerations.

Balloon Reliability: Balloon performance statistics have traditionally counted aborted flights as random balloon failures due to launch environment, unskilled crews, or some other unusual factor, and hence not amenable to correction by design or manufacturing changes. Using data from several sources, the Division assessed potential problems with large balloons which might be suitable for a high altitude BAMM flight. This study revealed that for 100 balloons greater than 26 million cu ft in volume, there had been only 6 in-flight failures while there were 18 ground aborts. A preliminary analysis of these flights revealed that the aborts were not randomly distributed; rather, they could be divided on the basis of the unbalanced bubble-erection force into two groups, one with a failure rate of 14 percent and the other with a failure rate of 25 percent. This information will be applied in the study of balloon design criteria scheduled for the next reporting period.

Balloon Instrumentation: Significant progress has been made in upgrading data telemetering systems and balloon control instrumentation. The driving force behind this continuing program has been our experimenters' increasing need to process selected experimental and flight-control data in real time. A dual approach has been pursued in meeting the demand for improved data-handling and control systems. The first method has been to adapt to balloon use the uhf command systems and the high-data-rate S-Band techniques originally developed for rocket instrumentation. The second has been to redesign completely the slower rate hf systems typically employed in balloon instrumentation.

The AFGL Detachment 1 permanent facility at Holloman AFB now has a very versatile, high-rate communication system for in-flight data recording, display and uplink commands. Both frequency modulation (FM) and pulse-code modulation (PCM) telemetry systems are available, with a variety of equipment for recovering, displaying and recording data from balloon-borne experiments.

Line printers, data formatters, cathode ray tubes, analog pen recorders, nine-track digital tape units and disks allow the users to monitor and record selected data in real time. The scientists can thus make

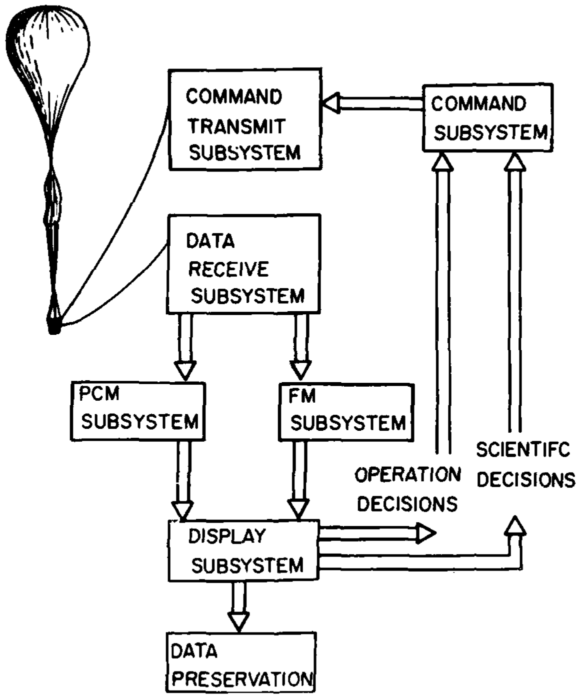

Balloon Telemetry Support System.

timely decisions to alter the experiment operation or to change the balloon trajectory. With the aid of the PDP-11/40 digital computer installed in 1975, they can process the received signals to display data in scientific form for ease of interpretation. Recorded data can be replayed at real-time speed or more slowly to verify operational readiness or to prepare for subsequent flights. For in-depth data reduction analysis, the recorded data can be made compatible with large-scale data reduction systems. Because the PCM system is flexible, the bit rates, bit order, word sizes and data content can be adapted to a wide range of formats. Nominal data rates for most applications are in the lower kilobit range. Data rates as high as 512,000 bits per second and 1600 frames per second have been successfully received and the data processed and displayed. Bit rates as high as two million bits per second could be handled. Software is available for the standard data set, and special programs can be developed for users with individual requirements.

The AFGL permanent balloon launch facility can cover flights at operating ranges as great as 250 miles when the balloon altitude is 50,000 ft or higher. This allows routine, real-time operational support for launches from Holloman AFB and the various other launch locations in and around the White Sands Missile Range. To provide coverage from remote launch locations or for flights at extended distances from Detachment 1, a mobile facility with similar data acquisition capability has been put into operation. It can be strategically located with a telephone communication link to the base facilities. This arrangement provides continuous display

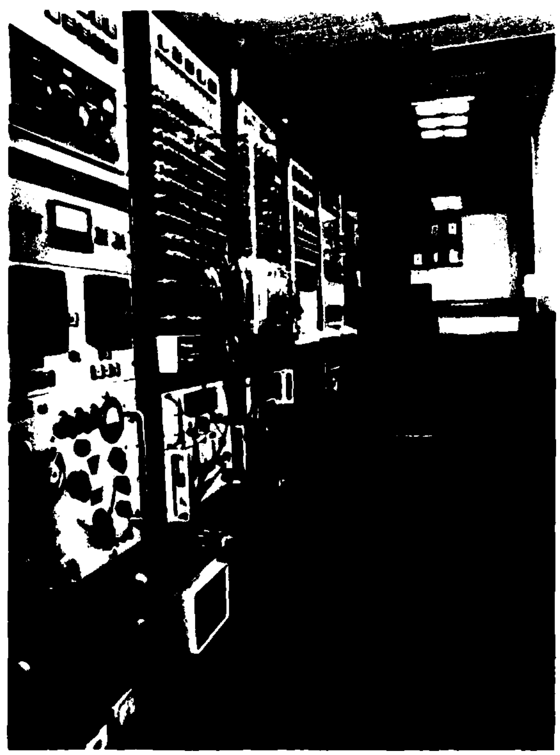

Interior of Mobile Telemetry and Command-Control Station for Balloon Flights.

of scientific data at the base facility, but because of the limited data rates achievable over standard telephone lines, only subsets of the total data packages are displayed.

Although traditional hf systems do not have the capability for high data rates, they are not limited to line-of-sight distances as are vhf and uhf systems. This advantage, their usefulness as secondary or backup command systems, and the continuing need for relatively simple balloon and ground station instrumentation on flights where data volumes are low, have kept hf systems in constant use. Their capabilities have not remained static. There has been an across-the-board, operationally qualified upgrading in which C-MOS logic circuits have been employed, both to increase reliability and to enhance data transmission rates. First, the standard hf balloon instrumentation package has been augmented with a 28-channel, high-resolution data encoder/timer unit and an 18-channel command decoder. The encoder resolves sequentially sensed voltages (from on-board experiments or flight controls) with 10 mV increments. Its pulse-duration 9-bit octal output code has a variable speed, ranging from slow (with hf transmissions) to rapid (with vhf and uhf). The decoder uses sequenced audio tones received from the ground to select a specific command channel. It also employs a reply code, in the same format as the encoder code, to verify channel selection. These changes to the standard balloon instrumentation package have been accompanied by the development of corollary ground station equipment such as a command-tone generator and decoding, display, and recording devices for incoming encoded data. A second area of improvement has encompassed hf in-flight transmitters and receivers. These items were redesigned with solid state components for greater reliability and uniformity. Frequency shift-keying (FSK) was also incorporated into the transmitter, while the receiver was given a dual channel capability. In addition, to increase the range of a 5 W vhf FM transmitter designed for use with the new encoder (to allow higher data transmission rates in line-of-sight operations), a ground-based vhf data repeater was successfully developed and operationally tested in the vicinity of Holloman AFB. Other balloon instrumentation developments include a "smart" ballast valve for tethered balloon applications (it remembers when it has been opened and it sounds an alarm on opening), a variable-opening helium gas valve, and a complicated flight-control package for the Air Launched Balloon System. The latter item controls a number of events with split-second accuracy, including the operation of a cryogenic, mid-air inflation system.

JOURNAL ARTICLES JANUARY 1979 - DECEMBER 1980

CARTEN, A.S., and WUEST, M.R.
Parachute Techniques Employed in the Air-Launched Balloon System (ALBS) Development Program
J. Aircraft 17, No. 2 (February 1980)

WILTON, R.E.
Printed Circuit Antennas for Solving Various Instrumentation Problems
Proc. Wkshp. Printed Circuit Antenna Technology (October 1979)

PAPERS PRESENTED AT MEETINGS JANUARY 1979 - DECEMBER 1980

CARTEN, A.S.
The Air-Launched Balloon System (ALBS) Phase II Design Improvement and Test Program
AIAA Parachute and Balloon Testing Capabilities Wkshp., Edwards AFB, CA (6-7 October 1980)

CARTEN, A.S., and WUEST, M.R.
Parachute Techniques Employed in the Air Launched Balloon System Development Program
6th AIAA Aerodynamic Decelerator and Balloon Technology Conf., Houston, TX (5-7 March 1979)

GRIFFIN, J.R., THORN, W., POIRIER, N.C., and FIKE, R.M.
Telemetry and Control Systems for the Balloon Altitude Mosaic Measurements Program
Int. Telemetry Conf., San Diego, CA (October 1980)

HOWARD, C.D., and RASMUSSEN, R.O.
Special Considerations to Assure Flight Success with Large, Expensive Rocket Payloads
5th ESA-PAC Symp. on European Rocket and Balloon Programmes and Related Res., Bournemouth, England (14-18 April 1980)

LAPING, H.
A Poor Man's Balloon Control and Data System
Int. Telemetry Conf., San Diego, CA (October 1980)

MCKENNA, E.F.
Post Burnout Thrust Measurements
5th ESA Symp. on European Rocket and Balloon Programmes and Related Res., Bournemouth, England (14-18 April 1980)
Post Burnout Thrust and Outgassing Characteristics of Solid Propellant Rocket Motors
AIAA 5th Sounding Rocket Technology Conf., Houston, TX (7-9 March 1979)

STEEVES, R.G.
ARIES Rocket Flight Vibrations Environment, Multispectral Measurements Program
AIAA 5th Sounding Rocket Technology Conf., Houston, TX (7-9 March 1979)

KREBS, C.P.
Prediction of Payload Internal Pressure
AFGL-TR-80-0260 (4 September 1980), ADA099339

LAPING, H.
BCS-18A Command Decoder-Selector
AFGL-TR-80-0249 (25 August 1980), ADA099384

NOLAN, G.F., WRINKLE, L.D., 1/LT, and GILDENBERG, B.D.
Modified Gas Valve for Improved Balloon Descent Control
AFGL-TR-80-0333 (30 October 1980), ADA099371

RICE, C.L. (Editor)
Proceedings, Tenth AFGL Scientific Balloon Symposium, 21 August to 23 August 1978
AFGL-TR-79-0053 (1 March 1979), ADA074469

WALKER, K.R., and GRIFFIN, J.R.
Microprocessor Controlled Pulse Amplitude Modulation Decommutator
AFGL-TR-80-0335 (28 October 1980), ADA100270

WILTON, R.E., and WATERMAN, A.
Telemetry Antennas for Large Diameter Sounding Rockets
AFGL-TR-79-0205 (4 September 1979), ADA082383

TECHNICAL REPORTS JANUARY 1979 - DECEMBER 1980

CARTEN, A.S., and SINDT, C.F.
Gas Replenishment Techniques for Use in High-Altitude, Long-Duration Scientific Balloon Flights
AFGL-TR-79-0278 (14 November 1979), ADA084486

DWYER, J.F.
The Problem: Instantaneously Effecting Controlled Balloon-System Descent from High Altitude
AFGL-TR-80-0277 (11 September 1980), ADA100255

GIANNETTI, A.A., and ERICKSON, J.C.
AFGL Balloon Telemetry Facility
AFGL-TR-80-0029 (23 January 1980), ADA084811

CONTRACTOR JOURNAL ARTICLES JANUARY 1979 - DECEMBER 1980

KEESE, D.L. (Texas A&M Univ., College Station, TX)
Zero-Pressure Balloon Design,
AIAA J. 17, No.1 (January 1979)

CONTRACTOR TECHNICAL REPORTS JANUARY 1979 - DECEMBER 1980

BEAN, S.P., and GROUND, J.R. (New Mexico St. Univ., Las Cruces, NM)
Balloon Systems and Launch Support
AFGL-TR-79-0175 (15 April 1979), ADA075385

BUCK, R.F. (Oklahoma St. Univ., Stillwater, OK)
Ten-Bit Resolution PCM Encoder (Falling Sphere Experiment)
AFGL-TR-80-0071 (1 February 1980), ADA092111

BUMGARNER, R.A., and GILCREASE, A.A. (New Mexico St. Univ., Las Cruces, NM)
Sounding Rocket and Balloon Systems Support
AFGL-TR-79-0166 (July 1979), ADA075384

DURNEY, G.P., and LAWRENCE, R.W. (ILC Dover, Frederica, DE)
Air Force Geophysics Laboratory Aerodynamically Shaped Tethered Balloon, 45,000 FT^3
AFGL-TR-80-0367 (December 1980), ADA096758

EBACHER, R.W. (Wentworth Inst. of Tech., Boston, MA)
Payload Instrumentation for Probing Rockets
AFGL-TR-80-0027, (December 1979), ADA083023

ERICKSON, J.C. (New Mexico St. Univ., Las Cruces, NM)
Support of AFGL Balloon Telemetry System
AFGL-TR-80-0372 (30 September 1980), ADA097735

FIKE, R.M. (Oklahoma St. Univ., Stillwater, OK)
TRADAT Microcomputer Based Trajectory System
AFGL-TR-80-0012 (November 1979), ADA083074

HOWELL, A.H. (Tufts Univ., Medford, MA)
Balloon-Supported Antenna for LORAN C/D Navigation System
AFGL-TR-80-0107 (January 1980), ADA087488
New Hardware for Tethered Balloons
AFGL-TR-80-0108 (January 1980), ADA086836
Payloads used in First Three Data-Gathering BAMM Flights
AFGL-TR-80-0109 (January 1980), ADA086839
Balloon-Supported LORAN Antenna, New Hardware for Tethered Balloons, and Payloads used in BAMM Flights
AFGL-TR-80-0034 (28 February 1980), ADA087487

MORIN, R.L. (Northeastern Univ., Boston, MA)
Command Control Consoles for Sounding Rocket Payloads
AFGL-TR-80-0019 (December 1979), ADA084097

OLSEN, J.F. (Aerojet Services Co., Sacramento, CA)
Engineering Services in Support of Sounding Rockets
AFGL-TR-80-0127 (November 1979), ADA087801

ROCHEFORT, J.S., O'CONNOR, L.J., and POIRIER, N.C. (Northeastern Univ., Boston, MA)
Communication and Instrumentation Systems for Space Vehicles
AFGL-TR-80-0189 (1 January 1980), ADA087944

THORN, W.F. (Northeastern Univ., Boston, MA)
FM Transmission of Television from Rockets and Balloons
AFGL-TR-79-0160 (11 July 1979), ADA075489

Space Shuttle Against the Auroral Arc. Future research in space physics will concentrate on understanding the effects of the aurora on military operations from the Shuttle.

IV SPACE PHYSICS DIVISION

The technical program of the Space Physics Division is concerned with space-environment effects on Air Force systems. Particles, such as electrons and protons, which permeate near-earth space, can degrade satellite electronics and sensors by radiation damage. They can also interfere with and disrupt on-board computer systems. Magnetic storms and substorms create ionospheric disturbances which degrade communications to and from satellites. They can cause surveillance, detection, and tracking systems to become ineffective or to give false information. Space is a dynamic environment with daily and seasonal variations and with naturally occurring disturbances. These variations and disturbances are caused by the sun. Therefore, the Division's program deals with solar activity and how to predict it, the radio and particle emissions resulting from such activity, and the propagation of solar particles through the interplanetary medium to the vicinity of the earth. It also is concerned with the interaction of such particles with the earth's magnetosphere, and with the particle fluxes and energies within the magnetosphere. Magnetic disturbances and storms and ionospheric irregularities resulting from particle precipitation and varying electron densities are included in its investigations.

In accomplishing its programs, the Division observes and monitors the important parameters in near-earth space with instruments carried by satellites and by a dedicated, heavily instrumented KC-135 which functions as an airborne ionospheric observatory. The flying observatory is used in a program of ionospheric mapping

PREVIOUS PAGE IS BLANK

and in the study of ionospheric disturbances both in the arctic and in the equatorial regions.

To complement the satellite and aircraft-borne observations, the Division maintains a number of ground-based observational sites such as the ionospheric observatory at Goose Bay, Labrador, its network of seven magnetic disturbance monitors across the United States, and its Solar Research Branch at the NSF-operated Sacramento Peak Observatory.

SOLAR RESEARCH

Solar research in the Space Physics Division is the responsibility of the Solar Research Branch. The Branch is a tenant at the Sacramento Peak Observatory (SPO), Sunspot, NM, a national center for solar physics operated by AURA, Inc., under contract to the National Science Foundation. Its task is to identify, predict, and understand physical mechanisms on the sun which give rise to the solar flares and high-speed solar-wind streams that produce geophysical disturbances known to disrupt Air Force systems. In addition, the Branch has an active program to restore images of the sun and of earth satellites that have been degraded by atmospheric turbulence. It is now in the third year of a study of variations in the sun's ultraviolet output to determine if these changes are large enough on a short enough time scale to affect the character of the ionosphere or influence weather patterns. The Solar Research Branch has recently begun investigations of the solar-stellar connection, a new area of research in which observations of active and variable stars are analyzed to better understand similar phenomena on the sun.

Flare Prediction: The capability to produce accurate predictions of solar flare activity will ultimately depend on a complete understanding of the physical processes occurring in flares, including the mechanisms for energy storage and release. At present, however, flare forecasting relies on statistical relationships between flare occurrence and solar pre-flare characteristics. The Solar Research Branch conducts in-house and contractual research in both flare physics and statistical methods. Both approaches utilize solar data obtained from the Air Weather Service (AWS) Solar Optical Observing Network (SOON) in addition to the telescopes available at SPO. The techniques developed through these studies are, in turn, applicable to SOON observing procedures and to the operation of the Air Force/NOAA Space Environment Services Center (SESC) in Boulder, Colorado.

Observations made earlier at SPO showed that flare energy may be built up and stored in sheared magnetic fields, as evidenced by relative motions between sunspots or solar-surface magnetic fields. Recent magnetograph measurements, combined with estimates of shear derived from the local geometry of solar atmospheric structures, have now indicated stored energy in amounts sufficient to power even the largest flares. Additional observations have also shown that the triggering of the flare may be associated with the emergence of new magnetic flux from beneath the solar surface. Measurements of the actual vector magnetic fields, although difficult to obtain, have been successfully completed under contract. These results confirm the presence of sheared field in association with sunspot motions and subsequent flare activity. The final product of this research is the design of observational parameters geared to quick identification of sheared fields and stored energy. These parameters are obtainable by SOON, which provides the bulk of the solar optical data transmitted to SESC.

Large flares occasionally produce emission in the optical continuum. These "white light" flares appear to be associated with the acceleration of high energy protons which subsequently reach the earth and produce geophysical disturbances. To

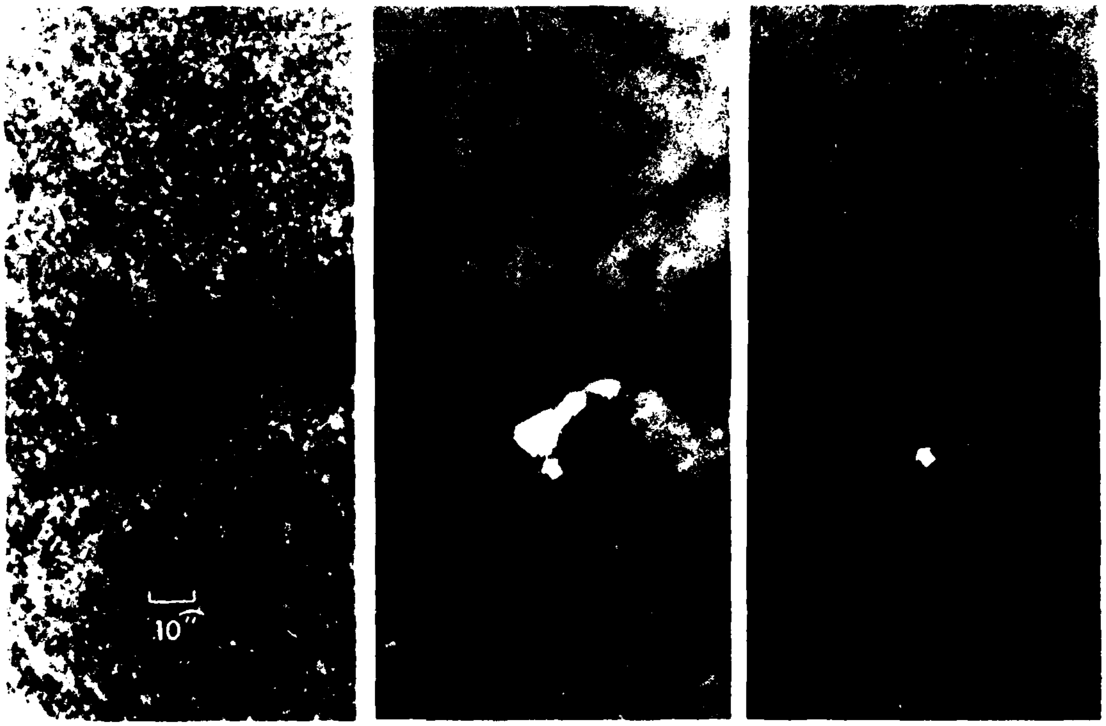

White Light Flare of July 1, 1980, Photographed: (a) in the Yellow-Green Prior to Onset, (b) in the Ultraviolet at Flare Maximum, and (c) in the Yellow-Green at Maximum. The scale represents 10 arcsec, which corresponds to about 7300 km on the solar surface.

study such flares, the Solar Research Branch has participated in the construction and operation of a special telescope at SPO capable of measuring the polarization and spectrum of flare emissions. Observations of a large flare on July 1, 1980, showed strong emission extending into the ultraviolet with no polarization. These data are compatible with the hypothesis that proton bombardment of the lower solar atmosphere causes the emission. The solar magnetic configuration and other preflare characteristics of this event are being investigated. It is likely that the actual site of the flare energy release occurs in the solar corona, at an altitude higher than the optical source.

The most recent work on the statistical approach to flare prediction uses improved algorithms for the Multivariate Discriminant Analysis (MVDA) technique developed earlier, and a larger data base for testing the method. Data for the years 1977 and 1978, collected by NOAA from SOON and other observatories, have been used in the MVDA computer program to produce daily forecast accuracies of 94, 32, and 59 percent for no flare, small flares, and large flares, respectively. During the same period, comparison predictions, subjectively derived using conventional NOAA methods, yielded accuracies of 95, 24, and 37 percent in the same categories. The greater accuracy in the forecasts for large flares is of particular interest to the Air Force because of the geophysical importance of these events. Other statistical methods, including logistic regression, have been tested under contract. Results are similar to those obtained from MVDA,

although they are more adversely affected by coding errors and missing data.

The MVDA technique has further application in a recently initiated effort to produce a short-term (10 minutes to 2 hours) flare forecast. Unlike the daily forecast, the short-term predictions will require real-time data and extremely short forecast-preparation time. Therefore objective, computer-generated predictions seem essential. A preliminary prediction scheme has already been outlined in a joint effort between the Solar Research Branch, the Plasmas, Particles and Fields Branch (which will provide the analysis of pre-flare solar radio data), NASA Marshall Space Flight Center (pre-flare soft x-ray data), NOAA World Data Center (pre-flare optical fluctuations), and AWS/SOON.

The Solar Research Branch provides assistance to and receives data from, AWS/SOON in a mutual effort to design more effective observing sequences for use in flare prediction. In particular, a trackball-operated mapping digital technique

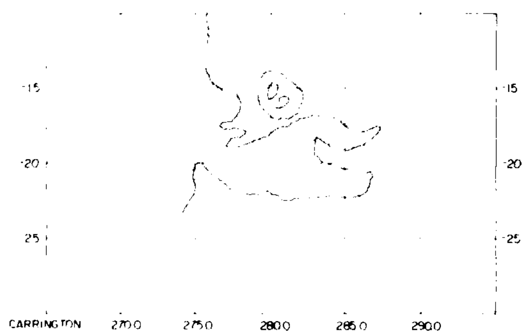

SOON Trackball Map Showing a Sunspot and the Magnetic Polarity Inversion Line. Coordinates are labeled in solar latitude (ordinate) and longitude (abscissa).

has been jointly developed to obtain data on sunspot dynamics, magnetic field development, and atmospheric structures (see figure). The main feature of the mapping program is its capability to superpose data of various types and times. Automatic corrections are also made for foreshortening of objects seen near the solar limb. This unique system should therefore prove ideal for rapid assessment of new flare-prediction parameters that will subsequently be incorporated into the MVDA technique. The Solar Research Branch has also been active in developing the SOON magnetograph hardware and software and in providing assistance to the SOON observer training schools.

In 1980 NASA successfully launched the Solar Maximum Mission (SMM) satellite, a series of experiments coordinated with ground-based observations; SMM was part of a larger international effort known as the Solar Maximum Year (SMY). During this period the Solar Research Branch participated in joint SMM/SMY experiments involving studies of the impulsive phases of flares as observed in x-rays, gamma rays, and optical emissions. One result was the observation of a white-light flare (discussed above) which coincided in time with a solar gamma-ray burst, providing further evidence for proton acceleration in flares.

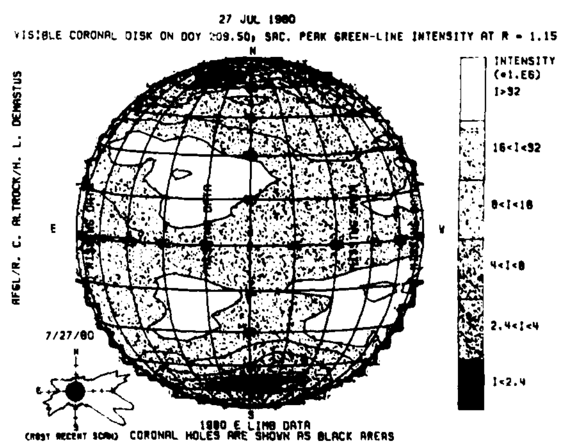

Map of the Coronal Green Line (FE XIV, 5303 A) as It Would Have Appeared Against the Solar Disk on July 27, 1980. Note coronal holes (black regions) near poles.

The Solar Research Branch also participated in the NASA/NSF Skylab Workshop on Solar Flares, which led to the most complete review and description yet available (published 1980) on the solar-flares. More recently, the Solar Research Branch contributed to the International Solar-Terrestrial Predictions Workshop and Study Group (1979), which reviewed and provided recommendations for the entire solar activity forecasting industry and its customers. Finally, the Solar Research Branch provided consultation to the Department of Energy's contracted study group, JASON, regarding techniques and research in solar activity forecasting.

Coronal Holes and the Prediction of Geomagnetic Disturbances: The Solar Research Branch has continued a program to supply data to the Air Force and other governmental agencies for the purpose of predicting geomagnetic disturbances. Previous research by Branch personnel has shown that the use of solar coronal green-line data (see below) can improve the prediction of such disturbances. These data are obtained by Branch personnel on a daily basis at SPO and telecopied to Air Force Global Weather Central (AFGWC) at Offutt AFB and the SESC. They consist of maps obtained by processing circular scans around the limb of the sun at various heights made in the green light of Fe XIV at 5303 Å. This light comes solely from the million-degree solar corona. Depressions in the intensity level of this light correspond to the existence of "coronal holes," which have been found to be correlated with high-speed solar wind streams and geomagnetic disturbances. These daily scans may be assembled into a single map representing how the corona would look on any given day if one were able to see it against the solar disk. Such maps are similar in appearance to maps obtained by rocket and satellite imagery of the sun in soft x-rays. These coronal maps, a new product of the Solar Research Branch, have found high acceptance among forecasters at both AFGWC and SESC. A sample, corresponding to the way the corona would have appeared against the disk on July 27, 1980, is shown here. In these maps, which are quickly produced by computer processing at the Solar Research Branch, coronal holes appear black. They may be quickly and easily recognized by geophysical forecasters, and the maps as a whole may be compared easily to other solar imagery available to forecasters, such as spectroheliograms in He I 10830 Å, or Hα 6563Å. The forecasting agencies receive telecopies of these maps on a twice-weekly basis. They are also utilized by Branch personnel for correlative studies with other solar data, geomagnetic disturbances, and satellite drag data.

Efforts are underway to assist SOON to obtain intensity maps of the sun in He 10830 Å. This atomic absorption line appears to be well-correlated with the location of coronal holes on the solar disk. Branch efforts are centering on utilizing the diode sensors of SOON optical telescopes to compare the intensity in this very weak line with that of the adjacent solar continuum. Whereas the green line can only be seen at the solar limb, the 10830 Å line has the advantage of being "observable" on the sun's disk itself, although it appears in the infrared and thus can be detected efficiently only by photosensitive diode detectors. Because the line's signal is so weak, Solar Research Branch scientists are having to develop special solar-scanning and data-reduction techniques to obtain usable data. The ultimate goal of these efforts is to enable each SOON installation to generate daily maps in the 10830 line.

Coronal Holes and Satellite Drag: At the request of Headquarters, Aerospace Defense Command (ADC), the Solar Research Branch investigated satellite drag data provided by ADC, relative to daily scans of the solar corona in the green line

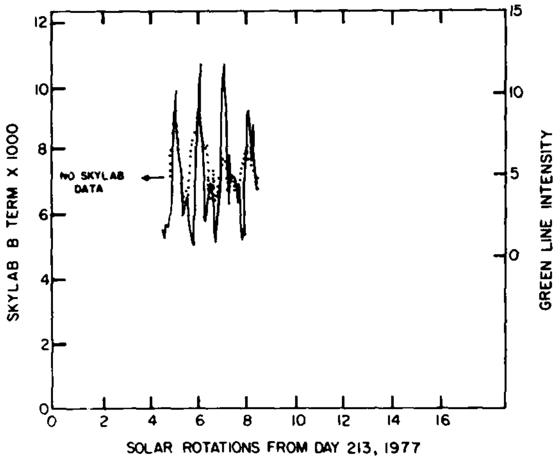

Total Satellite Drag Coefficient for Skylab, B (dotted line) and East-limb-west-limb Average Equatorial FE XIV 5303 Å Coronal Intensity, $\bar{I}_v$ (solid line) as a Function of Time. B is plotted as a function of observation time at the earth. A lag of 10 days from central meridian passage is introduced for $\bar{I}$ to simulate a hypothesized disturbance travel time from the sun to the earth. Prior to the period plotted, there were no data for B. *After the* period plotted, both signals became aperiodic.

obtained by the Solar Research Branch. The satellite drag data came from Skylab and other satellites, and showed unexplained variations in drag with periods ranging from 1 to about 27 days. Attempts had been made earlier at ADC to model the density of the upper atmosphere, but these modeling attempts were unsuccessful in removing the observed drag variations. The existence of the 27-day period in some of the data immediately implied a solar connection, as the solar rotation period near the equator as seen from the earth is approximately 27 days. The solar green-line data during that period in fact did show a 27-day periodicity in brightness near the solar equator. By shifting the coronal data slightly in time, relative to the satellite drag data, it was possible to produce a good correlation between maxima in the solar coronal intensity near the equator and maxima in the satellite drag (see figure). The transit time from the sun to the earth, which would be obtained by this procedure, turned out to be approximately 10 days.

One-Shot Coronagraph: After several years in design and construction, the new "one-shot" coronagraph at SPO has been completed with the help of Solar Research Branch personnel, and systematic patrol observations are now underway. The earlier monochromatic green-line coronagraph was fabricated during 1955, and observations began shortly afterwards. The quality of those observations was considered excellent for that time, with a minimum of instrumental scattered light and a high signal-to-noise ratio, producing photographs of even the faintest coronal structures. The new instrument is now yielding the best coronal photographs ever obtained by any instrument in the world. The system gives Fe X (6374 Å) and Fe

Superposed Photographs of the Sun Obtained Simultaneously with the New "One-shot" Coronagraph by the Solar Research Branch. Disk picture and inner limb are in Hα (6563 Å) formed at 10^4 degrees K, middle limb photo in Fe X (6374 Å) at 1×10^6 degree K, and outer limb in Fe XIV (5303 Å) at about 2×10^6 degrees K.

XIV (5303 Å) photos at the limb, and Hα (6563 Å), both at the limb and as full disk pictures (see figure). For the first time, a coronal image of the entire limb is obtained in a single exposure; hence the name, "one-shot." The photos are the best Solar Research Branch coronal expert Howard DeMastus has seen in 25 years of solar studies. They have exposure times less than one-half of those from the earlier instrument, resulting in far better temporal and spatial resolution. It may now be possible to observe some of the high-speed coronal transients predicted but not yet observed by ground-based coronagraphs.

The Solar Research Branch plans to use these new observations as a further tool in determining the relationship between flare-producing regions and transients in the corona as well as augmenting photoelectric observations of coronal holes. Although this instrument is not ideally suited for detecting coronal holes, which are normally observed with a coronal photometer, the one-shot observations can, nevertheless, indicate the nature of the inner corona adjacent to such coronal hole regions.

Energy Transport in the Solar Atmosphere: The Solar Research Branch continued its study of the fundamental processes involved in transporting energy through the solar atmosphere and into the interplanetary medium. Major advances were made in understanding the nature of convective overshoot, the scales of convective motion on the sun, the nature of oscillatory and wave motions of the solar atmosphere and of the sun as a whole, the determination of conditions in the interior of the sun from surface phenomena, and the interaction of motions with magnetic fields, leading to solar activity.

Tentative evidence for fast solar rotation has been observed by the Solar Research Branch. Features on the solar surface near the equator rotate with an average period of about 27 days. Analyses of sunspot motions from 1915 through 1977 indicate that motions having much shorter periods may also be present. Periods of 4.2, 8.4 and 16.8 days showed up in Fourier analysis, which agree with predictions based on the assumption that the invisible core of the sun is rapidly rotating.

Fluctuations in solar chromospheric emission as observed in the calcium K-line have been monitored for the past 5 years, a period coinciding with the rise in solar activity from minimum to maximum. The total calcium emission increased about 25-30 percent. The increase in the mean emission was well correlated with both the number of plage regions on the sun and the Zurich sunspot number. However, daily variations in the calcium emission seem to be poorly correlated with daily variations in either the number of plages or the sunspot number. This may have wide-reaching implications for how emergent flux affects the quiet chromosphere to create active regions.

Working with a contractor, the Solar Research Branch has extended observations of solar motions to larger areas of the solar surface and to longer periods of time. This has led to the discovery of a previously unknown intermediate scale of convection which has been labeled "mesogranulation." Mesogranules have lifetimes (1–4 hours) which are greater than granules (about 10 minutes) and shorter than supergranules (one to two days). Their spatial scale is approximately 5000 km, with velocities of about 100 meters per second. Mesogranulation may have a significant influence on the transport of energy and magnetic fields, and studies are continuing. The contractor has also provided theoretical models for the various scales of convection observed by the Solar Research Branch. He has found evidence that convective motions can be separated into two components: those motions controlled by magnetic fields and others that seem to be free of magnetic influence.

The Solar Research Branch has made considerable progress in interpreting the

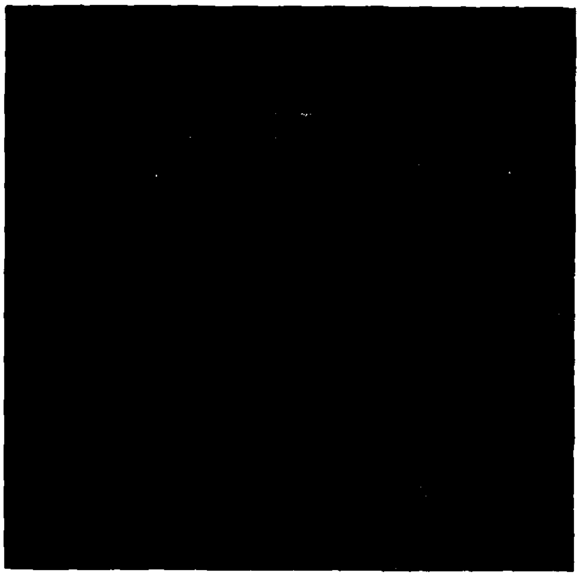

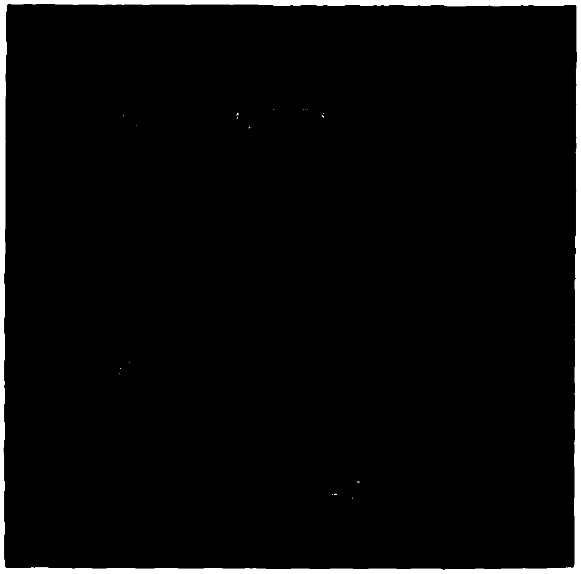

Velocity and Intensity Maps Made in He 10830 of Filaments Seen Against the Solar Disk. These figures illustrate data taken with a CCD chip and analyzed using the new image-processing system at Sacramento Peak Observatory. Units are km s^{-1} in the velocity figure and fraction of continuum intensity in line intensity image.

often confusing observations of small features seen at the solar surface. Knowledge of the behavior of these granulation elements, which are resolvable only under the best atmospheric "seeing" conditions, is fundamental to our understanding of the processes which channel energy flow from the sun's interior to its outer layers, and eventually into the solar wind and, thus, ultimately into the geophysical environment. The first comprehensive and accurate picture of the spatial and temporal behavior of individual convective elements has been obtained. Diagnostic methods, used to infer velocity fields, were shown to be faulty, and refined techniques were developed. A comprehensive set of calculations showing how highly resolved line profiles would behave under a number of different physical situations was made. Phenomena studied include granules, acoustic waves, oscillations, magnetic knots and faculae. It was shown that neither acoustic waves nor granulation can completely account for the breadth of solar spectral lines. These calculations will aid in the interpretation of high resolution observations that should result both from space shuttle programs, such as the Spacelab 2 and the Solar Optical Telescope (SOT) missions in which Solar Research Branch personnel are participating, and from the advances in imaging techniques described later.

Observations of the interaction between flows and magnetic fields were obtained. Flows of magnetic features in the "moats" surrounding sunspots have shown that moats typically develop and decay in less than a day, with a stable period lasting about 6 days. The sunspot always breaks up and disappears just before, or concurrently with, the decay of the moat. Appearance of a moat indicates that a spot is in its last decaying stage of evolution, having only a few days left to live. During the moat lifetime, moving magnetic features break off from the spot, stream across the moat, and disappear into the surrounding region. A theoretical model of the interaction of convection and magnetic flux tubes

has been formulated by the Solar Research Branch with collaborators from the University of Cambridge, United Kingdom, and the Max Planck Institut in West Germany.

The Solar Research Branch has made several advances in data acquisition and processing during this period. Silicon chips, charge-coupled devices (CCD) having a 100 x 100 pixel format, have been interfaced with telescopes and computers at both the big dome and tower telescopes at SPO. CCD devices have several advantages over film and linear diodes, which have been the primary detectors for solar observations. Advantages over film are (1) higher sensitivity, which permits maps of solar features in spectral regions previously difficult or impossible to obtain, (2) linear response to a wide range of light-levels, and (3) digital data-collection in real time. The major advantage over linear diode arrays is their two-dimensional structure, allowing simultaneous spectral and spatial coverage.

The accompanying figures show a solar filament (magnetic flux tube or arch above the solar surface) projected against a small portion of the solar disk, observed in the infrared He 10830 line with a CCD device and processed with the Branch's new image-processing facility. A strong correlation between line strength and velocity is evident. These represent the first direct He 10830 observations of line-of-sight velocities associated with solar filaments and will aid in understanding the mechanisms by which matter is transported in the presence of magnetic fields. Now that the feasibility of array detectors for solar work has been demonstrated successfully, work has begun on a sophisticated and powerful detector system consisting of eight such two-dimensional arrays to be operated simultaneously.

High Resolution Imaging: The Air Force continues to have a keen interest in high resolution imaging through the earth's atmosphere. A significant portion of Air Force basic research in this area is through in-house programs and contracts awarded by the Solar Research Branch. The primary objectives of these efforts are *to obtain distortion-free images of solar* surface features, to image earth satellites with increased resolution, and to lay the technical groundwork for utilizing the upcoming generation of giant, multiple-aperture telescopes for high-resolution observations.

Significant progress has also been made

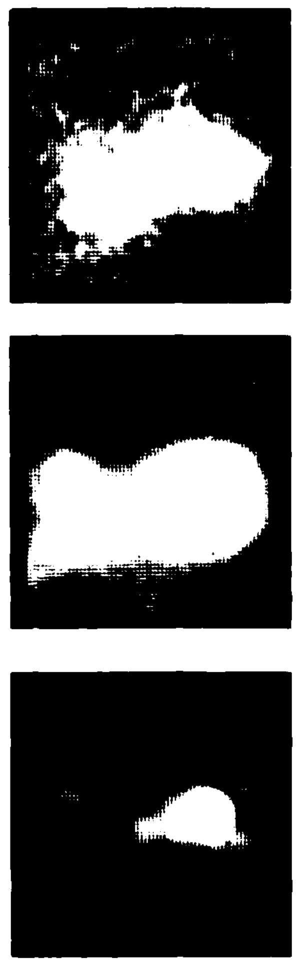

a

b

c

Reconstruction of a Complex Film-recorded Ca^{+} K Line Solar Feature: a. Single Input Frame; b. Direct Sum of 60 Frames; c. 60-Frame Reconstruction.

SATELLITE

STELLAR COMPARISON

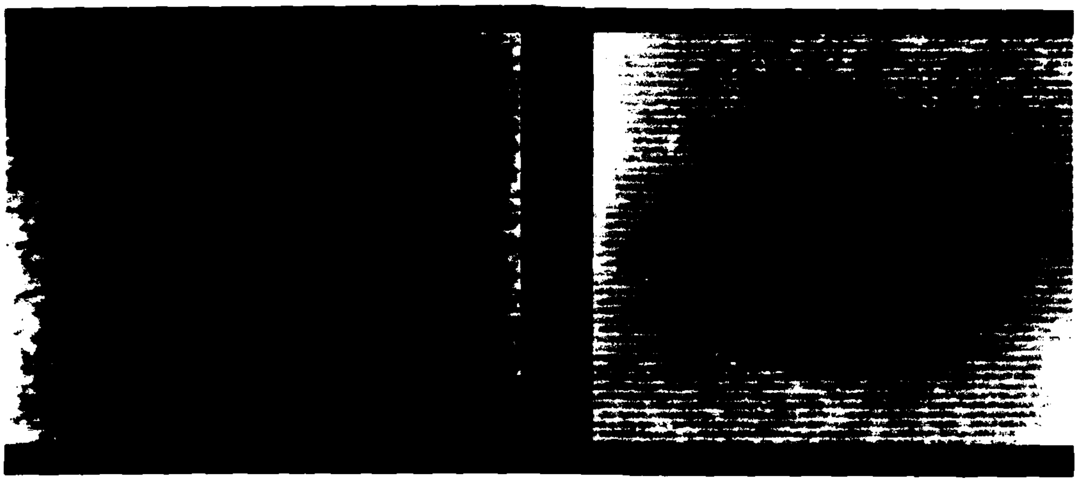

0.5 Arc Second

50 Meters at 20,000 Kilometers

0.5 Arc Second

Speckle observations of Soviet Molniya satellite and a stellar comparison. Dark central core of satellite auto-correlation function is slightly resolved. It shows an elongated shape and is larger than the circular function of the unresolved star. The satellite, about 5m in diameter, subtended only 0.05 arcsec when observed at an altitude of 2×10^4 km, barely above the theoretical resolving power (0.04 arcsec) of the 90 inch telescope at Kitt Peak.

in post-processing of images to enhance fine detail. A contractor has successfully used the Knox-Thompson speckle imaging algorithm to improve the resolution of solar features (see figure). Typically, about a hundred such images are taken in rapid sequence and then analyzed by Fourier techniques to obtain a single enhanced image.

Significant progress has been made in exploring methods for faint-object speckle imaging. In conjunction with a contractor, the Solar Research Branch has constructed a video speckle camera capable of detecting individual photon events. This camera recently demonstrated its ability by resolving detail in a quasar fully 10,000 times fainter than objects accessible with conventional speckle systems. It has also been used to confirm the discovery of Charon, the recently-found satellite of the planet Pluto, and to obtain observations which suggest that at least two asteroids (2 Pallas and 12 Victoria) have satellites. The highlight of this project to date has been the successful resolution of a Soviet Molniya communications satellite (see figure), a feat for which the Solar Research Branch was awarded the 1Q 1980 AFSC Technical Achievement Award.

The successful speckle observation of faint objects such as satellites entails a price in the form of an enormous increase (several hundredfold) in the quantity of data which must be processed. The Solar Research Branch is developing techniques for using modern image-processing facilities, including array processors and digital video displays, to ease this burden. Excellent progress has already been made. The time required to process a single speckle frame has been reduced from over 30 minutes to about 3 seconds. Since a single speckle observation involves hundreds, or even thousands, of individual

frames, such time savings are essential.

Solar Variability: The sun appears to have long-term (decades or centuries) and intermediate-term (1-10 years) energy-output variability. Shorter variations (months or a few years), if they exist, might affect terrestrial weather patterns and artificial satellite drag. Astronomers at Lowell Observatory in Flagstaff, Arizona, have reported changes in the brightnesses of outer planets that are inversely proportional to the number of sunspots, an indicator of solar activity. The brightness changes are as great as 2 percent per year, and are believed to be due to changes in the solar ultraviolet energy output. The magnitude of the change may, however, be caused by an amplification effect due to simultaneous changes in the planetary atmospheres.

Since 1978 the Solar Research Branch has been observing outer planets and satellites, some of which have atmospheres and some that do not, in an attempt to determine if the brightness changes are atmospheric in origin. Observations are made in visible photometric bands and in the near ultraviolet, using a high-precision photometer at the 48-inch telescope in Cloudcroft, New Mex.

Data on Neptune for the first two years of Cloudcroft observations have been reduced. No variability greater than about 1 percent per year has been seen in the ultraviolet. Results in the visible, especially for the 1980 season, were unusual and confusing. The variations are anomalously large over a season. Lowell confirms this behavior, which may have been induced by the recent solar activity maximum. Analyses of the results for Neptune are continuing, as are reductions of the observations of other planetary bodies. In addition, a third year of planetary monitoring observations, now underway during a period of declining solar activity, may well provide the information necessary to interpret the earlier solar-maximum results.

Generalizations of Solar Activity: An area of astronomy receiving increased attention and promising to provide important scientific breakthroughs during the next two decades is "The Solar-Stellar Connection." Many solar studies are severely limited because all the observed parameters refer to a single, very ordinary type star. By comparing these parameters with those of many other stars, it should become possible to understand numerous phenomena which have so far defied explanation, including perhaps, solar flares and activity. Stellar astronomers, on the other hand, are unable to test many of their theories because stars are, in general, spatially unresolvable, and thus must be treated as point sources. By using the nearby sun, with its wealth of small spatial details, as a testbed, they will be able to solve many difficult problems.

The Solar Research Branch has become involved in the solar-stellar connection during the past five years. Five solar-type stars known to have active chromospheres

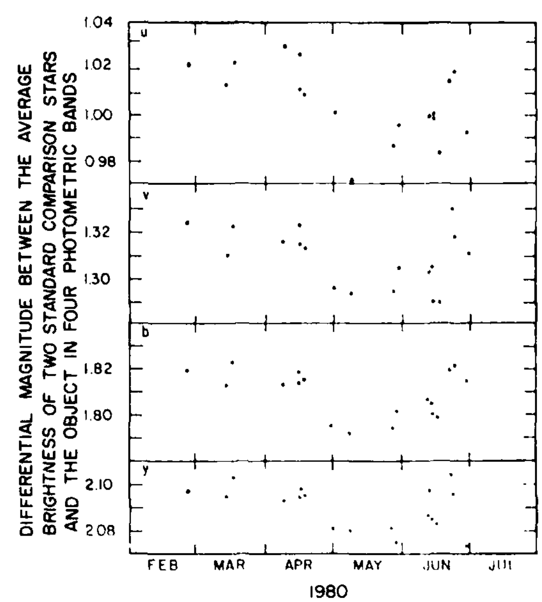

Photometric Variability in the Active Chromosphere star HD 115404.

were monitored for several months to determine the level of photometric variability. One star clearly varied at the 2 percent level. Satellite measurements of the sun taken over a roughly comparable period had maximum variations of 0.2 percent, an order of magnitude less. The variation in the active chromosphere star was probably irregular; observations have been resumed to check for periodic variations. The other four stars were constant to the 1 percent level, but showed indications of variability on a lower level. Analysis is underway to confirm such low-level variability.

The first detection of magnetic fields in solar-like stars was made by Solar Research Branch, SPO, and Kitt Peak astronomers. They used Fourier deconvolution techniques to compare the widths of a spectral line not sensitive to magnetic fields with the Ca II k line, which is field-sensitive. Three stars known to have strong k lines were observed. Magnetic fields were detected on two of them: ϵ Boo A was found to have a field strength of 2700 ± 500 gauss covering 20-40 percent of the disk. On 70 Oph A, a slightly weaker field covered 7-10 percent of the disk on one occasion, but no field was observed at another time. The percentage of the disk covered by strong fields is much greater than that covered by the sun, consistent with the great brightness of both stars at the center of the k line.

SOLAR RADIO RESEARCH

The Solar Radio Astronomy Section of the Trans-Ionospheric Propagation Branch analyzes radio observations of solar radiation in the 8 millimeter to 1.2 meter wavelength range. It also performs research on solar active regions and solar flares and studies the impact of these flares on the magnetosphere and ionosphere. In addition, it advises the Electronics Systems Division on the installation and acceptance testing of the Radio Solar Telescope Network (RSTN).

The radio observations analyzed are of two types: (1) whole-sun observations from RSTN patrols having antenna beamwidths larger than the sun's angular diameter (about 0.5°) and (2) high-resolution observations where the resolution is of the order of 1 arc-sec to 4 arc-min, making it possible to examine a single active region on the face of the sun. The Very Large Array in Socorro, NM, the Westerbork Synthesis Radio Telescope in the Netherlands, and the Aericibo telescope in Puerto Rico have all been used to make these high-resolution observations.

Patrol Based Research: Previous studies at AFGL of the large radio bursts associated with proton flares have shown that their microwave peak flux-density spectrum has a characteristic "U-shape," with a high flux-density response in the meter and centimeter regions and a dip at decimeter wavelengths. It has also been demonstrated that the spectral width of the "U" is related to the energy spectrum of the accelerated protons and that the integrated flux density at a single frequency (usually 8800 MHz) of the microwave burst associated with the proton flare is roughly proportional to the ensuing peak proton flux. This last result has recently been improved by integrating the proton-flare radio emission over a broad portion of the radio spectrum (rather than utilizing only a single frequency), as well as over time. Further improvement in this correlation was obtained by correcting for the flare's solar-longitude particle-propagation effect.

The delay to onset of a solar proton event can be defined as the interval between the inferred acceleration of the protons on the sun and their arrival at earth. A study based on a limited number of solar western hemispheric events has indicated that proton flares with longer rise times (at Hα, meter, and decimeter wavelengths) have

correspondingly larger delays to onset than more impulsive events. The correlation between the flare rise times and the delay intervals can be used for predictive purposes.

Two additional studies based on whole-sun patrol data have applicability for the 24-hour proton-event probability forecasts jointly issued (at present) by the AWS/NOAA forecast centers. The first of these was based on an earlier observation by members of the Solar Radio Astronomy Section that the geophysically important flares of August 1972 came from a region that also produced a large number of unusual impulsive bursts whose radio emission is confined to frequencies greater than 8800 MHz. An extensive review of historical data has revealed that these "sharp-cutoff" bursts are a fairly common characteristic of solar active regions that produce proton flares, and thus have predictive utility. The second study was based on the observation that proton flares tend to come in clusters, with a few large and complex regions producing a disproportionate number of events. It was found that one-third of all principal ($>$ 2dB) polar-cap absorption (PCA) events came from active regions that had produced a previous PCA. A simple persistence forecast technique based on the $>$ 8800 MHz peak flux density of the burst and solar longitude of the previous proton-flare from a given active region was developed to predict the likelihood of occurrence of these "subsequent" PCA events.

High Resolution Studies: A number of active regions were observed at 6 cm wavelength with the Very Large Array. In all cases the active region was resolved into one or more sources which were small ($\sim$20 arc-sec), bright ($\sim 10^6$K) and highly circularly polarized (30 percent to 100 percent). They dominated the active region emission at this wavelength. The locations of these sources were well correlated with the chromospheric plages as seen in Hα photographs. This enhanced 6 cm emission did not come from regions which directly overlay sunspots. The high brightness temperatures of the regions are indicative of coronal origin. A strong similarity was noted between circular polarization maps at 6 cm and photospheric magnetograms. The implication is that the polarization maps can serve as a "coronal magnetogram" to delineate the structure of the solar magnetic field high above the surface of the sun.

Radio Solar Telescope Network (RSTN): In the past two years, RSTN sites at Palehua, Hawaii, and Learmonth, Australia, have been completed and become operational. Solar Radio Astronomy Section personnel have played an integral role in the design, development, installation and acceptance testing of this system. A Near-East site (yet to be determined) will complete the four-station network. The Palehua and Learmonth sites are equipped with a Hewlett-Packard 1000 Model 45 computer that is used to detect significant flare-bursts, to format real-time burst-notification messages for transmission to AWS/NOAA forecast centers, and to archive the multi-frequency data on magnetic tape. Solar flux density data at the various frequencies are measured and recorded with a one-second time resolution.

ENVIRONMENTAL EFFECTS ON SPACE SYSTEMS

The Problem: Future operational space systems are expected to be more sensitive to the energetic particle environment than present systems. The newer microelectronic technology, while more compact and faster, tends to be less radiation-resistant. Therefore, particle-flux intensities will have a dominant role in determining the feasibility of future space systems. The technical or data base from which the present radiation models are derived is over ten to fifteen years old. Updated measurements are necessary if the Air

Force is to develop reliable space systems using modern technology.

Instrument Development: During the last two years the Air Force Geophysics Laboratory has undertaken an active development of state-of-the-art instrumentation. These instruments consist of an electron detector (fluxmeter) that measures electrons from 1 to 10 MeV in energy, a dosimeter that measures the total dosage behind shields of different thicknesses, a series of electrostatic analyzer instruments or J-sensors for the DMSP (Defense Meteorological Satellite Program), an electrostatic analyzer to be flown on board the European satellite METEOSAT-B, and a proton detector (1-100 MeV).

The electron detector consists of a series of solid-state detectors arranged in a telescopic fashion followed by a bismuth germanate crystal. The whole arrangement is encased in heavy shielding to prevent background particles from penetrating through the sides. The J-sensors (SSF/3) measure electrons from 30 eV to 20 KeV in energy and are being redesigned to include both electrons and protons (30 eV - 30 KeV). These sensors monitor precipitating particles in the auroral regions and are discussed in more detail below for the European Space Agency. An SSJ/3 instrument is also being flown on the METEOSAT-B spacecraft. Here it will monitor the electron environment for correlation with possible spacecraft upsets at geosynchronous altitudes. The dosimeter (SSJ*) is designed to monitor the dosage in a set of detectors individually mounted behind four different shielding thicknesses. This instrument, which will fly on the Block 5D2-F7 satellite, will also record the expected upset rate due to nuclear interaction of energetic protons and the passage of cosmic rays. These cause transient upsets or soft errors, degrading system reliability.

Soft Errors: A cooperative effort with the Deputy for Electronic Technology of the Rome Air Development Center investigated the effect of energetic protons (>20 MeV) on representative microelectronic devices. It was established for the first time that energetic protons could cause upsets via nuclear interactions. Previous calculations based only on ionization energy loss implied that this effect would not occur. This finding has an immediate impact on systems designed to fly near the inner radiation belt.

System Support: Orbital trade-offs in terms of expected radiation damage were performed for the ITV (Instrumented Test Vehicle) Program. Consultations were also held with GPS, Space Shuttle and Space Based Radar Program Offices.

Plasma Sheet Studies: The source of magnetospheric substorms resides in the earth's magnetotail. Plasma instabilities interrupt the cross tail current, leading to a rapid conversion of magnetic to kinetic energy. It is not known in detail what these instabilities are, how they develop, and whether they grow, or are dumped out. Recent research has emphasized the possible connection between single-particle motion and the generation of collective instabilities. It was shown that protons are normally magnetized (follow circular orbits) when the plasma sheet is expanded. They become demagnetized (follow non-circular orbits) when the plasma sheet is thinned. This leads to a modification of the stability criteria at the plasma sheet boundaries.

SOLAR PROTON EVENT STUDIES

Solar protons, accelerated in solar-active regions during solar-flare events, may drastically increase the radiation flux near the earth. The increased radiation can cause perturbations in the earth's aerospace environment and affect spacecraft operations, or systems operating in, or through, the polar ionosphere. Although the enhanced x-ray, radio and optical emissions during the solar flare

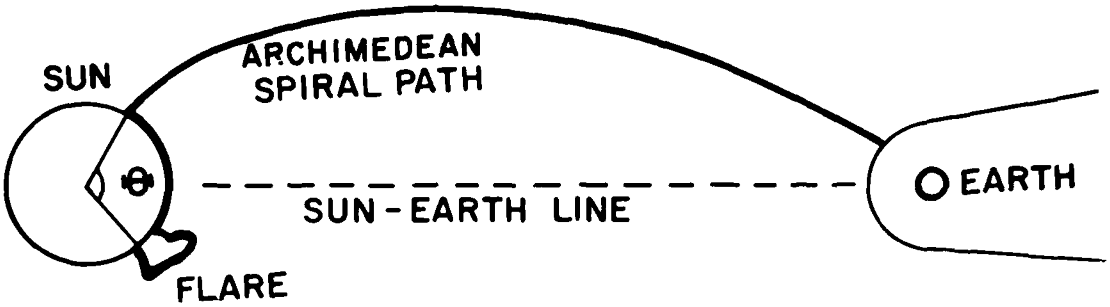

Illustration of the Propagation Concept. The coronal propagation distance 0 is illustrated by the heavy arc on the sun. Interplanetary propagation proceeds along the Archimedean spiral path from the sun to the earth.

event indicate that proton acceleration is occurring, the "U-shaped" spectral signature of the radio emission is generally regarded as the indicator that solar protons are being released from the solar-active region.

At the Solar-Terrestrial Predictions Workshop organized by the National Oceanic and Atmospheric Administration and co-sponsored by AFGL in 1979, Space Physics Division researchers reported the culmination of their efforts to predict the time-intensity profile of the solar proton flux expected at the earth after the occurrence of a solar flare. The concepts employed in the construction of the real-time computerized system to predict these fluxes, and presently in operational use by both the USAF and NOAA, were improvements, modifications, and generalizations of the results of a number of researchers throughout the world.

The propagation of solar protons from the flare site on the sun through interplanetary space to the earth can be separated into two distinct phases. The first phase is diffusion from the flare site through the solar corona to the "foot" of the Archimedean spiral path formed by the interplanetary magnetic field line between the sun and the earth. The second phase is the propagation in the interplanetary medium from the sun to the earth along interplanetary magnetic field lines with a velocity that is a function of the particle kinetic energy (see figure).

The prediction of the time-intensity profile of solar protons expected at the earth after the occurrence of a proton-releasing solar flare can be summarized as follows: There will be a delay between the time of the flare and the onset of enhanced flux at the earth as the particles propagate in the solar corona and along the interplanetary magnetic field lines from the sun to the earth. We have combined the results of a number of spacecraft to obtain a generalized onset-time algorithm such as illustrated here. The minimum in the figure corresponds to a flare at the "foot point" of the average Archimedean spiral path between the sun and the earth (57 degrees west of the sun's central meridian).

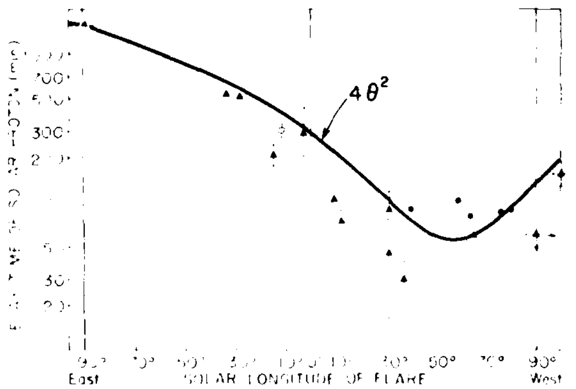

Distribution of Onset Time of 30 MeV Protons as Function of Solar Longitude.

The distribution of the predicted time of

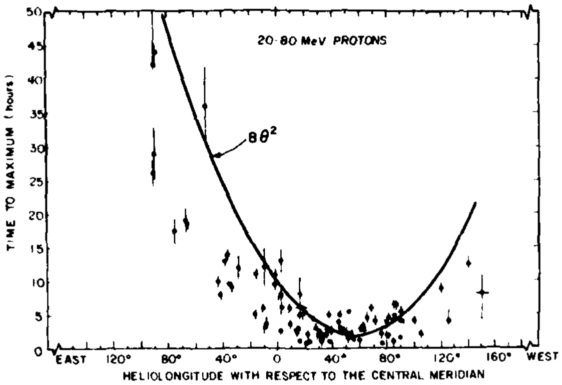

Distribution of Measured Time of Maximum of 20 to 80 MeV protons as Obtained by Spacecraft as Compared with the Coronal Propagation Parameters Utilized in the Prediction Technique.

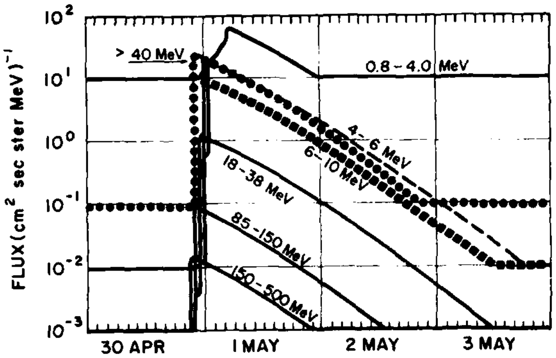

Time-Intensity Profiles Predicted for the Proton Energy Ranges Monitored by SMS/ GOES Satellites.

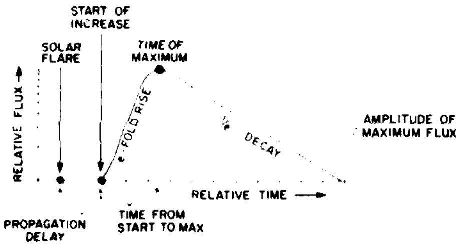

Conceptual Illustration of Typical Time-intensity Profile for Solar Proton Events.

maximum as a function of solar longitude is illustrated here, with the spacecraft-observed data points showing the typical range of variations that can be expected. The minimum in the curve again corresponds to a flare at the "foot point" of the Archimedean spiral path between the sun and the earth computed for nominal solar-wind speeds. A prediction of the time of the maximum flux and the magnitude of the maximum flux expected allows the construction of an exponential curve from the onset time to the time of maximum of the event. By specifying appropriate decay parameters, the form of the expected time-intensity profile may be generated. A conceptual time-intensity profile and a prediction for an actual event are shown here.

The prediction procedures are successful in predicting the types of events that generate increased ionization and perturb the polar ionosphere, specifically, phenomena caused or perturbed by solar protons in the energy range of a few mega-electron-volts to about 80 MeV. Our research has shown that in the range from hundreds of mega-electron-volts to giga-electron-volts (i.e., relativistic protons) the intensity of high-energy particles is consistently underpredicted.

Although relativistic solar cosmic-ray events occur on an average of once a year, these high-energy penetrating particles contribute significantly to the radiation dose in the initial phase of the event. At the present time it is not possible to predict which events will contain these relativistic particles. In fact, of the 28 events detected since 1956, a wide range of time-intensity profiles and energy spectra have been observed, making it difficult to develop a coherent model of these events.

The largest relativistic solar-particle event observed at the earth since 1960 occurred on May 7, 1978. The "event" was successfully predicted and the polar-cap absorption effects were adequately predicted; however, the high energy particle-flux intensities were seriously underpredicted. In an initial attempt to model this

event utilizing cosmic-ray data acquired by the world network of neutron monitors (there are essentially no spacecraft detectors that have good resolution at very high energies), AFGL scientists reported a fundamental new result: the release of relativistic solar protons from the solar corona is energy-dependent; that is, very energetic particles are released very efficiently and quickly from the corona whereas particles having lower energies—but still a few giga-electron-volts—have their major effective release a few minutes later. This analytical study and analysis verified previous theoretical work performed by other American scientists.

In a continuing study of significant solar-proton events, a table was published listing 34 riometer-sensed polar-cap absorption events for the period 1970-1972. This list includes the onset time, magnitude, time of maximum absorption and duration of each event and is self consistent with a previous AFGL publication covering the period 1955-1969 (TR-78-0028).

Geomagnetic Storm Prediction From Interplanetary Parameters: Perturbations of the geomagnetic field have a significant effect on the aerospace environment in which several USAF systems operate. These include systems that rely on high-frequency radio propagation through the ionosphere such as point-to-point communication, surveillance and detection systems, and space operations such as those affected by the changes in the density of the neutral atmosphere, which cause changes in the drag on spacecraft, thereby affecting their orbits. The geomagnetic storm is the result of a complex interaction between the interplanetary magnetic field transported in the solar wind and the geomagnetic field. Three of the most commonly obtained measures of geomagnetic activity are AE, Dst and Ap. AE is a geomagnetic index that characterizes the auroral electrojet, the primary index for magnetic activity in the polar regions. Dst is an index that characterizes the equatorial ring current. Ap is a "Planetary" index of the average magnetic activity.

A number of physical causal relationships have been established, and in concept, the prediction of the geomagnetic storm from measurements of the interplanetary plasma and field parameters is possible. An extensive investigation has been conducted correlating the measured interplanetary magnetic field and plasma

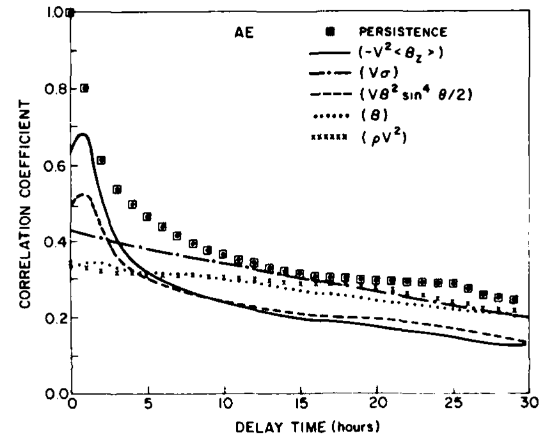

Auto-correlation and Cross-correlation Coefficients as Function of Lag (delay time) for AE with Various Solar Wind Parameters.

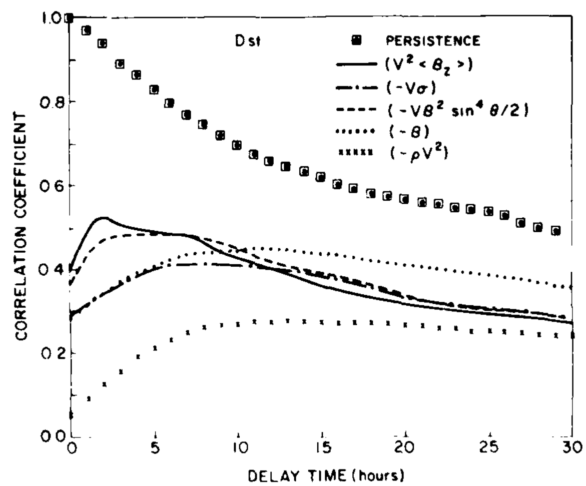

Auto-correlation and Cross-correlation Coefficients as Function of Lag (delay time) for Dst with Various Solar Wind Parameters.

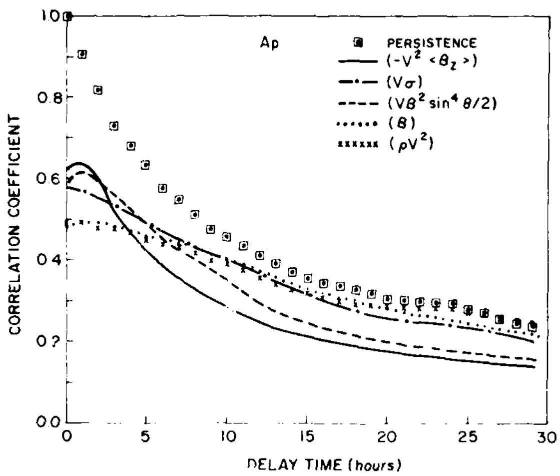

Auto-correlation and Cross-correlation Coefficients as Function of Lag (delay time) for Ap with Various Solar Wind Parameters. The "" are the cross-correlation coefficients of Ap prediction from the three parameters that have the highest correlation.

parameters with the geomagnetic activity. The result of this study shows that there are significant correlations between geomagnetic activity and specific interplanetary magnetic field and plasma parameters. These results are typified in the figures which display autocorrelations and cross correlation coefficients between the various measured interplanetary magnetic field and plasma parameters and the geomagnetic activity at the earth for various delay times ranging from 0 to 30 hours. These results show that there is considerable potential in being able to predict the onset and magnitude of geomagnetic disturbances from observations of the interplanetary parameters; however, ...tions a day or more in advance from ... earth interplanetary field and ...surements would be more dif- ... the correlation between the ...ved interplanetary mag- ...sma observations and ...vity 24 hours later is ... In fact, the predic- ...magnetic activity ...ld and plasma parameters is usually below the prediction that would be obtained by a simple persistence formula.

Charged Particle Access to Spacecraft: Research to study the access of cosmic radiation to an orbiting satellite has been conducted. In a cooperative effort with NASA, this research has been oriented toward comparing theoretical results with data measurements obtained from the

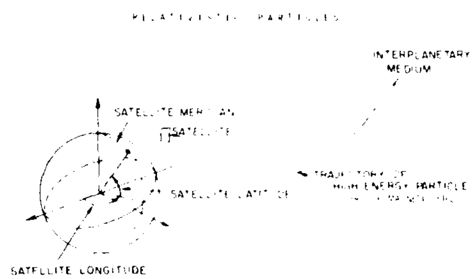

Typical Simple Cosmic-Ray Trajectory as a Particle Travels from the Interplanetary Medium through the Geomagnetic Field to an Orbiting Satellite.

HEAO-C spacecraft. As illustrated here the trajectory-tracing technique was used to determine cosmic ray orbits and cutoffs in the earth's magnetic field as modelled by the International Geomagnetic Reference Field 1975.0 modified to Epoch 1980.0 by use of the secular drift coefficients. Cosmic ray trajectories were computed at selected geographic grid intervals over a satellite orbit at 400 km. The definition of the solid angle of access at each grid location was accomplished by an azimuthal scan every 20 degrees in zenith up to zenith angles of 120 from the vertical direction. Early work to define the range of the solid angle of access did not find any allowed orbits at zenith angles of 140 from the vertical. Cutoff rigidity calculations were made for 67 different directions for each of 108 grid points, selected at 10 latitude intervals between 40 N and 40 S, and equi-spaced at 30 longitude intervals at each latitude. The objective of these cal-

culations was to provide basic information from which cutoffs at other points and directions could be interpolated.

An important effect was noted in the access of cosmic rays to orbiting satellites. From westerly directions cosmic rays may gain access to a spacecraft orbiting at 400 km from zenith angles up to 135° from the vertical. The V × B force allows these cosmic-ray charged nuclei to drop below the spacecraft horizon and have their paths bend upward, intersecting the spacecraft from below. Cosmic-ray geomagnetic cutoffs, ordered by the magnetic arrival direction, fold over smoothly about zenith angle 90° in westerly directions. In the magnetic west direction, the cutoff rigidity for a magnetic zenith angle of 60° is the same as the cutoff rigidity for a magnetic zenith angle of 120°.

For some types of spacecraft measurements it is important to be able to define the directions forbidden by the solid earth. The cosmic-ray shadow of the solid earth does not correspond to the solid angle subtended by the earth from the spacecraft position because of the bending of the charged-particle cosmic-ray trajectories in the geomagnetic field. From the general direction of the magnetic west (having a strong dependence on latitude) there is a "transmission notch" in the area forbidden by the solid earth that is the result of the $\overline{V} \times \overline{B}$ force "lifting" the cosmic ray trajectory up from the solid earth. The change in position and width of this "transmission notch" is shown in the figure, where the cosmic ray sphere of access to a satellite has been mapped onto two dimensions with an orthographic projection. The white areas of each of these projections indicate that cosmic rays of some energy have access to a spacecraft orbiting at 400 km. The dark areas around the nadir indicate directions where cosmic rays of all energies are forbidden by the solid earth. The apparent sharpness of the "transmission notches" is an artifact resulting from dividing the sphere of access into 67 segments and letting the access at the center of each segment typify the entire segment. The variation in the width and position of these "transmission notches" results from the different size of the cosmic-ray shadow generated by the solid earth, which has its geocenter displaced about 450 km from the effective magnetic center.

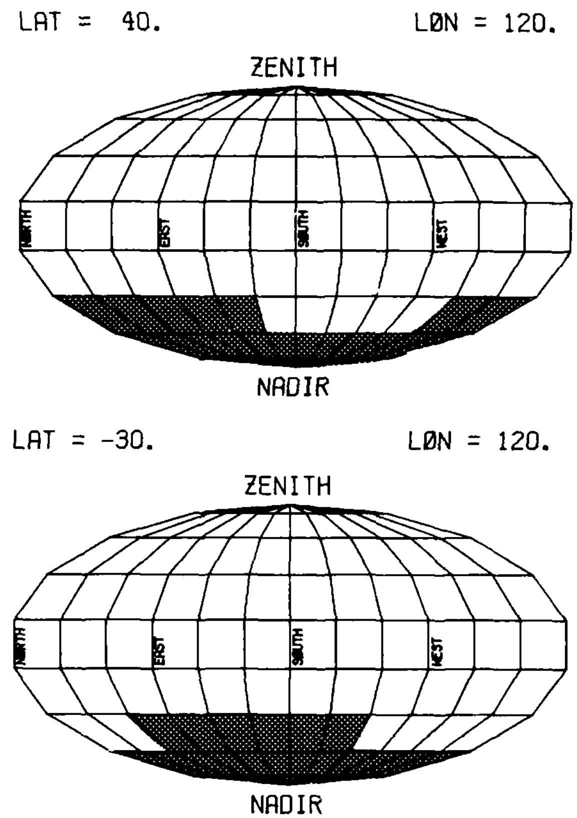

Orthographic Projection of the Three Dimensional Sphere of Cosmic Ray Access to a Spacecraft at 400 km. Zenith directions are indicated by parallels drawn every 20°; azimuthal directions, by meridians drawn every 30°. North (azimuth of 0°) is at the left of each projection; south (azimuth of 180°) is the center meridian line. White segments indicate that cosmic rays at some energy are allowed; shaded segments, that cosmic rays of all energies are forbidden.

Charged Particle Access to the Earth's Surface: In continuing research activities of particle propagation in the geomagnetic field, inconsistencies were noted in utiliz-

ing older published values of cosmic-ray cutoff rigidities for the analysis of cosmic-ray latitude survey data acquired in 1974 and 1975 (AFCRL-TR-74-0550). When these survey data were analyzed using cutoff rigidities calculated by AFGL scientists using a 1975 geomagnetic field model, these inconsistencies were considerably reduced. The results of this study show that cosmic radiation measurements are now of sufficient precision that the secular variations in the geomagnetic field must be considered in the analysis of cosmic ray data.

In collaboration with scientists from the University of Bern, Switzerland, a theoretical study has been conducted on the propagation of relativistic particles in the geomagnetic field during major geomagnetic storms. A mathematical model of the disturbed geomagnetic field was developed by including partial ring currents in the magnetosphere, and the trajectories of relativistic charged particles through this field configuration were calculated by numerical methods. The initial results of this study show that during major geomagnetic disturbances particles of considerably lower energy can be detected at selected geomagnetic latitudes than is possible during quiescent geomagnetic conditions.

New Passive High-Energy Proton Detectors: Methods of revealing the tracks of 1-10 MeV protons in a plastic track detector have been developed. Allyl diglycol carbonate (con nercially available as CR-39) has been shown to record 1 to 10 MeV protons at near normal incidence when etched in hot sodium hydroxide. The recorded tracks are clear and unambiguous, with the diameter a sensitive function of incident proton energy. A clear visual difference is seen between say 2 and 3 MeV protons, and resolution by measurement is a small fraction of a mega-electron-volt.

In recent years solid-state nuclear-track detectors have found widespread application. The production of tracks by energetic ions in insulating materials is a widely used technique for detection and identification of these ions. The use of these detectors has been shown to be very successful in the study of very heavy primary cosmic rays and the recording of fission fragments. The possibility of their application to detect protons has also been explored. Cellulose nitrate (CN) plastic has previously been used as a detector to record protons; however, CN is inhomogeneous and anistropic with regard to its physical characteristics. These defects manifest themselves in non-geometrical track profiles, differences in sensitivity in a given sheet, and variations in bulk etch rate. The use of plastic sheet cast from CR-39 monomer with excellent etching properties, high sensitivity, and high uniformity as a nuclear track detector was reported recently. This material was found to have a lower detection threshold than CN and a smaller variation of response to particles of a given ionization rate than Lexan polycarbonate. Commercially available, CR-39 is capable of recording protons of 10 MeV and below as well as 70 MeV alpha particles.

Cosmic Ray Exposure: A one square meter array of CR-39 plastic track detector was exposed to the cosmic radiation aboard a balloon (AFGL Designation H79-29) launched from Eielson Air Force Base, Alaska, on June 19, 1979. After a float altitude of 128,700 feet was reached, a squib was fired to shift a spring-loaded sliding plate to a new position, allowing cosmic-ray iron tracks which penetrated at float altitude to the main stack below to be separated from tracks which penetrated during the ascent phase. An attempt to stabilize and orient the payload utilizing a biaxial magnetometer combined with an electrical rotator was unsuccessful. The failure to maintain orientation during the flight required simple average mathematical assumptions to evaluate the effective solid angle for incident particles.

Final termination of the flight was about 200 miles west of Eielson AFB, with a total cosmic ray exposure of 3 hours, 29 minutes. The float altitude was maintained ± 700 feet during the 3 ½ hour period, this altitude corresponding to a vertical air mass of about 3 grams/cm^2 overhead.

The CR-39 plastics are being scanned for stopping cosmic-ray iron nuclei. The analysis should provide an accurate flux determination at this period near the maximum of the solar cycle when the expansion of the solar magnetic fields shields the earth from many of the low-energy cosmic rays.

A determination of the cosmic-ray iron flux is essential to an understanding of anomalies which have occurred in electronic computer memory elements on various satellites. Current accelerator studies of these anomalies indicate that energetic iron nuclei are capable of tripping micro-electronic memories. Results from this study will also be used to evaluate the background cosmic radiation buildup in a CR-39 track detector from cosmic radiation. The CR-39 material is being evaluated for use on the Long Duration Exposure Facility to be launched on the space shuttle.

Generalized Geometric Factor: A new method of computation of the generalized geometric factor for the response of electronic counters to the complex angular distribution of trapped particles has been developed. This method allows the correct perpendicular fluxes ($j_\perp$) to be computed from the observed count rates even at low altitudes when the trapped mirror planes are more narrow than the detector opening angles. Monte Carlo methods allow even the most complex geometric factors to be considered.

This Generalized Geometric Factor, G(n, λ), was formulated taking into account the anisotropy of the trapped radiation in analyzing the trapped proton data obtained by the instruments on board the U.S. Air Force Satellites S3-2 and S3-3. The detectors were the proton-alpha telescopes and the low-energy proton spectrometer. These instruments were designed to detect trapped protons of energies ranging from 0.1 to 6 MeV. Numerical and Monte Carlo methods were used to evaluate this factor. The results were applied to the reduction of the trapped proton data in the energy range above 100 keV. Since the factor depends on the radiation's anisotropy and the effective area of the detector system, these specific numerical values are applicable only to our data. However, the formulation of the factor and its variation with the index of the pitch-angle distribution as well as the spin-geomagnetic angle clearly illustrate the significance of the data-analysis and the conditions of the data collection performed by satellite-borne telescopes.

Low-Energy Electron Studies: AFGL has a major program to design, construct, calibrate and install a series of electrostatic analyzers, the SSJ/3, on DMSP (Defense Meteorological Satellite Program) Block 5D, flights 2, 3, 4 and 5. After the real-time data use for operational purposes, AFGL is currently analyzing the resulting data. The results of these analyses will be improved substorm models and better understanding of the mechanisms and sources of particle acceleration for investigating the possibility of specifying geomagnetic activity in real time.

Each J/3 package consisted of a set of two electrostatic analyzers which performed a differential energy analysis of electrons over the energy range from 50 eV to 20 keV. The analyzers were of the curved plate type and utilized channel electron multipliers to detect electrons of select energy ranges. A 16-point spectrum was produced each second. To protect the multipliers, a sun sensor was utilized to turn off the package when the sun was in the field of view. Calibrations for units 2 and 3 were performed at the Aerospace Corporation and results were compared

with a Monte Carlo computer simulation of the instrument. The two were in excellent agreement. Units 4 and 5 were calibrated using the more sophisticated beam facility at Rice University, where energy bands and geometric factors were determined. Delivery of the SSJ/4 package for the DMSP flight 6 has been completed. This unit provides the full electron analysis capability of the J/3 package, plus a similar capability for proton analysis.

Variations of this highly successful design have also been utilized for other programs. Two sets of two electrostatic analyzers, comprising the CRL-251 High Altitude Particle Spectrometer payload, were flown aboard AF satellite P78-1, launched on February 25, 1979, into a polar, circular sun-synchronous orbit at an altitude of approximately 600 km. The launch put the satellite into the noon-midnight meridian plane at an inclination of 97.73°. At launch, its period of revolution was 96.54 minutes. The satellite consists of a wheel section and a sail section.

Each set of analyzers has a low energy analyzer (50 eV to 1 keV) with eight energy channels and a high energy analyzer (1 to 20 keV) with eight energy channels. The two sets are placed 90° apart on the rim of the wheel section of the satellite, looking radially outward along the x and y axis of the wheel section. The spin axis is perpendicular to the plane of the wheel. The spin rate is 11 ± 1 rpm, the analyzers going through the full pitch angle cycle in 5.45 seconds. The four analyzers are swept simultaneously every 256 milliseconds. Thus, for each wheel spin each detector gives nearly 22 sixteen-point spectra.

The experiment has functioned normally since launch and is producing high-resolution pitch-angle data near the midnight and noon regions of the auroral ovals as well as in the polar cap regions. The data are being processed to study storm times, comparisons with DMSP electrocard optical data and SCATHA particle data.

Another version of the J/3 package has been delivered to the European Space Agency (ESA), and been integrated on the European METEOSAT-B satellite. The METEOSAT-B satellite launch has been delayed for about one year due to problems with the Ariane rocket. This satellite will be placed in a geostationary orbit and will act as a weather satellite for Europe.

The purpose of the AFGL sensor is to monitor the 50 eV - 20 KeV electron environment and to serve as a diagnostic tool for analyzing spacecraft anomalies. It will also provide useful correlative information when analyzed in conjunction with identical instruments on board DMSP satellites.

Auroral Boundary Studies: Over the past two years we have conducted an extensive program to study the location of the equatorward boundary of electron precipitation in the auroral zone and its variation with magnetic local time, with geomagnetic activity as measured by the magnetic index Kp, with solar wind speed, V, and the north-south component of the Interplanetary Magnetic Field (IMF), as a function of season and as a function of universal time. The equatorward boundary represents the mapping into the earth's ionosphere of the inner edge of the plasma sheet. Since the position of the inner edge is controlled by the large-scale convection electric field, a study of the equatorward boundary provides important information on the dynamics of the magnetosphere.

Approximately 18,000 boundaries of the oval were determined from plots of the data from the SSJ/3 electron detectors flown on the DMSP satellites. The boundaries were separated into one-hour zones in magnetic local time (MLT) with good coverage in 20 of 24 zones. In all zones the boundaries are found to move to progressively lower latitudes linearly as a function of increasing Kp. Linear correlation coefficients were generally greater than 0.8. The boundaries were found to move

equatorward similarly as a function of decreasing values of VB_z for values of B_z less than one nanotesla (nT), where V is the solar wind speed and B_z the north-south component of the IMF. (The nanotesla is the SI unit having the same magnitude as 1 gamma in the older nomenclature.) The linear relationship was weaker with VB_z than Kp, with correlation coefficients typically in the range from 0.6 to 0.7. For both Kp and VB_z the location of the boundary was projected into the equatorial plane of the magnetosphere and fitted to existing models of the magnetospheric electric field. This yielded an equation for the magnetospheric electric field parameterized in Kp and VB_z. The cross magnetospheric potential calculated from these equations was found to be in excellent agreement with measurements of the cross polar-cap potential. Such agreement argues strongly for the validity of the equations and for their use in modeling the magnetosphere.

In addition, the model clearly shows that the magnetosphere in its interaction with the solar wind and IMF acts as a half-wave rectifier. When Kp is small, or B_z is greater than 1 nT, the electric fields in the solar wind and magnetosphere do not couple directly and the magnetospheric electric field is small. For Kp greater than 2 and B_z less than 1 nT the two electric fields do couple directly and the magnetospheric electric field increases linearly with the solar-wind electric field.

In-Situ Measurements of Field-Aligned Current Systems: Experiments on board the polar-orbiting Air Force satellite, S3-2, provided, among others, measurements of the ambient vector magnetic field, the electric field and the fluxes of precipitating electrons in the energy range from 80 eV to 17 keV. The bulk of the data analyzed was taken in the ionosphere above the polar cap and the auroral ovals in the altitude range from 240 to 1560 km. Electrons were detected with a parallel-plate electrostatic analyzer which was mounted in the spin plane of the spacecraft, allowing it to sample through a full range of pitch angles. The instrument comprised of 32 energy bins swept through a complete spectrum in one second. The magnetic field components were measured with a triaxial fluxgate magnetometer whose sensor was extended 20 feet out from the spacecraft on the tip of an Astromast boom. By using an automatic ranging current source in conjunction with the magnetometer, a resolution of 5 nT was obtained in each of the field components despite a dynamic range of $\pm$ 64,000 nT. Deviations in the transverse (i.e., east-west) component of the magnetic field have been interpreted in terms of field-aligned current sheets which connect the horizontal currents flowing in the auroral ionosphere to their source regions deep in the magnetosphere.

The S3-2 magnetic field measurements were compared with similar measurements taken on the Triad satellite in several nearly coincident passes in the northern dawn-sector of the polar region. Such dual observations have made it possible to determine further characteristics of field-aligned (Birkeland) current sheets. They are spatial in nature, extending at least up to 1100 km in longitude, and are oriented very closely to the magnetic east-west direction. They do not show pronounced gradients with longitude. The current sheets move slowly in the north-south direction with velocities less than 0.15 km/sec. The major portion of the Region 1 (i.e., poleward portion) field-aligned currents was located equatorward of the convective electric field reversal, indicating that, for the most part, they exist on closed field lines.

Several consecutive orbits of the S3-2 satellite provided simultaneous measurements of magnetic and electric fields and auroral electron fluxes during a major magnetic storm when Kp reached a level of 8-. During such times of extreme magnetic disturbance, integrated precipi-

tating electron fluxes in excess of 5 x 10^9 electrons/cm^2-sec-sr were observed, as were field-aligned current densities approaching 20 μ A/m^2, and electric field intensities near 100 mV/m. Some of the principal results for these measurements are: (1) The observed direction of the electric field component indicated closure of the major field-aligned current pattern by Pedersen current flow in the ionosphere, consistent with a magnetospheric current source. (2) Values of the height-integrated Pedersen conductivity, calculated from the gradients of the electric and magnetic field components, were typically in the range from 10-30 Ω^{-1} in the current-carrying regions during active times. At such times particle precipitation on the nightside became the major factor in controlling the magnitude of the ionospheric conductivity, outweighing the influence which sunlight has in quiet times. (3) In regions of increased fluxes of precipitating electrons in the nightside auroral oval, current densities calculated from electron fluxes in the energy range from 0.08 to 17 keV accounted for up to 50 percent of the upward currents, increasing to better than 70 percent during the most intense substorm period.

DEFENSE METEOROLOGICAL SATELLITE PROGRAM

Topside Ionosphere Plasma Monitor: The Space Physics Division has developed, and will be supplying, a series of Topside Ionosphere Plasma Monitor instruments for flight on the Defense Meteorological Satellite Program (DMSP) Block 5D-2 satellites. The instrument, designated SSIES, will provide critical information about the characteristics of the space plasma above the peak of the F region as re-

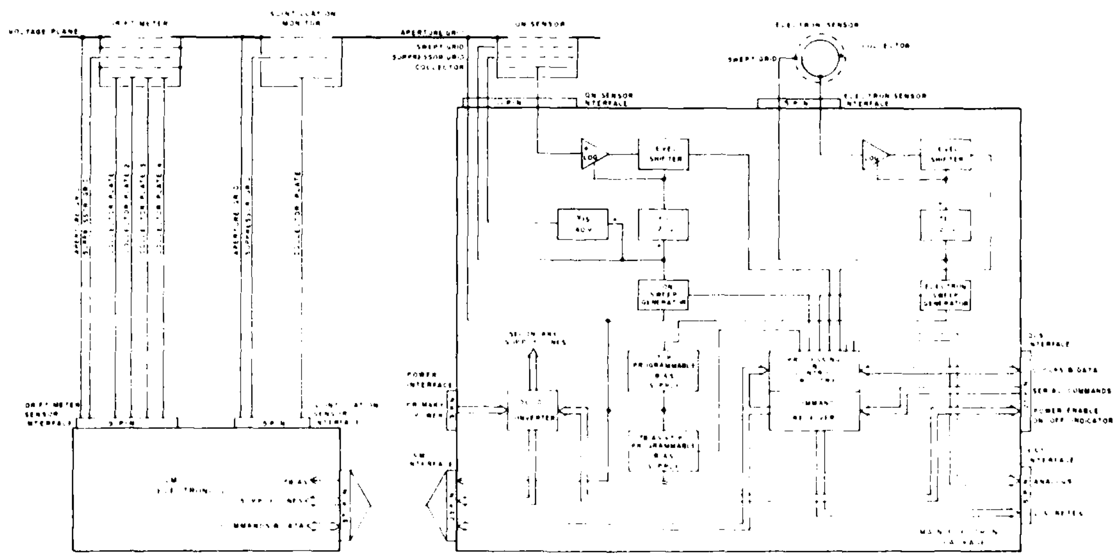

SSIES System Block Diagram.

quired for Air Force and communication systems.

Four electrostatic probes will measure ion and electron temperature, electron density, average ion mass, satellite potential, the power spectrum of irregularities, and two components of the ion drift-velocity vector known to be associated with concentration irregularities that cause scintillations of radio signals over a wide frequency range. In addition, the instrument will measure the polar wind on a routine basis to establish its morphological behavior.

The main features of the SSIES system are shown in the system block diagram. Control grids within the electron and ion sensors are biased and periodically sweep through small voltage ranges to determine the temperature and density of the particles collected. To produce meaningful data, these grids must be biased at a potential somewhere near that of the plasma with respect to the spacecraft. These bias potentials are determined by analysis of the data on the ground and are set by ground command; under certain operating modes, the electronics package will determine and set the bias potential automatically. In addition, the main electronics will analyze the sweep data and calculate the density and temperature of the detected electrons, hydrogen ions, and oxygen ions. At all times, the raw sensor data will be transmitted to ground stations for verification of on-board calculations.

Precipitating Particles Analysis: The Space Physics Division routinely provides electron and ion analyzers for the Defense Meteorological Satellite Program (DMSP). A new improved sensor package has been developed. The new instrument, designated SSJ 4, can measure both electrons and ions at twenty discrete energies between 30 eV and 30 keV once per second. The detectors are used by the Global Weather Central of the Air Weather Service to monitor the location and intensity of the auroral zone. To this end the Space Physics Division has developed software techniques for the Air Weather Service to use the data from the SSJ/4 sensors in near real time. The algorithm developed enables the Global Weather Central to determine the equatorward extent of the auroral oval with high accuracy: approximately 1° on the evening side of the oval and approximately 2° on the morning side of the oval.

In addition, the Global Weather Central has the need to extrapolate the global position of the oval from the measurements made by the SSJ 4 sensor at a point. To do this the Space Physics Division completed a large-scale statistical study of the variation in the location of the equatorward boundary with magnetic local time, activity, and the orientation of the Interplanetary Magnetic Field (IMF). Approximately 20,000 boundaries were scaled by hand.

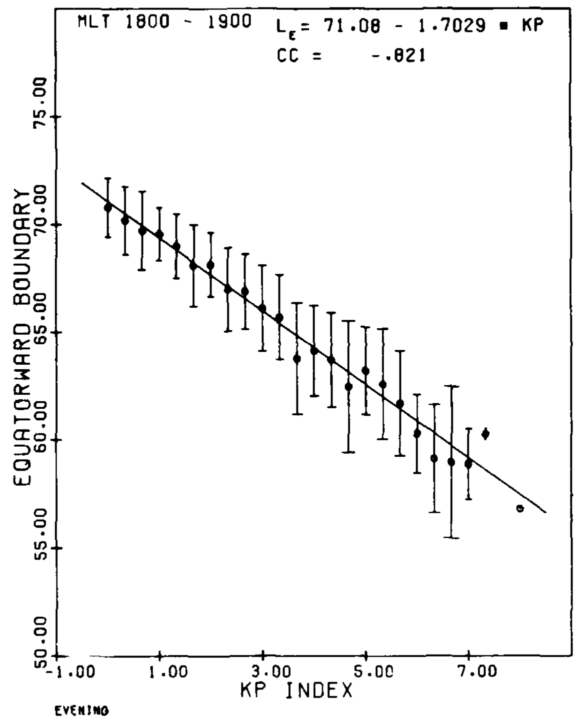

Field-aligned Currents and Electric Fields as seen by Polar Orbiting Satellite in Dawn-dusk Meridian.

The boundaries were separated by magnetic local time into one-hour zones. Within each zone, the location of the boundary was tested for correlations with Kp, the Z component of the IMF, the velocity in the solar wind times the Z component of the IMF, the square of the Z component, and the solar wind velocity times the square of the Z component. The correlations with Kp were very high. In the figure we show a typical example of the correlation with

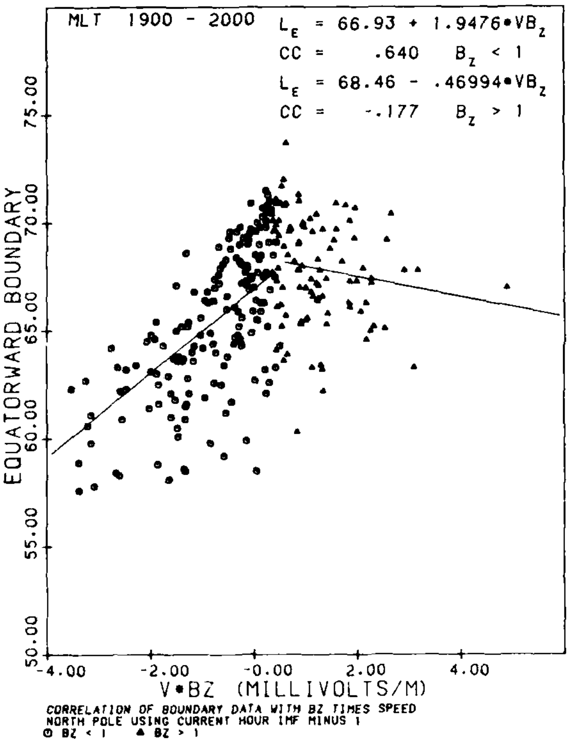

Idealized Electric Field and Magnetic Perturbation Measurements for Currents and Fields Shown in the Preceding Figure.

Kp, where the mean and standard deviations for the boundaries are determined. The line represents the linear least-squares-fit to the data. The equation for the line and the correlation coefficient are printed in the upper right hand corner. The coefficients approached -0.9 in the evening sector (1600 to 2400 magnetic local time) and were between -0.7 and -0.8 in the morning sector (0400 - 1200 MLT).

For quantities in the solar wind and IMF, the boundary correlated best with the solar wind velocity times the Z component of the IMF, when the correlation was limited to cases where the Z component was less than 1 nanotesla (nT). Above 1 nT, the correlation was weak or nonexistent. An example is shown in the figure for the magnetic local time 1900 to 2000. The two straight lines are the linear least-squares-fit to the data above and below 1 nT. The equations for the two lines are shown in the upper right hand corner. The break in behavior at 1 nT is consistent with the half-wave rectifier model of the magnetosphere; below 1 nT the magnetosphere and IMF are coupled and the solar wind and IMF drive the magnetosphere, while above 1 nT they are decoupled.

Equations relating the boundary position to Kp have been determined for all magnetic local time zones. From a single DMSP pass, the position of the oval boundary can be determined. By inserting this figure into the equation for the magnetic local time in which the boundary was determined, a provisional Kp can be calculated. This value, in turn, can then be inserted in the other equations to give the global specification needed.

Ionospheric Research From the DMSP and Other Satellites: In this subsection two topics are treated: (1) progress in identification of the large-scale electric field patterns in the polar ionosphere and their relationship to the orientation of the interplanetary magnetic field; (2) progress in the characterization of discrete, sun-aligned arcs in the polar cap.

Previous work on classifying the electric field pattern is summarized in the figure. The five classes shown are:

Type A: Uniform electric field across the polar cap observed with the OGO-6 satellite only in the northern (summer) polar cap.

Type B: Strong electric field near morn-

ing (evening) flank of the northern (southern) polar cap.

Type D: Strong electric field near the evening (morning) flank of the northern (southern) polar cap.

Type F: Strong electric fields along the flanks of the polar cap with weak fields in the central polar cap.

Type I: Irregular fields across the polar cap.

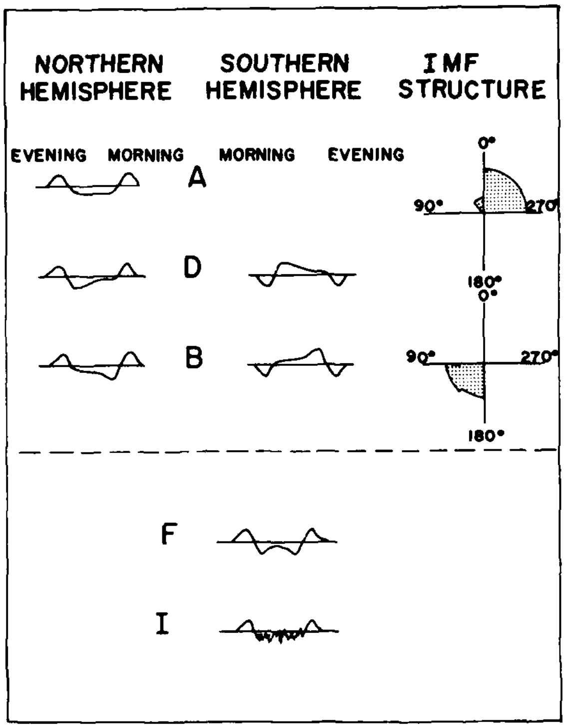

Types of Electric Field Patterns Observed by OGO-6 and Their Dependence on IMF B_x and B_y.

Types A and D (B) were found only when the Interplanetary Magnetic Field was pointed toward (away) from the earth.

During the last three months of 1976, the S3-2 satellite orbit was close to the dawn-dusk meridian. Data from this period were used to analyze the large-scale electric field patterns. The figure shows scatter plots of the patterns observed in S3-2 data as a function of the X and Y

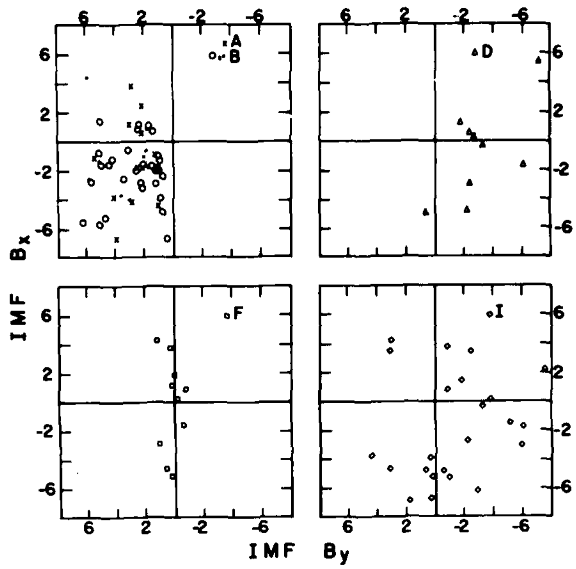

Scatter Plot of Convective Electric Field Patterns Observed by S3-2 as a Function IMF B_x and B_y.

components of the Interplanetary Magnetic Field. It is seen that types A and B are found only when the Y component is greater than 0. For both OGO-6 and S3-2, A-types are found only in the summer hemisphere and are associated with the IMF polarity that tends to produce strong electric fields along the evening flank of the polar cap. The occurrence ratio of A to B in S3-2 data was 2:1; the A-to-D ratio was 3:1 in the June, 1969, OGO-6 data. The dependence of D-types on the Y component of the IMF (upper right plot) agrees with OGO-6. The type F patterns were found when $B_y \sim 0$. The distribution of B, D and F patterns tends to confirm the critical role of the Y component. A survey of S3-2 measurements shows that A, B, D and F types are found when the Z component was less than 0.5 nT. Type I shows no correlation with X or Y components. The highly irregular electric fields are found only when the Z component was greater than 0. Type I patterns are further discussed below in connection with polar cap arcs.

An example of an electric field pattern

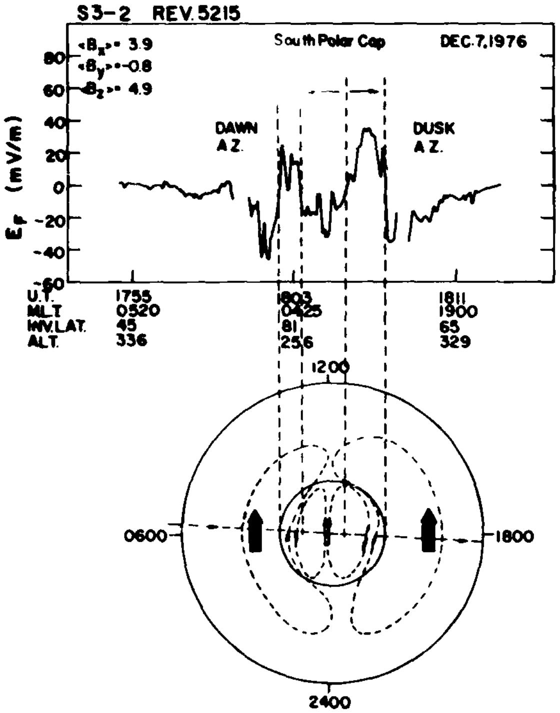

Example of Sunward Convection. Dusk-to-Dawn Electric Field in the Central Polar Cap During a Period of Northern IMF.

which was found in approximately half the summer polar-cap passes of S3-2 when the Z component of the IMF was greater than 0.7 nT is shown in the figure. During the S3-2 Rev 5215 southern high latitude pass, the Z component was found to equal 4.9 nT. As expected for driving sunward convection in the auroral oval, the electric field was directed from dusk to dawn. At the poleward boundary of the oval, the electric field reversed polarity, becoming dawn to dusk near the morning and evening flanks of the polar cap. Within the central polar cap, the electric field was directed from dusk to dawn. Sunward convection in the central polar cap is inconsistent with a viscous interaction model. Sunward convection in the summer polar cap during periods of northward B_z is consistent with ground magnetometer and laboratory simulation results.

Polar Cap Arcs: Investigations of discrete arcs in the polar cap have shown that polar cap arcs tend to be sun-aligned and are most frequently observed during periods of magnetic quieting when the interplanetary magnetic field has a northward component. Visible arcs are caused by precipitating electrons with energies of $\leq$ 2 keV. Another class of subvisual arcs are produced at the altitude of the iono-

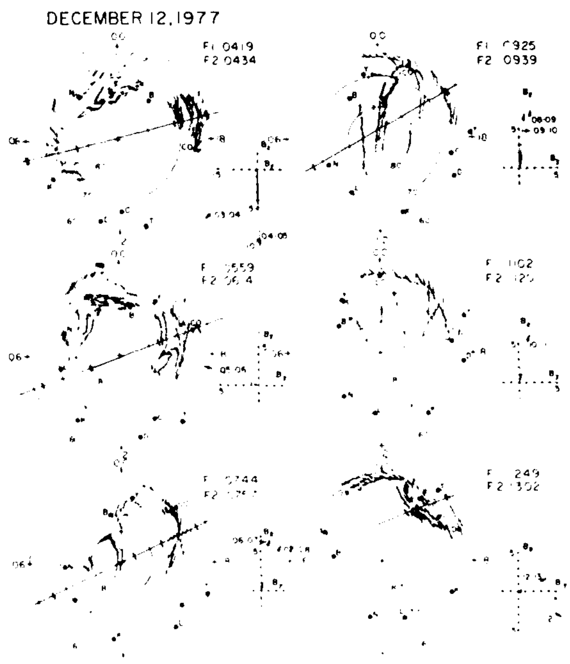

Cartoon Representation of Sequential DMSP High Latitude Imagery on December 12, 1977.

sphere F layer by electrons with energies of a few hundred electron volts. Here we illustrate many of the known characteristics of polar cap arcs using data from the USAF satellites S3-2 and DMSP (Defense Meteorological Satellite Program). At the times of interest, both satellites were in orbits close to the dawn-dusk meridian. Satellite S3-2 measured the electric and magnetic fields, and the fluxes of electrons with energies between 80 eV and 17 keV.

DMSP satellites are stabilized in three axes and are in circular, sun-synchronous orbit at an altitude of 840 km. All DMSP satellites are equipped with scanning, optical imagers. Some, but not all, are also equipped with spectrometers that look toward local zenith and measure fluxes of electrons with energies between 50 eV and 20 keV.

The accompanying cartoon represents, in magnetic latitude and local time, composites of visible imagery from DMSP/F1 and DMSP/F2 taken over the northern hemisphere during a period of magnetic quieting on December 12, 1977. Solid, straight lines give the portions of F2

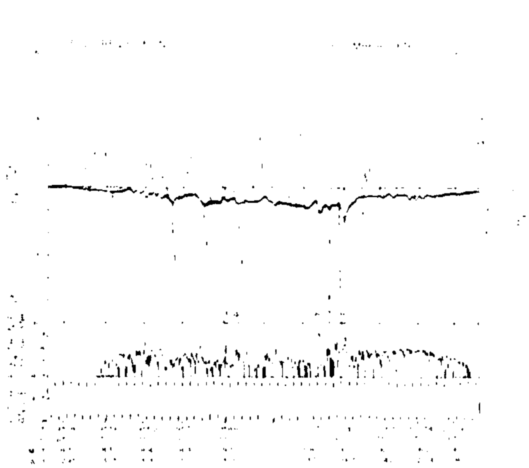

Top Panel Gives the Dawn-to-Dusk Electric Field Component and the Transverse Magnetic Field Deflection (heavy line). Bottom Panels Give the Directional Electron Flux and Pitch Angles. Data were taken over winter polar cap with IMF B_z northward.

trajectories during which electron data were taken. To the right of each cartoon, the hourly average values of the interplanetary magnetic field Y and Z components are shown. During the initial period of southward Z component, the polar cap was clear of visible emissions and only uniform, polar rain fluxes were detected. Approximately one hour after the IMF turned northward, sun-aligned arcs were found in the polar cap. Polar cap arcs persisted until the interplanetary magnetic field again turned southward. An hour after a second northward turning of Z components, arcs returned to the polar cap. The sun-aligned arcs were embedded in a region of high-density ($\sim$ 0.1 cm^{-3}) polar rain. Within the arc, the up-looking DMSP spectrometer detected three spectral components: a cold (100 eV) high density (1.5 cm^{-3}) population, a peaked primary distribution with a temperature of 350 eV that had been accelerated through a potential drop of $\sim$ 750 V, and a secondary and/or degraded primary population. Burch et al. found that over polar showers the low-energy component was highly field-aligned. The secondary and accelerated primary populations were nearly isotropic in pitch angle.

A plot of the electric field, the deviation in the magnetic fields, and the directional flux of electrons (cm^2-sec-ster)$^{-1}$ and electron pitch angles measured during S3-2 Rev 5231 are given here as functions of invariant latitude, magnetic local time and altitude. The pass occurred while the satellite was near apogee over the north polar cap, where it passed within 1° of the magnetic pole along the dawn-dusk meridian. The X, Y and Z components of the interplanetary magnetic field were -3.4, 3.8, and 7.4 nT, respectively. As compared with the idealized uniform polar cap fields, the electric and magnetic signatures were highly irregular. In the northern hemisphere a positive electric field corresponds to sunward convection and the field-aligned current is out of the ionosphere in regions where the deviations in the magnetic field have a negative slope. Eight regions of negative slope in the deviation of the magnetic field accompanied by enhanced electron fluxes are noted here. As evidenced by their being embedded in polar rain, at least events 3 through 7 lie in the polar cap.

Event 6 was analyzed in detail. The

field-aligned current out of the ionosphere was found to have an intensity of 2.8 μA/m^2. It was carried by electrons with a temperature of 200 eV that had been accelerated through a potential drop of ~ 1 kV. A nearly isotropic pitch-angle distribution of electrons across event 6 suggests a field-aligned potential drop extending for large distances along B. The measured electron energy fluxes of 2.5 ± 0.5 ergs cm^{-2}-sec-ster were sufficient to produce a visible arc. The figure gives an idealized, two-dimensional projection of the electric fields and currents associated with event 6. As predicted by Lyons, the arc is in a region of negative electric-field divergence.

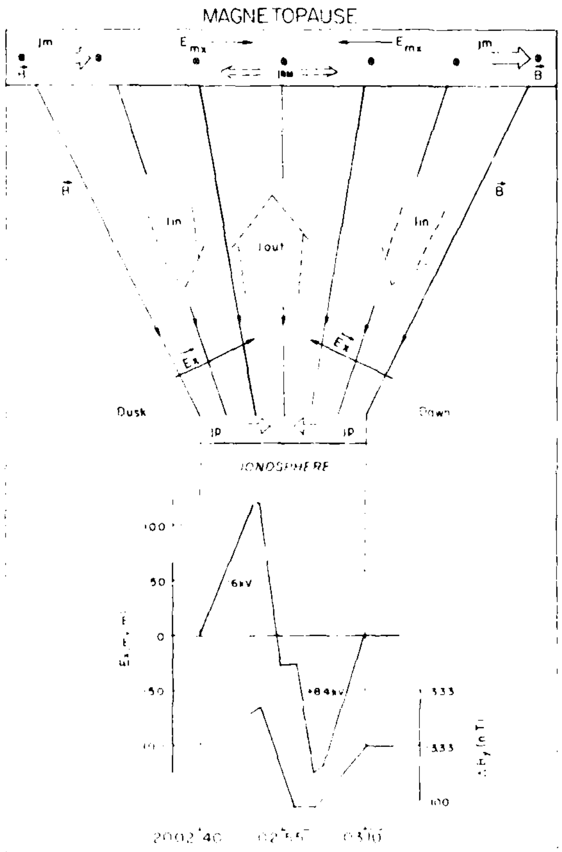

Idealized Two-Dimensional Projection of Electric Fields and Currents in Vicinity of Event 6 in the Preceding Figure

Electric Field Instrumentation: The Space Physics Division supplied electric field instrumentation to be flown on one of four rocket payloads to be launched from the Poker Flat Research Range, Fairbanks, Alaska, during March, 1981.

IONOSPHERIC EFFECTS RESEARCH

Statistics and Morphology of Signal Scintillation: Experiments on a near global scale have been performed to determine the characteristics of transionospheric signals which undergo heavy scintillation. In December 1979, a combined air and ground campaign was initiated at Goose Bay, Canada, Thule, Greenland, and Ascension Island. The ground results in the auroral and polar regions showed the presence of a moderate amount of scin-

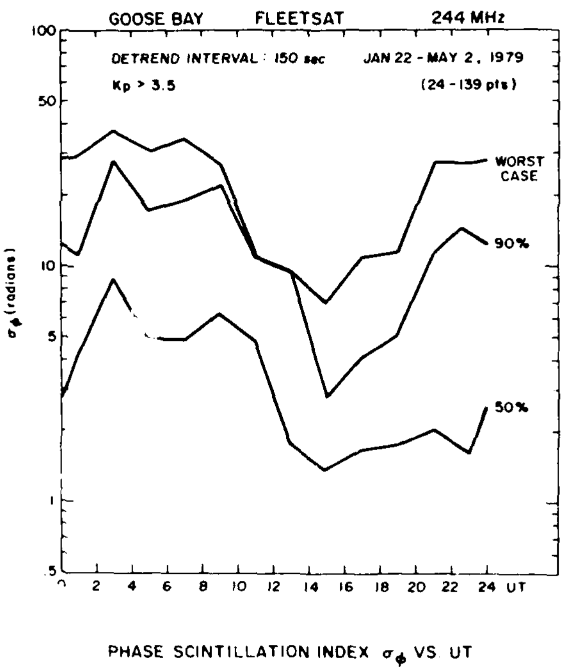

Diurnal Variation of Phase Scintillation at Goose Bay, Labrador.

tillation, indicating a slightly disturbed ionosphere at Goose Bay, with a much more disturbed ionosphere at Thule, and consequently a great deal heavier scintillation. For the first time, phase-scintillation measurements were taken on the ground using a three aerial baseline at both locations. Complications in the data-recording reduction and analysis processes have delayed the publication of results from the polar and auroral experiments, but early findings include rapid phase fluctuations of up to 20 radians.

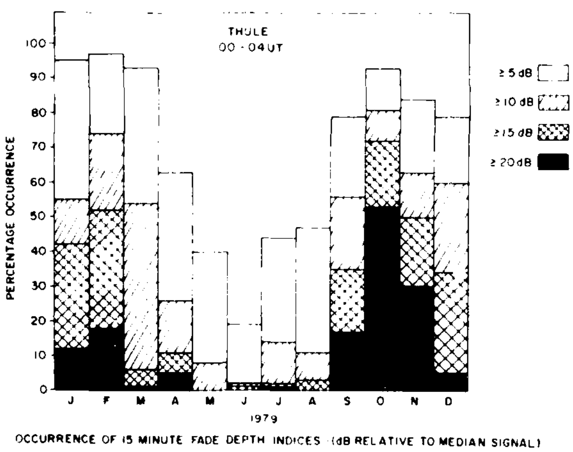

Occurrence of Scintillation at Thule, Greenland, 00-04 UT, 1979.

From other campaigns and on-going experiments, a statistical analysis of a year's data (1979) has shown maximum occurrence of scintillation greater than 20 dB (at 244 MHz) during the month of October and minima during May, June, and July. The overall distribution was generally bimodal (data for Thule given here). Statistics compiled in the same way for Goose Bay, Canada (see figure), failed to show the October maximum, and showed much lower probability of occurrence overall. The May, June, and July minima were obscured during daytime hours, possibly indicating the effects of E-region activity.

Perhaps the most interesting result of the December 1979 experiment was the discovery of an extremely irregular ionospheric structure near Ascension Island. During the Apollo experiment of 1970, signals from Ascension Island were reported to have undergone scintillation which was unprecedented for its frequency regime (2200 MHz). During the December, 1979, campaign, signal scintillation of up to 30 dB was found at 1541 MHz (see figure) when Marisat was observed at very high elevation angles from Ascension. These data can be compared with the data from Natal, Brazil, or Huancayo, Peru, where scintillation was never found in excess of 8 dB.

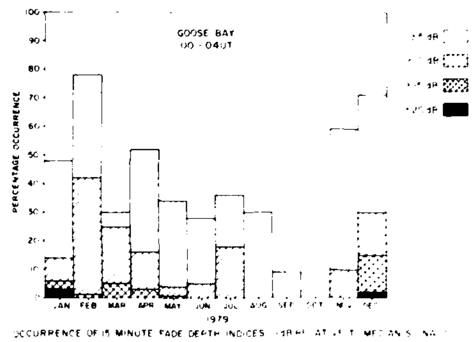

Occurrence of Scintillation at Goose Bay, Labrador, 00-04 UT, 1979.

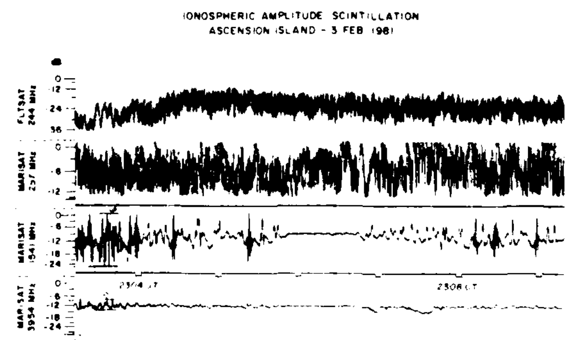

Example of Intense Scintillation at Ascension Island.

It has long been known that the irregu

AD-A126 004 REPORT ON RESEARCH AT AFGL JANUARY 1979-DECEMBER 1980 2/3
(U) AIR FORCE GEOPHYSICS LAB HANSCOM AFB MA
A B MCGINTY APR 82 AFGL-TR-82-0132

UNCLASSIFIED F/G 5/1 NL

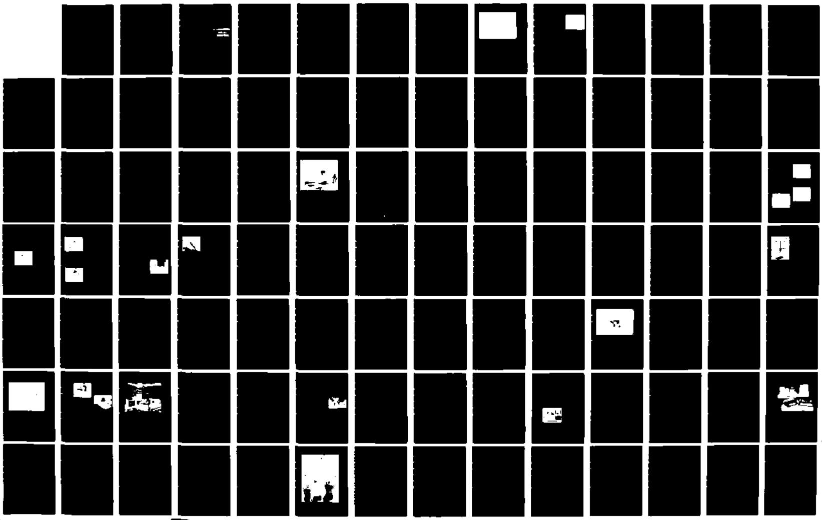

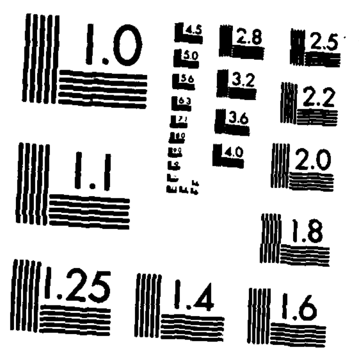

MICROCOPY RESOLUTION TEST CHART
NATIONAL BUREAU OF STANDARDS-1963-A

lar ionosphere varies diurnally, seasonally, latitudinally, and, most recently, longitudinally. Scintillation occurrences at Huancayo, Peru, Natal, Brazil, and Accra, Ghana, have been compared with Guam data supplied by the Naval Ocean Systems Center. All the observatories in the African/American zone exhibit similar occurrence patterns. Huancayo is typical of this group and is compared with Guam here. Guam leads or lags by six months. While Huancayo showed a minimum of occur-

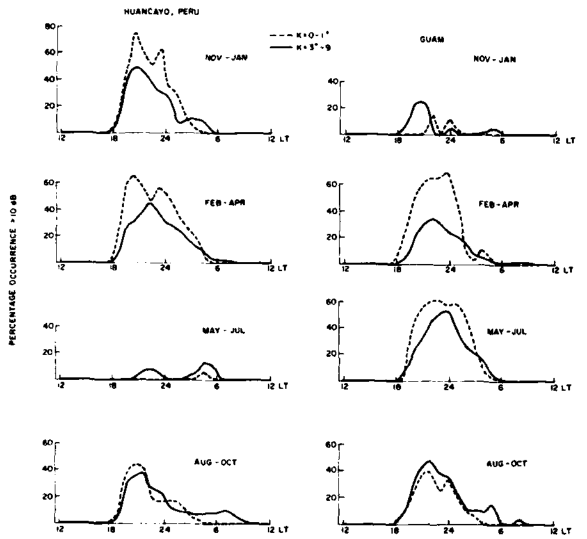

Comparison of Occurrence of Strong Scintillation at Huancayo, Peru, and Guam, March, 1978, to June, 1979, for Low and High Magnetic Index.

rence during May, June, and July, and showed a maximum in November, December, and January; Guam showed a minimum in November, December, and January, with a maximum in May, June, and July (see figure). As of this writing, the precise initiating mechanism for the generation of the regions of irregularities has not been observationally verified, nor has the reason for such pronounced longitudinal effects as those described been found.

Goose Bay Ionospheric Observatory: Real time support to the 414L Over-the-Horizon Backscatter Radar System has been a principal focus for activities at the AFGL Goose Bay Ionospheric Observatory (GBIO) during the period. The Electronic Systems Division 414L System Project Office has been conducting a Systems Performance Test (SPT) of the Experimental Radar System (ERS). The Transmitter site and the Receive-Operations site (Columbia Falls AFS) in Maine were completed in 1979 and the SPT has been conducted in 1980. The ionosonde, magnetometer, and total electron content data provided to Air Force Global Weather Central (AFGWC) by the GBIO in its operational role has been a cornerstone of the AFGWC support to the ERS. A special remote data-display

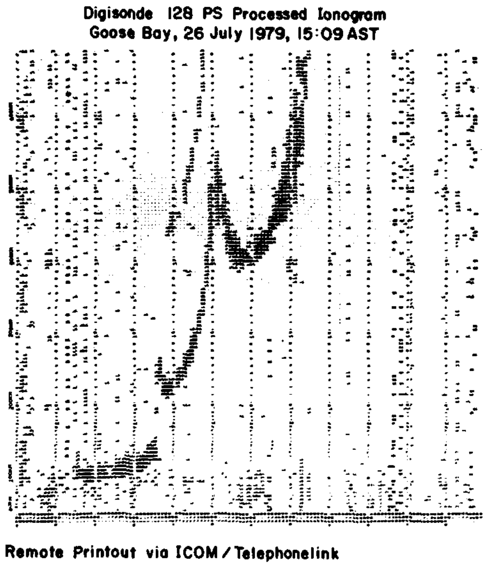

Remote Real-time Printout of a Digital Ionogram. The ionogram recorded at the Goose Bay Ionospheric Observatory in Canada was immediately printed out at the Columbia Falls AFS, the 414L Receive-Operations site in Maine, using the ICOM system. The frequency and virtual height scales were added before transmission.

system known as the Ionogram Communicator (ICOM) was installed between the GBIO and the Receive-Operations site. Ionograms made by the GBIO digital ionosonde are immediately transmitted over a dedicated telephone line and printed out

at Columbia Falls (see figure). The ERS operators have the benefit of constant updates on the overhead ionosphere at Goose Bay to use in frequency management and in understanding operation of the radar system.

At 65 degrees corrected geomagnetic latitude, GBIO is optimally located to investigate the high latitude ionosphere near and within the auroral oval. The study of amplitude and phase scintillation, important to Air Force Command, Control, and Communications, has been one of the more important AFGL study areas. Amplitude scintillation measurements have been made at GBIO for many years. More recently, phase-scintillation measurement systems based on microcomputers have been installed. Within the past year, the phase scintillation measurements have been augmented by installation of a spaced antenna array with a 500 meter baseline. The location of the GBIO near or within the auroral oval during nighttime is significant, since scintillation activity is enhanced in the auroral oval during this time period.

Space Data Communication: AFGL has a program for the development of a prototype Space Environmental Support System (SESS) Data Communicator (SESSDAC). The SESSDAC prototype will be used at the GBIO to automate some of the SESS data now being manually submitted by operators. Consideration has been given to developing a unit that could be used at other SESS data-reporting locations. SESSDAC will automatically acquire data from the sensor systems now in use, process the data in the same way as the observers, and automatically communicate the data to AFGWC, using the data message formats and communications circuits now in use. SESSDAC operation will be successful if AFGWC doesn't know whether data were submitted by an observer or by SESSDAC. SESSDAC is constructed using standard single-board microcomputer modules. Most of the component boards and other units are available from more than one source. They could also be leased under a service contract, with equipment servicing handled by the contractor. SESSDAC is being tested at the Air Weather Service Sagamore Hill Radio Observatory in Massachusetts. Total Electron Content (TEC) values are being successfully reduced from

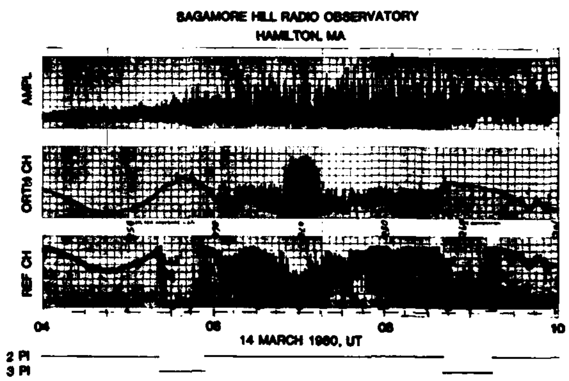

Example of Difficult Radio Polarimeter Data. SESSDAC successfully followed the phase angle change-overs and calculated total electron content correctly despite rapidly changing amplitude and phase angle values during testing at the Air Weather Service Sagamore Hill Radio Observatory.

radio polarimeter measurements. The successful determination of TEC requires SESSDAC to overcome problems of noisy data and to keep track of the integral number of signal phase revolutions during the diurnal variation of TEC (see figure).

Ionosonde Data-Analysis Automation: AFGL research on the application of digital techniques to ionospheric data has continued. Digital ionosondes have been under development since 1970 and are now in operation at the GBIO in Iceland in support of 414L testing, and aboard the AFGL Airborne Ionospheric Observatory, a specially instrumented KC-135. The Geomonitor was developed to preprocess digital ionograms, reducing the number of data characters needed to portray an ionogram from 21,600 to 2340 (see figure). The

ninefold reduction in data enables remote data communication to use shared communications links rather than dedicated

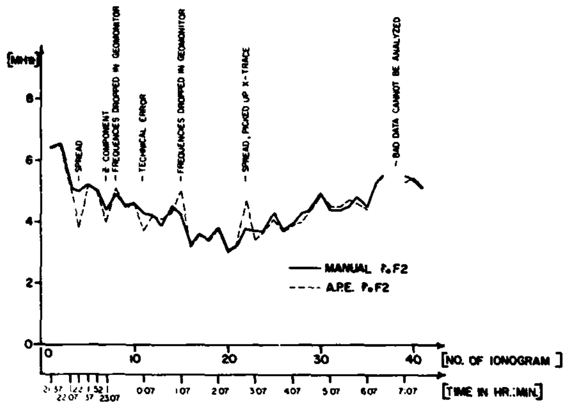

Preliminary Results of Automated Ionosonde Data Analysis. The values of the F2 layer ordinary critical frequency, foF2, determined by the automated analysis algorithm and by manual scaling are compared. Possible explanations for lack of agreement of individual cases are given.

links. The Geomonitor techniques provided a basis for current research into complete automation of digital ionosonde data to provide the ionospheric parameters now analyzed by the observers. This research is still in an early stage and results directly usable by the Air Force cannot be expected for several years. The problem is complicated by the amount of information potentially available from digital ionosonde measurements of the ionosphere and by the subtle variations in the measurement data which are significant to the ionospheric parameters derived for submission to AFGWC. Indeed, there is still not universal agreement in the scientific community on the interpretation of the ionospheric parameters used by the Air Force in ionospheric monitoring and modeling.

Auroral Oval: Radio wave propagation and communications through the high-latitude ionosphere are severely affected by the enhanced and irregular ionization observed in the area covered by the auroral oval. The statistical auroral oval, developed by the Russians Feldstein and Starkov (1965) from IGY all-sky camera data, has for a long time served as the framework for high-latitude ionospheric models. Optical observations from the Defense Meteorological Satellite Program (DMSP) have over the last decade pro-

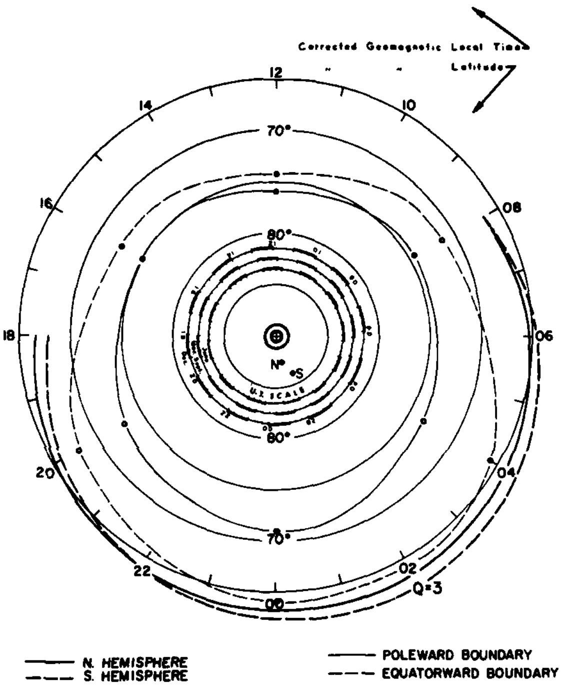

Equatorial Edge of Diffuse Aurora, Feldstein Oval. Inner and outer boundaries of the Feldstein auroral oval for Q = 3 are found at 71° and 64° corrected geomagnetic latitudes (CGL) at 0° corrected geomagnetic time (CGT). The equatorward boundaries of the continuous (diffuse) aurora determined from DMSP data are at 63° and 62° for the Northern and Southern Hemispheres, respectively. The latitude difference between the equatorward boundary of the diffuse aurora and that of the Feldstein oval increases both in the evening and morning sectors.

vided a large data base useful for the verification of the oval concept and the study of the dynamics of the oval boundaries. An analysis of the location of the equatorward boundary of the diffuse (or continuous) aurora, corresponding to the equatorward

boundary of auroral precipitation, was made using data covering the period 1972 through 1975. Grouped by the high-latitude magnetic activity index Q, the DMSP-derived particle precipitation boundaries were found systematically 1° to 2° (for very quiet conditions 3°) equatorward of the respective Feldstein oval boundaries. The analysis also indicates a systematic difference between the location of the oval boundaries in the southern and northern hemispheres, with the boundary of the oval in the southern hemisphere up to 1° more equatorward. The results permit a refinement of the specification of the oval boundary from the available magnetic activity (Q) data for use by rf systems such as the Over-the-Horizon Backscatter (OTH-B) radar operating in the high-latitude ionospheric environment.

An Experimental (OTH-B) Radar System (ERS) is presently being tested in Maine, to study the effects of the auroral and subauroral ionosphere on the radar's performance. At 09:00 Corrected Geomagnetic Local Time (CGLT), the Q = 3 oval affects only 10 percent of the ERS coverage area, whereas at 21:00 CGLT, it affects 40 percent of the area. To estimate the duration for which, under given magnetic activity conditions, the coverage area of the radar would be affected by the aurora, the Q-index magnetic-activity data base from Sodankyla (Finland) was analyzed to provide the probability distribution of Q. The Q-values from a single station show, due to the changing distance of the station from the oval, a strong diurnal dependence. After the Q-data is detrended with empirical time-dependent factors, it is possible to forecast the level and duration

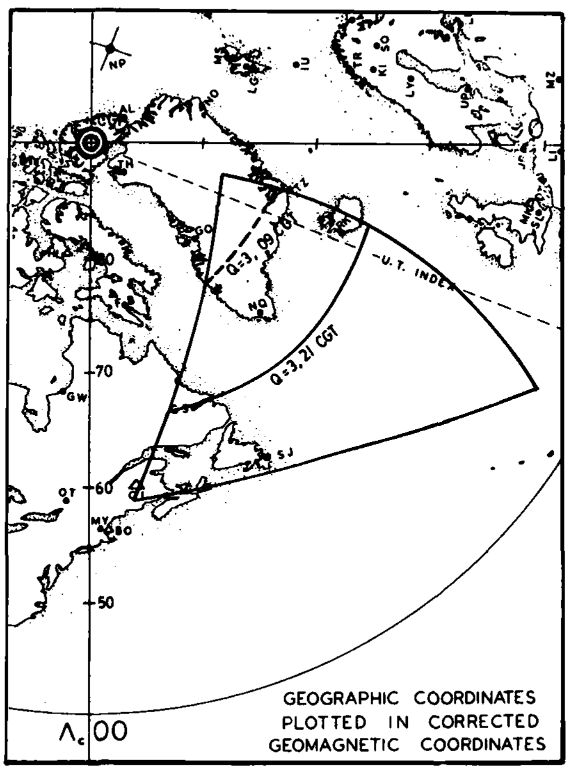

Surveillance Area under ERS Testing Shown in Corrected Geomagnetic (CG) Coordinates. At 09 CGT the Q = 3 oval covers 10 percent of the surveillance area, whereas at 21 CGT the oval covers 40 percent of the area (from the northern tip). The region in the test area, below the respective curves, is free of auroral disturbance.

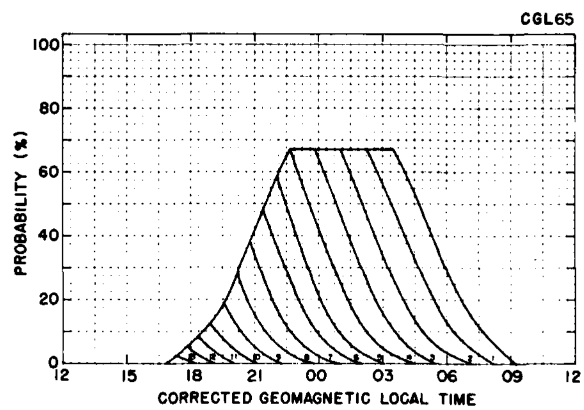

Probability of Occurrence of Auroral Disturbances of Indicated Duration (in hours) at 65° CGL in the ERS Test Area. Curve number 10 (disturbances lasting for 10 hours) shows that an auroral disturbance beginning at 17 CGT has 12 percent probability of lasting for 10 hours. The probability that this disturbance will last for 4 hours (curve 4) is 68 percent. The period 09-16 CGT is statistically free of auroral disturbance at 65° CGL.

of disturbances in the test region of the ERS. For example, at 65° corrected geomagnetic latitude (CGL) in the test area, the probability of auroral disturbance is high, 68 percent, for 4 hours, 23-04 CGT; the region is practically free of any auroral disturbance for 8 hours from 09-17 UT. Such predictions are useful for determining the duration of efficient or inefficient periods of surveillance due to changing space environments.

Photoelectron Flux and Optical Emissions: These studies seek to determine to what extent altitude profiles of electron and neutral densities can be determined by remote satellite sensing of optical emissions.

At the request of Space Division, AFGL has undertaken a program in the remote sensing of daytime electron and neutral density altitude profiles at midlatitudes from satellite optical measurements. To do this, a sufficiently accurate theory for the photoelectron flux is needed; once it is known, volume emission rates at selected wavelengths may easily be calculated. Satellite optical-emission measurements can then be used to determine altitude profile information.

At AFGL, a new approach (combining the Boltzmann and Fokker-Planck equations) was used to calculate the photoelectron flux for the daytime, bottomside ionosphere. We have found steady-state solutions of the Boltzmann-Fokker-Planck (BFP) equation for the electron distribution function in the 1 to 60 eV energy range which are in good agreement with experiment for electron energies from 20 to 30 eV, but in poor agreement for electron energies from 2 to 6 eV. In the 2 to 6 eV energy range we have developed a nonlinear BFP-Poisson theory and used it to study small electrostatic perturbations to the ionospheric plasma. In doing so, we have found that our steady-state solutions from 2 to 6 eV are unstable, and upper hybrid and electron cyclotron waves are generated. We feel that these instabilities lead to weak plasma turbulence, which in turn modifies the electron distribution function in the 2 to 6 eV range. The electron distribution function from 2 to 6 eV greatly affects certain optical emissions. It is our hope that a more accurate theory can be developed so that local ionospheric properties can be inferred from remote satellite optical measurements. In the future, these methods will be generalized so that properties of the topside ionosphere that are of interest to Space Division and the Air Weather Service can be studied.

The Auroral E Layer/Continuous Aurora: Considerable progress has been made in the description of the auroral E layer: the particles which produce it, the latitudinal and longitudinal distributions, and the dynamics of the entire night sector. These results are based on combined measurements from satellites, AFGL's Airborne Ionospheric Laboratory, and ground stations which span nearly 12 years.

When integrated over the loss cone, particles which precipitate to produce the auroral E layer are Maxwellian. Both electrons and protons contribute to the ionization, but the electrons predominate.

The critical frequency of the E layer is found to be in one-to-one correspondence with the precipitating particle energy flux. In addition, the virtual height of the E layer is related to the characteristic energy of the particles. The coordinated theoretical work shows promise of putting these relations on a quantitative basis so as to permit the calculation of the E-layer ionosphere from measured particle parameters. Of equal importance is the converse process by which one may use the ionospheric soundings to measure the particle characteristics and consequently probe the plasma sheet, the magnetospheric source of these particles.

The latitudinal distribution of the precipitating particles, both energy flux and characteristic energy, are well described by Gaussian functions. Furthermore, at a

given instant the Gaussian energy flux is constant in magnetic local time throughout the entire night sector in a frame of reference which has as its origin a pole which is offset from the magnetic pole.

This uniformity can exist through large changes in auroral activity. Thus, for a large range of conditions, the entire nighttime auroral E layer can be specified by two parameters: the maximum energy flux and the radius of this maximum about the offset pole.

Auroral E Program: The purpose of this program is to study the feasibility of remotely sensing electron density profiles in the auroral ionosphere by satellite measurements of optical emissions. The program consists of coordinated rocket, satellite, aircraft and ground-based measurements, and a theoretical effort to analyze the data.

The continuous aurora/auroral E region was chosen as the subject of this investigation based on the results of the aforementioned research program. These results showed that, of all auroral phenomena, this one offered the closest approach to conditions for controlled experimental measurement. The regularity, large extent, and stability of this aurora permit multiple rocket experiments to be performed under nearly identical conditions. The high probability of occurrence of this aurora means experimenters can wait for optimum conditions. The experience of measuring this aurora makes it possible to determine when these optimum conditions occur by means of ionospheric and optical measurements on AFGL's Airborne Ionospheric Observatory. The existence of equilibrium means this region is the most favorable one for the study of the complex physics and chemistry of the ionosphere.

The experimental program is planned for a February-March 1981 window at Poker Flat, Alaska, and consists of the following measurements: electron and proton energy spectra by satellite and rocket; volume emission rates at selected wavelengths by rocket; electron, ion and neutral particle temperatures by rocket; electric fields by rocket; electron densities by the Chatanika incoherent scatter radar; and other ionospheric, geomagnetic, photographic and photometric quantities by the Airborne Ionospheric Observatory and ground facilities.

The theoretical program consists of the application of the methods of transport theory to calculate most of the experimentally-determined quantities. Experiment and theory can then be compared, and the feasibility of determining electron density profiles from satellite optical measurements assessed.

Real Height of the Auroral Region of the Ionosphere: A simplified procedure has been developed for the determination of real height in the auroral region from virtual height data obtained in the presence of a magnetic field. The basis of the method is the representation of the relation between index of refraction and electron density by a simple power law. The resulting relation between real height and virtual height can then be easily solved for the real height. A numerical study of two parabolic models of the ionosphere indicates that the calculated values of real height are in very good agreement with the exact values.

SPACECRAFT CHARGING TECHNOLOGY

The space environment has caused hundreds of operating anomalies on communications and surveillance satellites. Anomalies include amplifier gain-control logic switching, thermal control degradation, sensor data noise, erroneous operation of attitude control systems, and power system failure.

Definition of the Problem: The complex interaction between a satellite and the earth's space plasma (electron and proton) environment that leads to spacecraft

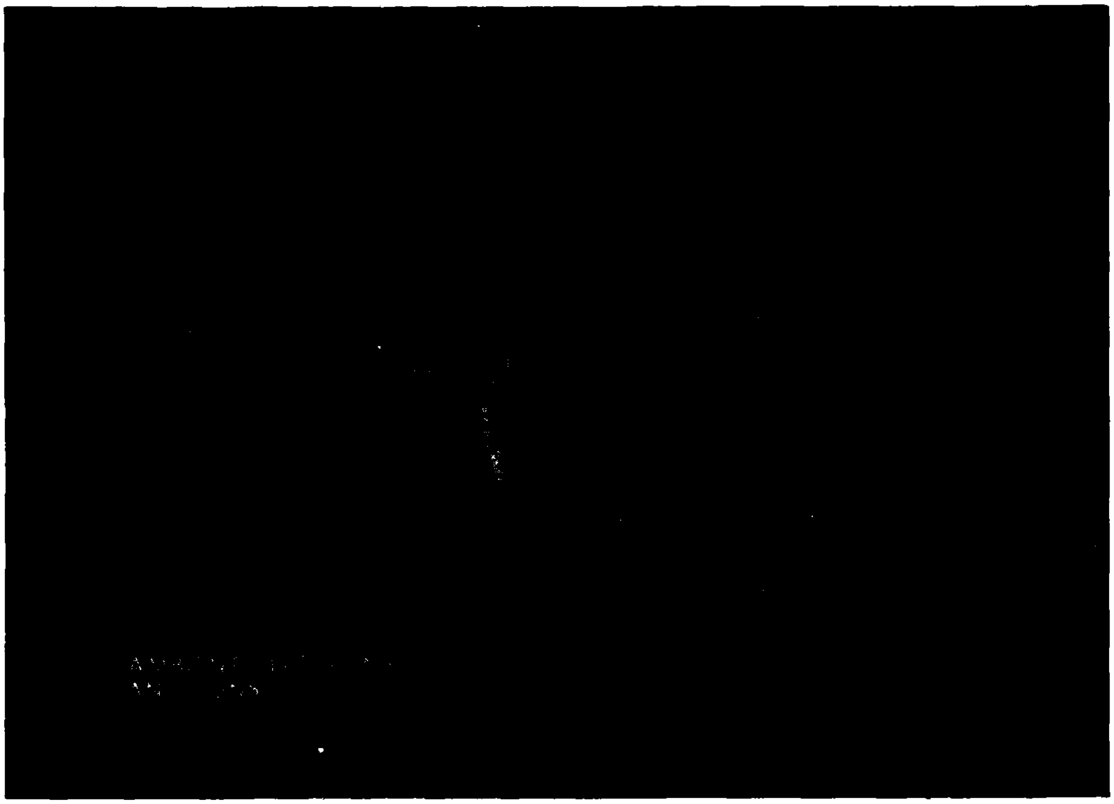

Interaction of Satellite and Space Plasma Environment of Earth.

charging is depicted in the figure. During a magnetospheric substorm, the ambient electron and ion temperatures at geosynchronous orbit altitudes (about 36,000 km, or 6.6 earth radii) increase by about a factor of four for periods of 1 to 2 hours. When substorms occur, satellite surfaces acquire a net charge from the flux of high energy electrons. Secondary emission from high-energy electrons and ions, ambient thermal ions, and photoemission tend to reduce the charging. The charging level increases significantly when the satellite is in eclipse and the source of photoelectrons is removed. When the satellite is in sunlight, high differential potentials in the kilovolt range may be developed between the illuminated and shadowed portions of the spacecraft. When sufficient voltage stresses occur, current discharges can follow, which produce electromagnetic interference (EMI). The EMI has caused hundreds of operating anomalies observed on communications and surveillance satellites.

Another suspected cause of spacecraft charging is due to the penetration of high-energy electrons into spacecraft dielectrics. In this case, charge is stored in the dielectric which, in turn, can lead to electrical breakdown when the breakdown potential of the material is reached. For example, dielectric films are charged by 20-100 keV electrons; while cables and printed-circuit boards are charged by mega-electron volt electrons.

AFSC/NASA Technology Program: Technology involving spacecraft charging is one of the many interdependent research areas in aeronautics and astronautics that are coordinated by the Air Force Systems Command (AFSC) and NASA Space Research and Technology Review Group. NASA and AFSC strive to identify their common technical problems and

then assign agency responsibility for providing the required technology. Spacecraft charging is a six-year investigation between AFSC's Director of Science and Technology and NASA's Office of Aeronautics and Space Technology. A steering committee incorporates NASA and AFSC requirements into the investigation. Each technology element of the investigation is assigned to either NASA or the Air Force with well-defined accountability. Contractual and in-house efforts are devoted to this investigation.

The goal of the spacecraft-charging technology investigation is to protect our satellites from the harmful effects of high-voltage arc discharges. The objectives of the investigation are to develop the design criteria, materials, techniques, test and analytic methods to ensure control of absolute and differential charging of spacecraft surfaces. Technology elements of the investigation include: (1) specification of the space environment which induces the charging; (2) development of analytical tools to model the interactions between the environment and the spacecraft surfaces; (3) development of ground facilities to conduct materials and systems evaluations; (4) development of new or modified spacecraft materials for charge control; and (5) analysis and interpretation of satellite flight data to validate predictions of the analytical tools and to calibrate ground facilities.

SCATHA Satellite Results: The SCATHA (*S*pacecraft *C*harging *at* *H*igh *A*ltitudes) satellite, shown here, is an integrated satellite experiment that measures the characteristics of the spacecraft charging phenomenon, determines the response of the satellite to the charging process, and evaluates charge-control techniques. The primary SCATHA mission objective is to obtain information for an Air Force Military Standard concerning spacecraft charging.

The SCATHA satellite is part of the DOD Space Test Program managed by

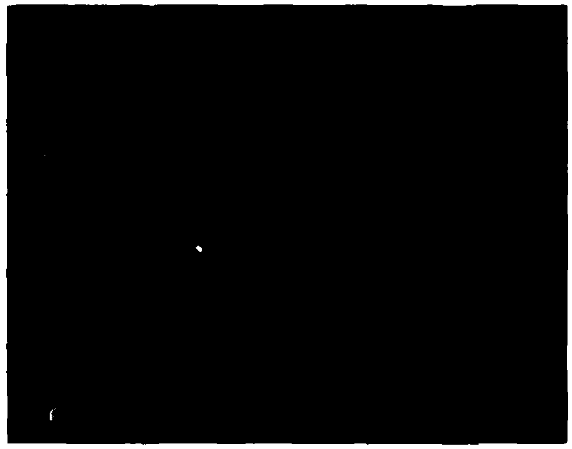

SCATHA Satellite.

AFSC's Space Division. Martin Marietta was the prime spacecraft contractor. Launch was on a Delta 2914 from the Eastern Test Range on January 30, 1979. SCATHA has an equatorial orbit with an apogee of 7.7 earth radii (42,000 km) and perigee of 5.3 earth radii (28,000 km) and drifts easterly at 6 degrees per day. The thirteen experiments on SCATHA are provided by Air Force, Navy, NASA, Defense Nuclear Agency, industry and university groups. Engineering experiments measure potentials on the satellite surface and the effects of discharges on spacecraft surfaces and on subsystems. Environmental experiments measure the characteristic fields and fluxes. An electron beam system and a positive-ion beam system are used to develop techniques to actively control spacecraft charging. The engineering, environmental and charge control experiments were selected to work in concert and, thus, relate cause and effect in spacecraft charging.

Characterized Geosynchronous Environment: A comprehensive specification of the space environment at geosynchronous altitudes is being developed through scientific analysis and interpretation of the SCATHA satellite data stream. The specification contains a statistical

treatment (histograms, time averages, and standard deviations) of physical quantities which characterize the space plasma population at geosynchronous altitudes. The specification will be included in the spacecraft charging Military Standard and in NASA's Design Guidelines Monograph for spacecraft charging. The specification can then be used in the design of all future Air Force geosynchronous satellites. A preliminary environmental specification was used in engineering studies for the Defense Satellite Communications Systems III.

Characterized Arc Discharges: The frequency and time characteristics of arc discharge on SCATHA have been measured with the Aerospace Corporation's Charging Electrical Effects Analyzer. Computer fitting of the one waveform indicated that it was composed of two damped sinusoids: one with a frequency of 11.1 MHz and an amplitude of 0.9 V and the other with a frequency of 25 MHz and an amplitude of 0.7 V. The waveform characteristics will be used by Aerospace in developing systems-level test requirements for spacecraft charging.

Demonstrated Active Charge Control: An optimum technique for actively controlling spacecraft charging has been selected based on analysis of the SCATHA charge-emission experiments. Direct comparison between operation of an electron emitter, a heated filament, and a plasma discharge source indicates that the plasma source is the best technique for use in active spacecraft charge control. Based on this result, an automatic charge-control system is now being designed to include a plasma discharge source as well as a spacecraft potential monitor, a pulse monitor, and a control unit.

NASCAP: A theoretical description of the process of spacecraft charging by space plasmas has been prepared in the form of a computer code called NASCAP (*NASA* *Charging* *Analyzer* *Program*). NASCAP was developed under NASA and Air Force sponsorship. The NASCAP code computes the voltage distributions on and around spacecraft due to the space environment. The NASCAP code performs a dynamic, fully three-dimensional simulation of the electrostatic charging processes acting on an object in space or in a ground test chamber environment. In particular, the code predicts surface potentials on spacecraft (see the figure showing a Defense Support Program spacecraft), identifies high-field areas of possible discharge sites, predicts response to environmental charge, predicts and interprets particle-detector response, and assesses the effects of particle emission from charge emitters. NASCAP is the most advanced satellite-charging code available. It has also been employed in the analysis of spacecraft charging on SCATHA, on the Instrumented Test Vehicle (ITV), and on the commercial LEASAT and Satellite Business system (SBS) satellites. The code is being used in contamination and charging studies on the Inertial Upper Stage (IUS)/DSP interface.

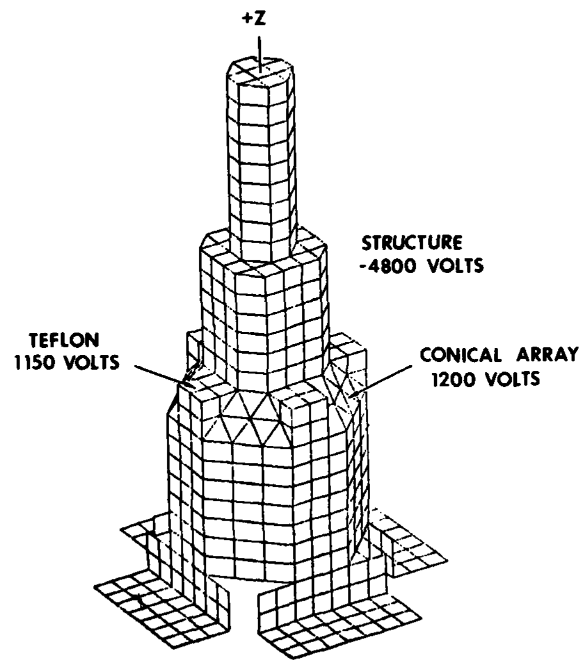

Defense Support Program Spacecraft: Finite Elements.

JOURNAL ARTICLES
JANUARY 1979 – DECEMBER 1980

AARONS, J., MACKENZIE, E., and BHAVNANI, K.
High-Latitude Analytical Formulas for Scintillation Levels
Radio Sci. 15, No.1 (January 1980)

AHMED, M., SAGALYN, R.C., WILDMAN, P.J.L., and BURKE, W.J.
Topside Ionospheric Trough Morphology: Occurrence Frequency and Diurnal, Seasonal, and Altitude Variations
J. Geophys. Res. 84, No.A2 (February 1979)

ALTROCK, R.C.
Anomalous Satellite Drag and the Green-line Corona
Solar Terr. Predictions Proc. 4 (March 1980)

BASU, SANTIMAY, BASU, SUNANDA, JOHNSON, A.L., KLOBUCHAR, J.A., and RUSH, C.M.
Preliminary Results of Scintillation Measurements Associated with Ionosphere Heating and Possible Implications for the Solar Power Satellite
Geophys. Res. Lett. 7, No.8 (August 1980)

BASU, SANTIMAY, MCCLURE, J.P., BASU, SUNANDA, HANSON, W.B., and AARONS, J.
Coordinated Study of Equatorial Scintillation and In-Situ and Radar Observations of Nighttime F Region Irregularities
J. Geophys. Res. 85, No. A10 (October 1980)

BASU, SUNANDA, and AARONS, J.
The Morphology of High-Latitude VHF Scintillation Near 70°W
Radio Sci. 15, No.1 (January-February 1980)

BASU, SUNANDA, BASU, SANTIMAY, MULLEN, J.P., and BUSHBY, A.
Long-Term 1.5 GHz Amplitude Scintillation Measurements at the Magnetic Equator
Geophys. Res. Lett. 7, No.4 (April 1980)

BECKERS, J.M., BREEDLOVE, W.O., DEMASTUS, H.L., DEVEGVAR, P.G.N., JOHANSEN, E.E., GILLIAM, L.B., MANN, G.R., MAUTER, H.A., and PHILLIS, G.L.
The Night Sky Conditions at the Sacramento Peak Observatory II: Cloud Cover, Seeing, and Precipitable Water
Publ. Astron. Soc. Pac. (December 1980)

BESSE, A.L., and RUBIN, A.G.
A Simple Analysis of Spacecraft Charging Involving Blocked Photoelectron Currents
J. Geophys. Res. 85 No. A5 (May 1980)

BINDER, O.H., SHEA, M.A., and SMART, D.F.
The Effect of Altitude Differences and Secular Changes on the Utilization of Cosmic-Ray Variational Coefficients
IL Nuovo Cimento 1 C, No.3 (1978)

BUCHAU, J., GASSMANN, G.J., PIKE, C.P., and WAGNER, R.A.
Radar Propagation Errors in the Arctic Ionosphere
Air Force Surveys in Geophysics No. 231 (April 1980)

BUCKNAM, D.B., and SHEA, M.A.
Event Oriented Data Collection for the Ground-Level Solar Cosmic Ray Event of 30 April 1976
Proc. 15th Int. Cosmic Ray Conf. 11 (September 1979)

CHRISTOU, J., and WORDEN, S.P.
The Diameter of CYGNI by Speckle Interferometry
Astron. J. 85, No. 3 (March 1980)

COHEN, H.A., SHERMAN, C., and MULLEN, E.G.
Spacecraft Charging Due to Positive Ion Emission: An Experimental Study
Geophys. Res. Lett. 6, No.6 (June 1979)

DANDEKAR, B.S.
Relationship Between the IMF, the Midday Gap, and Auroral Substorm Activity
J. Geophys. Res. 84, No. A8 (August 1979)

DRYER, M., and SHEA, M.A.
Requirements for Predictions and Real-time Monitoring for the Study of Travelling Interplanetary Phenomena
Solar Terr. Predictions Proc. 2 (1979)

DUFOUR, R.J., TALBOT, R.J., JR., JENSEN, E.B., and SHIELDS, G.A.
M 83 II: Spectral Characteristics and Chemical Abundances of H II Regions
Astrophys. J. 236 (February 1980)

EATHER, R.H., MENDE, S.B., and WEBER, E.J.
Dayside Aurora and Relevance to Substorm Current Systems and Dayside Merging
J. Geophys. Res. 84, No. A7 (July 1979)

ESSEX, E.A., and KLOBUCHAR, J.A.
Mid-Latitude Winter Nighttime Increases in the Total Electron Content of the Ionosphere
J. Geophys. Res. 85, No. A11 (November 1980)

FILZ, R., RAO, Y.V., and DAVIS, A.
An Experiment for Measuring Heavy Cosmic Ray Spectra, Solid State Nuclear Track Detectors
Ed. by H. Francois, Pergamon Press, Oxford and New York (1980)

FLUCKIGER, E., DEBRUNNER, H., SMART, D.F., and SHEA, M.A.
Calculations of Changes in Cosmic Ray Cutoff Rigidities Due to a Partial Ring Current System in the Magnetosphere
16th Int. Cosmic Ray Conf., Conf. Papers 4 (1979)

FORBES, J.M., and GARRETT, H.B.
The Solar Cycle Variability of Diurnal and Semi-diurnal Thermospheric Temperatures
J. Geophys. Res. 84, No.A5 (May 1979)

FOUGERE, P.F.
Sunspots: Power Spectra and a Forecast
Solar Terr. Predictions Proc. (1979)

GARRETT, H.B.
Review of Quantitative Models of the 0-to-100 keV Near-Earth Plasma
Rev. Geophys. and Space Phys. 17, No.3 (May 1979)
Spacecraft Charging: A Review
Progress in Astronautics and Aeronautics 71 (1980)

GARRETT, H.B., and DEFOREST, S.E.
Time-Varying Photoelectron Flux Effects on Spacecraft Potential at Geosynchronous Orbit
J. Geophys. Res. 84, No.A5 (May 1979)

GARRETT, H.B., and GAUNT, D.N.
Spacecraft Charging During Eclipse Passage
Progress in Astronautics and Aeronautics 71 (1980)

GARRETT, H.B., RUBIN, A.G., and PIKE, C.P.
Prediction of Spacecraft Potentials at Geosynchronous Orbit
Solar Terr. Predictions Proc. 8, No.120 (1980)

GUIDICE, D.A.
Observatory Report: Sagamore Hill Radio Observatory
Bull. AAS 11, No.1 (1979); Bull. AAS, 12, No.1 (1980)

HARDY, D.A., HILLS, H.K., and FREEMAN, J.W.
Occurrence of the Lobe Plasma at Lunar Distance
J. Geophys. Res. 84, No.A1 (January 1979)

HIRMAN, J.W., NEIDIG, D.F., SEAGRAVES, P.H., FLOWERS, W.F., and WIBORG, P.H.
The Application of Multivariate Discriminant Analysis to Solar Flare Forecasting
Solar Terr. Predictions Proc. 3, Ed. by R.F. Donnelly (March 1980)

HUBBARD, G., HEGE, K., REED, M.A., STRITTMATTER, P.A., WOOLF, N.J., and WORDEN, S.P.
Speckle Intereferometry. I. The Steward Observatory Speckle Camera
Astronom. J. 84, No.9 (September 1979)

HUMBLE, J.E., SMART, D.F., and SHEA M.A.
Cosmic Ray Cutoffs at 400 km Applicable to the HEAO-C Satellite
16th Int. Cosmic Ray Conf., Conf. Papers 4 (1979)

JENSEN, E.B., and THUAN, T.X.
A Detailed Photometric Study of the Edge-On Spiral NGC 4565
Photometry, Kinematics and Dynamics of Galaxies, Ed. by D.S. Evans, Univ. of Texas Pr. (1979)

KANE, S.R., CRANNELL, C.J., DATLOWE, D., FELDMAN, U., GABRIEL, A., HUDSON, H.S., KUNDU, M.R., MATZLER, C., NEIDIG, D., PETROSIAN, V., and SHEELEY, N.R., JR.
Impulsive Phase of Solar Flares
Solar Flares, Colorado Assoc. Univ. Pr., Boulder, CO (June 1980)

KEIL, S.L.
The Structure of Solar Granulation. I. Observations of the Spatial and Temporal Behavior of Vertical Motions
Astrophys. J. 237 (May 1980)
II. Models of Vertical Motion
Astrophys. J. 237 (May 1980)
The Interpretation of Solar Line Shift Observations
Astron. Astrophys. 82 (1980)

KELCH, W.L., LINSKY, J.L., and WORDEN, S.P.
Stellar Model Chromospheres. IX. Chromospheric Activity in Dwarf Stars
Astrophys. J. 229 (April 1979)

KERSLEY, L., and KLOBUCHAR, J.A.
Storm Associated Protonospheric Depletion and Recovery
Planet. Space Sci. 28, Pergamon Pr. Ltd. (1980)

KERSLEY, L., AARONS, J., and KLOBUCHAR, J.A.
Nighttime Enhancements in Total Electron Content Near Arecibo and Their Association with VHF Scintillations
J. Geophys. Res. 85, No. A8 (August 1980)

KRUKONIS, A.P., and WHALEN, J.A.
Occurrence and Lifetimes of Discrete Auroras Near Midnight
J. Geophys. Res. 85, No. A1 (January 1980)

KUHN, J.R., and WORDEN, S.P.
Evidence of Long-Period Solar Velocity Fluctuations
Astrophys. J. 228 (March 1979)

LINSKY, J.L., WORDEN, S.P., MCCLINTOCK W., and ROBERTSON, R.M.
Stellar Model Chromospheres. X. High Resolution, Absolute Flux Profiles of the Ca II H and K Lines in Stars of Spectral Types FO-M2
Astrophys. J. Suppl. Ser. 41 (September 1979)

MENDOZA, N.M., PIKE, C.P., and SEIKEL, G.R.
Common Threads in the Aerospace Science
Aerospace Sciences Mtg. in Review, Astronautics and Aeronautics 18 (5) (May 1980)

MEYER, F., SCHMIDT, H.U., SIMON, G.W., and WEISS, N.O.
Buoyant Magnetic Flux Tubes in Supergranules
Astron. Astrophys. 76 (1979)

MIKKELSEN, I.S., AARONS, J., and MARTIN, E.
Geometrical Considerations of 136 MHz Amplitude Scintillation in the Auroral Oval
J. Atmos. Terr. Phys. 40 (February 1979)

MISCHKE, C.F.W., RAUBENHEIMER, B.C., STOKER, P.H., VAN DER WALT, A.J., SHEA, M.A., and SMART, D.F.
Experimental Observations of Secular Changes in the Vertical Cutoff Rigidity
16th Int. Cosmic Ray Conf., Conf. Pap. 4 (1979)

NEIDIG, D.F.
High Resolution Observations of Fibril Changes in a Small Flare
Sol. Phys. 61 (1979)
Solar Rotation Studies Using Sunspot Data (1967-1974)
Sol. Phys. 66 (1980)

NEIDIG, D.F., WIBORG, P.H., SEAGRAVES P.H., HIRMAN, J.W., and FLOWERS, W.E.
Multivariate Discriminant Analysis Applied to Solar Flare Forecasting
Preprint Vol., 6th Conf. Probability and Statistics in Atmos. Sci. (October 9 1979)

NOVEMBER, L.J., TOOMRE, J., GEBBIE, K.B., and SIMON, G.W.
The Height Variation of Supergranular Velocity Fields Determined From Simultaneous OSO 8 Satellite and Ground-Based Observations
Astrophys. J. 227 (January 15 1979)

PARDON, L., WORDEN, S.P., and SCHNEEBERGER, T.J.
The Lifetimes of Sunspot Moats
Sol. Phys. 63 (September 1979)

PAULIKAS, G.A., BAKER, D.N., BARRON, W.R., DOMINGO, V., HIGBIE, P.R., IMHOF, W.L., LYONS, L.R., MCPHERRON, R.L., ROELOF, E.C., SCHOLER, M., SHEA, M.A., SMART, D.F., SPJELDVIK, W.N., and VETTE, J.I.
Prediction of Energetic Particle Disturbances
Sol.-Terr. Predictions Proc. 2 (1979)

PIKE, C.P.
A Comparison of the North- and South-Polar F Layers
J. Geophys. Res. 76, No.28 (October 1 1971)

PIKE, C.P., and DANDEKAR, B.S.
Evening Sector Auroral Oval Dynamics From DMSP Photographs
J. Geophys. Res. 84, No. A7 (July 1 1979)

PIKE, C.P., DAILEY, C.C., GARRETT, H.B., KELLEY, J.G., MITZ, M.A., NOYES, J.C., OGILVIE K.W., and WU, S.T.
Highlights 1979 Space Sciences & Astronomy
AIAA Comm. on Space Sci & Astron., C.P. Pike, Chrmn (1980)

PIKE, C.P., GARRETT, H.B, JOHNSON, R.G., SIMON, G., and STERK, A.
Aerospace Highlights of 1978: Space Sciences and Astronomy
Astronautics and Aeronautics (January 1979)

RADICK, R.R., and TETLEY, W.C.
The 10 February 1977 Lunar Occultation of Uranus. Radius, Limb Darkening, and Polar Brightening at 6900 A
Icarus, 4J (1979)

RASTOGI, R.G.
Seasonal Variation of Equatorial Spread F in the American and Indian Zones
J. Geophys. Res. 85, No. A2 (February 1 1980)
Seasonal and Solar Cycle Variations of Equatorial Spread-F in the American Zone
J. Atmos. Terr. Phys. 42 (1980)

RASTOGI, R.G., AARONS, J.
Nighttime Ionospheric Radio Scintillations and Vertical Drifts at the Magnetic Equator
J. Atmos. Terr. Phys. 42 (1980)

RICH, F.J., SAGALYN, R.C., and WILDMAN, P.J.L.
Electron Temperature Profiles Measured up to 8000 km by S3-3 in the Late Afternoon Sector
J. Geophys. Res. 84, No. A4 (April 1 1979)

RICH, F.J., BURKE, W.J., KELLEY, M.C., and SMIDDY, M.
Observations of Field-Aligned Currents in Association with Strong Convection Electric Fields at Subauroral Latitudes
J. Geophys. Res. 85, No.A5 (May 1 1980)

ROBINSON, R.D., WORDEN, S.P., and HARVEY, J.W.
Observations of Magnetic Fields on Two Late-Type Dwarf Stars
Astrophys. J. 236 (March 15 1980)

ROTHWELL, P.L., and YATES, G.K.
A Dynamical Model for the Onset of Magnetospheric Substorms, Dynamics of the Magnetosphere
Ed. by S.I. Akasofu, D. Reidel (1980)

ROTHWELL, P.L., RUBIN, A.G., and YATES, G.K.
A Simulation Model of Time-Dependent Plasma-Spacecraft Interactions
Proc. Spacecraft Charging Tech. Conf. (Reprinted 10 April 1979)

RUBIN, A.G., and GARRETT, H.B.
ATS-5 and ATS-6 Potentials During Eclipse
NASA Conf. Pub. 2071 (1979)

RUBIN, A.G., KATZ, I., MANDELL, M., SCHNUELLE, G., STEEN, P., PARKS, D., CASSIDY, J., and ROCHE, J.
A Three Dimensional Spacecraft-Charging Computer Code
Prog. in Astronautics and Aeronautics 71 (1980)

SCHNEEBERGER, T.J., WORDEN, S.P., and WILKERSON, M.S.
High Resolution Line Profiles of T Tauri Stars
Astrophys. J. Supp. Ser. 41 (November 1979)

SCHNEEBERGER, T.J., WORDEN, S.P., and AFRICANO, J.L.
Observational Astronomy at Cloudcroft Observatory
Proc. Southwest Regional Conf. Astron. and Astrophys. 5 (April 1980)

SHEA, M.A.
Cosmic Ray Trajectory Calculations and Their Applications
Proc.,Indo.-U.S. Wkshp. Sol-Terr. Phys. (February 1980)

SHEA, M.A., and SMART, D.F.
Significant Solar Proton Events; 1970-1972
Sol-Terr. Phys. and Meteorology: Working Document III(1979)
A Comparison of the Characteristics of Solar Proton Events for the Last Two Solar Minima, Space Res.
Ed. by M.J. Rycroft, Pergamon Pr. (1979)

SHEA, M.A., SMART, D.F., TANSKANEN, P.J., and HUMBLE, J.E.
Neutron Monitor Response to Non-Vertical Arrival Directions During GLE's
Conf. Pap., 16th Int. Cosmic Ray Conf. 12 (1979)

SHEA, M.A., SMART, D.F., ARENS, M., BERCOVITCH, M., CHIBA, T., DEBRUNNER, H., DORMAN, L.I., DUGGAL, S.P., FENTON, A.G., FLUCKIGER, E., GALLI, M., HATTON, C.J., HUMBLE, J.E., JODOGNE, J.C., KONIG, P.J., LAZUTIN, L.L., LOCKWOOD, J.A., POMRANTZ, M.A., ROHRS, K., SHAFER, Y.G., STOKER, P.H., STORINI, M., TAKAHASHI, H., TANSKANEN, P.J., VENKATESAN, D., WADA, M., and WIBBERENTZ, G.
The Ground-Level Relativistic Solar Proton Event of May 7 1978: A Composite Report
16th Int. Cosmic Ray Conf., Conf. Pap. 5 (1979)

SMART, D.F.
Prediction of the Time-Intensity Profile of Solar Proton Events
Proc. Indo-U.S. Wkshp. Sol-Terr. Phys., (1980)

SMART, D.F., GARRETT, H.B., and SHEA, M.A.
The Prediction of AE, ap, and Dst at Time Lags Between 1 and 30 hours
Solar-Terrestrial Predictions Proceedings, Vol. 2: Working Group Reports and Reviews. Edited by Richard F. Donnelly, Environment Research Laboratories, National Oceanic and Atmospheric Administration, U.S. Department of Commerce, Boulder, Colorado, 399-414 (1979)

SMART, D.F., and SHEA, M.A.
PPS76—A Computerized "Event Mode" Solar Proton Forecasting Technique
Sol-Terr. Predictions Proc. 1, Prediction Grp. Report (1980)
Current Status of Short-Term Solar Proton Predictions
Space Res., XIX, Ed. by M.J. Rycroft, Pergamon Pr. (1979)

SMART, D.F., SHEA, M.A., HUMBLE, J.E., and TANSKANEN, P.J.
A Model of the 7 May 1978 Solar Cosmic Ray Event
16th Int. Cosmic Ray Conf., Conf. Pap. 5 (1979)

SMART, D.F., SHEA, M.A., LUND, N., RASMUSSEN, I.L., BYRNAK, B., and WESTERGAARD, N.J.
Cosmic Ray Penumbral Patterns Derived From the Trajectory Calculations for the HEAO-C Satellite
16th Int. Cosmic Ray Conf., Conf. Pap. 12 (1979)

SMIDDY, M., BURKE, W.J., KELLEY, M.C., SAFLEKOS, N.A., GUSSENHOVEN, M.S. HARDY, D.A., and RICH, F.J.
Effects of High-Latitude Conductivity on Observed Convection Electric Fields and Birkeland Currents
J. Geophys. Res. 85, No.A12 (December 1 1980)

TALBOT, R.J., JR., and JENSEN, E.B.
Multicolor Surface Photometry of M83
Photometry, Kinematics and Dynamics of Galaxies, Ed. by D.S. Evans, Univ. Texas Pr. (December 1979)

TALBOT, R.J., JR., JENSEN, E.B., and DUFOUR, R.J.
Anatomy of a Spiral Galaxy
Sky and Telescope 60 (July 1980)

VAMPOLA, A.L., ALTROCK, R., ATWELL, W., BACKSTROM, R.C., GARRETT, H.B., HICKMAN, D., JOHNSON, R.G., PEREYASLOVA, N.H., ROBBINS, D., SLOWEY, J., SROGA, J., STASSINOPOULOS, E., TEAGUE, M., and VAUGHAN, W.W.
User Requirements of Solar-Terrestrial Predictions for Spacecraft Applications
Sol-Terr. Predictions Proc. II (December 1979)

WEBER, E.J., BUCHAU, J., and MOORE, J.G.
Airborne Studies of Equatorial F Layer Ionospheric Irregularities
J. Geophys. Res. 85, No. A9 (September 1980)

WILKERSON, M.S.
Neutral-Hydrogen Observations of Smooth-Arm Spiral Galaxies
Astrophys. J. 240 (September 1980)

WORDEN, S.P.
Interferometric Determinations of Asteroid Diameters
Asteroids, Ed. by T. Gehrels, Univ. of Arizona Pr. (December 1979)

WORDEN, S.P., and STEIN, M.K.
Angular Diameter of the Asteroids Vesta and Pallas Determined From Speckle Observations
Astron. J. 84 No. 1 (January 1979)

YOUNG, P.S., HOLEMAN, E.G., PARSIGNAULT, D.R., HAGAN, M.P., and FILZ, R.C.
The Generalized Geometrical Factor of Particle Telescopes for Trapped Radiations
16th Int. Cosmic Ray Conf., Conf. Pap., 3, Code No. MG2-7 (August 1979)

PAPERS PRESENTED AT MEETINGS JANUARY 1979 - DECEMBER 1980

AARONS, J., and WHITNEY, H.E.
Recent Observations of Equatorial and High Latitude Scintillations
AGARD Symp on Prop. Eff. on Earth/Space Paths, London, U.K. (12 - 16 May 1980); URSI - COSPAR Mtg., Warsaw, Poland (19-23 May 1980)
New Studies in Ionospheric Scintillation on Trans-Ionospheric Paths
Prop. Eff. on Earth/Space Paths, London, U.K. (12-16 May 1980)

AARONS, J., MULLEN, J.P., WHITNEY, H.E., COUSINS, M., and LIVINGSTON, R.C. (SRI Intl., Menlo Pk., CA.)
Phase and Amplitude Scintillations Over Discrete Aurora
Natl. Radio Sci. Mtg., Univ. of Colorado, Boulder, CO (5-8 November 1979)

AFRICANO, J.L., QUIGLEY, R.W. (W. Wash. Univ.), SCHNEEBERGER, T.J., and WORDEN, S.P.
Photometric Eclipse Timings of RW Trianguli
154th AAS Mtg., Wellesley, MA (12-14 June 1979)
The Cloudcroft Observatory 48" Telescope
153rd Am. Astronom. Soc. Mtg., Mexico City, Mexico (7-11 January 1979)

ALLEN, R.S., and KLOBUCHAR, J.A.
Use of NAVSTAR-GPS Transmissions to Study the High Latitude Ionosphere
AGARD Consultant Lecture, Kjeller, Norway (20-25 August 1979)

ALTROCK, R.C., and MUSMAN, S.
The Evolution of an Average Solar Granule
Internat. Astron. Union Colloq. No. 51 on "Turbulence in Stellar Atmospheres," London, Ontario, Canada (27-30 August 1979)

ALTROCK, R.C., GARRETT, H.B., ET AL.
User Requirements of Solar Terrestrial Predictions for Spacecraft Applications
Internat. Solar Terr. Predictions Proc., (NOAA) Boulder, CO (October 1979)

ALTROCK, R.C., and MUSMAN, S.
Time Development of Solar Granulation
153rd Am. Astronom. Soc. Mtg., Mexico City, Mexico (7-11 January 1979)
Physical Development of an Average Solar Granule
155th Am. Astronom. Soc. Mtg., San Francisco, CA (13-18 January 1980)

ALTROCK, R.C.
Solar Photospheric Evolution During the Lifetime of a Granule
156th Am. Astronom. Soc. Mtg., College Park, MD (16-18 June 1980)

BAKSHI, P. (Boston Coll., Boston, MA.), and BARRON, W.R.
Prediction of Riometer Absorption from Solar Flare Radio Burst Characteristics
Solar-Terr. Predictions Wkshp., Boulder, CO (23-27 April 1979)
Prediction of Solar Flare Proton Spectrum from Radio Burst Characteristics
Solar-Terr. Predictions Wkshp., Boulder, CO (23-27 April 1979)

BARRON, W.R., and BAKSHI, P.
Prediction of Solar Flare Proton Spectrum from Radio Burst Characteristics
Solar-Terr. Prediction Wkshp., Boulder, CO (23-27 April 1979)
Application of Solar Flare Radio Burst Fluxes to the Prediction of Solar Energetic Proton Flux Increases
Solar-Terr. Prediction Wkshp., Boulder, CO (23-27-April 1979)

BASU, B. (Boston Coll., Newton, MA.), CHANG, R. (MIT, CAMBRIDGE, MA), and JASPERSE, J.R.
Electrostatic Plasma Instabilities in the Daytime Ionospheric E-Region
Am. Geophys. Un. Mtg., Fall, San Francisco, CA (8-12 December 1980)

BASU, S. (Emmanuel Coll., Boston, MA), and AARONS, J.
Results Obtained from Equatorial Irregularity Campaigns
XXIInd Plenary Mtg. of COSPAR, Banglaore, India (29 May - 9 June 1979)
Review of Multi-Technique Observations of F-Region Equatorial Irregularities
Symp. on Sci. and Engineering Uses of Satellite Radio Beacons, Warsaw, Poland (19-23 May 1980)

BASU, S. and BASU, SUNANDA (Emmanuel Coll., Boston, MA)
Model of Phase and Amplitude Scintillations from In-Situ Measurements
Solar-Terr. Predictions Conf., Boulder, CO (23-27 April 1979)

BASU, S. and WHITNEY, H.E.
A Study of Multifrequency Intensity Scintillation Spectra Near the Magnetic Equator
6th Internat. Symp. of Equatorial Aeron., Aguadilla, Puerto Rico (17-24 July 1980)

BASU, S., JOHNSON, A.L. (Avionics Lab., Wright-Patterson AFB, Ohio), RUSH, C.M. (U.S. Dept. of Commerce, ITS, Boulder, CO), and KLOBUCHAR, J.A.
Preliminary Results of Scintillation Measurements Associated with Ionospheric Heating in the Overdense and Underdense Modes
Symp. on Sci. and Engineering Uses of Satellite Radio Beacons, Warsaw, Poland (19-23 May 1980)

BASU, SUNANDA, BASU, S., GANGULY, S. (NAIC, Arecibo Obs., Puerto Rico), HANSON, W.B., and KLOBUCHAR, J.A.
Multi-Technique Study of Natural Midlatitude Irregularities
Symp. on Sci. and Engineering Uses of Satellite Radio Beacons, Warsaw, Poland (19-23 May 1980)

BASU, SUNANDA, BASU, S., GANGULY, S., and KLOBUCHAR, J.A.
Simultaneous Incoherent Scatter and Scintillation/Total Electron Content Observations in the Midlatitude Ionosphere
XXIInd Plenary Mtg. of COSPAR, Bangalore, India (29 May - 9 June 1979)

BURKE, W.J. (Boston Coll., Boston, MA)
Simultaneous Measurements of Electric Fields, Birkeland Currents and Electron Precipitation by S3-2 in the Vicinity of Discrete Auroral Arcs
Chapman Conf., Univ. of Alaska, Alaska (20-25 July 1980)

BURKE, W.J., HARDY, D.A., RICH, F.J. (Regis Coll., Weston, MA), and KELLEY, M.C. (Cornell Univ., Ithaca, N.Y.)
Electrodynamic Structures in the Late Evening Sector of the Auroral Zone
Am. Geophys. Un. Mtg., Spring, Washington, DC (28 May - 1 June 1979)

BURKE, W.J., GUSSENHOVEN, M.S. (Boston Coll., Boston, Ma.), RICH, F.J. (Regis Coll., Weston, MA), HARDY D.A., and SMIDDY, M.
Electrodynamic Structures in the Polar Cap During Periods of Geomagnetic Quieting
Yosemite High Latitude Elec. Flds. Conf., Yosemite Nat'l Pk., CA (30 January - 2 February 1980)

BURKE, W.J., GUSSENHOVEN, M.S., FEYNMAN, J. (Boston Coll., Boston, MA), COHEN, H., HARDY, D.A., CHESLEY, A.
Plasma Observations During Operation of the Electron and Ion Beam Systems on SCATHA
Am. Geophys. Un. Mtg., Fall, San Francisco, CA (3-7 December 1979)

BURKE, W.J., LAI, S.T. (Boston Coll., Boston, MA), and COHEN, H.A.
A Theoretical Investigation of Virtual Electrode Formation Near the SCATHA Satellite
Am. Geophys. Un. Mtg., Fall, San Francisco, CA (3-7 December 1979)

CLIVER, E.W., GUIDICE, D.A.
Sharp-Cutoff Short-Cm Wavelength Bursts from Proton Activity Centers
Am. Astronom. Soc., Univ. of Maryland, Coll. Pk., MD (15-18 June 1980)

CLOUGH, S.A., KNEIZYS, F.X.; DAVIES, R.W. and GAMACHE, R. (Univ. of Lowell, Lowell, MA); and TIPPING, R. (Univ. of Nebraska, Nebraska)
Theoretical Line Shape for H_2O Vapor; Application to the Continuum
Wkshp. on Atmospheric Water Vapor, Vail, CO (11-13 September 1979)

COHEN, H.A., HUBER, W.B., and MASEK, T.
Preparation, Integration and Initial Operations of SPIBS on the P78-2 Satellite
AIAA Fall 79 Mtg., Princeton, NJ (30 September - 1 October 1979)

COHEN, H.A., DALE, F., LYNCH, W. and MCGEE, K.
A Semi-Portable Pumping System for Ground Tests of a Space Vehicle Positive Ion Source
26th Nat'l Symp. of the Am. Vacuum Soc., New York, NY (2-5 October 1979)

COHEN, H.A., MULLEN, E.G., HUBER, W.B., and MASEK, T.
The Sounding Rocket Flight of a Satellite Positive Ion Beam System
AIAA Fall 79 Mtg., Princeton, NJ (30 October - 1 November 79)

COHEN, H.A.
P78 Satellite and Payload Responses to Electron Beam Operations on March 30, 1979
Spacecraft Charging Technology Conf. III, USAF Academy, Colorado Springs, CO (12-14 November 1980)
A Direct Comparison of Three Techniques of Discharging Satellites
Spacecraft Charging Technology Conf. III, USAF Academy, CO (12-14 November 1980)

COOKE, D.J. (Univ. of Utah, Utah), HUMBLE, J.E. (Univ. of Tasmania, Tasmania, Australia), SMART, D.F., and SHEA, M.A.
The Cosmic Ray Penumbrum and Its Relationship to the Geomagnetic Field
Int. Union of Geodesy and Geophys., XVII General Assembly, Canberra, Australia (3-14 December 1979)

DANDEKAR, B.S.
Morphology of the Polar Cap Arcs
Am. Geophys. Un. Mtg., Spring, Washington, DC (28 May - 1 June 1979)
Morphology of Polar Cap Arcs From Periods of Strong Auroral Activity
Am. Geophys. Un. Mtg., Fall, San Francisco, CA (7-11 December 1980)

DONATELLI, D.E. (Regis Coll., Weston, MA), and ALLEN, R.S.
Ionospheric Refractive Correction Using an Adaptive Procedure
Int. Solar-Terr. Predictions Wkshp., NOAA/ERL, Boulder, CO (23-27 April 1979)

DONATELLI, D.E., BURKE, W.J., and SAGALYN, R.C.
The Longitudinal Distribution of Topside Plasma Bubbles
Am. Geophys. Un. Mtg., Spring, Washington, DC (28 May - 1 June 1979)

DOYLE, M.A. and RICH, F.J. (Regis Coll., Weston, MA), BURKE, W., AND SMIDDY, M.
Field Aligned Currents Observed in the Region of the Dayside Cusp
Am. Geophys. Un. Mtg., Spring, Toronto, Canada (22-27 May 1980)

DRYER, M. (Space Environment Laboratory, NOAA-ERL, Boulder, CO) and SHEA, M.A.
Requirements for Predictions and Real-Time Monitoring for the Study of Travelling Interplanetary Phenomena
Int. Solar-Terr. Predictions Wkshp., Boulder, CO (23-27 April 1979)

DUBS, C.W.
Restriction in Phase Space and the Lifetime of Geomagnetically Trapped Particles
Am. Geophys. Un. Mtg. Spring, Toronto, Canada (28 May - 1 June 1979)

ESSEX, E.A., KLOBUCHAR, J.A., PHILBRICK, C.R., MENDILLO, M. (Boston Univ., Boston, MA), and LEO, R.E. (Montana State Univ., Bozeman, MT)
Total Electron Content Observations During the February 26, 1979 Total Solar Eclipse Over North America
Nat'l. Rad. Sci. Mtg., Univ. of Colorado, Boulder, CO (5-8 November 1979)

FEYNMAN, J., SPJELKVIK, W.N., and FRITZ, T.A. (NOAA/ERL/SEL, Boulder, CO), and HARDY, D.A.
Scatha and ATS-6 Observations of Outer Radiation Zone Particle Injections During a Multi-Substorm Magnetic Disturbance
Am. Geophysics. Un. Mtg., Fall, San Francisco, CA (3-7 December 1979)

FEYNMAN, J.
300 Years of Auroral Variability
NATO Advanced Study Inst. on Exploration of the Polar Upper Atmos., Norway (May 1980)

FILZ, R.C.
Long Duration Exposure Emulsion Package (LDEEP)
Am. Phys. Soc. Mtg., Washington, DC (23-26 April 1979)
Measurement of 55 MeV Trapped Proton Fluxes with H MIN—300 km at Solar Maximum
Am. Geophys. Un. Mtg., Fall, San Francisco, CA (8-12 December 1980)

FILZ, R.C., PARSIGNAULT, D.R., and HOLEMAN, E. (Emmanuel Coll., Boston, MA)
0.1-100 MeV Proton Fluxes at the Outer Edge of the Inner Trapped Region
Am. Geophys. Un. Mtg., Spring, Toronto, Canada (22-27 May 1980)

FILZ, R.C., RAO, Y.V., DAVIS, A. and HAGAN, M.P. (Emmanuel Coll., Boston, MA)
CR-39 Plastic Track Detector Experiment for Measurement of Charge Composition of Primary Cosmic Rays
IUPAP/IAU Symp. No.94, Origin of Cosmic Rays, Bologna, Italy (11-14 June 1980)

FLUCKIGER, E., and DEBRUNNER, H. (Physikalisches Institut, Univ. of Bern, Bern, Switzerland), SMART, D.F., and SHEA, M.A.
Calculations of Changes in Cosmic Ray Cutoff Rigidities Due to a Partial Ring Current System in the Magnetosphere
16th Int. Cosmic Ray Conf., Kyoto, Japan (6-18 August 1979)
Theoretical Study of the Effects of a Partial Ring Current in the Magnetosphere on Cosmic Ray Cutoffs
XVII International Union of Geodesy and Geophysics/International Association of Geomagnetism and Aeronomy General Assbly., Canberra, Australia (3-14 December 1979)
On the Significance of Cosmic Ray Measurements as Additional Tool for Magnetospheric Studies
Seventh European Cosmic Ray Symposium, Leningrad, USSR (11-15 September 1980)

FOUGERE, P.F.
Sunspots: Power Spectra and a Forecast
Int. Solar-Terr. Prediction Wkshp., Boulder, CO (23-27 April 1979)
Maximum Entropy Power Spectrum Estimation
Ecole Polytechnique, Montreal, Canada (15-21 June 1980)
High-Time Resolution Study of the September 21, 1977 Sudden Commencement Using AFGL Magnetometer Data
NOAA (April 1979)
The Maximum Entropy Method and Some Applications
Am. Statistical Assoc. Joint Mtg, Washington, DC (13 August 1979)
Geomagnetic Pulsation Observations Using the AFGL Magnetometer Network
IAGA Gen. Assbly., Australia (December 1979)

FOUGERE, P.F., and TSACOYEANES, C.
AFGL Magnetometer Observations of the Mount St. Helen's Eruption of MAY 18 1980
Am. Geophys. Un. Mtg., San Francisco, CA (Fall, 1980)

GARRETT, H.B.
Low Energy Magnetospheric Plasma Interactions with Space Systems - The Role of Predictions
Int. Solar-Terr. Predictions Wkshp., Univ. of Colorado, CO (23-27 April 1979)
Review of the Near-Earth Spacecraft Environment
Soc. Photo-Optical Instrum. Engineers, No. Hollywood, CA (4 February 1980)

GARRETT, H.G., CAPT., USAF, RUBIN, A.G., and PIKE, C.P.
Prediction of Spacecraft Potentials at Geosynchronous Orbit
Int. Solar-Terr. Predictions Mtg., NOAA/ERL, Boulder, CO (23-27 April 1979)

GARRETT, H.B., and SCHWANK, D.C.
ATS-5 and ATS-6 Quantitative Models of the Geosynchronous Plasma
IUAGG/IAGA Mtg., Canberra, Australia (3-14 December 1979)

GARRETT, H.B., SCHWANK, D., HIGBIE, P.R., and BAKER, D.N. (Los Alamos Scientific Laboratory)
Comparison Between the 30-80 KeV Electron Channels on ATS-6 and 1976-059A During Conjunction and Application to Spacecraft Charging Prediction
Am. Geophys. Un. Mtg., Spring, Washington, DC (28 May - 1 June 1979)

GARRETT, H.B., SMART, D.F., and SHEA, M.A.
Correlation Studies of AE, ap and Dst at Time Lags Between 0 and 30 Hours
XVII IUGG Gen. Assembly, IAGA Session, Canberra, Australia (3-14 December 1979)

GEBBIE, K.B., and TOOMRE, J. (Joint Inst. for Laboratory Astrophysics, Boulder, CO), SIMON, G.W.
The Variation with Height of Supergranular Velocity Fields
153rd Am. Astronom. Soc. Mtg., Mexico City, Mexico (7-11 January 1979)

GUSSENHOVEN, M.S. (Boston Coll.), HARDY, D.A., and BURKE, W.J.
DMSP Electron Observations of Equatorward Auroral Boundaries and Their Relationship with Magnetospheric Electric Fields
Am. Geophys. Un. Mtg., Fall, San Francisco, CA (3-7 December 1979)
Quasi Static Injection Boundaries: DSMP Predictions and P78-2(SCATHA) Observations
Am. Geophys. Un. Mtg., Spring, Toronto, Canada (22-27 May 1980)

GUSSENHOVEN, M.S., COHEN, H., HARDY, D.A., BURKE, W.J., and CHESLEY, A.
Analysis of Ambient and Beam Particle Characteristics During the Ejection of an Electron Beam from a Satellite in Near-Geosynchronous Orbit on March 30 1979
Spacecraft Charging Tech. Conf. III, USAF Academy, Colorado Springs, CO (12-14 November 1980)

GUSSENHOVEN, M.S., BURKE, W.J., HARDY, D.A., and RICH, F.J. (Regis Coll., Weston, MA)
Electric and Magnetic Field Structures at High Latitudes with a Northward IMF
Am. Geophys. Un. Mtg., Spring, Washington, DC (28 May - 1 June 1979)

HAISH, B.M., and LINSKY, J.L. (Inst. for Lab. Astrophysics, Boulder, CO), SLEE, O.B. (CSIRO, Sydney, Australia), and WORDEN, S.P.
Simultaneous X-Ray, UV, Optical and Radio Observations of the Flare Star, Proxima Centauri
154th Am. Astronom. Soc. Mtg., Wellesley, MA (12-14 June 1979)

HARDY, D.A., RICH, F.J., and BURKE, W.J.
Auroral Dynamics During a Substorm Near the Dawn Dusk Meridian
Am. Geophys. Un. Mtg., Spring, Washington, DC (28 May - 1 June 1979)

HARDY, D.A., BURKE, W.J., GUSSENHOVEN, M.S., and FEYNMAN, J.
Spatial and Temporal Variation of Electron and Proton Pitch Angle Distributions Near Geosynchronous Altitude
Am. Geophys. Un. Mtg., Fall, San Francisco, CA (3-7 December 1979)

HARDY, D.A., BURKE, W.J., and GUSSENHOVEN, M.S.
Optical and Electron Measurements of Polar Cap Arcs
Am. Geophys. Un. Mtg., Spring, Toronto, Canada (22-27 May 1980)

HARDY, D.A., GUSSENHOVEN, M.S., BURKE, W.J., and HOLMAN, E. (Emmanuel Coll., Boston, MA)
The Relationship Between the Equatorward Boundary of Auroral Electron Precipitation and the State of the Interplanetary Magnetic Field and Solar Wind
Am. Geophys. Un. Mtg., Fall, San Francisco, CA (8-12 December 1980)

HEGE, E.K., COCKE, W.J., HUBBARD, E., GRESHAM, M., and STRITTMATTER, P.A. (Steward Obs., Tucson, Arizona), WORDEN, S.P.. AND RADICK, R.R.
Speckle Interferometric Observations of Pallas
156th Am. Astronom. Soc. Mtg., College Pk., MD (16-18 June 1980)

HOUMINER, Z. (NRC Sr. Research Assoc.), and AARONS, J.
Plasmapause and Auroral Oval Irregularities During Magnetic Storms
No. Am. Radio Sci. Mtg and IEEE/AP-S Int. Symp., Univ. Laval, Cite Universitaire, Quebec, Canada (2-6 June 1980)

HUGHES, W.J. (Boston Univ., Boston, MA)
A Global Study of Pi2 Pulsations
Am. Geophys. Un. Mtg., Spring, Ontario, Canada (22-27 May 1980)

HUMBLE, J.E. (Univ. of Tasmania, Australia), SMART, D.F., and SHEA, M.A.
Cosmic Ray Cutoffs at 400 km
Am. Geophys. Un. Mtg., Spring, Washington, DC (28 May - 1 June 1979)

HUMBLE, J.E., SMART, D.F., and SHEA, M.A.
Cosmic Ray Cutoffs at 400 km Applicable to the HEAO-C Satellite
16th Int. Cosmic Ray Conf., Kyoto, Japan (6-18 August 1979)

JASPERSE, J.R., and STRICKLAND. D.J. (Science Applications, McLean, VA)
An Analytic Solution for the Primary Auroral Electron Flux in the Forward-Scattering and Average, Discrete, Energy-Loss Approximations
Am. Geophys. Un. Mtg., Fall, San Francisco, CA (3-7 December 1979)

JASPERSE J.R., BASU, B.
Approximate Analytic Solutions for the Auroral Proton and Hydrogen Fluxes and Related Quantities
Am. Geophys. Un. Mtg., Fall, San Francisco, CA (8-12 December 1980)

KEIL, S.L.
Some Comments on the Interpretation of Photospheric Line Shifts
154th Am. Astronom. Soc. Mtg., Wellesley, MA (12-14 June 1979)
Dynamical Models of Convective Penetration and High Spatial Resolution Observation
156th Am. Astronom. Soc. Mtg., College Pk., MD (16-18 June 1980)
Line Asymmetries Due to Granular Motion
155th Am. Astronom. Soc. Mtg., San Francisco, CA (13-18 January 1980)

KEIL, S.L., and CRAM, L.E. (Sac. Peak Obs., Sunspot, NM)
Dynamical Processes in the Solar Atmosphere: Observational and Theoretical Results Concerning the Nature of Turbulence
153rd Am. Astronom. Soc. Mtg., Mexico City, Mexico (7-11 January 1979)

KELLY, J.G. (AFGL West Coast Office) and PIKE, C.P.
Space Weather Environment and Its Effects on Present and Future Space Systems
Military Ops. Research Soc. Mtg., Vandenberg AFB, CA (4-6 December 1979)

KLOBUCHAR, J.A., MENDILLO, M. (Boston Univ., Boston, MA)
Unified Presentation of Ionospheric F-Region Storm Effects over the L=2 to 5 Latitude Range
Am. Geophys. Un. Mtg., Spring, Washington, DC (28 May - 1 June 1979)

KLOBUCHAR, J.A., RASTOGI, R.G.; BUSHBY, A. (Geophys. Institute of Peru, Peru), CHANDRA, H., SETHIA, G., and DESHPANDE, M.R. (Physical Research Lab., Ahmedabad, India)
A Comparison of Near-Equatorial Electron Content in the Indian and American Longitudes
22nd Plenary Mtg. COSPAR, Bangalore, India (29 May - 9 June 1979)

KLOBUCHAR, J.A., and MENDILLO, M.
A Morphology-Based Prediction Scheme for the Coupled Latitudinal and Local-Time Development of F-Region Storms
Solar-Terr. Predictions Wkshp., Boulder, CO (April 1979)

KLOBUCHAR, J.A., PHILBRICK, C.R., MENDILLO, M., ESSEX, E.A.
Total Electron Content Observations During the February 26, 1979 Total Solar Eclipse Over North America
Am. Geophys. Un. Mtg., Spring, Washington, DC (28 May - 1 June 1979)

KLOBUCHAR, J.A.
Present State of Ionospheric Time Delay Prediction
Symp. of Scientific and Engineering Uses of Satellite Radio Beacons, Warsaw, Poland (19-23 May 1980)

KLOBUCHAR, J.A., and SOICHER, H. (U.S. Army Communications R&D Command, Ft. Monmouth, NJ)
A Preliminary Evaluation of the Two-Frequency Ionospheric Correction for the NAVSTAR-Global Positioning System
AGARD Symp., London, England (12-16 May 1980)

KROHL, H.W. (NOAA/EDIS/NGSDC, Boulder, CO), TANSKANEN, P.J., HARDY, D.A., and GUSSENHOVEN, M.S.
Comparative Studies of the Location of the Optical Oval, Discrete and Diffuse Auroras During Moderately Quiet Conditions
Am. Geophys. Un. Mtg., Spring, Toronto, Canada (22-27 May 1980)

KUHN, J.R. (Princeton Univ., Princeton, NJ), and WORDEN, S.P.
Evidence of Long Period Solar Velocity Fluctuations
153rd Am. Astronom. Soc. Mtg., Mexico City, Mexico (7-11 January 1979)

LAI, S.T. (Boston Coll., Boston, MA), and COHEN, H.A.
Space Charge Effects on Ion and Electron Beams Emitted from P78-2 Satellite
Am. Geophys. Un. Mtg., Fall, San Francisco, CA (8-12 December 1980)

LAI, S.T., and COHEN, H.A.
Virtual Anode Formation During Beam Operations
Am. Geophys. Un. Mtg., Spring, Toronto, Canada (18-22 May 1980)

MARCOS, F.A., CHAMPION, K.S.W., and PHILBRICK, C.R.
Empirical Model of Lower Thermospheric Density for Low Solar Flux and Geomagnetic Activity
COSPAR, Bangalore, India (29 May - 9 June 1979)

MENDILLO, M. (Boston Univ., Boston, MA)
The HEAO Hole in the Ionosphere
Am. Geophys. Un. Mtg., Spring, Toronto, Canada (22-27 May 1980)

MISCHKE, C.F.W., SHEA, M.A., SMART, D.F., RAUBENHEIMER, B.C., STOKER, P.H., and VAN DER WALT, A.J. (of Potchefstroom Univ., Potchefstroom, South Africa)
Experimental Observations of Secular Changes in the Vertical Cutoff Rigidity
16th Int. Cosmic Ray Conf., Kyoto, Japan (6-18 August 1979)

MOORE, J.G., and WEBER, E.J. (Regis Coll., Weston, MA)
OI 6300 and 7774 Airglow Measurements of Equatorial Plasma Depletions
Int. Symp. on Equatorial Aeron., Aguadilla, Puerto Rico (17-24 July 1980)

MULLEN, E.G., GARRETT, H.B., HARDY, D.A., and WHIPPLE, E.C. (Univ. of California at San Diego, CA)
P78-2 SCATHA Environmental Data Atlas
Spacecraft Charging Tech. Conf., USAF Academy, Colorado Springs, CO (12-14 November 1980)

MULLEN, J.P., WHITNEY, H.E., AARONS, J., and YEH, K.C. (Univ. of Illinois, Urbana, IL)
Longitudinal Sensitivity of Equatorial Scintillation as Discovered in the 1978 Equatorial Scintillation Campaign
Int. IEEE/APS Symp. and Nat'l. Radio Sci. Mtg., Univ. of Washington, Seattle, WA (18-22 June 1979)

MULLEN, J.P., and AARONS, J.
UHF Scintillation Activity Over Polar Latitudes
Danish Comm. for Scientific Res in Greenland, Copenhagen, Denmark (7 May 1980)

NEIDIG, D.F.
Multivariant Discriminant Analysis Applied to Solar Flare Forecasting
6th Conf. on Probability and Statistics in Atmospheric Science, Banff Centre, Banff, Alberta, Canada (9-12 October 1979)

NOPPER, R.W., JR. (NAS-NRC Assoc.), HUGHES, W.J. (Boston Univ., Boston, MA), MACLENNAN, C.G. (Bell Labs., Murray Hill, NJ), MCPHERRON, R.L. (Univ. of California at Los Angeles)
Pulsation Events of July 29 1977
Am. Geophys. Un. Mtg., Spring, Toronto, Canada (22-27 May 1980)

ODOM, D.B., and VIENS, N.P. (Raytheon Co., Wayland, MA), KLOBUCHAR, J.A.
Analysis of Unusual Signal Strength Variations Observed in the 14 and 21 MHz Bands Following an Atlas-Centaur Rocket Launch
URSI Mtg., Quebec, Canada (June 1980)

PIKE, C.P.
Spacecraft Charging Technology
IEEE Electro 79, New York, NY (April 1979)

PIKE, C.P., and STEVENS, N.J. (NASA Lewis Research Center)
Agreement for NASA OAST - USAF AFSC Space Interdependency on Spacecraft Environment Interaction
Spacecraft Charging Tech. Conf., USAF Academy, Colorado Springs, CO (12-14 November 1980)

PIKE, C.P., and STEVENS, N.J. (NASA Lewis Research Center)
Space Systems Environmental Interactions Technology
AF/NASA Spacecraft Charging Tech. Conf. III, USAF Academy, CO (12-14 November 1980)

RADICK, R.R.
Possible Eclipses Involving the Short Period Components of Beta Capricorni
155th Am. Astronom. Soc. Mtg., San Francisco, CA (13-18 January 1980)

RAO, Y.V., DAVIS, A., and HAGAN, M.P. (Emmanuel Coll., Boston, MA), and FILZ, R.C.
CR-39 Plastic Track Detector Experiment for Measurement of Charge Composition of Primary Cosmic Rays
IUPAP/IAU Symp. No. 94, Bologna, Italy (11-14 June 1980)

RASTOGI, R.G. (NRC Resident Res. Assoc.)
Nighttime Equatorial UHF Radio Scintillation and E and F Region Irregularities
Nat'l. Radio Sci. Mtg., Univ. of Colorado, Boulder, CO (5-8 November 1979)
Spread F and Scintillations of Radio Waves
IAGA Gen. Assbly., Canberra, Australia (2-15 December 1979)

RASTOGI, R.G., AARONS, J., WHITNEY, H.E., MULLEN, J.P., PANTOJA, J. (Geophys. Inst. of Peru, Huancayo, Peru), DESHPANDE, M.R., VATS, H.O., and CHANDRA, H. (Phys. Research Lab., Ahmedabad, India) and DAVIES, K. (NOAA Res. Lab., CO)
Multifrequency Equatorial Ionospheric Scintillations in American and Indian Zones
22nd PLENARY Mtg. of COSPAR, Bangalore, India (29 May - 9 June 1979)

RICH, F. (Regis Coll., Weston, MA), CATELL, C. (Space Science Lab., Univ. of California, Berkeley, CA), BURKE, W.J., and SMIDDY, M.
Height Variations of Field Aligned Currents and Electrostatic Shocks Obtained from Simultaneous Observations
Am. Geophys. Un. Mtg., Spring, Toronto, Canada (22-27 May 1980)

RICH, F.J., BURKE, W.J., and HARDY, D.A.
Observed Electric and Magnetic Field Structure Over the Harang Discontinuity
Am. Geophys. Un. Mtg., Spring, Washington, DC (May 1979)

ROTHWELL, P.L., and YATES, G.K.
The Conservation of the First Adiabatic Invariant and Substorm Onsets
Chapman Conf. on Waves and Instabilities in Space Plasma, Boulder, CO (Summer 1979)
Magnetic Instabilities in the Plasma Sheet Caused by Single Particle Motion
Am. Geophys. Un. Mtg., Spring, Toronto, Canada (28 May - 1 June 1979)
Rayleigh-Taylor Instabilities and Field Line Reconnection in the Plasma Sheet
Am. Geophys. Un. Mtg, Spring, Toronto, Canada (22-27 May 1980)

RUBIN, A.G., and SCHNUELLE, G. (Systems, Science & Software, Inc., CA)
SCATHA Satellite Detector Modeling
Am. Geophys. Un. Mtg., Spring, Washington DC (28 May - 1 June 1979)

RUBIN, A.G., COHEN, H.A., HARDY, D.A.; TAUTZ, M.F. (Radex Corp., Carlisle, MA), SAFLEKOS, N.A. (Boston Coll., Boston, MA)
Computer Simulation of Spacecraft Charging on SCATHA
Spacecraft Charging Tech. Conf. III, USAF Academy, Colorado Springs, CO (12-14 November 1980)

RUBIN, A.G., COHEN, H.A., TAUTZ, M.F., SAFLEKOS, N.A., and AGGSON, T. (Goddard Space Flight Ctr., NASA)
Computer Simulation of Spacecraft Charging on SCATHA
Am Geophys. Un. Mtg., Spring, Toronto, Canada (22-27 May 1980)

RUBIN, A.G., GARRETT, H.B., and WENDEL, A.
Materials Effects on Spacecraft Charging
IEEE Annual Conf. on Nuclear and Space Radiat. Eff., Santa Cruz, CA (17-20 July 1979)

SAFLEKOS, N.A., SHUMAN, B.M., POTEMRA, T.A. (JHV/APL, Laurel, MD)
Dual Satellite Observations of Geomagnetic Disturbances in Auroral Regions
Am. Geophys. Un. Mtg., Fall, San Francisco, CA (3-7 December 1979)

SAFLEKOS, N.A., TAUTZ, M.F., BHAVNANI, K.H. (Radex Corp.), RUBIN, A.G., MCINERNEY, R.E., and MIZERA, P.F. (The Aerospace Corp., El Segundo, CA)
Spacecraft Charging: A Comparison Between Model and Experiment from SCATHA
Am. Geophys. Un. Mtg., Fall, San Francisco, CA (3-7 December 1979); Spacecraft Charging Tech Conf III, USAF Academy, Colorado Springs, CO (12-14 November 1980)

SAMIR, U., WILDMAN, P.J.L., SAGALYN, R.C., and RICH, F.J.
The Contributions of Satellite Size, Satellite Potential, and Plasma Parameters in Determining Ion Distribution Around S3-2 Satellite—an Experimental Assessment
Am. Geophys. Un. Mtg., Spring, Washington, DC (May 1979)

SCHNEEBERGER, T.J., WORDEN, S.P., and AFRICANO, J.L. (AURA, Inc., Sac Peak Obs., Sunspot, NM)
Observational Astronomy at the Cloudcroft Observatory
Southwest Regional Conf. on Astron. and Astrophys. Mtg., Little Rock, AR (20-21 May 1979)

SCHNEEBERGER, T.J., WORDEN, S.P., AFRICANO, J.L., and QUIGLEY, R. (Western Wash. Univ., Bellingham, Washington)
New Photometric Observations of EX Hydrae
155th Am. Astronom. Soc. Mtg., San Francisco, CA (13-18 January 1980)

SCHNEEBERGER, T.J., WORDEN, S.P., DELUCCA, E. (Wesleyan Univ., Middletown, CT), and GIAMPAP, M. (Steward Obs., Tucson, AZ)
High Resolution Spectra of Stellar Flares
155th Am. Astronom. Soc. Mtg., San Francisco, CA (13-18 January 1980)

SCHNEEBERGER, T.J., WORDEN, S.P., KUHN, J.R. (Princeton Univ., Princeton, NJ), and AFRICANO, J.L.
Flare Activity on T Tauri Stars
155th Am. Astronom. Soc. Mtg., San Francisco, CA (13-18 January 1980)

SCHNUELLE, G.W., KATZ, I., MANDELL, M.J. (All of Systems, Science, and Software, Inc.), and RUBIN, A.G.
Simulation of the Charging of the SCATHA (P78-2) Satellite
Am. Geophys. Un. Mtg., Fall, San Francisco, CA (3-7 December 1979)
Simulation of a Natural Charging Event on the SCATHA (P78-2) Satellite
Am. Geophys. Un. Mtg., Spring, Toronto, Canada (18-22 May 1980)

SHEA, M.A.
Cosmic Ray Trajectory Calculations and Their Application
Indo-U.S. Workshop on Solar-Terrestrial Physics, Udaipur, Rajasthan, India (12-16 June 1979)
Solar Cosmic Ray Emissions as Registered by Ground Stations
Astronomical Observatory Seminar, Ondrejov, Czechoslovakia (23 June 1980)

SHEA, M.A., and SMART, D.F.
Relativistic Solar Particle Events During STIP Intervals II and IV
STIP Symposium on Solar Radio Astronomy, Interplanetary Scintillations, and Co-ordination with Spacecraft, Narrabri, N.S.W., Australia (28-30 November 1979)
Preliminary Study of Neutron Monitor Intensity vs. Geophysical and Solar Parameters
COSPAR Specialized Symposia on Cosmic Rays in the Heliosphere, XXIII Plenary Meeting of COSPAR, Budapest, Hungary (2-14 June 1980)
Possible Evidence for a Rigidity-Dependent Release of Relativistic Protons from the Solar Corona
STIP Symp. on Shock Waves in the Solar Corona and Interplanetary Space, Smolenice, Czechoslovakia (15-19 June 1980)

SHEA, M.A., SMART, D.F., ARENS, M., BERCOVITCH, M., CHIBA, T., DEBRUNNER, H., DORMAN, L.I., DUGGAL, S.P., FENTON, A.J., FLUCKIGER, E., GALLI, M., HATTON, C.J., HUMBLE, J.E., JODOGNE, J.C., KONIG, P.J., LAZUTIN, L.L., LOCKWOOD, J.A., POMERANTZ, M.A., ROHRS, K., SHAFER, YU.G., STOKER, P.H., STORINI, M., TAKAHASHI, H., TANSKANEN, P.J., VENKATESAN, D., WADA, M., and WIBBERENZ, G.
The Ground-Level Relativistic Solar Proton Event of May 7, 1978: A Composite Report
16th Int. Cosmic Ray Conference, Kyoto, Japan (6-18 August 1979)

SHEA, M.A., SMART, D.F., and TANSKANEN, P.J. (Univ. of Oulu, Oulu, Finland), HUMBLE, J.E. (Univ. of Tasmania, Hobart, Australia)
Neutron Monitor Response to Non-Vertical Arrival Directions During GLE'S
16th Int. Cosmic Ray Conf., Kyoto, Japan (6-18 August 1979)

SHUMAN, B.M., VANCOUR, R.P., SMIDDY, M., SAFLEKOS, N.A., RICH, F.J.
Field-Aligned Current, Convective Electric Field, and Auroral Particle Measurements During a Major Magnetic Storm
Am. Geophys. Un. Mtg., Spring, Toronto, Canada (22-27 May 1980)

SIMON, G.W.
The Role of the Astronaut in Space Research
5th Air Univ. Airpower Symp., Air War Coll., Maxwell AFB, AL (23-25 February 1981)

SMART, D.F.
Prediction of Time Intensity Profiles of Solar Proton Events
Indo-U.S. Workshop on Solar-Terrestrial Physics, Udaipur, Rajasthan, India (12-16 June 1979)
Prognosis of Cosmic Ray Emissions from Solar Flares
Astronomical Observatory Seminar, Ondrejov, Czechoslovakia (23 June 1980)

SMART, D.F., and SHEA, M.A.
PPS76 - A Computerized "Event Mode" Solar Proton Forecasting Technique
Solar-Terrestrial Prediction Workshop, College Inn, Boulder, CO (23-27 April 1979)
A Summary of Solar Particle Prediction Research
Indian Space Research Organization Seminar, Bangalore, India (18 June 1979)
The Predictability of Solar Proton Events
Radio Science Division Seminar, National Research Laboratories, New Delhi, India (20 June 1979)

SMART, D.F., SHEA, M.A., HUMBLE, J.E.
Characteristics of Cosmic Ray Cutoffs for a Satellite Orbiting at 400 km
Symp. on Cosmic Rays in the Heliosphere, COSPAR, Budapest, Hungary (2-14 June 1980)

SMART, D.F., and SHEA, M.A., HUMBLE, J.E., and TANSKANEN, P.J.
A Model of the May 7 1978 Solar Cosmic Ray Event
16th Int. Cosmic Ray Conf., Kyoto, Japan (6-18 August 1979)

SMART, D.F., SHEA, M.A.; LUND, N., RASMUSSEN, I.L., BYRNAK, B., WESTERGAARD, N.J. (All of Danish Space Research Inst., Lyngby, Denmark)
Cosmic Ray Penumbral Patterns Derived from the Trajectory Calculations for the HEAO-C Satellite
16th Int. Cosmic Ray Conf., Kyoto, Japan (6-18 August 1979)

SMIDDY, M., HARDY, D.A., SHUMAN, B., BURKE, W.J., SAFLEKOS, N.A. (Boston Coll., Boston, MA), RICH, F.J. (Regis Coll., Weston, MA), KELLEY, M.C. (Cornell Univ., Ithaca, NY), POTEMRA, T.A. (Johns Hopkins Univ., Laurel, MD)
Observed Relationships Between High-Latitude Fields and Large Scale Birkeland Current Systems
Yosemite High Latitude Electric Fields Conf., Yosemite Nat'l Pk., CA (30 January - 2 February 1980)

SMIDDY, M., RICH, F.J., BURKE, W.J., HARDY, D.A., and WOLFE, R.A.
Observations of Field-Aligned Currents in Association with Strong Convection Electric Fields in the Trough
Am. Geophys. Un. Mtg., Spring, Washington, DC (May 1979)

SMIDDY, M., and SAGALYN, R.C.
Department of Defense Electric Field Studies in the Eighties
Yosemite High Lat. Electric Fields Conf., Yosemite Nat'l Pk., CA (30 January - 2 February 1980)

SPIRO, R.W., HAREL, M., REIFF, P.H., and RICH, F.J.
Substorm Simulation Results: II Subauroral Electric Fields and Evolution of the Plasmapause
Am. Geophys. Un. Mtg., Spring, Washington, DC (May 1979)

SU, S.Y. (Lockheed Engineering & Management Services Co., Houston, TX), and KONRADI, A. (NASA Johnson Space Ctr., Houston, TX)
Comparison of the Average Plasma Environment at Geosynchronous Orbit with the Environment at Lower L-Values
Am. Geophys. Un. Mtg., Spring, Toronto, Canada (22-27 May 1980)

TANSKANEN, P.J., HARDY, D.A.
Electron Spectra in the Region of Discrete Auroral Arcs as Observed with DMSP-Satellites
Am. Geophys. Un. Mtg., Spring, Washington, DC (28 May - 1 June 1979)
The Persistence of Auroral Features and the Pattern of Electron Precipitation in Consecutive DMSP Satellite Passes
Am. Geophys. Un. Mtg., Spring, Toronto, Canada (22-27 May 1980)

TOOMRE, J. (Joint Inst. for Laboratory Astrophysics, CO), NOVEMBER, L.J. (Sac. Peak Obs., Sunspot, NM), and SIMON, G.W.
Mesogranulation—An Intermediate Scale of Motion on the Sun
155th Am. Astronom. Soc. Mtg., San Francisco, CA (13-18 January 1980)

VAMPOLA, A.L., ALTROCK, R.C., ET AL.
User Requirements of Solar-Terrestrial Predictions for Spacecraft Applications
Solar-Terr. Predictions Wkshp., Boulder, CO (1979)

WEBER, E.J.
AFGL Equatorial Scintillation Campaigns: Airborne Optical Measurements of 6300Å Airglow Depletions
Wkshp. on the Physics of the Equatorial Ionosphere, Cornell Univ., Ithaca, NY (22-23 October 1979)

WENDEL, A.H.
Real-Time Earth-Based Predictors of Spacecraft Charging During Eclipse Passage
Am. Geophys. Un. Mtg., Fall, San Francisco, CA (3-7 December 1979)
Compensation for Band-Pass Error in 10-100 keV Particle Data from ATS-5, ATS-6 and SCATHA
Am. Geophys. Un. Mtg., Fall, San Francisco, CA (8-12 December 1980)

WHALEN, J.A., and SHARBER, J.R. (of Inst. of Space and Atmos. Studies, Florida Inst. of Tech., Melbourne, FL)
Spectral and Latitudinal Characteristics of the Electron Precipitation in the Continuous (Diffuse) Aurora Near Midnight
Am. Geophys. Un. Mtg., Spring, Washington, DC (28 May-1 June 1979)

WHALEN, J.A.
Latitude and Local Time Dependence of the Continuous Aurora
Am. Geophys. Un. Mtg., San Francisco, CA (3-7 December 1979)

WHITNEY, H.E., MULLEN, J.P., and AARONS, J.
The Statistics of Scintillation Activity Over Polar and Auroral Latitudes During a Period of High Solar Flux
Nat'l Radio Sci. Mtg., Univ. of Colorado, Boulder, CO (12-15 January 1981)

WILKERSON, M.S.
Comparisons of the Orientations of Double-Lobed Radio Sources and Their Associated Elliptical Galaxies
Astronom. Soc. of the Pacific Ann. Mtg., Tucson, AZ (7-12 July 1980)

WORDEN, S.P. (Sac. Peak Obs., Sunspot, NM)
Solar Large Scale Velocity Periodicities in the Range 4d-18d
IAU Jt. Discussion, Montreal, Canada (14-23 August 1979)
Detecting Planets in Binary Systems with Speckle Interferometry
Life in the Universe, NASA Ames Res. Ctr., Moffett Fld., CA (19-20 June 1979)
High Angular Resolution Astronomical Techniques: Speckle Interferometry and Related Methods
SPIE Mtg., San Diego, CA (25 July - 1 August 1980)
Image Reconstruction Using Speckle Interferometry
153rd Am. Astronom. Soc. Mtg., Mexico City, Mexico (7-11 January 1979)

WORDEN, S.P., and KEIL, S.L.
Sources of Noise in Solar-Limb Definitions
154th Am. Astronom. Soc. Mtg., Wellesley, MA (12-14 June 1979)

WORDEN, S.P., and HEGE, E.K., HUBBARD, E.N., WOOLF, N.J., STRITTMATTER, P.A. (all of Univ. of Arizona, Tucson, AZ)
Speckle Interferometry, A Test on an Earth Orbital Satellite
NORSIC 12 Spacecraft Identification Conf. (NORAD), Colorado Springs, CO (13-15 August 1980)

YOUNG, E.R., RICH, F.J. (Regis Coll., Weston, MA), and SMIDDY, M., SAGALYN, R.C.
Observations of Equinoctial Density Enhancements in the Equatorial Topside Ionosphere Near the Sunset Terminator
Am. Geophys. Un. Mtg., Toronto, Canada (22-27 May 1980)

YOUNG, E.R., BURKE, W.J., RICH, F.J., SAGALYN, R.C., and SMIDDY, M.
The Global Distribution of Equatorial Spread F in the Topside Ionosphere during Equinoctial Periods
Symp. on the Eff. of the Iono. on Radio Sys., Naval Res. Lab., Washington, DC (April 1981)

YOUNG, P.S. (Miss. State Univ.), HOLEMAN, E.G., PARSIGNAULT, D.R., HAGAN, M.P. (Emmanuel Coll., Boston, MA), and FILZ, R.C.
The Generalized Geometrical Factor of Particle Telescopes for Trapped Radiation
16th Int. Cosmic Ray Conf., Kyoto, Japan (6-18 August 1979)

TECHNICAL REPORTS

AARONS, J., MULLEN, J.P., WHITNEY, H.E., and MACKENZIE, E.M.
The Dynamics of Equatorial Irregularity Patch Formation, Motion, and Decay
AFGL-TR-80-0090 (26 March 1980), ADA083154

BARRON, W.R., CLIVER, E.W., GUIDICE, D.A., and BADILLO, V.L.
An Atlas of Selected Multi-Frequency Radio Bursts from the Twentieth Solar Cycle
AFGL-TR-80-0098 (2 April 1980), ADA088220

BURKE, W.J., HARDY, D.A., CAPT., RICH, F.J., KELLEY, M.C., SMIDDY, M., SHUMAN, B., SAGALYN, R.C., VANCOUR, R.P., WILDMAN, P.J.L., LAI, S.T., and BASS, J.
A Case Study of S3-2 Observations in the Late Evening Auroral Oval
AFGL-TR-79-0011 (8 January 1979), ADA072996

CLIVER, E.W.
Almost-Necessary Conditions for a Solar Active Region to Produce a Subsequent Polar Cap Absorption Event
AFGL-TR-80-0151 (17 April 1980), ADA088882

DANDEKAR, B.S.
Study of the Equatorward Edge of the Auroral Oval from Satellite Observations
AFGL-TR-79-0010 (9 January 1979), ADA072997

DUBS, C.W.
Phase Space Coordinates of Long Lifetime Trapped Radiation From Stormer Mapping
AFGL-TR-79-0029 (18 January 1979), ADA072995
On the First and a Related Adiabatic Invariant with a Force in the Direction of the Velocity
AFGL-TR-80-0193 (25 June 1980), ADA099338

FILZ, R.C.
Long Duration Exposure Emulsion Package (LDEEP)
AFGL-TR-79-0156(19 July 1979), ADA077362

FINKE, R.C., and PIKE, C.P.
Spacecraft Charging Technology - 1978
AFGL-TR-79-0082 (1979), ADA084626

FORBES, J.M., and GARRETT, H.B., CAPT.
Atmospheric Effects on Time-Varying Photoelectron Flux from Satellite Surfaces
AFGL-TR-80-0185 (16 June 1980), ADA092446

GARRETT, H.B., CAPT.
The Current Status of Predictions of Low Energy Plasma Interactions with Space Systems
AFGL-TR-79-0089 (4 April 1979), ADA074523

GARRETT, H.B., CAPT., MCINERNEY, R.E., DEFOREST, S.E., and JOHNSON, B.
Modeling of the Geosynchronous Orbit Plasma Environment - Part 3. ATS-5 and ATS-6 Pictorial Data Atlas
AFGL-TR-79-0015 (15 January 1979), ADA067843

GAUNT, D.M.
Large Space Structure Charging During Eclipse Passage
AFGL-TR-80-0022 (15 January 1980), ADA084810

HANSER, F.A., HARDY, D.A., CAPT., and SELLERS, B.
Calibration of the Rapid Scan Particle Detector Mounted in the SCATHA Satellite
AFGL-TR-79-0167 (18 July 1979), ADA082382

HARDY, D.A., CAPT., and MACKEEN, R.
An Algorithm for Determining the Boundary of Auroral Precipitation Using Data From the SSJ/3 Sensor
AFGL-TR-80-0028 (24 January 1980), ADA084482

HARDY, D.A., GUSSENHOVEN, M.S., and HUBER, A.
The Precipitating Electron Detectors (SSJ/3) for the Block 5D/Flights 2-5 DMSP Satellites: Calibration and Data Presentation
AFGL-TR-79-0210 (14 September 1979), ADA083136

HOUMINER, Z., and AARONS, J.
Behavior of High-Latitude Irregularities During Geomagnetic Disturbances
AFGL-TR-80-0194 (24 June 1980), ADA094120

KLEIN, M.M.
A Method for Direct Determination of Real Height from Virtual Height Data for the Auroral Region of the Ionosphere
AFGL-TR-79-0276 (14 November 1979), ADA083139

KNECHT, D.J., HUTCHINSON, R.O., and TSACOYEANES, C.W.
An Introduction to the AFGL Magnetometer Network
AFGL-TR-79-0108 (April 1979), ADA068879
Archive Data Tapes of the AFGL Magnetometer Network
AFGL-TR-79-0212 (20 September 1979), ADA084483

KRUKONIS, P.A., WHALEN, J.A., and REILLY, A.E.
Short Duration Sporadic E and Discrete Auroral Events
AFGL-TR-79-0004 (4 January 1979), ADA069800

MAZZELLA, A., TOBENFELD, E., and RUBIN, A.G.
AFSIM - An Air Force Satellite Interactions Model
AFGL-TR-79-0138 (29 June 1979), ADA078032

MULLEN, E.G., GARRETT, H.B., HARDY, D.A., and WHIPPLE, E.C.
P78-2 SCATHA Preliminary Data Atlas
AFGL-TR-80-0241 (11 August 1980), ADA094122

RICH, F., SMIDDY, M., SAGALYN, R.C., BURKE, W.J., ANDERSON, P., BREDESEN, S., and SULLIVAN, W.P.
In-Flight Characteristics of the Topside Ionospheric Monitor (SSIE) on the DMSP Satellite Flight 2 and Flight 4
AFGL-TR-80-0152 (17 April 1980), ADA088879

RICH, F.J., CATTELL, C.A., KELLEY, M.C., and BURKE, W.J.
Simultaneous Observations of Auroral Zone Electrodynamics by Two Satellites: Evidence for Height Variations in the Topside Ionosphere
AFGL-TR-80-0342 (10 November 1980), ADA100237

RUBIN, A.G., BHAVNANI, K.H., and TAUTZ, M.F.
Charging of Spinning Spacecraft
AFGL-TR-79-0261 (29 October 1979), ADA084807

RUBIN, A.G., GARRETT, H.B., and WENDEL, A.H.
Spacecraft Charging on ATS-5
AFGL-TR-80-0168 (14 May 1980), ADA090508

SAGALYN, R.C., HUTCHINSON, R.O., and GUSSENHOVEN, S. (Editors)
Proceedings of the Air Force Geophysics Laboratory Workshop on Geomagnetism: April 6-7, 1979
AFGL-TR-79-0192 (20 August 1979), ADA082308

SHUVAL, A., KLOBUCHAR, J.A., and SOICHER, H.
Correlation Studies of Protonospheric Electron Content Over the U.S.
AFGL-TR-79-0064 (6 March 1979), ADA073080

TSIPOURAS, P., and GARRETT, H.B.
Spacecraft Charging Model - 2 Maxwellian Approximations
AFGL-TR-79-0153 (13 July 1979), ADA077907

VANCOUR, R.P., and SHUMAN, B.M.
Comparison of Results from the S3-2 Satellite and the Chatanika Radar in an Early Morning Aurora
AFGL-TR-79-0254 (22 October 1979), ADA086861

WENDEL, A.H., 2nd LT, USAF
Ground-Based Predictors of Spacecraft Charging During Eclipse Passage
AFGL-TR-80-0088 (20 March 1980), ADA090338

WHITNEY, H.E.
Report on Peru Scintillation Tests
AFGL-TR-79-0030 (22 January 1979), ADA072994

WILDMAN, P.J.L.
The Dynamics of a Rigid Body in the Space Plasma
AFGL-TR-79-0201 (28 August 1979), ADA084806

CONTRACTOR JOURNAL ARTICLES JANUARY 1979 – DECEMBER 1980

AKASOFU, S-I.
Prediction of the Occurrence and Intensity of Magnetospheric Substorms
Geophys. Res. Lett. 6, No. 11 (November 1979)

BASU, SANTIMAY, BASU, SUNANDA, MULLEN, J.P., and BUSHBY, A.
Long-Term 1.5 GHz Amplitude Scintillation Measurements at the Magnetic Equator
Geophys. Res. Lett. 7, No.4 (April 1980)

BASU, SANTIMAY, BASU, SUNANDA, JOHNSON, A.L., KLOBUCHAR, J.A., and RUSH, C.M.
Preliminary Results of Scintillation Measurements Associated with Ionosphere Heating and Possible Implications for the Solar Power Satellite
Geophys. Res. Lett. 7, No. 8 (August 1980)

BASU, SANTIMAY, MCCLURE, J.P., BASU, SUNANDA, HANSON, W.B., AARONS, J.
Coordinated Study of Equatorial Scintillation and In-Situ and Radar Observations of Nighttime F Region Irregularities
J. Geophys. Res. 85, No. A10 (October 1980)

BASU, SUNANDA, and AARONS, J.
The Morphology of High-Latitude VHF Scintillation Near 70°W
Radio Sci. 15, No. 1 (January-February 1980)

BASU SUNANDA, and KELLEY, M.C.
(Emmanuel Coll., Boston, MA)
A Review of Recent Observations of Equatorial Scintillations and Their Relationship to Current Theories of F-Region Irregularity Generation
Radio Sci. 14, No.3 (May-June 1979)

BURKE, W.J., BRAUN, H.J., MUNCH, J.W., and SAGALYN, R.C.
Observations Concerning the Relationship Between the Quiet-Time Ring Current and Electron Temperatures at Trough Latitudes
Planet. Space Sci. 27 (1979)

BURKE, W.J., SAGALYN, R.C., SMIDDY, M., KELLEY, M.C., and LAI, S.T.
Electric Fields at High Latitudes in the Topside Ionosphere Near the Dawn-Dusk Meridian
Space Research XIX, Ed. by M.J. Rycroft, Pergamon Pr. (1979)
Polar Cap Electric Field Structures with a Northward Interplanetary Magnetic Field
Geophys. Res. Lett. 6, No.1 (1979)

BURKE, W.J., DONATELLI, D.E., SAGALYN, R.C., and KELLEY, M.C.
Low Density Regions Observed at High Altitudes and Their Connection with Equatorial Spread F
Planet. Space Sci. 27 (1979)

BURKE, W.J., SAGALYN, R.C., and KANAL, M.
Observed Heating Effects of Conjugate Photoelectrons
Planet. Space Sci. 27 (1979)

BURKE, W.J., SAGALYN, R.C., RASTOGI, R.G., AHMED, M., RICH, F.J., DONATELLI, D.E., and WILDMAN, P.J.L.
Postsunrise Refilling of the Low-Latitude Topside Ionosphere
J. Geophys. Res. 84, No. A8 (August 1979)

BURKE, W.J., DONATELLI, D.E., and SAGALYN, R.C.
The Longitudinal Distribution of Equatorial Spread F Plasma Bubbles in the Topside Ionosphere
J. Geophys. Res. 85, No. A3 (March 1980)

BURKE, W.J., HARDY, D.A., RICH, F.J., KELLEY, M.C., SMIDDY, M., SHUMAN, B., SAGALYN, R.C., VANCOUR, R.P., WILDMAN, P.J.L., and LAI, S.T.
Electrodynamic Structure of the Late Evening Sector of the Auroral Zone
J. Geophys. Res. 85, No. A3 (March 1980)

BURKE, W.J., GUSSENHOVEN, M.S., RICH, F.J., HARDY, D.A., SMIDDY, M., and KELLEY, M.C.
Electrodynamic Structures in the Polar Cap During a Period of Geomagnetic Quieting
Proc. of Chapman Conf. on High Lat. Electric Field (January - February 1980)

CHACKO, C.C. (Dept. of Astronomy, Boston Univ., Boston, MA)
The High-Latitude Behavior of HmF2 and NmF2 Along the Noon-Midnight Meridian Under Quiet Conditions
J. Geophys. Res. 83, No.A 12 (December 1978)

CRAM, L.E., KEIL, S.L., and ULMSCHNEIDER, P.
Some Effects of Acoustic Waves on Spectral-Line Profiles
Astrophys. J., No. 234 (December 1979)

DEUBNER, F.L., ULRICH, R.K., and RHODES, E.J.
Solar P-Mode Oscillations as a Tracer of Radial Differential Rotation
Astron. Astrophys., 72 (1979)

EATHER, R.H., MENDE, S.E., and WEBER, E.J. (KEO Consultants, Newton MA)
Dayside Aurora and Relevance to Substorm Current Systems and Dayside Merging
J. Geophys. Res. 84, No. A7 (July 1979)

GIAMPAPA, M.S., WORDEN, S.P., and GILLIAM, L.B.
The Effects of Chromospheric Activity on Metallicity Measurements
Astrophys. J. 229 (May 1979)

HATHAWAY, D.H., GILMAN, P.A., and TOOMRE, J. (Univ. of Colorado, Boulder, CO)
Convective Instability when the Temperature Gradient and Rotation Vector Are Oblique to Gravity
Geophys. and Astrophys. Fluid Dynamics 13 (1979)

HUBBARD, G., REED, M., STRITTMATTER, P., HEGE, K., and WORDEN, S.P.
Digital Speckle Interferometry to Measure the Angular Diameters of Faint Objects
Proc. of Colloq. No. 50, Int. Astronom. Un. (1979)

KAN, J.R., and AKASOFU, S.-I. (Univ. of Alaska, Fairbanks, AK)
A Model of the Auroral Electric Field
J. Geophys. Res. 84, No. A2 (February 1979)

LIU, C.H., and YEH, K.C. (Univ. of Illinois, Champaign, IL)
Pulse Spreading and Wandering in Random Media
Radio Sci. 14, No. 5 (September-October 1979)

RHODES, E.J., DEUBNER, F.L., and ULRICH, R.K.
A New Technique for Measuring Solar Rotation
Astrophys. J., No. 227 (January 1979)

RICH, F.J., BURKE, W.J., KELLEY, M.C., and SMIDDY, M.
Observations of Field-Aligned Currents in Association with Strong Convection Electric Fields at Subauroral Latitudes
J. Geophys. Res. 85, No. A5 (May 1980)

SCHNEEBERGER, T.J., LINSKY, J.L., McCLINTOCK, W., and WORDEN, S.P.
Chromospheric Emission Lines in the Red Spectrum of AD Leonis. II. Physical Conditions in Flares
Astrophys. J. 231 (July 1979)

SCHNEEBERGER, T.J., WORDEN, S.P., AFRICANO, J.L., and TYSON, E.
Cloudcroft Observatory Today
Sky and Telescope 59 (February 1980)

SCHNEEBERGER, T.J., WORDEN, S.P., and BECKERS, J.M.
The Night Sky Conditions at the Sacramento Peak Observatory. I. Sky Brightness
Publ. Astron. Soc. Pac. 91, No. 542 (August 1979)

SCHUNK, R.W., and RAITT, W.J. (Utah St. Univ., Logan, UT)
Atomic Nitrogen and Oxygen Ions in the Daytime High-Latitude F Region
J. Geophys. Res. 85, No. A3 (March 1980)

SOJKA, J.J., FOSTER, J.C., RAITT, W.J., SCHUNK, R.W., and DOUPNIK, J.R. (Utah St. Univ., Logan, UT)
High-Latitude Convection: Comparison of a Simple Model with Incoherent Scatter Observations
J. Geophys. Res. 85, No. A2 (February 1980)

SOJKA, J.J., RAITT, W.J., and SCHUNK, R.W.
High-Latitude Plasma Convection: Predictions for Eiscat and Sondre Stromfjord
Geophys. Res. Lett. 6, No. 11 (November 1979)
Effect of Displaced Geomagnetic and Geographic Poles on High-Latitude Plasma Convection and Ionospheric Depletions
J. Geophys. Res. 84, No. A10 (October 1979)
A Comparison of Model Predictions for Plasma Convection in the Northern and Southern Polar Regions
J. Geophys. Res. 85, No. A4 (April 1980)

ULRICH, R.K., RHODES, E.J., and DEUBNER, F.L.
The Effect of a Radial Rotational Velocity Gradient on p-Mode Eigenfrequencies
Astrophys. J. 227 (January 1979)

WHELAN, J.A.J., WORDEN, S.P., RUCINSKI, S.M., and ROMANISHIN, W.
AH Cancri: A Contact Binary in M67
Mon. Not. R. Astr. Soc. 186 (1979)

CONTRACTOR TECHNICAL REPORTS JANUARY 1979 – DECEMBER 1980

ALBANO, R.K., LEE, L.C., and KAN, J.R. (Geophys. Inst., Univ. of Alaska)
Non-Neutral Field-Aligned Current Sheet and Auroral Electric Field
AFGL-TR-79-0066 (February 1979), ADA072852

AKASOFU, S.-I. (Geophys. Inst., Univ. of Alaska)
Interplanetary Energy Flux Associated with Magnetospheric Substorms
AFGL-TR-79-0141 (July 1979), ADA071388

ANANTHAKRISHNAN, S., COLES, W.A., KAUFMAN, J.J., and RICKETT, B.J. (Dept. of Electrical Engineering, Univ. of California)
The Latitudinal Structure of Solar Wind Streams from Radio Scintillation Observations
AFGL-TR-79-0234 (September 1979), ADA081462

BADILLO, V.L. (Manila Obs., Manila, Philippines)
Solar Microwave Bursts Accompanying Proton Events
AFGL-TR-79-0171 (31 July 1979), ADA081461

BAKER, K.B., and PAPAGIANNIS, M.D. (Dept. of Astronomy, Boston Univ., Boston, MA)
Correlation of High Latitude Coronal Holes with Solar Wind Streams High Above or Below the Ecliptic
AFGL-TR-80-0123 (April 1980), ADA087525

BANDES, D., and BARRETT, T.B. (Parke Mathematical Lab., Carlisle, MA)
Groundrange and Bearing Error Determination and Display for an OTH Backscatter System with an Arctic Through Ionosphere
AFGL-TR-80 0055 (II) (February 1980), ADA087010

BARRETT, T.B. (Parke Mathematical Lab., Carlisle, MA)
Spectral Analysis of Scintillation Data Taken From an Aircraft
AFGL-TR-80-0055 (I) (February 1980), ADA086837

BASU, SANTIMAY, and BASU, SUNANDA (Emmanuel Coll., Boston, MA)
Modelling of Equatorial Phase and Amplitude Scintillations from OGO-6 and AE Irregularity Data
AFGL-TR-80-0141 (November 1979), ADA087011

BELLEW, W., DAVIS, A., HAGAN, M.P., HOLEMAN, E., HUBER, A., PANTAZIS, J., PARSIGNAULT, D., and RAO, Y.V. (Emmanuel Coll., Boston, MA)
Energetic Particle Studies: Instrumentation and Analysis
AFGL-TR-79-0223 (September 1979), ADA081714

BHAVNANI, K.H., TAUTZ, M.F., and ZIEMBA, E.J. (Radex Inc., Carlisle, MA)
Analysis of Spacecraft Charging and Geophysical Data Bases
AFGL-TR-80-0173 (31 July 1980), ADA090020

BOYLE, R.P., and PARSIGNAULT, D.R. (Emmanuel Coll., Boston, MA)
Auroral X-Ray Contamination in the Polar Regions of the Low Energy Proton Spectrometer on the S3-2 Satellite
AFGL-TR-80-0265 (August 1980), ADA097713

CARDUS, J.O., ALBERCA, L.F., and GALDON, E. (Observatorio del Ebro, Roquetas, Spain)
Total Electron Content Model From INTASAT Data
AFGL-TR-79-0182 (3 May 1979), ADA073233

CHACKO, C.C., and MENDILLO, M. (Dept. of Astronomy, Boston Univ., Boston, MA)
DMSP Auroral Images and the Goose Bay Ionosphere
AFGL-TR-79-0023 (January 1979), ADA077023

CHAMBERLAIN, M.T. (Photometrics, Inc., Lexington, MA)
Data Analysis of Film from AFGL Rocket A31.603
AFGL-TR-79-0195 (20 August 1979), ADA092705

CHEN, C.K., WOLF, R.A., HAREL, M., KARTY, J.L., SPIRO, R.W., and ERICKSON, G.M. (William Rice Univ., Houston, TX)
Study of Magnetospheric Currents and Resultant Surface Magnetic Variations
AFGL-TR-80-0139 (17 April 1980), ADA093928

DALGARNO, A., and CONSTANTINIDES, E. (Smithsonian Astrophys. Obs., Cambridge, MA)
Calculations Pertaining to the Energy Balance and Plasma Motions in the Ionosphere
AFGL-TR-79-0270 (November 1979), ADA083010

DEVANE, J.F., and JOHNSON, E.R. (Boston Coll., Boston, MA)
Investigation of Magnetic Field Phenomena in the Ionosphere
AFGL-TR-79-0044 (October 1979), ADA075356

DONATELLI-DULONG, D.E. (Regis Coll., Weston, MA)
Development and Evaluation of Adaptive Techniques for Reducing Ionospheric-Induced Radar Tracking Errors in Real Time
AFGL-TR-79-0256 (30 September 1979), ADA081460

EATHER, R.H. (KEO Consultants, Newton, MA)
Ionization and Emission Processes in the Auroral and Equatorial Ionosphere
AFGL-TR-80-0326 (15 October 1980), ADA095296

FELLI, M., LANG, K.R., and WILLSON, R.F. (Dept. of Physics, Tufts Univ., Medford, MA)
VLA Observations of Solar-Active Regions I. The Slowly Varying Component
AFGL-TR-80-0225 (1 August 1980), ADA091722

GROSSI, M.D., and GUPTA, A.K. (Smithsonian Astrophys. Obs., Cambridge, MA)
Adaptive HF Propagation Path Utilization
AFGL-TR-79-0236 (15 September 1979), ADA090023

HALVERSON, W.D. (Spire Corp., Bedford, MA)
Techniques for the Simulation of the Space Plasma Environment
AFGL-TR-80-0337 (September 1980), ADA097734

HANSER, F.A., and SELLERS, B. (Panametrics, Inc., Waltham, MA)
Design, Construction and Testing of a Magnetic Electron Spectrometer for Detecting Electrons to 10 MeV, Including a Preliminary Design for a Flight Unit
AFGL-TR-79-0229 (September 1979), ADA078516

HAREL, M., WOLF, R.A., SPIRO, R.W., REIFF, P.H., CHEN, C.K., BURKE, W.J., RICH, F.J., and SMIDDY, M. (William Marsh Rice Univ., Houston, TX)
Quantitative Simulation of a Magnetospheric Substorm. I. Model Logic and Overview
AFGL-TR-80-0128 (23 January 1980), ADA087699
Quantitative Simulation of a Magnetospheric Substorm. II. Comparison with Observations
AFGL-TR-80-0129 (23 January 1980), ADA087700

HAREL, M., WOLF, R.A., REIFF, P.H., and SMIDDY, M.
Birkeland Currents and Ring Currents in the Computer Simulation of the Substorm of 19 September 1976
AFGL-TR-79-0041 (February 1979), ADA073852
Study to Analyze and Synthesize Satellite Data
AFGL-TR-79-0024 (15 January 1979), ADA070947

HARDY, J.W. (Itek Corp., Lexington, MA)
Solar Imaging Experiment
AFGL-TR-80-0338 (September 1980), ADA102283

HEDEMAN, E.R., and PRINCE, H.D. (Johns Hopkins Univ., Applied Physics Lab., Laurel, MD)
Study of Geomagnetic Storms, Solar Flares, and Centers of Activity in 1976, The Year Between Solar Activity Cycles 20 and 21
AFGL-TR-80-0267 (2 September 1980), ADA098936

HOLEMAN, E., SPENCER, T., RAO, Y.V., and HAGAN, M.P. (Emmanuel Coll., Boston, MA)
A Table of Parameters for Heavy Ion Tracks in CR-39 Nuclear Track Detector
AFGL-TR-80-0035 (January 1980), ADA083070

KANAL, M., TORABI, A.F. (Clark Univ., Worcester, MA)
Electron Transport at High Altitude
AFGL-TR-80-0314 (30 September 1980), ADA108185

LANG, K.R. (Dept. of Physics, Tufts Univ., Medford, MA)
Very Large Array (V.L.A.) Observations of Solar Active Regions
AFGL-TR-79-0037 (April 1979), ADA066780

LANG, K.R., and WILLSON, R.F. (Dept. of Physics, Tufts Univ., Medford, MA)
Fine-Scale Radio Studies of the Sun
AFGL-TR-80-0190 (1 July 1980), ADA090021

LAQUEY, R.E. (Maya Development Corp., San Diego, CA)
A Very Low Energy Electrostatic Analyzer
AFGL-TR-80-0023 (31 December 1979), ADA090016

LAZARUS, A.J. (Center for Space Res., Mass. Inst. of Technology, Cambridge, MA)
Analysis of Solar Wind Data from the SOLRAD 11A and 11B Spacecraft
AFGL-TR-79-0056 (February 1979), ADA070945

MENDILLO, M., and LYNCH, F.X. (Astronomy Dept., Boston Univ., Boston, MA)
The Influence of Geomagnetic Activity on the Day-to-Day Variability of the Ionospheric F-Region
AFGL-TR-79-0074 (January 1979), ADA070966

MENG, C.I. (Applied Physics Lab., Laurel, MD)
The Investigation of the Magnetospheric Dynamics in Conjunction with the SCATHA Satellite Observations
AFGL-TR-80-0070 (December 1979), ADA087433

MERTZ, L. (Lockheed Palo Alto Res. Lab., Palo Alto, CA)
Solar Magnetic Field Studies (Photon Counter)
AFGL-TR-79-0240 (October 1979), ADA082242

MICHELS, H.H. (United Technologies Res. Ctr., East Hartford, CT)
Theoretical Research Investigation upon Reaction Rates to the Nitric Oxide (Positive) Ion
AFGL-TR-80-0072 (31 January 1980), ADA104303
Theoretical Research Investigation upon Reaction Rates to the Nitric Oxide (Positive) Ion
AFGL-TR-79-0190 (Rpt. #1) (31 July 1979), ADA104136

MOREL, P.R., HANSER, F.A., and SELLERS, B. (Panametrics, Inc., Waltham, MA)
Design of Instrumentation Suitable for the Investigation of Charge Buildup Phenomena at Synchronous Orbit
AFGL-TR-79-0235 (October 1979), ADA081378

PARKER, L.W. (Lee W. Parker, Inc., Lexington, MA)
Time-Dependent Computer Model of Plasma Space Charge Interactions with a Finite-Cylindrical Spacecraft
AFGL-TR-80-0018 (31 December 1979), ADA084892

QUINN, S.B., JR. (Dept. of Elec. Engineering, Univ. of Illinois, Champaign, IL)
Studies of Transionospheric Scintillation Using Orbiting Satellite Data
AFGL-TR-80-0092 (April 1980), ADA085448

RICH, F.J., and ANDERSON, P.B. (Regis Coll. Res. Ctr., Weston, MA)
Space Environmental Studies: Instrumentation and Data Analysis Related to the Ionosphere
AFGL-TR-80-0218 (2 September 1980), ADA091816

ROELOF, E.C., and GOLD, R.E. (Johns Hopkins Univ., Laurel, MD)
Research on Prediction Techniques for the Time Dependence of Solar Particle Events and Geomagnetic Activity from Results of Synoptic Analysis of Solar and Interplanetary Particle Plasma and Field Observations
AFGL-TR-80-0100 (March 1980), ADA086817

SAMIR, U., WILDMAN, P.J., RICH, F., BRINTON, H.C., and SAGALYN, R.C. (Univ. of Michigan, Ann Arbor, MI)
About the Parametric Interplay Between Ionic Mach Number, Body-Size and Satellite Potential in Determining the Ion Depletion in the Wake of the S3-2 Satellite
AFGL-TR-80-0329 (December, 1980), ADA095507

SCHATTEN, K.H., and MENDILLO, M. (Dept. of Astron., Boston Univ., Boston, MA)
Short Term Periodicities in Ionospheric Total Electron Content
AFGL-TR-80-0096 (March 1980), ADA084756

SMITH, S., REINISCH, B.W., TANG, J.S., and BIBL, K. (Univ. of Lowell, Ctr. for Atmospheric Res., Lowell, MA)
Automatic Ionospheric Parameter Extractions from Digital Ionogram Data
AFGL-TR-80-0102 (November 1979), ADA084101

SPIRO, R.W., HAREL, M., WOLF, R.A., and REIFF, P.H. (William Marsh Rice Univ., Houston, TX)
Quantitative Simulation of a Magnetospheric Substorm. 3. Plasmaspheric Electric Fields and Evolution of the Plasmapause
AFGL-TR-80-0130 (25 January 1980), ADA087948

STEIN, R.F. (Dept. of Astron. and Astrophys., Michigan St. Univ., East Lansing, MI)
Solar Atmospheric Dynamics
AFGL-TR-80-0208 (May 1980), ADA092910

THOMAS, J.H., CLARK, A., JR., and SCHEUER, M.A. (Dept. of Mechanical and Aerospace Sci., Univ. of Rochester, Rochester, NY)
Dynamical Phenomena in Sunspots
AFGL-TR-80-0064 (15 February 1980), ADA086010

TSIPOURAS, P., and D'AGOSTINO, R. (Bedford Research Assoc., Bedford, MA)
Statistical Goodness-of-Fit Techniques Applicable to Scintillation Data
AFGL-TR-80-0345 (30 June 1980), ADA104511

VANCE, B., and MENDILLO, M. (Boston Univ., Boston, MA)
Finite Element Simulation of Processes in the Auroral Ionosphere
AFGL-TR-79-0003 (January 1979), ADA065551

VECCHIA, D.F., TRYON, P.V., CALDWELL, G.A., and JONES, R.H. (Statistical Engineering Div., National Bureau of Standards, Boulder, CO)
Statistical Methods for Solar Flare Probability Forecasting
AFGL-TR-80-0336 (September 1980), ADA092708

VONDRAK, R.R. (SRI International, Menlo Park, CA)
Simultaneous Measurements of the Auroral Ionosphere by the Chatanika Radar and by the S3-2 Satellite
AFGL-TR-79-0048 (January 1979), ADA067939

WERNIK, A.W. (Dept. of E.E., Univ. of Illinois, Champaign, IL)
Model Computations of Radio Wave Scintillation Caused by Equatorial Bubbles
AFGL-TR-79-0165 (July 1979), ADA077028

WINNINGHAM, J.D., and SHEPHERD, G.G. (Univ. of Texas, Richardson, TX)
Auroral Data Analysis
AFGL-TR-79-0071 (26 March 1979), ADA070180

YOUNG, E.R., TORR, D.G., and RICHARDS, P. (Space Phys. Res. Lab., Univ. of Michigan, Ann Arbor, MI)
A Simulation of the Midlatitude Plasmasphere and Ionosphere
AFGL-TR-79-0125 (31 May 1979), ADA073892

ZIRIN, H., and MOORE, R.L. (California Inst. of Tech., Pasadena, CA)
Physics of Flares: Analysis of Simultaneous Hα and X-Ray Observations
AFGL-TR-80-0008 (20 December 1979), ADA084751

125

Man-Computer Interactive Data Access System

V METEOROLOGY DIVISION

The research program of the Meteorology Division is concerned with atmospheric effects on Air Force systems. Present-day military operations are at least as dependent upon the weather as at any time in the past. While it is true that some Air Force operations will be less affected by weather elements, newer operations will involve more complex and sophisticated systems that are weather-dependent. Thus, the search for better methods of observing and predicting meteorological conditions continues to be a vital part of the Air Force's geophysical research efforts.

During the period 1979-80, projects in the Meteorology Division have included: research on cloud and precipitation physics; development of techniques for the processing and display of Doppler weather radar data used in detecting significant features of storms and predicting their motion and severity; consideration of laser techniques in the measurement of low-altitude wind hazards; development and testing of automated techniques of observing, disseminating, displaying and predicting critical airfield weather elements; use of meteorological satellite data in short-range mesoscale weather forecasting; development of climatological techniques for use in the design and operation of Air Force systems; and research in the modeling of mesoscale and global atmospheric circulations.

CLOUD PHYSICS

The cloud physics program involves research on clouds and associated hydro-

meteors such as rain, snow and ice crystals. Advanced development is performed to support Air Force functions or systems that have environmental problems in the area of cloud or precipitation physics.

The ultimate goal of geophysical research is to learn how to better live with, or control, the environment. Before any modification or control of weather is possible, however, we must learn how to successfully predict the weather. To predict, we should understand the physics of weather, in particular, the processes that create first ice crystals, then snow and rain. Detailed descriptions of the microphysical and dynamical processes occurring in storm systems in the atmosphere are thus needed. Such descriptions require observations, and the observations require instrumentation.

Our cloud physics program therefore includes development of new instrumentation, collection of cloud physics observations through the depth of the troposphere, development of physical models describing the microphysics, understanding the underlying physical, microphysical and dynamical processes operating within the clouds, and the development of techniques to predict cloud and hydrometeor parameters. We shall discuss each in turn.

Instrumentation: Laser shadowgraphs of ice, snow and rain are obtained in digital form by Particle Measurement System (PMS) equipment. Pattern recognition programs were developed to automatically distinguish the different types of hydrometeors and to provide ice or water mass content. Because of the large density variations of snowflakes in the melting layer, the PMS equipment does not provide accurate water-mass content values. Three instruments to alleviate this deficiency are in various stages of development and testing. The EWER (*E*vaporate *W*ater that aggravates *E*rosion on *R*eentry) is still undergoing flight tests and design improvements but is providing useful data. The TWCI (*T*otal *W*ater *C*ontent *I*ndicator), which operates by collecting ice, snow and rain in a carrier fluid and then measuring the water mass in the carrier fluid, is scheduled for installation in AFGL's MC-130E aircraft during February and March, 1981. A third instrument called an "M-meter" is under development using computer simulation models. The principle is to measure the change in angular momentum of a light-weight, rapidly rotating ring when the ring is struck by the hydrometeors while the aircraft is flying at an airspeed of approximately 100 m/sec. A Rosemount Ice Detector was also modified and mounted on the MC-130E to obtain details of the icing rate under various meteorological conditions.

To assure that instruments were indeed in the free air and that the stream flow around the aircraft had minimum impact on the quality of the hydrometeor data, computer models simulating flow about three-dimensional bodies and the trajectories of the hydrometeor were utilized. For the EWER and the Ice Detector, the collection efficiency was shown to be a function of particle size but was sufficiently high over the range of particle sizes most pertinent to their function to make the EWER and the Ice Detector useful sources of data.

Measurements of the mass of small ice crystals found in high cirrus clouds were studied both in-house and under a university contract because the current measurement techniques are not completely satisfactory. Scattering and imaging techniques are insufficiently developed at the present time for measuring total mass when ice particles are present. Two untried techniques show some promise for measurement of mass. The first is the evaporation of the ice particles and ultraviolet detection of the vapor plume. The second technique uses the impaction and time history of evaporation for determining both size and mass.

Extensive comparisons of instruments used to measure the liquid water content

in clouds were performed under a university contract. Scattering probes were found to overestimate the liquid water content by a factor of two or three. The best technique for obtaining instantaneous measurements of the total mass when only liquid particles are present seems to be a hot wire device which is still in an experimental stage.

Investigations of lidar and radar as airborne cloud microphysical probes concluded that routine lidar investigations of cirrus clouds above the aircraft should await improvements in laser power, efficiency and pulse repetition rate. The weather avoidance radar on a Learjet 36 was modified to provide recorded radar reflectivity data to perform more detailed intercomparisons of in-situ and radar reflectivity relationships. Such data would allow detailed investigations of microwave attenuation in heavy precipitation environments.

In most storms, the maximum total water content is in the melting layer. As the snowflakes melt the dielectric constant increases and so does the returned radar signal. The wet exterior of the snowflake returns the signal and masks the snow, water and air in the interior. For this reason the radar signals from the melting layer, or bright band, have not been used quantitatively. Knowledge of how snowflakes melt, whether there is ventilation through the snowflakes or whether air is trapped inside the residual water drops, is required to interpret the bright band signals. To study the melting of individual snowflakes and ice crystals, a melting chamber has been designed and is being constructed.

Observations: To make theoretical calculations of the attenuation of laser-beam weapon systems as the light waves pass through cirrus clouds, the Air Force Weapons Laboratory (AFWL) required data on the density and particle-size distribution of cirrus particles. A number of flights were made by the AFGL instrumented MC-130E in the New Mexico region, and the data and analysis were published in a series of reports entitled "Cirrus Particle Distribution Studies" (see the bibliography at the end of the chapter). Two flights were also conducted in the marine boundary layer to provide AFWL with particle-size distributions up to 1000 feet in essentially clear air. The concentration and size distribution of the salt spray in the marine boundary layer were found to vary with height and wind speed.

The PMS instruments indicated the presence of ice crystals during some flights in clear air when the horizontal visibility was over 100 miles. These were verified by the mission director using a snow stick. One of the PMS two dimensional (2-D) precipitation probes was modified to measure low particle densities, and values of the order of one particle larger than 100 microns in diameter in an eight cubic meter sample volume were found in subvisible cirrus.

Measurements of icing rates and other in-situ meteorological parameters were provided for the Aircraft Icing Probabilities program which is discussed below in the section on Climatology.

Observations of total water content, particle type and size distributions were made from the Learjet 36 and the MC-130E in support of ABRES (*A*dvanced *B*allistic *R*e-*E*ntry *S*ystem) and Minuteman testing of ICBMs during reentry at the Kwajalein Missile Range in the central Pacific.

To perform in-flight icing tests on DOD aircraft, the Air Force Flight Test Center (AFFTC) uses a KC-135 tanker to produce an icing spray. The AFGL MC-130E was used to verify that the supercooled drops in the spray were similar in size to those found in actual icing conditions. Calibrations were taken at various flow rates, temperatures and distances from the spray nozzle. A rain-rate spray nozzle was also calibrated at above-freezing temperatures.

Observations were taken for three basic research projects. Large Scale Cloud Systems (LSCS) were sampled at various levels in the northeast section of wintertime cyclonic storms. This section of the storm was chosen because it is generally the most uniform and contains the least convective activity. Penetrations were made on successive days as the storms crossed the United States from the midwest to the Atlantic Ocean during which time the characteristics of the storms changed. Working with the University of Washington and the National Center for Atmospheric Research (NCAR), AFGL sampled Pacific storms passing over Seattle by aircraft, radars and rawinsondes to obtain microscale and mesoscale features of mature winter cyclonic storms prior to their modifications by the mountains east of Seattle. Specific flights into the melting layer over the eastern United States began in late 1980 to provide data for models of the microphysics of the melting layer. Future plans are to use a dual Doppler radar system to provide the microscale and mesoscale dynamics of the melting layer in conjunction with the aircraft observations.

Description: The description of particle types, size distributions, ice and water mass content, and synoptic situations were provided as reports for the various projects. Seven reports prepared for AFWL describe the cirrus particle environment over New Mexico during winter months (see the bibliography at the end of the chapter). Two other reports describe the distribution of particles found between 100 ft and 1000 ft over the Pacific Ocean off the coast of California (see bibliography). Another report describes the microphysics of a storm which was sampled as it tracked across the United States. In addition to the raw data and observations provided to AFFTC, a report describing the mission data and meteorological conditions of one of the icing spray tests was published.

Cirrus clouds formed from the condensation of water vapor at high levels in the atmosphere were found to be made up of crystals in the form of bullet rosettes, bul-

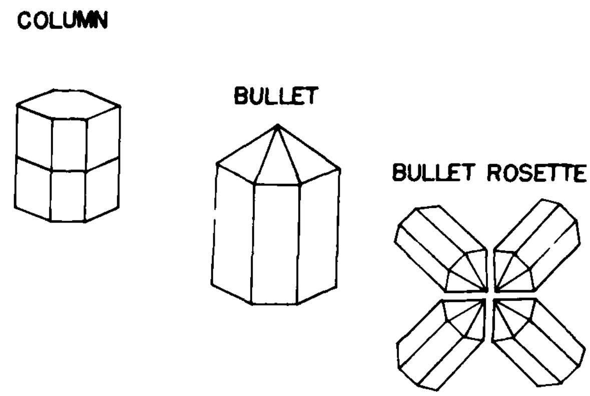

Snow Crystal Shape from High-Level Cirrus Clouds.

lets, or columns, as shown in the diagram. Unlike water clouds, such as fair-weather cumulus or stratus, cirrus clouds usually do not have sharp visual boundaries. Particle concentration values obtained from the PMS instruments show a more continuous range of particle densities at cirrus levels which we have called "subvisible" cirrus. Cirrus uncinus, commonly called "mare's tails," consists of the larger cirrus ice particles that are heavy enough to fall out of the cirrus-generating cells. Since these precipitation particles generally evaporate at lower levels, the mare's tails are by definition a form of virga, or streak.

At altitudes of 20,000 to 30,000 feet in clear air, the PMS scatter probes generally detect a consistent background of particles in the 2 to 10 micron range. Larger ice particles with diameters in excess of 100 microns sometimes fall from higher levels. Intermediate size particles are rarely observed because they generally do not survive. This leads to a bimodal distribution of particle sizes in clear air when particles are generated at higher levels. This precipitation of large ice crystals in

clear air, or where there are high cirrus clouds present, has also been observed at the surface in arctic regions and is referred to as "diamond dust."

Understanding: The description of cirrus particles in clear air has led to a better understanding of the processes operating in the atmosphere and has substantiated theoretical calculations which indicate that large cirrus particles can survive falls of up to 2 km in clear air before evaporating.

The joint University of Washington, NCAR and AFGL program at Seattle provided an improved understanding of the mesoscale features of cyclonic storms and the role of convective cells, fronts, lifting motions and cirrus generating cells in the life cycle of large scale, cyclonic storm systems. Such storms provide the major amount of precipitation over the Continental United States. Cirrus-generating cells were observed seeding lower, moisture-laden layers. However, the precipitation released by these lower layers was so diffused in space and time that the seeding from an individual generating cell could not be followed to the ground. The lower layers were acting to spread out the trigger action of the generating cells in both time and space.

Descriptions of the changes of particle-size spectra for ice crystals and snowfall through deep cyclonic storms were provided, utilizing a flight profile developed by Prof. Passarelli, of M.I.T. The changes in the spectra delineated regions where aggregation occurred. Regions where deposition dominated were also observed. A better understanding of these processes acting within the storm opens the possibility of delaying or advancing the onset of aggregation, which could have an effect on the distribution of ground level precipitation.

Prediction: Testing of ICBM nosecones in the reentry corridor at Kwajalein Missile Range required the development of techniques to predict particle types and size distributions, as well as ice and water mass content along the reentry trajectories. These techniques were developed, tested and modified to meet the individual test criteria. Initially, the tests were conducted in heavy weather in deep storms, but some baseline tests had to be conducted in clear air with no cirrus clouds present. This led to forecasting for "severe clear" missions, which were as difficult to predict as the heavy weather missions. The instrumented Learjet 36 became the major source of data for the severe clear mission since neither the radars nor the weather satellites could detect the thin cirrus layers which were of concern.

Using correlations between water-content values measured by the aircraft and data obtained from the weather satellites in the visible and infrared bands derived from the AFGL McIDAS system (Man-computer Interactive Data Access System), AFGL made predictions of total water-content values in and around Kwajalein. These forecasts were passed to Kwajalein in real-time for mission support.

As mentioned above, the radar reflectivity values do not give water-content values directly. The standard method has been to develop new relationships between the water-content values obtained by the PMS equipment aboard the aircraft and the radar returns. New relationships were developed for each layer for each mission. A new method was developed for using the raw PMS data which was faster and more accurate in converting the radar values into ice and water mass values. The new parameters are more stable in time and areal extent and have smoother vertical profiles. Anomalies are thus easier to recognize and the end results are more reliable.

Prediction of the maximum size particles is now possible using the PMS data, which is truncated at the upper end because of instrumentation limitations. Data taken by other instruments mounted

on the aircraft clearly show the upper limits, and an empirical relation was found which gives the limiting size as a function of the slope of the exponential distribution as determined by the PMS precipitation probe data. This information on the largest size particles is critical in converting radar reflectivity data to ice and water mass content for the nosecone erosion tests at Kwajalein. In addition, this extrapolation technique is extremely important in the investigations of the melting layer, where the largest snowflakes and snowflake aggregates are found in the atmosphere.

GROUND-BASED REMOTE-SENSING TECHNIQUES

The Meteorology Division has steadfastly devoted a major share of its resources to support a strong program of research in radar meteorology. During recent years, this investment has reached the payoff stage, through the development and successful testing of storm diagnostic and processing techniques. These provide the cornerstone of a new operational weather radar system for protection against storm hazards by concerned agencies of the Departments of Commerce, Defense, and Transportation. The new radar, dubbed NEXRAD (Next Generation Weather Radar), is in an early procurement phase, with a design philosophy which is based in large part on research conducted by the Weather Radar Branch of the Meteorology Division. The bridge between research and the future operational weather radar system was the Joint Doppler Operational Project (JDOP), sponsored by the Air Weather Service (AWS), the National Weather Service (NWS), and the Federal Aviation Agency (FAA).

The Joint Doppler Operational Project was conducted in Oklahoma, as a cooperative effort by the Meteorology Division of AFGL and the National Severe Storms Laboratory (NSSL), during the spring severe-storm seasons of 1977, 1978, and 1979. Results during the first two years established the superiority of Doppler techniques for reliable identification of tornadoes and other damaging windstorms (results for 1979 will be discussed below). Nearly all tornadoes originate in a larger rotating vortex, called a mesocyclone, located at mid-storm levels. Mesocyclones can be detected by Doppler radar long before any severe weather appears at the earth's surface. Consequently, the JDOP warnings of tornadoes and severe storms, based on Doppler techniques, had far fewer false alarms than the standard warnings issued by the National Weather Service, which were based on public reports and conventional radar lacking Doppler capability. The Doppler-based warnings for tornadoes also provided the public more than twenty minutes of precious lead time for protective action before the tornado struck, in comparison with just two minutes attained by the standard methods currently in use by forecast offices. These remarkable test results evoked unanimous agreement by the operational agencies to insist on Doppler technology for NEXRAD.

Automated Analysis of Weather Radar Data: Another technique pioneered by JDOP was a computerized tracking program which provided real-time estimates of the future positions of storm echoes. The success of this program during the 1978 JDOP test led to a continuation of efforts to refine and expand the processing capabilities. The data processing system (WEATRK) is designed to assimilate large amounts of data from the Doppler radar (10 million bits in 40 seconds) and display them in an easily and quickly understood manner.

The WEATRK system is configured around a general purpose minicomputer. The computer is interfaced to both the radar and a color display in such a fashion as to (1) automatically accept all the fine-scale data available from the Pulse Pair

Processor, (2) enable the meteorologist to make manual entries into the data base via a hardwired trackball cursor, and (3) present the results of the automated analyses of fine-scale data as well as manual inputs, geographic overlays, and manual annotations on a color display. Other features of the system include a 320 K byte core memory for rapid "on-the-fly" processing of the data, a 10 megabyte disc for the storage of programs and intermediate analysis results, a 1600 bpi 9-track tape recorder for the storage of analytical results, a line-printer for the display of alphanumeric results in hard copy form, and a CRT terminal for the control of computer operations.

The data analysis considers the characteristics of storms defined by the volume

DATE:12Ø TIME:1823 ELEVATION: Ø.2 ZTHRES: 3Ø

CELL ID	3	5	1	4	2	11	12
CELL ID	3	5	1	4	2	B	C
RANGE (KM)	22Ø	224	142	1Ø2	5Ø	126	216
AZIM (DEG)	297	31Ø	329	325	342	323	11
HT (HM)	58	58	3Ø	14	5	28	48
BASE (HM)	-39	-39	-18	-1Ø	-3	-14	-37
TOP (HM)	88	92	89	-98	-46	76	54
VOL(KM2E2)	975	521	499	22Ø	177	116	98
MXREF(DBZ)	47	52	48	57	53	53	48
ALT (HM)	56	56	52	18	28	43	54
MXVEL(M/S)	-18	-16	-18	-16	-32	Ø	-9
MXSTD(M/S)	1Ø	9	11	9	11	Ø	8
ALT	39	56	52	61	-46	76	54
MASS(K	328	326	246	175	1Ø2	84	46
SPEED(M	16	16	22	4	12	1Ø	999
DIR (DEG)	231	218	192	2Ø7	258	243	999

DISPLAY AVERAGE VELOCITY IS 224 DEGREES AT 13 M/S
DISPLAY TOTALS - CELLS 9 MASS 1336 E+2 KTONS FLUX 1Ø48 KTONS/HR

Computer Printout of Storm Characteristics.

enclosed within a predefined reflectivity threshold. Appropriate significance and size filters reject small or unimportant volumes. For each volumetric scan of the radar, three-dimensional reflectivity-weighted centroid locations are computed for the twelve cells having the largest masses, and an abbreviated list of storm characteristics is prepared. Along with volume centroid locations (azimuth, range and altitude), other characteristics computed for each volume included the volume, mass, base, top, maximum reflectivity and its altitude, the maximum velocity with the storm, the maximum spectral width and its altitude, and the speed and direction of storm movement. These storms are numbered according to their mass and are displayed on a line printer and/or a CRT terminal. A typical characteristic display is shown here.

After successive volume scans, the centroid locations are correlated with time, and a least-squares analysis of past centroid locations together with cell-speed measurements are used to forecast the positions of the storm two- and four-scan sequences (approximately 12 and 24 minutes) later. Upon completion of this analysis, a color display picture is generated showing three reflectivity levels, past tracks, extrapolated positions, an abbreviated characteristics list, radar and analysis parameters, and an overlay map of the local area. An example of this product is presented in the next section.

The trackball cursor permits the interrogation of color display data, providing a convenient and useful means for the semiautomatic measurement and annotation of particular storm features. The data associated with the cursor positions are automatically entered into a cursor analysis program, and the results are presented on the color display. The results include the display number, the color value, the 3-dimensional location of the cursor (azimuth, range, and altitude) and, if the velocity display is interrogated, the shear and distance over which the shear is computed. The interactive use of the cursor analysis on the Doppler signature of mesocyclones, tornado vortices, high shear and gust fronts eases the meteorologists' workload in identifying and monitoring these phenomena.

1979 Joint Doppler Operational Project: Objectives for the third season of JDOP experiments were directed toward the automation, remote transmission, and display of Doppler information. These objectives were: (1) to evaluate the format and effectiveness of the manually aided

automatic display products described previously, (2) to evaluate the transmission of these products over telephone data lines, and (3) to provide inputs to the warning agencies from the remote radar location. To accomplish these objectives, manually aided automated display products from the AFGL 5-cm wavelength Doppler radar, supplemented by 10-cm Doppler observations from the co-located NSSL radar, were transmitted once each six minutes to operational settings in central Oklahoma and Texas for use by meteorologists from the NWS, AWS, and FAA.

A severe storm that struck Vance Air Force Base, Oklahoma, on May 2 provides a good example of the operational importance of the kinds of information contained in the 1979 JDOP display product. This example is illustrated well here. At 1517 CST, or nine minutes prior to the data in the first figure, JDOP meteorologists identified a mesocyclone in a storm approximately 180 km to the northwest of the radar and, moreover, the cell track showed the troublesome echo moving toward Vance Air Force Base. The AWS forecaster in Oklahoma City issued his first tornado warning at 1526.

The information transmitted to the AWS forecaster every six minutes enabled him to give the people at Vance a con-

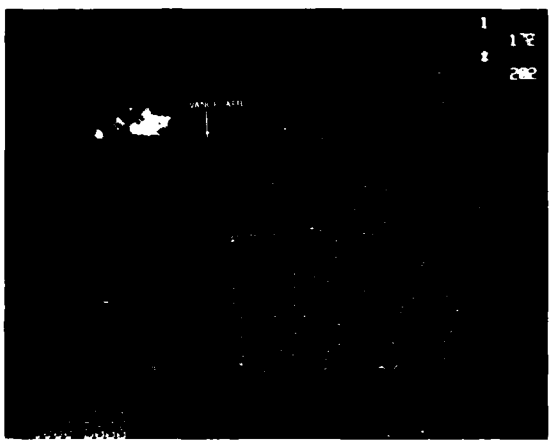

Computer-synthesized Echo Track Display for May 2, 1979, 1526 CST. Superimposed on County-line Map of Oklahoma. A mesocyclone had been identified and the first tornado warning was issued for echo "1", which was moving slowly toward Vance AFB.

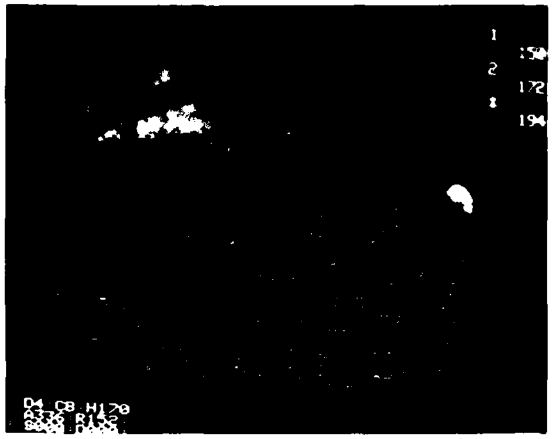

Computer-synthesized Echo Track Display for May 2, 1979, at 1613 CST. The mesocyclone is still rotating vigorously and echo "1" has intensified sufficiently to indicate large hail as well as a tornado.

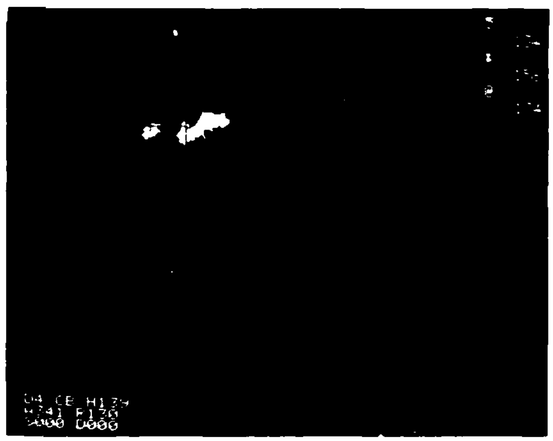

Computer-synthesized Echo Track Display at 1704 CST. The computer has renumbered the tornadic storm from "1" to "5". Large hail is also indicated. The eastern edge of the storm is now over Vance AFB, and base personnel are seeking safe shelter. Aircraft have already been moved into hangars.

tinuous and fairly accurate picture of the weather bearing down on their base. Shortly before 1600, the storm spawned its first small tornado. At 1613, the high reflectivities in the core of the cell indicated hail, and the mesocyclone circulation was still evident. At 1704, the JDOP forecaster identified a tornado vortex signature in the velocity data, and the strong core reflectivities continued to indicate hail. Contact with Vance personnel was lost soon after and was not re-established until after 1754. The continued existence of the

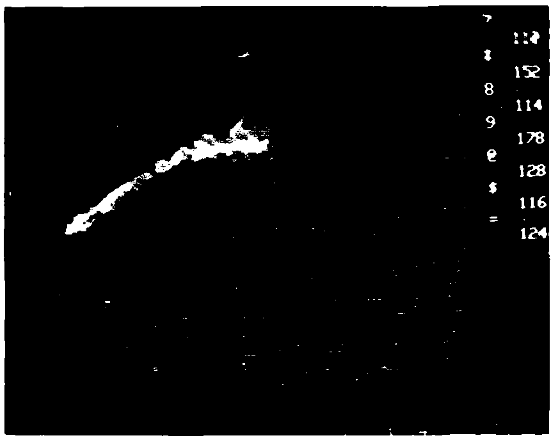

Computer-synthesized Echo Track Display at 1754 CST. All clear: the severe storm hazards have moved east of Vance AFB.

mesocyclone and high reflectivities showed that this storm was still quite dangerous; however, careful analysis indicated that the mesocyclone center had moved to the east of Vance. Once communications with Vance were resumed, the impact of the frequent and detailed advisories on Vance's operations came to light.

Responsible officials at Vance had taken the warnings seriously and acted prudently. They moved their entire fleet of fifty-two T-38 aircraft into hangars, and all personnel were advised to take shelter in the Base Command Post. A tornado heavily damaged the adjacent town of Lahoma and lifted slightly as it crossed the base at approximately 1730. The Vance weather station recorded a sharp dip in pressure and peak gusts of 70 knots as the tornado passed nearby. Golf-ball sized hail was found on the T-38 parking ramps, and baseball-sized hail was found in the base housing area. No personnel were injured, however, and no T-38 aircraft damaged.

An important lesson was learned on another occasion. During the afternoon of April 10, 1979, three supercell thunderstorms originated in a relatively small area of Texas, a short distance south of the Red River. They all moved into southwestern Oklahoma and toward our radar site. Each supercell featured one or two maxi-tornadoes and several smaller ones. Unfortunately, several of the maxi-tornadoes moved through heavily populated areas of cities, killing and injuring many people despite the warnings issued by the National Weather Service. Wichita Falls, Texas, where entire city blocks were reduced to rubble, was hit the hardest. The maxi-tornadoes had damage path lengths of 20 to 100 km. A great amount of non-tornadic wind damage also occurred, and hailstones as large as 3 inches in diameter were reported.

The NSSL 10-cm radar detected the mesocyclonic circulation of this storm in all three supercells, at distances in excess of 200 km. The co-located AFGL 5-cm radar, however, produced velocity patterns that could not be interpreted as an organized circulation. Part of the difficulty was excessive velocity folding. With the desired 115-km unambiguous range, the unambiguous velocity limit of the 5-cm radar is only $\pm$ 17.5 ms^{-1}. If true velocities in the storms covered a spread of more than 105 $m\,s^{-1}$, which is not at all unlikely in view of the large size and incredible violence of these maxi-tornadoes, then the 5-cm Doppler velocities would undergo triple folding. Each color on the velocity display could represent any of four different

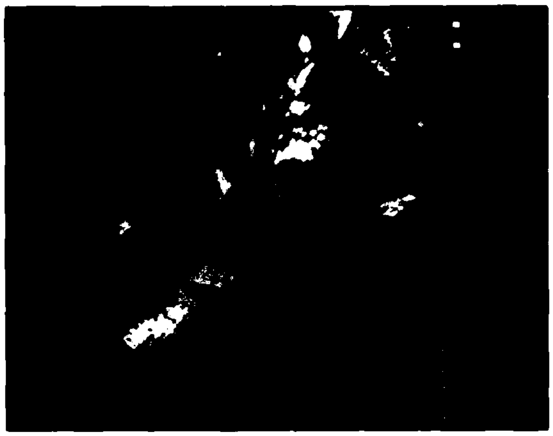

Reflectivities Measured with 5-cm Radar, 0.5° Elevation Angle, at 1730 CST, April 10, 1979. Range-mark interval is 64 km. The Wichita Falls tornadic storm is crossing the outer range marker.

velocity intervals separated by multiples of 35 m s^{-1}.

Excessive attenuation was experienced by the 5-cm AFGL radar. As the Wichita Falls storm approached its target, it moved directly behind the even more monstrous Harrold-Marlow storm, which was in south-central Oklahoma at the time.

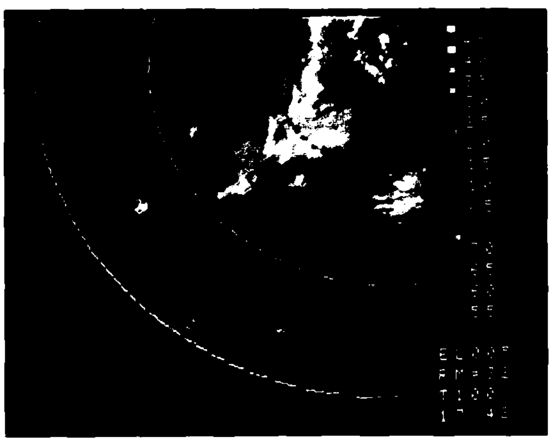

Reflectivities Measured with 5-cm Radar, 0.5° Elevation Angle, at 1742 CST. The Wichita Falls storm has been almost completely attenuated by the intervening storm.

Almost unbelievably, the Wichita Falls storm echo almost faded from view as its tornado was devastating the city. Dramatic "before" and "after" views of this extraordinary attenuation are shown here. The southern end of the Harrold-Marlow storm echo, which contained its mesocyclone and severe weather, also suffered heavy 5-cm attenuation through its intense core. The relatively unattenuated NSSL 10-cm low-level reflectivity in the Harrold-Marlow storm, as well as a conveniently placed network of Agricultural Research Service rain gauges, indicated peak instantaneous rainfall rates greater than 150 mm hr^{-1}, with a very large area of 100 mm hr^{-1} lined up along the same direction as the Wichita Falls storm.

It seems ironic that the AFGL 5-cm Doppler radar suffered such extreme disability in its aborted attempt to observe the Red River Valley supercells, because, 11 years earlier, this same radar was used in Massachusetts to make the first real-time Doppler measurements of a mesocyclone. The 5-cm radar was hopelessly outclassed and overpowered by the much larger, more intense, and more violent storms found in Texas and Oklahoma.

The Red River Valley storms shattered a dangerous assumption. Designers of operational weather radars had flirted with the seemingly attractive idea of employing a 5-cm radar, which would achieve the same angular resolution as a 10-cm radar with an antenna of only half the diameter and hence would be much lower in cost. For stratiform precipitation, and for most ordinary convective storms, a 5-cm radar would be suitable. In extremely vigorous, intense, high-velocity storms, however, a 5-cm radar is useless. Although the monster storms are rare, they are the killers. An operational system which could protect people in marginal storms, but would be completely inadequate in an outbreak of maxi-tornadoes, would be a waste of taxpayers' money. Consequently, all JDOP staff members

are now in unanimous agreement that future operational weather radars must employ 10-cm radiation.

Forecasters who utilized the display products provided by the 1979 JDOP effort were invited to submit comments on its strong and weak points. Gratitude was expressed by the Air Weather Service for the excellent forecast of severe weather at Vance AFB on May 2 that saved base personnel from injury and aircraft from damage. Also, from Fort Sill, served by AWS, came the word that JDOP had prevented false alarms on two occasions. During the April 10 tornado outbreak, a major tornado crossed the southern sections of Lawton, Oklahoma, inflicting heavy damage, killing three persons, and injuring scores of others. Fort Sill is adjacent to the northern edge of Lawton. As the tornadic storm approached Lawton, the Fort Sill forecasters had the benefit of accurate mesocyclone locations and predicted storm tracks provided by JDOP, which indicated that Fort Sill would be spared this time. It was. On May 2, several hours after the Vance AFB storm, the National Weather Service issued a tornado warning for Lawton on the basis of a hook echo noted on the conventional (non-Doppler) WSR-57 radar, and possibly a mistaken public report of a funnel cloud. The JDOP display showed only high reflectivities, indicative of hail, and occasional measurements of high shear, but no organized mesocyclone. Having faith in JDOP, the Fort Sill forecaster did not issue a tornado warning, which proved to be correct. Although 3/4-inch hail fell on Fort Sill, no tornadoes were confirmed anywhere in the vicinity.

The 1979 program demonstrated that operationally significant Doppler data displays can be synthesized in a manually aided automatic fashion in nearly real time, and, moreover, that agency forecasters, some with little or no Doppler training, can be very effective in the use of this information. Forecaster comparisons of JDOP Doppler information with conventional information sources were quite favorable on such things as the frequency of update of significant information, the detailed information on cells, and the use of color. Moreover, their endorsements of the operational importance of the projections of storm-cell movement and the concise identification of severe-weather elements were emphatic. The JDOP experience gained in the Vance AFB storm certainly supports such conclusions.

Gust Front Detection: During the JDOP observations in Oklahoma, gust fronts were occasionally detected by Doppler radar, running ahead of advancing thunderstorms. At the earth's surface, a gust front is manifested by a line of shifting wind direction, closely followed by suddenly increasing wind speeds, which may sometimes attain damaging intensity. Doppler radar offers the opportunity not only to monitor the approach of high surface winds, but also to observe the vertical structure of a gust front which may inflict hazards on low-flying aircraft. Sample velocity displays of two contrasting types of gust fronts are portrayed here.

Doppler Velocity Pattern Observed in Hazardous Gust Front of April 30, 1978. Range-mark interval is 32 km.

The April 30, 1978, gust front traveled at an average speed of 19 m s^{-1}. Peak sur-

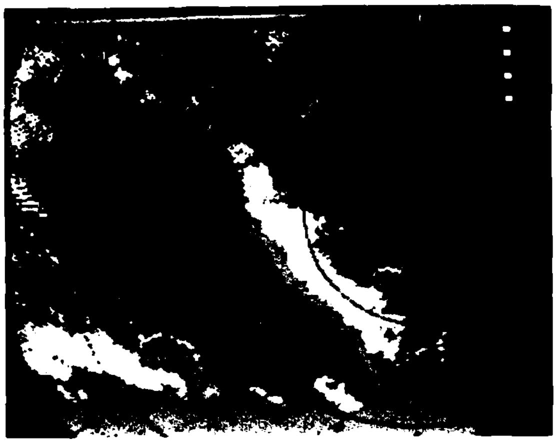

Doppler Velocity Pattern Observed in Shallow Gust Front of May 2, 1978.

face winds, measured at two stations traversed by the gust front, were 17 and 18 m s^{-1}, a shade lower. However, the figure indicates that peak winds measured by Doppler radar increased two-fold from the surface up to a height of 300 meters, resulting in dangerous vertical wind shear in excess of 0.05 s^{-1} (5 m s^{-1} per hundred meters). The highest Doppler velocities of 40 m s^{-1} occurred at heights between 1 and 2 km, where peak radial shear values greater than 0.1 s^{-1} were found along the radar beam.

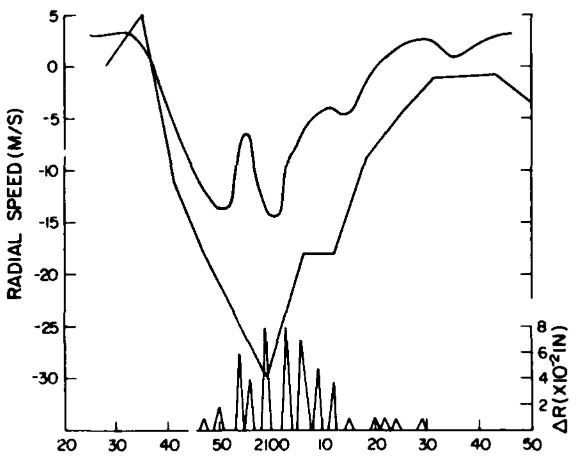

Comparison of Radial Velocities Derived from Surface Wind Measurements (upper line), Doppler Radial Velocities Observed 300 Meters above This Surface Station (middle line), and Rainfall Amounts (lower triangles) during Passage of April 30, 1978, Gust Front.

The observations of this gust front provide a good illustration of why it is safer to drive than to fly near a violent thunderstorm complex. Peak gust speeds were more than doubled from ground level to an altitude of a few hundred meters. More significantly, extremely hazardous wind shears frequented the gust front, and especially its boundaries, within the lowest 2 km. Furthermore, the presence of velocities in certain regions with magnitudes more than double the speed of translation of the gust front, and normal to the front, suggests the existence in nearby regions of vertical velocities of comparable magnitude which are not sensed by a radar looking more or less horizontally. Nearly all of this potentially dangerous activity took place in weak reflectivity, outside the heavy rain area. Low-flying aircraft, particularly those engaged in landing and takeoff, would do well to avoid any maneuvers in the vicinity of lively gust fronts. Doppler radar with real-time shear presentation can provide an excellent warning.

The May 2, 1978, gust front, in contrast, was extremely shallow, with peak westerly winds of 16 m s^{-1} at a height of about 140 meters above the ground. This gust front displayed no hazardous shear, and had no velocities in excess of its travel speed. However, it occurred within an area of widespread precipitation, and so might have been difficult for a pilot to recognize visually. Also, surface winds ahead of the gust front were from the east. An aircraft descending from a height of 1 km into this gust front would encounter a surprising shift from head winds of over 40 knots to a tail wind of over 30 knots. The unfortunate pilot caught in such a situation at an airport having no Doppler radar might be challenged to take strenuous measures to

compensate for his loss of airspeed and miscalculation of expected touchdown point.

Turbulence Detection by Doppler Radar: The detection of turbulence in storm environments by radar methods has been a frequent subject of investigation during the past two decades. The interpretations of Doppler radar data in these efforts have generally been qualitative, in the sense that actual turbulent parameters were not estimated and the effects of the range of the storm and its particle size distribution were not taken into account. A new effort is directed at incorporating these varied effects in the interpretation of radar data to more reliably estimate storm turbulent parameters.

A Doppler radar essentially measures the distribution of precipitation velocities, termed the "Doppler power spectrum," along the viewing direction of the radar. The data from any one measurement are acquired from a small volume in space, called the "radar pulse volume," which is typically formed from a circular beam of about one degree in width and about 100 meters in range. The spectrum power at each spectral value is proportional to the sum of the sixth powers of the diameters of the particles moving with that radial velocity value. Thus, a large particle contributes more power to the Doppler spectrum than a small particle. Unfortunately, a large particle, because of its greater inertia, follows the random turbulent air motions less faithfully than the smaller particles. Thus, the parameters derived from the Doppler power spectrum, namely mean velocity and the variance about this mean, may not be representative of the true turbulent air motions. Furthermore, as the pulse volume size increases with increasing range from the radar, the degree to which the turbulent fluctuations are mapped into fluctuation of the Doppler mean velocity varies, altering the interpretation of the data. Thus, proper interpretation of radar data in terms of turbulent parameters requires the inclusion of these varied effects into the radar turbulence theory.

Theoretical analyses, assuming rain as precipitation tracers, show that precipitation effects can be significant. For example, one may analyze the fluctuations of the Doppler mean velocity to form the turbulent power density spectrum, which essentially describes the intensity of turbulent motion as a function of turbulent eddy size. Results show that at eddy sizes less than about 200 m, the radar turbulent-energy estimates are a small fraction of the true atmospheric values. At ranges greater than about 20 km, it is more reasonable to use Doppler spectrum variance as a tool in estimating turbulent intensity. Analyses show that exclusion of precipitation effects at shorter ranges can lead to a 60 percent underestimate of turbulent intensity. At ranges greater than about 20 km, the underestimate from exclusion of precipitation effects is closer to 15 to 25 percent. Of further significance is the finding that, at ranges greater than about 20 km, the turbulent intensity estimate is more strongly dependent upon the maximum eddy size than the precipitation environment. Unfortunately, there is at present no proven reliable method of estimating this maximum eddy size by radar methods. Nonetheless, it can be demonstrated that a good estimate of turbulence severity can be obtained with a reasonable guess of this parameter. This result is significant since it demonstrates that radar data can be used to estimate well the severity of storm turbulence even though exact knowledge of no turbulent parameter is at hand.

Verification and fine tuning of the theoretical results discussed above require data analysis. During the spring of 1981, AFGL is participating in a multiagency program at Wallops Island, Virginia. The emphasis of this program is to determine the lightning and turbulent characteristics of thunderstorms, as de-

tailed by both airborne and ground-based sensors. It is felt that the data from this experiment will support the theoretical findings and lead to refined techniques for turbulence identification within thunderstorms.

Laser Measurement of Wind Hazards: Aircraft in the landing and takeoff stage of flight are particularly vulnerable to effects of low-altitude wind shear, down drafts, turbulence, and the wake vortex flow from preceding aircraft. The standard wind measuring equipment cannot provide a sufficient density of measurements in the airfield vicinity to positively identify the location of hazardous conditions. The continued development of Doppler radar capability for locating and measuring these hazards is encouraging. However, the ground clutter environment around airports offers serious technical difficulties to radar, particularly at short ranges and at the very low elevation angles representative of the nominal 3° glide slope. Consequently, laser techniques are being considered as a possible alternative.

A new program was recently initiated to develop a prototype moderate-power pulsed CO_2 laser/scanner system. The laser will have a heterodyne Doppler velocity measurement capability over the range from 1 to 50 m s^{-1}. The distance over which measurements are made will depend upon the aerosol content of the air and cloud attenuation effects. Under most conditions, it is expected that a range of 15 to 25 km will be achieved. The basic laser/scanner system is being constructed under contract. The signal processing and display systems that will be used to provide near real-time depictions of wind and turbulence patterns at airfields are being developed in the Laboratory.

MESOSCALE OBSERVING AND FORECASTING

The primary emphasis of the research and development program of the Mesoscale Forecasting Branch during this reporting period has dealt with objective, or automated, capabilities to observe, predict, disseminate, and display aviation-related weather. Other aspects of the mesoscale research and development program have dealt with the development of objective weather prediction schemes for short-range forecasting and procedures to more effectively use high-resolution data available from both polar orbiting and geostationary weather satellites.

Automated Weather System Development: Air Force needs for weather support span a wide range and are largely dependent on the particular mission to be satisfied. As a result, the whole concept of automated weather support has been built around a modular design to ensure flexibility. A specific modular design of an automated system for peacetime airfield weather support underwent a two-year demonstration test which ended in January, 1979. The test of that system, called MAWS (Modular Automated Weather System), demonstrated that a microprocessor-based approach to airfield weather support can be accomplished with state-of-the-art, commercially available hardware/software systems which have been hardened to function in an operational environment. An automated system can routinely and continuously provide supplemental information which can be critically important in marginal and adverse weather situations. During such weather, the need for two or more independent observations of airfield visibility and wind conditions was clearly documented. In particular, measurements of visibility 25 meters or higher above the ground were shown to provide improved guidance to landing aircraft when conditions were near landing minima. Other important features, routinely available through an automated system but tedious and time consuming to obtain in the manpower-intensive operational environment, are the so-called "metwatch" parameters.

Routine calculation and display of such factors as crosswind component and wind chill can provide valuable detection and warning information to specific user groups.

During the period of the demonstration test, automated processing of the rotating beam ceilometer (RBC), used to measure cloud base height, was not fully achieved. In a follow-on development effort, a fully automated capability to process and digitally display the RBC's output, in real-time, was accomplished. Relying again on capabilities emerging from the micro-computer industry, a stand-alone system was designed, fabricated and tested in an operational environment. It automatically interfaces the operational RBC, performs data validation and smoothing functions, converts the received signal for digital display, and performs an objective evaluation of the current cloud data to provide an up-to-date cloud base height determination. New cloud height profiles (scans) are supplied by the RBC and processed by the system ten times per minute. Subsequent processing of the cloud height scan can yield representative cloud observations by applying objective procedures. In a test conducted at the Weather Test Facility at Otis AFB, it was shown that reliable observations of low cloud height, low cloud amount, and ceiling can be obtained from hierarchical clustering techniques applied to an updated thirty-minute sample of individual scan data. That test demonstrated that only slight improvement is realized in specification accuracy by adding basic information from a second and third RBC on or near the airfield.

More accurate and reliable surface weather instruments are being sought to replace aging inventory sensors and to measure weather elements which now require a human observer. During this reporting period, primary emphasis has been on sensors appropriate for use at tactical or bare-base airfields. Several observing techniques and instruments having good potential for use in fully automated systems are being evaluated at AFGL and at the Weather Test Facility at Otis AFB, Massachusetts. The Weather Test Facility was established to permit rigorous, long-term evaluation of new and improved instruments at a location which frequently has cloudiness, reduced visibility, and many forms of precipitation.

In its documented requirements for a modernized weather support capability, the Air Weather Service seeks to have a fully automated observational capability which is deployable to tactical, or bare-base, airfields during periods of hostility. For this purpose there is a great need for rugged but lightweight and durable sensors and processing systems. A survey was conducted to establish the current capabilities in tactical weather measurements operationally, alternative state-of-the-art instruments and measurement techniques, and engineering modifications required for automated system compatibility. Based on the survey, deficiencies were identified and development efforts undertaken. Deficiencies exist mainly in sensible weather observations; that is, visibility, cloud conditions and "weather" determination. Of the three, the development of a visibility sensor suitable for bare-base airfield use is closest to fruition. A substantial redesign of the forward scatter visibility meter has yielded a model with improved operating characteristics and compactness. Transportability improvements, weight reduction, self-calibrating options and an improved capability for covert operations have been incorporated.

Intercomparison and reliability tests, conducted at the Otis Weather Test Facility during the fall fog season of 1980, documented that the redesigned sensor provides measurements of extinction coefficient highly correlated with standard transmissometer measurements in periods of fog and precipitation. Tests are presently underway of the Army's AN/

GVS-5 hand-held laser rangefinder to establish its utility as a cloud height sensor at tactical airfields. It suffers from two potentially serious characteristics: (1) its design limits its "near-field" capability to 600 feet and beyond, which means it is ineffective in very low, aviation-critical ceiling conditions; (2) it uses a neodymium laser source, which is not eye-safe. This factor could prevent its use at tactical airfields. Consideration is also being given to ceilometers using other, eye-safe, laser sources and/or microwave radar ceilometers.

Historically, wartime planning and operations have been hampered by incomplete and/or inaccurate information of weather conditions within uncontrolled or enemy-controlled battle areas and airspace. With the emergence of precision munitions, guided by laser, television, infrared or millimeter target-sensing capabilities, the importance of knowing the enemy's airspace characteristics is increased substantially. In 1980 a new program was initiated called "Weather Systems Advanced Development," whose overriding goal is to develop a broad capability to observe, collect and process weather information from hostile areas. Another major program objective is to develop techniques to present the information to tactical air and ground forces in the form of tactical decision aids for the purpose of maximizing the use of environmentally-sensitive and expensive precision-guided munitions.

Short Range Forecasting: AFGL's mesoscale (short range) forecasting research is aimed at developing objective procedures to aid the field forecaster responsible for the prediction of critical weather elements for time periods up to six hours. Techniques under investigation range from single-station, single-element statistically based models to numerically-based fog-forecasting models.

Single-station statistical prediction algorithms have been developed and tested for glidescope slant-visual range and cloud-base height conditions at airfields. In both cases the Regression Estimation of Event Probabilities (REEP) technique yielded superior probability prediction algorithms for forecast intervals ranging from 30 minutes to 3 hours. While the prediction equations rely, to a large extent, on the most recent observation of the element to be forecasted, the incorporation of "measures of trend" and measurements of related, but independent, variables was found to increase forecast skill.

A potentially powerful source of weather information, particularly in hostile tactical environments, is the meteorological satellite. Geosynchronous satellites, which provide frequent views of the same wide geographical area, can be used effectively in sensible weather prediction models. The visible and infrared wavelength imagery so provided has been incorporated into automated data extraction, analysis, interpretation and short-range prediction techniques. Initial experiments have sought extrapolation techniques which predict the position of cloud brightness areas (visible wavelength) up to three hours ahead. Successive images of cloud brightness (with 1-km video resolution) were evaluated using five different statistical correlation techniques to determine the overall displacement, or motion, of cloud features. This motion vector is then applied to the latest imagery field, which is extrapolated in space without allowing for changes in the cloud features due to development or decay. The five motion-vector techniques included variations on fast Fourier transform covariance and pattern recognition/tracking approaches. Testing on simulated cloud patterns and several cases of geosynchronous satellite imagery data confirmed that the binary cross-covariance technique yielded higher verification scores than the other techniques tested. However, as much as 75 percent of the changes that occur in cloud

reflectivity were found to be due to processes other than simple extrapolation or translation.

In addition to seeking a capability to predict the future distribution of satellite brightness fields, one also needs a procedure to transform imagery predictions into cloud, precipitation and visibility forecasts. Central to the development of accurate specification algorithms is the establishment of an accurate and statistically-complete data base. Particular care must be taken to minimize the uncertainties in the relative and absolute values of satellite visible imagery. Precision navigation to properly earth-locate the satellite data, normalization which accounts for varying solar illumination and irregular scattering effects, and the establishment of clear column background brightness values as a function of season and solar elevation angle were accomplished. Specific algorithms (statistical relationships) have been developed using visible imagery only for cloud cover, precipitation occurrence probability, and rainfall rate. Studies presently underway are evaluating the extent to which the specifications are improved by incorporating infrared imagery and by using a multiple predictor approach.

Studies are also underway at AFGL and under contract to develop and evaluate forecaster-interactive techniques for short range prediction purposes. Relying on the power of computer-driven interactive graphical display systems, the potential for substantial improvements in the ways in which meteorologists process and utilize weather data in short-range forecast preparation is being investigated. AFGL's interactive system is called McIDAS (Man-computer Interactive Data Access System). It provides to the meteorologist, in near real-time, meteorological satellite imagery and conventional surface and upper-air weather data. Software resident within McIDAS permits the generation and display of basic and derived meteorological parameters in mapped or listed form. For example, the operator can easily invoke key-in commands to compute and display streamlines, isobars, temperature and its advection, single-station and vertical cross-section analysis of atmospheric structure, individual visible and IR Satellite imagery maps, and time loops of satellite maps to assess motion characteristics. Studies have been undertaken, through participatory short-range forecast preparation, to assess the utility of an interactive system like McIDAS, to identify its advantages/disadvantages, and to define a program of research and development to improve procedures for man-interactive short-range prediction, a mode of operation anticipated within the Air Force later this decade. Objective techniques being developed under contract will be integrated into AFGL's Mc IDAS for test and evaluation. These include convective-cell extrapolation techniques, frontal advection models, manually-digitized radar-processing algorithms, and cloud displacement/rotation models.

Investigations of the mesoscale spatial and temporal variability of wind near airfields are being pursued. The horizontal characteristics of wind regimes are being studied from wind-speed and direction observations gathered over a 3-year period in an eastern Massachusetts mesonetwork. The data, which were collected from some 26 stations separated by distances ranging from one to eight km and representing a wide range of topographic features, are being analyzed for spatial and temporal (diurnal and seasonal) variations. Additionally, vertical wind profile data, obtained from tower-mounted anemometers and a Doppler acoustic sounder, are being analyzed for the development of vertical wind-shear specification and short-range prediction techniques.

The impact of reduced visibility due to fog formation can be substantial on avia-

tion operations and safety, particularly along coastal zones where fog is apt to be more frequent and denser. Our limited ability to predict fog formation is largely due to our limited knowledge and understanding of the detailed micro-structure and dynamics of the fog-prone environment. In this regard, a two-year laboratory and field program at the Weather Test Facility on Cape Cod has been undertaken to collect and analyze data on fog drop size and concentration, condensation nuclei, temperature, humidity, wind and visibility data before, during, and after fog events. Data collected during five major fog episodes which occurred in July, 1980, are being evaluated to formulate a descriptive model of the fog-evolution process. The descriptive model, in turn, will form the basis for an improved numerical fog-prediction model applicable to coastal airbases impacted by maritime fog regions.

Satellite Specification Studies: The Defense Meteorological Satellite Program (DMSP) consists of a series of polar-orbiting satellites, each with a specific set of standard and special purpose sensors. Among the standard sensors are fine-mode visible and infrared imagers which permit detection of small-scale cloud features in potentially greater detail than do most civilian satellites. Research being conducted in AFGL's Meteorology Division seeks to improve the utilization of the fine mode imagery for the identification and characterization of cloud features. In a recently completed study, a spectral technique was used in which the original image was transformed by a two-dimensional fast Fourier transform which, in turn, was used to classify the contents of the image. Basically, the Fourier transform defines the spatial distribution of brightness in the image and estimates cloud size and organization better than first-order statistics. Using the McIDAS facility, a computer-based processor was formulated to label a small cloud area (25 × 25 nm) with one of nine possible cloud type categories. Classification accuracy based on visible and infrared images in combination was found to be substantially greater than using either of them singly. Small-scale cloud features such as cumulus and cirrus clouds, which can be difficult to detect and identify using first-order statistical techniques, were handled well by the Fourier transform approach.

An alternative approach to cloud typing and cloud coverage is being pursued through a clustering, or segmentation, of cloud masses, using low-resolution infrared imagery from the geosynchronous (GOES) satellite. Using a histogram approach, we subdivided areas in infrared images into one to four clusters, each representing a range of infrared temperatures. Conversion algorithms, which will identify the clustered cloud masses as one of eighteen simple or complex cloud regions, are being sought. Consideration is being given, in the development of conversion algorithms, to basic and complex (gradients, textures) measures of the visible and infrared characteristics of the cloud clusters.

One of the special imaging sensors flown on one DMSP satellite was designed to respond to electromagnetic radiation in the so-called near-infrared range (about 1.5 μm). It has a response characteristic that permits the discrimination of snow on the ground from clouds in the atmosphere to a much greater extent than is possible with just the visible and infrared images. This response characteristic also offers the potential of distinguishing clouds made up of ice particles from clouds made up of water droplets and clouds of a mixed phase. The phase of a cloud can be important to certain aerospace operations, such as missile re-entry and cruise missile trajectories. Using AFGL's McIDAS facility, we have undertaken diagnostic studies to develop specification algorithms and to provide an experimental data base for cloud-

free line-of-sight and surface visibility studies.

Weather Modification: Operations at many airports can be hampered by the presence of dense fog. Likewise, the presence of low stratus clouds can seriously hamper military tactical and surveillance operations. The ability to disperse these types of atmospheric phenomena would enhance Air Force mission success. AFGL studies, concluded during this reporting period, addressed techniques for operational fog and stratus dispersal. Warm fog dispersal by means of ground-based heat sources and supercooled stratus dispersal by means of silver iodide flares were studied. Both weather modification projects were terminated in 1978. AFGL does not presently have a program in weather modification.

DESIGN CLIMATOLOGY

Atmospheric effects on materiel and systems design can be vital to successful accomplishment of the Air Force mission. Both materiel and systems design require the careful consideration of various atmospheric elements, including their variability and extremes. Overdesign may be ineffective as well as uneconomical, whereas underdesign can result in failure, with possible loss of life and materiel. Consequently, climatological research is continuing in order to more clearly describe atmospheric structure and its effect on Air Force plans, and the design and operation of equipment. Included in this effort are empirical models and algorithms which are being developed to improve the utility of climatic information.

Kwajalein Reference Atmospheres: Rocketsonde and rawinsonde measurements of temperature, density and wind have been used to derive consistent, hydrostatic models of atmospheric properties at the Kwajalein Missile Range (KMR), Marshall Islands. A mean annual model and 12 monthly models of the thermodynamic properties have been constructed for altitudes up to 120 km, including estimates of the day-to-day and diurnal variations of density, temperature and wind, plus time and space variability to 200 nautical miles and time intervals to 6 hours. Information is also provided on the speed of sound, viscosity, humidity, index of refraction, molecular weight, acceleration of gravity, and interlevel correlations of density, temperature and wind.

Stratosphere-Mesosphere Relationships: The time and space variations of atmospheric density in tropical regions have been examined as part of an on-going investigation of atmospheric structure and its effect on aerospace vehicles. The figure shows the rate of decay in correlation between densities at two points with increasing horizontal distance for altitudes between the surface and 60 km. The rate of decay in the horizontal decreases substantially with increasing altitude. At 50 km, for example, zero correlation is reached at about 2400 nautical miles (4450 km), which indicates that large-scale tidal and planetary waves are the dominant factors at these altitudes.

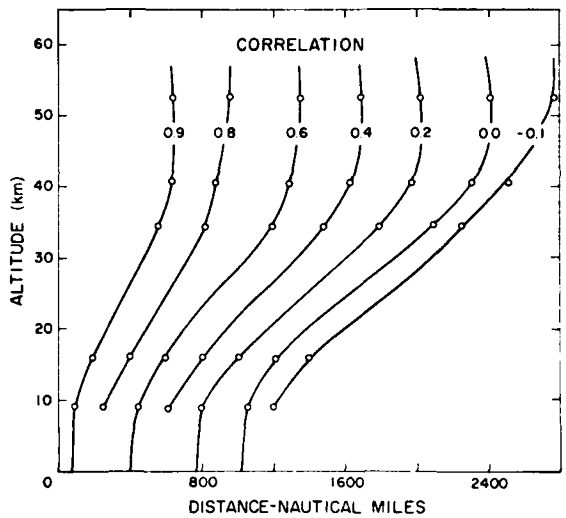

Rate of Decay of Density Correlation with Distance.

KM KILOMETERS ABOVE SEA LEVEL
MEAN AVERAGE OF OBSERVED VALUES
STDV STANDARD DEVIATION OF VALUES TIMES 10
N NUMBER OF VALUES AT EACH ALTITUDE

KM	26	28	30	32	34	36	38	40	42	44	46	48	50	52	54	56	58	60
MEAN	220	222	226	230	233	239	246	253	260	267	270	269	267	263	260	257	254	254
STDV	40	42	54	61	62	65	89	93	87	81	71	61	47	55	62	73	76	92
N	43	47	50	50	50	50	50	50	50	50	50	50	50	50	49	46	43	37
28	86	**																
30	58	75																
32	36	45	83															
34	33	39	75	88														
36	-3	8	49	65	78													
38	-9	-1	17	38	58	78												
40	-25	-16	-2	13	34	52	80											
42	-14	-17	-7	5	26	35	64	81										
44	-24	-33	-22	-11	1	19	44	54	69									
46	-16	-26	-27	-20	-8	14	33	47	57	71								
48	-13	-25	-26	-10	2	23	31	45	59	61	74							
50	2	-2	-6	8	15	21	25	31	40	44	45	72						
52	15	13	-6	4	0	-4	3	-1	10	7	15	38	68					
54	14	26	2	4	5	7	10	7	5	-8	0	16	39	73				
56	36	37	6	1	2	-9	-14	-13	-5	-19	-13	3	25	59	84			
58	32	37	-5	-11	-12	-17	-23	-15	-9	-20	1	13	27	49	65	81		
60	21	27	-10	-18	-25	-27	-35	-30	-21	-25	4	3	22	42	47	64	89	

** MULTIPLY TABULAR VALUES BY 0.01 TO OBTAIN CORRELATION COEFFICIENTS

Correlation of January Temperatures (°K) at White Sands Missile Range from 26 km to 60 km.

These investigations emphasize day-to-day density variability on the mesoscale, that is, for horizontal distances from 50 to 200 nautical miles and time periods of from 1 to 12 hours; root-mean-square (rms) differences for these distances and time intervals have been estimated for altitudes up to 60 km.

Middle Atmosphere Climatology: A technique has been developed that can be used to obtain estimates of the integrated effect of density, temperature and wind on the trajectories and impact points of reentry vehicles. Statistical arrays of monthly means, standard deviations of the day-to-day variability, and interlevel correlations of a given element provide the required information in compact form. An example of such an array for altitudes between 26 and 60 km is given here. This array provides density data in a format that can be readily used to estimate the distributions of vertical density gradients and the effects of day-to-day density variations on aerospace vehicles. A statistical method has also been developed to estimate the probability of extreme wind speeds for specific locations and altitudes up to the mesopause (80 km).

Preliminary research has begun on the manner in which correlation between densities at two levels decays with increasing vertical separation. A number of empirical models have been proposed for specific atmospheric elements. These models, however, are valid only over restricted ranges. An exponential representation of correlation decay for density between 26 and 60 km is given here. Although this

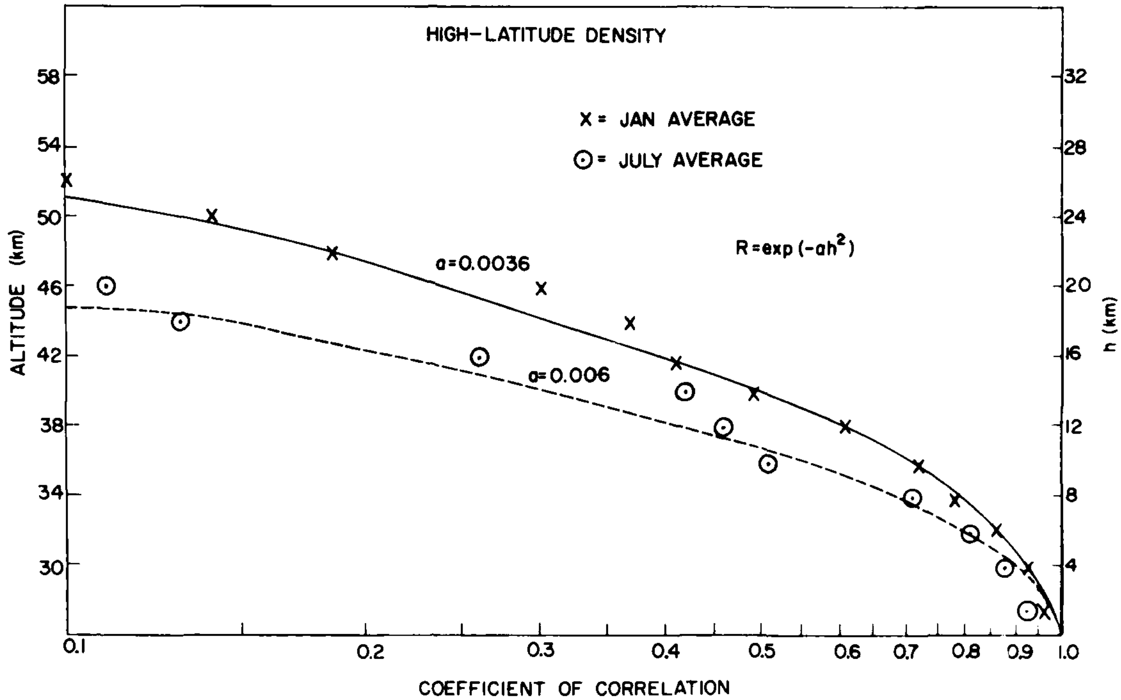

Exponential Representation of Correlation Decay from Density between 26 km and 60 km.

exponential fit appears promising, other regions and altitudes are being examined to explore the utility of this and related exponential models.

Surface Ice Accretion: The Air Force needs information on surface ice accretion to design and locate structures such as communications towers, radio antennas and radars. Unfortunately, standardized observations of icing amounts are not available in sufficient quantity to make objective estimates of the probability of ice accretion. This has resulted in the loss of inadequately designed Air Force structures. For example, a combination of ice and strong winds caused the destruction of an important Air Force communications tower in Europe during 1979. Since more reliable design decisions could be made if there were a more accurate data base, AFGL was asked to develop a method for objectively observing ice accretion. Such icing observations, taken in conjunction with measurements of other meteorological elements, could be used to develop a model for a climatology of icing.

An off-the-shelf, aircraft-type ice detector, chosen because of its potential for objectively measuring ice amounts, was tested in a climatic chamber. During the tests, which simulated natural icing conditions, detector output was found to be highly correlated with measurements of mass and thickness of ice on simulated structural members. The ice detection system was then deployed at four New England locations during the winter of 1979-1980 to evaluate its effectiveness for determining ice accumulations in the natural environment. Results indicate that the ice detector would make an excellent instrument for objectively measuring rime icing amounts on mountain tops. This information is important in the design of contemporary line-of-sight communications systems which are usually located on high,

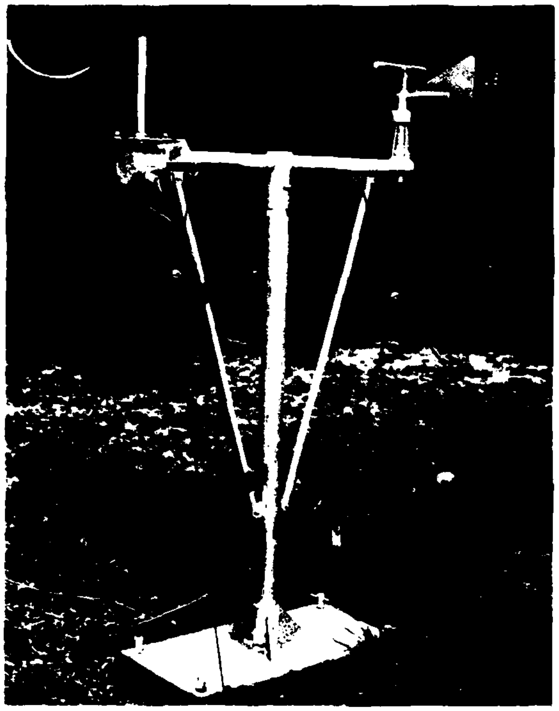

Ice Detector at Field Test Site.

exposed sites. A slight modification and additional testing would be necessary to use the instrument to measure glaze icing, which results from freezing rain or drizzle. The ice detector is shown here on a stand at one of the field test sites. The cylinder on the co-located vane was used to make comparative measurements of the mass and thickness of accumulated ice.

Station Cloud-Cover Frequencies: Climatological tables normally summarize cloud information in terms of the frequency of cloud cover, in tenths, from clear (0/10) to overcast (10/10), and in terms of the frequency of ceiling height from the ground to as high as 10 km. Clouds form a ceiling at a given height when they cover more than 5/10 of the sky at that height. As useful as the climatic summaries are, however, more information is needed, such as: (1) the average sky cover as a function of elevation above the ground; (2) the average amount of cloud cover in layers, and at specific levels of the atmosphere; and (3) the frequency distribution of cloud cover, from 0/10 to 10/10, at any level, or in any layer between levels that are defined by point of observation and target.

A model to estimate the areal coverage of clouds has been published recently in the open literature, which is used to accomplish the above purposes. A typical result of its application is shown in the figure. For example, the average cloud cover at the ground (that is, fog) is 0.11 for a January morning in Berlin, Germany.

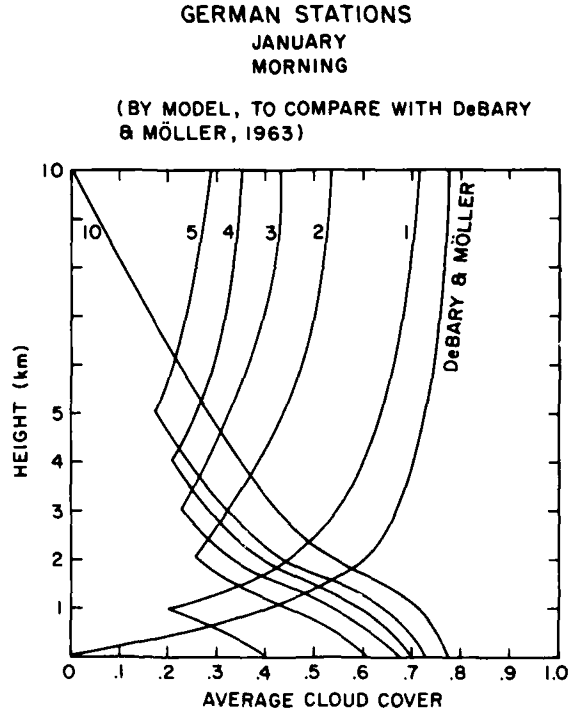

Average Cloud Cover at and between Levels, Berlin, Germany, January Morning.

But the average cloud cover for all heights up to 10 km is 0.78. At the 1-km level the cloud cover, on the average, is 0.2; it is 0.4 in the layer between ground and the 1-km surface, 0.6 in the layer from 1 to 5 km, and 0.71 in the entire layer to 10 km.

Further application of the model yields the estimates of frequency distributions.

If, for example, the layer of interest is that between 3 and 10 km over an area of 100 km^2 at Bedford, Mass., in January, noontime, the model yields estimates of probabilities as follows: full overcast, 19 percent; clouds covering 1/10 to 5/10, 9 percent; all clear, 66 percent. If the interest were in a much larger area, such as 100,000 km^2, or a square area roughly 300 km to the side, the probability estimates would be: full overcast, 0.1 percent; clouds covering 1/10 to 5/10, 80 percent; all clear, 3 percent.

Duration of Events: Under an AFGL contract, the University of Rochester has developed a model, based on the Markov process (a process in which all that is used for the probability of future events is the current information), to give analytic answers for the probability of the duration of weather events. In the Ornstein-Uhlenbeck process, a commonly used type of Markov process, the serial correlation coefficient of a variable decreases exponentially with time. The hour-to-hour correlation coefficient is approximately 0.95 for variables such as air temperature, visibility, ceiling, and other weather elements. The analytical expressions for probable durations have been programmed on the CDC-6600 computer. By use of third-order polynomials, however, approximate solutions have been made possible on desk-top computers. To illustrate their use, the following values have been computed, for the probability of continuous periods of no-rain, for the indicated duration at Boston, Mass., in July, where the hour-to-hour probability of no-rain is 0.9503. For 1/2 hour the probability of continuous periods of no-rain is 0.93; for 1 hour, 0.92; 6 hours, 0.86; 12 hours, 0.81; 1 day, 0.72; 2 days, 0.58; 3 days, 0.48; 7 days, 0.21. It appears, therefore, that there is a 50-50 chance of rain in a 3-day period. The probability of no-rain at all during the whole month of July is estimated to be 0.2 percent.

Stochastic Modeling of Station Climate: An AFGL contract with the University of Central Florida (UCF) has expanded the application of stochastic models to develop probability distributions of weather elements. The DOD has had a continuing need to provide climatological information to weapon systems designers and operators, and to planners on both the strategic and tactical levels. The UCF studies were motivated by the goal of achieving a capability to determine, expeditiously, the climatic probability of above-threshold conditions of weather relative to the success of an Air Force mission anywhere at any time. The studies focused on the following five weather elements, for which probabilistic models were obtained: visibility, sky cover, windspeed, rainfall, and ceiling. Each model has two to three distribution parameters that need to be estimated to fit the desired weather elements at a given station. The usual method for estimation of parameters is maximum likelihood. At UCF a slightly different position was taken in the goals of modeling. The cumulative distribution function (CDF) was made the center of interest as opposed to the probability density function. The parameter estimates were obtained to minimize the sums of squares of the differences between estimates and the empirical CDF's. Although the models are basically nonlinear with respect to the parameters, a linearization has been effected through a first-order Taylor Series expansion. These probabilistic models have proved useful at nearly all the stations tested.

AIRCRAFT ICING PROGRAM

In the last few years, the Air Force has turned to low level operations as a means of increasing the survivability of its aircraft. This is caused in part by the sophisticated high and mid-level air defense equipment now generally available. A return to low levels brings us back into a

region of the atmosphere not frequently traversed by the United States Air Force since the advent of the high-performance jet engine. This step "back" over 20 years has resurrected a 20-year old problem: aircraft icing.

Aircraft recently added to the inventory, such as the F-16, A-10 and HH-53, are encountering disturbing problems with icing. Potentially severe problems have been anticipated for the cruise missile, which was designed without anti-icing or de-icing capabilities.

In response to an Air Weather Service Geophysical Requirement, the Meteorology Division initiated a program with three goals: (1) to evaluate the current AWS techniques used in forecasting aircraft icing; (2) to develop, as required, new automated forecast techniques based on standard meteorological data which can be used on the AF Global Weather Center computers; and (3) to develop a procedure for obtaining a climatology of aircraft icing based on standard archived data.

Because the radiosonde observations are the primary input to the current forecast techniques, the immediate goal is to collect objectively-measured ice accretion observations and to relate them to concurrent observations of liquid water content, drop-size distributions and air temperature. To improve icing forecast techniques, it is necessary to achieve a better understanding of the microphysical processes of the atmosphere containing those elements which produce icing conditions. This requires in-situ measurements of these atmospheric elements. During the 1979-80 winter season, a meteorologically-instrumented HC-130E research aircraft collected icing data for sixteen case studies for a total of twenty-three sampling hours in which the HC-130E flew in the immediate vicinity of radiosonde ascents. A similar amount of sampling is being conducted during the 1980-81 winter season with an increased emphasis on the study of icing conditions associated with active frontal zones.

ATMOSPHERIC DYNAMICS

The modern science of weather forecasting as it has developed during the last quarter century is based on the belief that numerical models of the atmosphere can simulate the evolution of the real atmosphere. Prediction is possible from such a simulation only when it can be produced faster than the speed at which the natural evolution takes place. Prediction can be accurate only to the extent that the simulation is. Consequently, efficiency and accuracy have been regarded as the two most important attributes of numerical models throughout the history of the development of numerical weather prediction.

The accuracy of a simulation or, more generally, of a numerical model, depends on the accuracy of the postulated physical laws, the accuracy with which the physical laws are expressed as mathematical statements, and the accuracy with which the mathematical statements are carried out computationally. Similarly, the efficiency of a model may be seen to be a composite of the efficiencies of the three individual elements. The research efforts at AFGL during the last two years have been mainly directed toward improving efficiencies in the mathematical and computational aspects. Investigations covered both the global and regional domains and included both stationary and transient problems.

Digital Filters on Spherical Surfaces: A perennial problem in the numerical simulation of the atmospheric evolution is the presence of noise that arises from computational errors. Left unchecked, the noise will interact with the real signal in a model to produce unrealistic simulations. Therefore, the removal or damping of unwanted noise in a numerical simulation has been considered to be an important subject of research in numerical weather prediction. The so-called "ideal filter" is defined to be an algorithm that would remove only the unwanted waves and leave

all other waves intact in both amplitude and phase.

Although such a filter had been developed earlier for flows represented on a plane, the proper form of filtering for flows in a spherical domain remains to be selected. We have studied the characteristics of several different forms of a highly scale-dependent low-pass filter for scalar variables on the surface of a sphere. The phase and amplitude response functions of the various forms of the filter indicate that the simplest form approaches most closely the criteria established for the ideal filter, although it does not preserve area-weighted mean values. This form of the filter has been adopted in our study of interactions of model dynamics and numerical errors in a global barotropic model of the atmosphere. Our experience indicates that the filter is computationally efficient and very effective in removing spurious short waves generated by numerical errors in the process of a numerical time integration.

Model Dynamics and Numerical Errors: Numerical experiments have been carried out on a global atmospheric model to study the suitability of certain numerical methods in atmospheric modeling. Specifically, using idealized initial conditions and a scale-dependent spatial filter, we have investigated the capabilities and limitations of second-order finite-difference approximations commonly used in simulation and prediction studies. Comparisons with analytic solutions reveal that, for dynamically stable flows, second-order finite-difference approximations, together with a digital filter appropriate for a spherical surface, are adequate in yielding approximate solutions to the modeling differential equations. For dynamically unstable flows, numerical errors are amplified as part of the dynamics of the unstable system. The use of finite-difference approximations may yield solutions which bear no resemblance whatsoever to the true solution of the differential equations in spite of the maintenance of computational stability by a digital filter. Interactions of model dynamics and numerical errors in a numerical model may prove to be another major obstacle in numerical prediction of an unstable flow.

Fourier Series on Spheres: In spectral simulation and prediction of atmospheric flows, the choice of basis functions is important because it dictates both the accuracy and economy of the computational procedure. For global spectral models, a popular current practice is to expand the dependent variables in terms of spherical surface harmonics. While such expansions give rise to spectral equations that possess many desirable numerical properties, these model equations have a serious drawback in that an inordinate amount of computer time and computer storage is required for their numerical solution. This drawback is due to the associated Legendre functions, one of the basis functions of the surface-harmonics, which are not amenable to fast transforms. Since it is the transform method that makes spectral methods competitive with finite-difference methods in terms of computer economy, it is desirable that an expansion yield equations that can be handled by fast transforms. Fourier series as basis functions in a global spectral model appear most attractive, because very efficient numerical transform algorithms that require little computer storage are now available.

Based on geometric considerations we have developed a Fourier series representation of a scalar variable on the surface of a sphere. Such a representation can also be derived from considerations of the properties of spherical surface harmonics. In fact, we have provided a unified derivation for three known expressions for the Fourier decomposition of a scalar function on spheres, and have shown that the expression which is consistent with geometric considerations is superior.

Limited-Area Models: There are two compelling reasons for developing limited-area models that are motivated by the desire for better and/or more detailed forecasts. One is the uneven distribution of the meteorological network that measures that state of the atmosphere. There are more weather stations over well-populated than less-populated areas. The other is the limitation on the capacity and speed of the computers used for the numerical weather prediction. With given limits and a given model, a larger forecast domain must utilize a coarser computational resolution than a smaller domain.

To prepare a better and/or more detailed forecast locally in the area of particular concern we identify a region containing the area and generate simulations over the region using a computational resolution which is finer than that used in the outside. In so doing, we create an artificial boundary along which the values of the variables must be provided during the period of forecast. These boundary values must be specified externally by another model which covers a larger domain and, therefore, has a coarser resolution.

To investigate the effects of the computational resolution on the forecast accuracy of such a limited-area model we carried out a series of controlled experiments on a model with a hypothetically fixed observational network. The experiments used wind velocity as the variable of observation and prediction. The requisite initial and boundary conditions for a given computational resolution were estimated through interpolation. Two spatial interpolations of different degrees of sophistication and the linear temporal interpolation were considered in the experiments.

Using the root-mean-squares of forecast errors and the skill scores as the measures, we have found that the more sophisticated spatial interpolation does not necessarily yield better accuracy. The required interpolation in space and/or time has been found to produce errors of a magnitude which tends to offset smaller truncation errors that result from the reduction in the grid interval. The advantage of a finer computational resolution has been found only at shorter wavelengths and during the second half of the twenty-four hour period.

JOURNAL ARTICLES
JANUARY 1979 - DECEMBER 1980

BARNES, A.A., JR.
Observations of Ice Particles in Clear Air, Journal de Recherches Atmospheriques
14, No. 3-4 (1980)

BUNTING, J.T.
Sensing Ice Clouds from Satellites, Light Scattering by Irregularly Shaped Particles
Ed. by D.W. Schuerman, Plenum Pub. Co. (1980)

BURGESS, D.W., and WILK, K.E. (National Severe Storms Lab, Norman, OK), BONEWITZ, J.D. (Capt., USAF Air Weather Service, Norman, OK), GLOVER, K.M. (AFGL), HOLMES, D.W. (National Weather Service, Silver Springs, MD), and HINKELMAN, J. (Federal Aviation Administration, Washington, DC)
The Joint Doppler Operational Project
Weatherwise 32, No. 2 (April 1979)

GRINGORTEN, I.I.
Probability Models of Weather Conditions Occupying a Line or an Area
J. Appl. Meteorol. 18, No. 8 (August 1979)

KUNKEL, B.A.
A Modern Thermo-Kinetic Warm Fog Dispersal System for Commercial Airports
J. Appl. Meteorol. 18, No. 6 (June 1979)
Fog: Man's Attempt to Control It
Weatherwise 33 (June 1980)

LUND, I.A.
Climatology
McGraw-Hill Yearbook of Science and Technology (1980)

LUND, I.A., and GRANTHAM, D.D.
Estimating the Joint Probability of a Weather Event at Two Locations
J. Appl. Meteorol. 18, No. 1 (January 1979)
Estimating Recurrence Probabilities of Weather Events
J. Appl. Meteorol. 18, No. 7 (July 1979)

Estimating Probabilities of Cloud-Free Fields of View from the Earth Through the Atmosphere
J. Appl. Meteorol. 19, No. 4 (April 1980)
Estimating the Joint Probability of a Weather Event at More Than Two Locations
J. Appl. Meteorol. 19, No. 9 (September 1980)

MOROZ, E.Y.
Lidar Visibility Measurements, Light Scattering by Irregularly Shaped Particles
Ed. by D.W. Schuerman, Plenum Pub. Co. (1980)

PLANK, V.G., BERTHEL, R.O., and BARNES, A.A., JR.
An Improved Method for Obtaining the Water Content Values of Ice Hydrometeors from Aircraft and Radar Data
J. Appl. Meteorol. 19, No. 11 (November 1980)

SHAPIRO, R.
An Examination of Certain Proposed Sun-Weather Connections
J. Atmos. Sci. 36, No. 6 (June 1979)
Book Review: Sun, Weather and Climate
by Herman, J.R., and Goldberg, R.A., Am. Geophys. Un., EOS 61 (1980)

YEE, S.Y.K.
Studies on Fourier Series on Spheres
Mon. Weather Rev. 108, No. 5 (May 1980)

PAPERS PRESENTED AT MEETINGS JANUARY 1979 - DECEMBER 1980

ALLEN, R.H., CAPT. (Hq. AWS, Scott AFB, IL), BURGESS, D.W. (National Severe Storms Lab., Norman, OK), and DONALDSON, R.J.
Severe 5 cm Radar Attenuation of the Wichita Falls Storm by Intervening Precipitation
19th Conf. on Radar Meteorology, Miami, FL (15-18 April 1980)

BARNES, A.A., JR.
Ice Particles in Clear Air
I.A.M.A.P.-I.C.C.P., VIIIth Int. Conf. on Cloud Phys., Clermont-Ferrand, France (15-19 July 1980)

BJERKAAS, C.L., CAPT., and FORSYTH, D.E., CAPT. (Univ. of Oklahoma, Norman, OK)
Real-Time Automated Tracking of Severe Thunderstorms Using Doppler Weather Radar
11th Conf. Severe Local Storms, Kansas City, MO (2-5 October 1979)
Operational Test of a Three-Dimensional Echo Tracking Program
19th Conf. Radar Meteorology, Miami, FL (15-18 April 1980)

BOEHM, A.R., MAJ., DITTBERNER, G.J., MAJ. (USAF/ETAC, Scott AFB, IL), and GRINGORTEN, I.I.
Evaluation of Forecasts with Scores Based on Climatic Probabilities
Int. Sym. on Probabilistic and Statistical Methods in Weather Forecasting, Nice, France (8-12 September 1980)

BOUCHER, R.J.
Snowfall Rate Determined from Radar Reflectivity within a 50 km Range
19th Conf. Radar Meteorology. Miami, FL (15-18 April 1980)

BUNTING, J.T.
Sensing Ice Clouds from Satellites
Int. Wkshp. on Light Scattering by Irregularly Shaped Particles, SUNY, Albany (5-7 June 1979)
Sensing Snow and Clouds at 1.6 μm.
Cloud/Climate Wkshp., New York, NY (29-31 October 1980)

BURGESS, D.W. (National Severe Storms Lab. Norman, OK), and DONALDSON, R.J.
Contrasting Tornadic Storm Types
11th Conf. on Severe Local Storms, Kansas City, MO (2-5 October 1979)

COHEN, I.D., CAPT., and VARLEY, D.J., LT. COL.
Aircraft Observations of Particle Concentrations in the First 1000 Feet Above the Ocean Surface
3rd Conf. on Ocean-Atmosphere Interaction, Los Angeles CA (30 January - 1 February 1980)

DONALDSON, R.J.
Severe Storm Warning by Meteorological Doppler Radar
Natl. Weather Assoc. Hanscom AFB, MA (4 December 1980)
Gust Front Structure Observed by Doppler Radar
11th Conf. on Severe Local Storms, Kansas City, MO (2-5 October 1979)

DONALDSON, R.J., and BJERKAAS, C.L., CAPT.
Gust Front Structure Observed by Doppler Radar
19th Conf. on Radar Meteorology, Miami, FL (15-18 April 1980)

GEISLER, E.B., CAPT., and DENGEL, R.C. (SASC, Lexington, MA)
Objective Prediction of Slant Visual Range During Advective Fog Conditions
8th Conf. on Weather Forecasting and Analysis, Denver, CO (10-13 June 1980)

GLOVER, K.M.
On the Automation of Weather Radar Information for Air and Ground Operations
19th Conf. on Radar Meteorology, Miami, FL (15-18 April 1980)

GRANTHAM, D.D.
The AFGL Aircraft Icing Program
In-Flight Icing Met'l Surveys Coordination Mtg., Fed. Aviation Admn. Tech. Ctr., Atlantic City, NJ (6 August 1980)

GROGINSKY, H.L. (Raytheon Co., Wayland, MA), and GLOVER, K.M.
Weather Radar Canceller Design
19th Conf. on Radar Meteorology, Miami, FL (15-18 April 1980)

HAWKINS, R.S.
A Clustering Technique for Satellite Imagery Analysis
8th Conf. on Weather Forecasting and Analysis, Denver, CO (10-13 June 1980)

JAGODNIK, A.J., and YOUNG, M.J. (Raytheon Co., Wayland, MA), BANIS, K.J., and GLOVER, K.M.
A Programmable Fault-Tolerant Meteorological Radar Signal Processor
Government Microcircuit Appl. Conf., Washington, DC (1980)

KEILSON, J., and ROSS, H.F. (Univ. of Rochester, Rochester, NY)
The Maximum Over an Interval of Meteorological Variates Modeled by the Stationary Gaussian Markov Process
6th Conf. on Probability and Statistics in Atmospheric Sci., Banff, Canada (9-12 October 1979)

KRAUS, M.J., and BJERKAAS, C.L.
An Analysis of PPI Patterns of Radial Velocity Shear
19th Conf. on Radar Meteorology, Miami, FL (15-18 April 1980)

KUNKEL, B.A.
Acoustic Sounding of Marine Fog at a Massachusetts Coastal Station
Second Conf. on Coastal Meteorology, Los Angeles, CA (30 January - 1 February 1980)

LUND, I.A., and GRANTHAM, D.D.
Estimating the Joint Probability of a Weather Event at More than Two Locations
6th Conf. on Probability and Statistics in Atmospheric Sci., Banff, Canada (9-12 October 1979)

MOROZ, E.Y.
Lidar Visibility Measurements
Int. Wkshp. on Light Scattering by Irregularly Shaped Particles, SUNY, Albany (5-7 June 1979)

MUENCH, H.S.
Local Forecasting Through Extrapolation of GOES Imagery Patterns
8th Conf. on Weather Forecasting and Analysis, Denver, CO (10-13 June 1980)

PASSARELLI, R.E., JR., and SRIVASTAVA, R.C.
A New Aspect of the Vertical Incidence Doppler Spectrum of Falling Snowflakes
19th Conf. on Radar Meteorology, Miami, FL (15-18 April 1980)

PETROCCHI, P.J., and BANIS, K.J.
Computer Analysis of Raindrop Spectral Data Acquired by RD-69 Disdrometers During the 1979 NSSL SESAME Project
19th Conf. on Radar Meteorology, Miami, FL (15-18 April 1980)

PLANK, V.G., BERTHEL, R.O., and DELGADO, L.V.
The Shape of Raindrop Spectra for Different Situations and Averaging Periods
I.A.M.A.P.-I.C.C.P. VIIIth Int. Conf. on Cloud Phys., Clermont-Ferrand, France (15-19 July 1980)

SOMERVILLE, P.N., and BEAN, S.J. (Univ. of Central Florida, Orlando, FL)
Probability Modeling of Weather Elements
6th Conf. on Probability and Statistics in Atmospheric Sci., Banff, Canada (9-12 October 1979)

TECHNICAL REPORTS JANUARY 1979 - DECEMBER 1980

BERTHEL, R.O.
A Method to Predict the Parameters of a Full Distribution from Instrumentally Truncated Data
AFGL-TR-80-0001 (7 January 1980), ADA085950

BJERKAAS, C.J., CAPT., and FORSYTH, D.E., CAPT.
An Automated Real-Time Storm Analysis and Storm Tracking Program (WEATRK)
AFGL-TR-80-0316 (1 October 1980), ADA100236

BROWN, H.A.
Preliminary Assessment of an Automated System for Detecting Present Weather
AFGL-TR-79-0137 (26 June 1979), ADA078031
Automation of Visual Weather Observations
AFGL-TR-80-0097 (1 April 1980), ADA088881

BUNTING, J.T., and FOURNIER, R.F.
Tests of Spectral Cloud Classification Using DMSP Fine Mode Satellite Data
AFGL-TR-80-0181 (2 June 1980), ADA094119

BUNTING, J.T., and TOUART, C.N.
Horizontal Scale Variations in Satellite Estimates of Weather Erosion Parameters for Reentry Systems
AFGL-TR-80-0209 (26 June 1980), ADA092447

CHISHOLM, D.A., LYNCH, R.H., WEYMAN, J.C., CAPT., and GEISLER E.B., CAPT.
A Demonstration Test of the Modular Automated Weather System (MAWS)
AFGL-TR-80-0087 (24 March 1980), ADA087070

COHEN, I.D., CAPT.
Cirrus Particle Distribution Study, Part 5
AFGL-TR-79-0155 (13 July 1979), ADA077361
Marine Boundary Layer Sampling Flight No. 2
AFGL-TR-79-0242 (11 October 1979), ADA083158

COHEN, I.D., CAPT., and BARNES, A.A., JR.
Cirrus Particle Distribution Study, Part 6
AFGL-TR-80-0261 (4 September 1980), ADA096772

COLE, A.E., KANTOR, A.J., and PHILBRICK, C.R.
Kwajalein Reference Atmospheres, 1979
AFGL-TR-79-0241 (9 October 1979), ADA081780

COLE, A.E., KANTOR, A.J., and BERTONI, E.A.
Interlevel Correlations of Temperature and Density, Surface to 60km
AFGL-TR-80-0163 (14 May 1980), ADA090515

DELGADO, L.V., CAPT.
Icing Nozzle Element Optimization Test, January 1979
AFGL-TR-79-0193 (20 August 1979), ADA081175

DONALDSON, R.J., JR., and GLOVER, K.M.
Joint Agency Doppler Technology Tests
AFGL-TR-80-0357 (21 November 1980), ADA100208

DYER, R.M., and BARNES, A.A., JR.
The Microphysics of Ice Clouds - A Survey
AFGL-TR-79-0103 (8 May 1979), ADA077020

FITZGERALD, D.R.
Applications of Ground-Based Remote Sensing Techniques
AFGL-TR-80-0315 (1 October 1980), ADA097044

GEISLER, E.B.,CAPT.
Development and Evaluation of a Tower Slant Visual Range System
AFGL-TR-79-0209 (14 September 1979), ADA082384

IZUMI, Y., and TOUART, C.N.
A Test of the Climatic Normality of Synthetic Profiles of Atmospheric Liquid Water Content Over the USSR in 1973
AFGL-TR-79-0154 (12 July 1979), ADA077021

KANTOR, A.J., and COLE, A.E.
Time and Space Variation of Density in the Tropics
AFGL-TR-79-0109 (10 May 1979), ADA074472
Wind Distributions and Interlevel Correlations, Surface to 60 km
AFGL-TR-80-0242 (19 August 1980), ADA092670

KUNKEL, B.A.
A Preliminary Assessment of the Monostatic Acoustic Sounder as a Forecast Aid in the Prediction of Advection Fogs at a Massachusetts Coastal Station
AFGL-TR-80-0341 (6 November 1980), ADA100271

LUND, I.A., and BERTONI, E.A.
Some Comparisons Between Probabilities of Cloud-Free Lines-of-Sight Estimated from Aircraft and from Sky Cover Observations
AFGL-TR-80-0046 (8 February 1980), ADC021847

LUND, I.A., GRANTHAM, D.D., BERTONI, E.A., and ELAM, C.B., JR.
Atlas of Cloud-Free Line-of-Sight Probabilities Part 5: North Africa and the Middle East
AFGL-TR-79-0275 (9 November 1979), ADA088156

MOROZ, E.Y., and BROUSAIDES, F.J.
Survey of Sensors for Automated Tactical Weather Observations
AFGL-TR-80-0195 (25 June 1980), ADA094121

MUENCH, H.S.
Short-Range Forecasting Through Extrapolation of Satellite Imagery Patterns Part II: Testing Motion Vector Techniques
AFGL-TR-79-0294 (10 December 1979), ADA086862

MUENCH, H.S., and HAWKINS, R.S.
Short-Range Forecasting Through Extrapolation of Satellite Imagery Patterns Part I: Motion Vector Techniques
AFGL-TR-79-0096 (26 April 1979), ADA073081

MUENCH, H.S., and KEEGAN, T.J.
Development of Techniques to Specify Cloudiness and Rainfall Rate Using GOES Imagery Data
AFGL-TR-79-0255 (26 October 1979), ADA084757

SHAPIRO, R.
Linear Filtering on the Surface of a Sphere
AFGL-TR-79-0263 (29 October 1979), ADA082386

TATTELMAN, P.
Climatic Chamber Tests of a Surface Ice Accretion Measurement System
AFGL-TR-79-0079 (26 March 1979), ADA077022

TOUART, C.N., and IZUMI, Y.
Comparison Study of Models Used to Prescribe Hydrometeor Water Content Values Part II: USSR Data
AFGL-TR-79-0213 (18 September 1979), ADA082385

VARLEY, D.J., LT. COL.
A Marine Boundary Layer Sampling Flight In Clear Air
AFGL-TR-79-0013 (10 January 1979), ADA069723
Microphysical Properties of a Large Scale Cloud System, 1-3 March 1978
AFGL-TR-80-0002 (7 January 1980), ADA083140

VARLEY, D.J., LT. COL., and BARNES, A.A., JR.
Cirrus Particle Distribution Study, Part 4
AFGL-TR-79-0134 (18 June 1979), ADA074763

VARLEY, D.J., LT. COL., and COHEN, I.D., CAPT.
Cirrus Particle Distribution Study, Part 7
AFGL-TR-80-0324 (16 October 1980), ADA100269

YEE, S.Y.K.
Double Fourier Series Solution of Poisson's Equation on a Sphere
AFGL-TR-80-0334 (29 October 1980), ADA099385
Fourier Series on Spheres - A Geometric Perspective
AFGL-TR-80-0021 (15 January 1980), ADA084484

YEE, S.Y.K., and SHAPIRO, R.
Numerical Studies on a Global Barotropic Vorticity Equation Model of the Atmosphere
AFGL-TR-79-0295 (1979), ADA084487

CONTRACTOR JOURNAL ARTICLES JANUARY 1979 - DECEMBER 1980

AUFDERHAAR, G.C., and LIOU, K.N. (Univ. of Utah, Logan, UT)
Cylindrical Cloud Model for Microwave and Infrared Radiative Transfer: Applications to DMSP Microwave Sounders
1980 Int. Radiation Symp. Volume (1980)

CAMPBELL, W.C., CHADWICK, R.B., EARNSHAW, K.B., and MORAN, K.P. (Wave Propagation Lab., Boulder, CO)
Low Elevation Angle Wind Measurements By FM-CW Radar
Preprint Vol. 19th Conf. on Radar Meteorology (April 1980)

CHADWICK, R.B., and MORAN, K.P. (Wave Prop. Lab., CO)
Long-Term Measurements of C_n^2 in the Boundary Layer
Radio Sci. 15, No. 2 (March-April 1980)

CHADWICK, R.B., MORAN, K.P., and CAMPBELL, W.C.
Design of a Wind Shear Detection Radar for Airports
IEEE Trans. on Geoscience Elec. GE-17, No. 4 (October 1979)

CHADWICK, R.B., and STRAUCH, R.G.
Processing of FM-CW Doppler Radar Signals from Distributed Targets
IEEE Trans. on Aerospace and Elec. Sys. AES-15, No. 1 (January 1979)

LIOU, K.N., and DUFF, A.D. (Univ. of Utah, Logan, UT)
Atmospheric Liquid Water Content Derived From Parameterization of Nimbus 6 Scanning Microwave Spectrometer Data
J. Appl. Meteorol. 18 (1979)

PASSARELLI, R.E., JR. (MIT, Cambridge, MA), and SRIVASTAVA, R.C. (Univ. of Chicago, Chicago, IL)
A New Aspect of the Vertical Incidence Doppler Radar Spectrum of Ice Particle Fall Speeds
J. Appl. Meteorol. 19 (November 1980)

YEH, H.Y., and LIOU, K.N. (Univ. of Utah, Logan, UT)
Infrared and Microwave Sounding of the Cloud Liquid Water Content and Temperature Profile in Cloudy Atmospheres
1980 Int. Radiation Symp. Vol. (August 1980)

CONTRACTOR TECHNICAL REPORTS JANUARY 1979 - DECEMBER 1980

ASTLING, E.G., and LIOU, K.N. (Univ. of Utah, Salt Lake City, UT)
Analyze, Calculate, and Develop Techniques for Weather Satellite Imagery Data
AFGL-TR-79-0140 (15 June 1979), ADA077292

BEAN, S.J., and SOMERVILLE, P.N. (Univ. of Central Florida, Orlando, FL)
Some Models for Windspeed
AFGL-TR-79-0180 (16 July 1979), ADA077048

BEAN, S.J., SOMERVILLE, P.N., and HEUSER, M. (Univ. of Central Florida, Orlando, FL)
Some Models for Ceiling
AFGL-TR-79-0221 (31 August 1979), ADA078033

BERKOFSKY, L. (Ben Gurion Univ. of the Negev, Sde Boker, Israel)
Desert Convective Clouds
AFGL-TR-80-0140 (February 1980), ADA083965

BLOOD, D.W., and CRANE, R.K. (Environmental Res. and Technology, Inc., Concord, MA)
Assessment of Radar Parameters for Hydrometeor Scatter Measurement Using the ALCOR and TRADEX Radars at Kwajalein
AFGL-TR-80-0031 (November 1979), ADA083071

BRINGI, V.N. (Dept. of Elec. Engineering, Ohio St. Univ., Columbus, OH)
Correlation Properties of Differential Reflectivity and Their Implications for Radar Meteorology
AFGL-TR-80-0356 (1 October 1980), ADA104049

BURKE, S.L. (Regis Coll., Weston, MA)
Meteorological Studies: Atmospheric Analysis, Automated Weather System Development, Satellite Studies
AFGL-TR-79-0047 (28 February 1979), ADA067937

CHIN, D., and HAMILTON, H.D. (Systems and Applied Sciences Corp., Riverdale, MD)
Synoptic Analysis Case 2 - 23 March 1978 - 27 March 1978
AFGL-TR-79-0007 (5 January 1979), ADA065555
Synoptic Analysis Case 3 - 23 February 1977 - 25 February 1977
AFGL-TR-79-0021 (18 January 1979), ADA066981

CRANE, R.K. (Environmental Res. and Technology, Inc., Concord, MA)
Automatic Weather Radar Echo Assessment and Tracking
AFGL-TR-79-0248 (March 1979), ADA081061

D'ENTREMONT, R.P. (Systems and Applied Sciences Corp., Riverdale, MD)
Performance of the Discrete Fourier Transform Satellite Imagery Classification Technique
AFGL-TR-80-0175 (17 June 1980), ADA095364

GERLACH, A.M. (ED.) (Systems and Applied Sciences Corp., Riverdale, MD)
Computer-Based Weather Research
AFGL-TR-80-0069 (29 February 1980), ADA094020

HAASS, U.L., and BRUBAKER, T.A. (Colorado St. Univ., Fort Collins, CO)
Estimation of Lateral and Rotational Cloud Displacement from Satellite Pictures
AFGL-TR-79-0287 (October 1979), ADA085810

HALLETT, J. (Univ. of Nevada, Desert Res. Inst., Reno, NV)
Characteristics of Atmospheric Ice Particles: A Survey of Techniques
AFGL-TR-80-0308 (September 1980), ADA093927

HARDY, K.R. (Environmental Res. and Technology, Inc., Concord, MA)
Meteorological Data Analyses in Support of the ABRES Program
AFGL-TR-79-0084 (January 1979), ADA070946

HEUSER, M., SOMERVILLE, P.N., and BEAN, S.J. (Univ. of Central Florida, Orlando, FL)
Least Squares Fitting of Distributions Using Non-Linear Regression
AFGL-TR-80-0362 (30 September 1980), ADA097039

KEILSON, J., and ROSS, H.F. (Univ. of Rochester, Rochester, NY)
Gaussian Markov Related Variates for Meteorological Planning
AFGL-TR-79-0282 (14 November 1979), ADA081382

KUO, H.L., and RAYMOND, W.H. (Univ. of Chicago, Chicago, IL)
A Quasi-One-Dimensional Cumulus Cloud Model and Parameterization of Cumulus Heating and Mixing Effects
AFGL-TR-79-0272 (November 1979), ADA083024

LIOU, K.N., YEH, H.Y., CHEN, F.M., HUTCHISON, K., and ASTLING, E. (Univ. of Utah, Salt Lake City, UT)
Development of Infrared and Microwave Techniques for Cloud Parameter Inference from Satellite Imagery and Sounder Data
AFGL-TR-80-0263 (30 August 1980), ADA097592

LORENZ, E.N. (MIT, Cambridge, MA)
The Feasibility of a Low-Order Model of a Moist General Circulation
AFGL-TR-80-0354 (30 November 1980), ADA096704
Numerical Evaluation of Moist Available Energy
AFGL-TR-79-0083 (March 1979), ADA067725

MACK, E.J., WATTLE, B.J., ROGERS, C.W., and PILIE, R.J. (Calspan Corp., Buffalo, NY)
Fog Characteristics at Otis AFB, MA
AFGL-TR-80-0340 (30 October 1980), ADA095358

METCALF, J.I., HOLM, W.A., BODNAR, D.G., MARTIN, E.E., TREBITS, R.N., and STEINWAY, W.J. (Georgia Inst. of Tech., Engineering Experiment Station, Atlanta, GA)
Design Study for a Coherent Polarization-Diversity Radar
AFGL-TR-80-0262 (April 1980), ADA096757

NORMENT, H.G. (Atmospheric Sci. Assoc., Bedford, MA)
Collection and Measurement Efficiencies of the EWER Cloud Water Meter for Hydrometeors
AFGL-TR-79-0122 (May 1979), ADA072827
Airflow Effects on Riming Measurements by a Wing Tip-Mounted Ice Detector on the MC-130E Research Airplane
AFGL-TR-79-0194 (August 1979), ADA077019

NORQUIST, D.C. (Systems and Applied Sciences Corp., Riverdale, MD)
An Investigation of Three Methods of Completing a Staggered Data Field on Square Grid
AFGL-79-0197 (24 August 1979), ADA082330

PARKER, L.W., and KASEMIR, H.W. (Lee W. Parker, Inc., Concord, MA)
Airborne Lightning Warning Systems: A Survey
AFGL-TR-80-0226 (July 1980), ADA095354

PICKETT, R.M., and BLACKMAN, E.S. (Bolt Beranek and Newman, Inc., Cambridge, MA)
Automated Processing of Satellite Imagery Data: Test of a Spectral Classifier
AFGL-TR-79-0040 (February 1979), ADA068663

SHAPIRO, R. (AFGL) and STOLOV, H.L. (City College of the City University of New York, NY)
A Search for a Solar Influence on the Skill of Weather Forecasts
AFGL-TR-79-0031 (30 January 1979), ADA064481

SOMERVILLE, P.N., and BEAN, S.J.
A New Model for Sky Cover
AFGL-TR-79-0219 (27 August 1979), ADA078368
Stochastic Modeling of Climatic Probabilities
AFGL-TR-79-0222 (November 1979), ADA080559
Some Additional Models for Rainfall
AFGL-TR-79-0220 (31 August 1979), ADA077872

SOMERVILLE, P.N., BEAN, S.J., and FALLS, S. (Univ. of Central Florida, Orlando, FL)
Some Models for Visibility
AFGL-TR-79-0144 (30 June 1979), ADA075490

VALI, G., POLITOVICH, M.K., BAUMGARDNER, D.G., and COOPER, W.A. (Univ. of Wyoming, Laramie, WY)
Conduct of Cloud Spectra Measurements
AFGL-TR-79-0251 (12 October 1979), ADA081127

WASH, C.H., WHITTAKER, T.M., and JOHNSON, D.R. (Univ. of Wisconsin, Madison, WI)
Initial Studies in Objective Forecasting of Meso-scale Weather Using Interactive Computer System
AFGL-TR-79-0247 (15 June 1979), ADA077343

WASH, C.H., O'KEEFE, R., WHITTAKER, T.M., EDMAN, D.A., and JOHNSON, D.R. (Univ. of Wisconsin, Madison, WI)
Studies in Objective Forecasting of Mesoscale Weather Using Interactive Computer System, Report No. 2
AFGL-TR-80-0309 (15 June 1980), ADA091752

Readying Borehole Tiltmeter for Installation at Pinon Flat Crustal Observatory, near San Diego, CA.

VI TERRESTRIAL SCIENCES DIVISION

The Terrestrial Sciences Division performs research in seismology, geology, geodesy and gravity. This research supports the deployment and operation of strategic systems for delivery of Air Force weapons. To measure worldwide geophysical phenomena, the Division designs and produces instruments at varying scales and accuracy levels to meet specific needs. It conducts field work whenever and wherever necessary, collecting data with a variety of instrumented test beds designed to be operated on land, in the air, or in space. The Division also develops quantitative theoretical models of geophysical phenomena for comparison with observations.

During the reporting period, the Division investigated automated position and azimuth determination, lunar laser ranging, very long baseline interferometry, absolute gravimetry, satellite altimetry, and geopotential modeling. It also conducted research in crustal motion and the development of tiltmeter technology for Air Force geophysical applications, and determined detailed aspects of the motion environment of specific portions of the Western states of particular interest to the Air Force.

GEODESY AND GRAVITY

Geodesy is concerned with the size, shape and mass distribution of the earth, and its orientation in inertial space. Accurate geodetic information is necessary for the accurate determination of positions, distances and directions for launch sites,

tracking sensors and targets. The geodetic and gravimetric parameters for the earth and geodetic information for positioning not only form the structural framework for mapping, charting and navigational aids, but are also direct data inputs for missile inertial guidance systems. Current geodetic information is inadequate to meet the requirements of future USAF weapon systems.

The Division conducts continuing research and development programs in geometric geodesy and in physical geodesy (or gravity). These programs are directed toward improving the fundamental knowledge of the earth's size, shape, and gravity field and the techniques used for determining position, distance and direction on the earth's surface and in terrestrial and inertial three-dimensional coordinate systems.

In programs such as satellite altimetry, gravity gradiometry and very long baseline interferometry, AFGL participates and cooperates with the Defense Mapping Agency, the Army, the Navy, the National Aeronautics and Space Administration, the National Oceanic and Atmospheric Administration, the U.S. Geological Survey, other civilian agencies, and academic observatories. The Terrestrial Sciences Division also participates with the International Gravity Commission in the development of a worldwide gravity reference network. A worldwide system of earth-tide profiles is being established in cooperation with the International Center for Earth Tides, Brussels, Belgium.

Laser Ranging and Radio Interferometry: Earth-based laser ranging systems routinely make accurate measurements to the moon and high-altitude geodetic satellites, and radio interferometers routinely make accurate phase measurements of signals from quasars and navigation satellites. AFGL and its contractors analyze these measurements, significantly advancing geodesy and geodynamics.

AFGL has participated in the lunar laser-ranging program, along with NASA, since its inception. From 1970 to 1980 more than 3000 range measurements were made between the McDonald Observatory in Texas and four of the retroreflectors placed on the moon by Apollo and Soviet space missions. Scientists from AFGL and its contractors have analyzed these data, using the Planetary Ephemeris Program, a large computer program developed by the Massachusetts Institute of Technology under contract by AFGL and other DOD agencies. The data analyses have led to significant advances in the fields of geodesy, geophysics, celestial mechanics and fundamental physics. Most recently, research has concentrated on studying earth rotation and polar motion. Variations of latitude and UTO (Universal Time uncorrected for polar motion) have been determined from the McDonald Observatory lunar laser-ranging observations. The typical formal uncertainties are 0.006 arcsec (approximately 20 cm on the earth's surface) for the latitude variation and 0.5 msec (during which time the earth rotates approximately 20 cm at the latitude of the observatory) for UTO. When corrected for polar motion, the UTO values may be used to estimate changes in the length of the day. Changes in length-of-day values determined from lunar laser-ranging data have been compared to those inferred, using the principle of conservation of angular momentum, from determinations of the angular momentum of the global atmosphere computed from analyses of zonal winds. Both agree closely, in amplitude and phase, in identifying an oscillation in the length of the day of about 0.2 msec with a cycle approximately 50 days long.

Another technique being used for geodetic measurements is very long base line interferometry (VLBI). A plane wave front from a distant quasar source arrives at two radio observatories at different times depending on the direction of the source, the orientation of the earth, and the locations

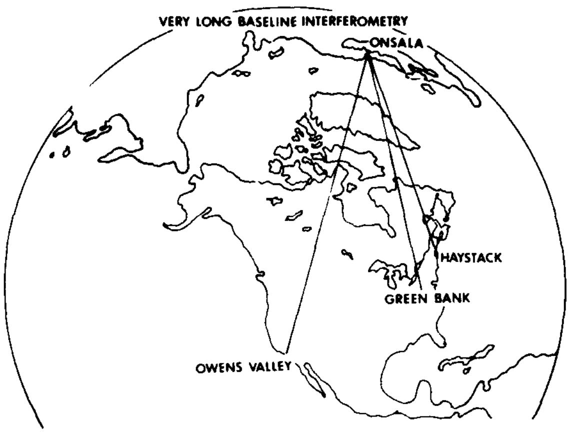

VLBI Becomes an Intercontinental Linear *Measuring Technique.*

of the observatories on the earth. VLBI is a technique for precisely determining the time difference by the cross correlation of the signals recorded at the two observatories. As the earth rotates, the time difference changes, and the VLBI data can be used to determine earth rotation and polar motion, source directions, and the relative positions of the observatories. AFGL sponsored the adaptation of the radio observatory at Onsala, Sweden, for VLBI applications and, subsequently, the data collection experiments and data analyses by MIT. At different dates, the orientation of the pole has been determined to better than 0.01 arcsec and UT1 (Universal Time corrected for polar motion) has been determined to better than 0.3 msec. As a by-product of this technique, the following distances between Onsala and U.S. radio observatories have been determined:

Haystack, Mass.
- Onsala 5,599,719,678 ± 34 mm

Green Bank, W. Va.
- Onsala 6,319,317,765 ± 37 mm

Owens Valley, Calif.
- Onsala 7,914,131,242 ± 40 mm

Radio interferometry for geodetic measurements can be performed using artificial satellites instead of quasars as radio sources. On December 17, 1980, portable miniature interferometric terminals for earth surveying (MITES) antennas were set atop three survey marks near the Haystack Observatory, Westford, Mass. These antennas yielded radio interferometric observations of the NAVSTAR/Global Positioning System satellites which were analyzed to determine the vector baselines between the survey marks. Observations were repeated 12 days later with different antennas on the marks. To determine each baseline on each day, all the observations from the entire time that five satellites were above 20° elevation angle (1.3 hours) were used. On each day, the triangle of separately estimated baselines closed within 1 cm in each vector component. For each baseline, the two determinations agreed within 1 cm. This is the first step in AFGL's program to develop inexpensive portable MITES systems for surveying over long or short baselines using NAVSTAR satellites as radio sources, but without having to know the NAVSTAR codes.

Automated Position Determination: Geodesy is concerned not only with positioning but also with the orientation of a site in inertial space. The conventional reference standards for inertial orientation are the stars, and the usual orientation angles are known as astronomic latitude, longitude and azimuth. Other inertial reference standards besides the stars exist (the lunar orbit and gyroscopes, for instance) but currently the stars are the best and most widely used inertial reference standards available to geodesists.

Studies have shown that the human being can be the largest error source in astronomic position determination. Therefore, all AFGL's position determining, transferring, and monitoring experiments deal with various phases of automating one or more of the components involved in this very specialized type of position determination.

The present research and development program in automated positioning deter-

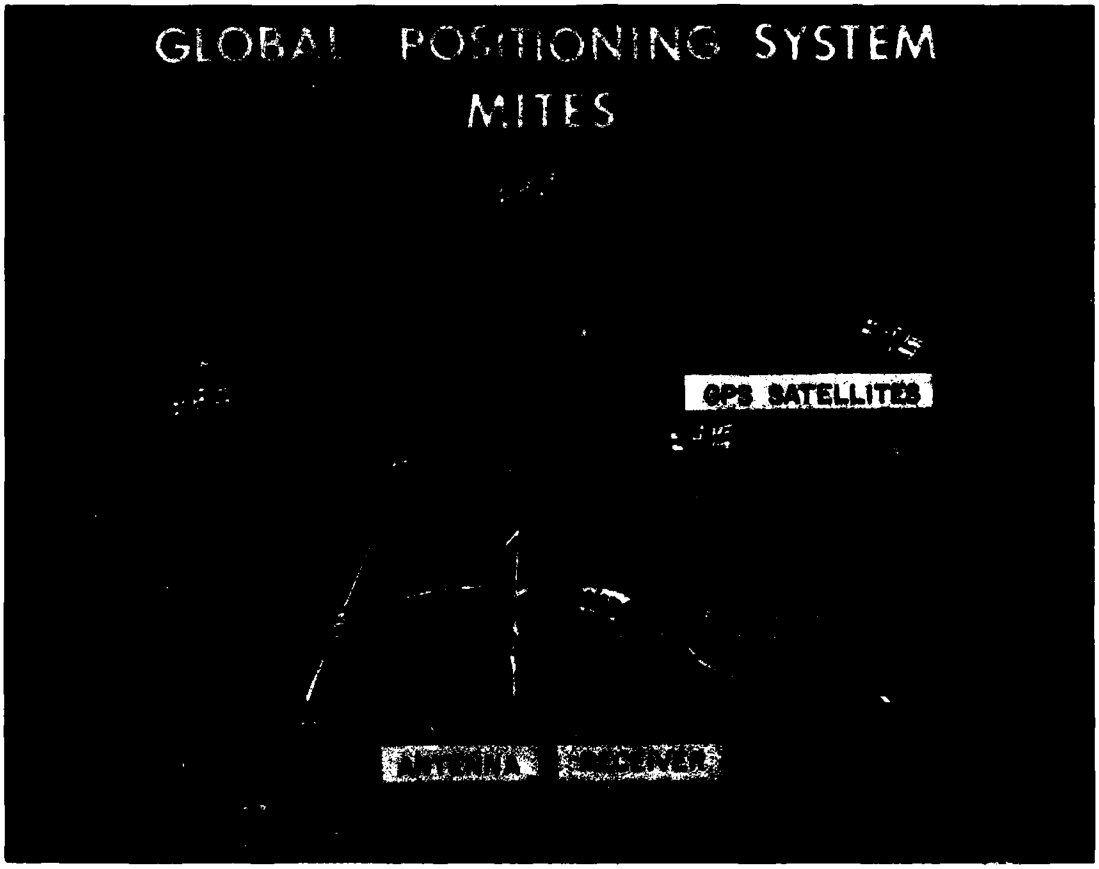

MITES System (Miniature Interferometric Terminals for Earth Surveying) for Precise Measurement of Geodetic Baselines.

mination encompasses four areas: (1) determination of azimuth or a reference direction that can serve as a precise azimuth reference; (2) transfer of azimuths and monitoring of azimuths to determine their stability; (3) automation of astronomic position determinations; and (4) experimentation in methods of measuring refraction at the point of observation.

To determine azimuth or a reference direction based on the precise location of the earth's rotational axis, AFGL sponsors contractor experiments to detect the earth's rotation. For example, a ring laser program will investigate the feasibility of developing a system capable of determining azimuth and latitude to sub-arcsecond precision. These programs are directed towards the development of gyroscopes that will be geodetically and geophysically significant instruments in finding the local direction of the earth's rotational axis. Given this axis, the precise value of astronomic latitude and azimuth can be determined.

AFGL and the National Geodetic Survey (National Oceanic and Atmospheric Administration) are cooperating to test a device that automatically transfers an azimuth reference. This experiment will produce a completely automated device for turning highly precise, repeatable azimuth reference angles. The device consists of a telescope mounted on a computer-controlled indexing table that has a silicon photo-diode linear sensor in the focal

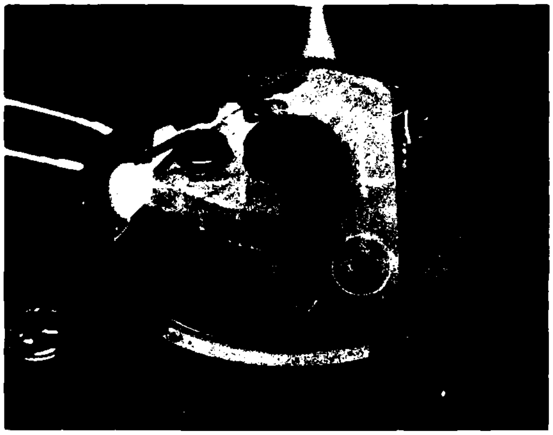

Ring Laser Gyroscope—Test of an Azimuth Determination Technique.

plane for use as a vernier aiming device. The indexing table automatically positions the telescope in azimuth by means of the computer controller that drives the indexing table in 1-degree increments and uses the movable linear photo-diode to position a target within one arc-second of the optical axis of the telescope. The instrument is leveled with an electronic capacitance level, eliminating the need for manual fine adjustments. After initial settings of the telescope on the azimuth reference marker, all horizontal movements are controlled and recorded with the computer controller. The azimuth transfer head has been completed and is now being tested at the National Geodetic Survey.

An AFGL azimuth monitoring experiment is designed to employ the differing characteristics of plane mirrors and prismatic reflectors for monitoring rotational and translational movements of an azimuth reference, or any other reference station whose positional stability must be closely monitored. The experiment uses a small helium-neon laser as its light source. The light is split and transmitted into two mirrors at the site to be monitored. One of these mirrors is a plane mirror, the other a retroreflecting prism. Each mirror is so aligned that it will return its image of the laser to a position monitor consisting of a silicon-diode junction barrier capable of monitoring the movement of the centroid of the return image in two axes. Rotational movements are discriminated from translational movements by comparing the images reflected from the plane mirror and the retroreflector. A constant record of the fluctuations of the position of the centroids of the two returning images is recorded on magnetic tape.

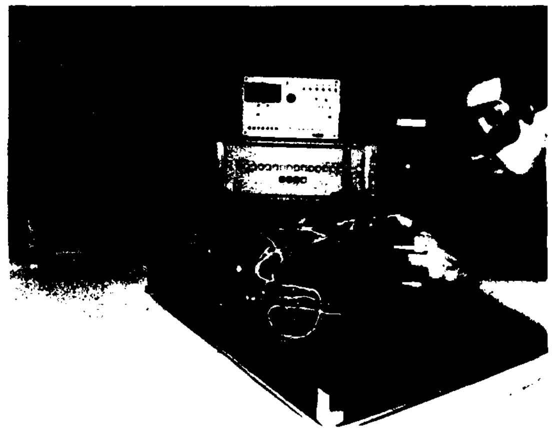

AFGL Azimuth Monitoring Experiment.

AFGL, the Defense Mapping Agency, and the University of Maryland are cooperating to develop a photosensor to replace the visual eyepiece on a T-4 geodetic theodolite. This photo-electric "camera" head automatically records the passage of a star across the field of view of a coded system of photosensors. Reduction of these observations with known time and instrument elevation and axis permits the development of astronomic positions. Making theodolite observations automatic can reduce the operational skill level required for the astro survey teams. Human effects on the instrument and "personal equation" effects can be reduced and the reproducibility of the measurement procedure can be improved. The immediate goal of tests now underway is to produce stellar observations with internal

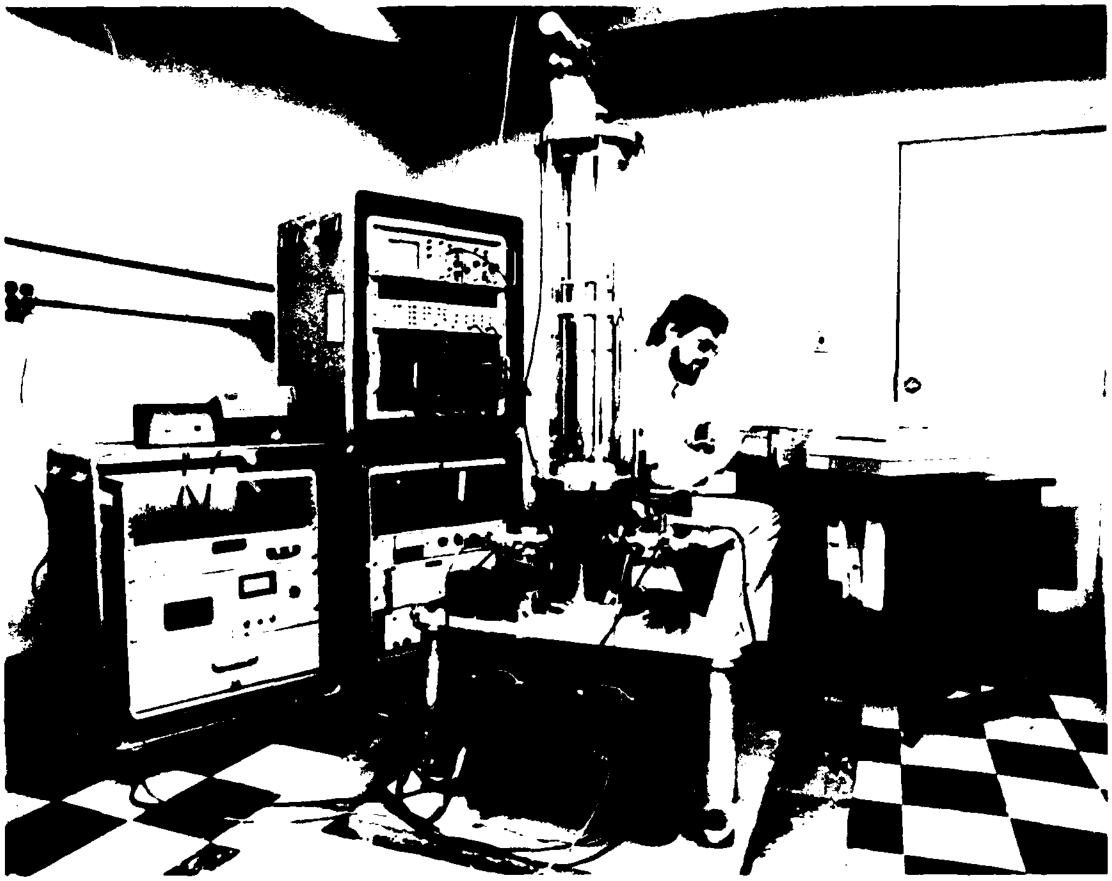

New Absolute Gravity Measuring System

consistencies equaling, or exceeding, visual observations.

AFGL also sponsors a University of Maryland program to develop a field device for real-time measurement of astronomic refraction. The two-color refractometer measures very precisely the differential refraction between the blue and red portions of the image of the star. The total refraction is calculated from the measured differential refraction. The next phase will consist of the development of a small scale instrument capable of being taken to geodetic survey sites where the two-color observations will be used to determine astronomic refraction at the point of survey.

Absolute Gravimetry: The Terrestrial Sciences Division's program in absolute gravity is divided into three main areas. First, it supports both research into measurement techniques by other organizations and comparisons of measurements with other absolute instruments. Second, the physics of measurement techniques is studied and new instruments are developed. Finally, the AFGL transportable system is used to measure gravity in the laboratory and at selected field sites.

The outside work supported by AFGL includes that of the Joint Institute for Laboratory Astrophysics in Boulder, Colorado. AFGL is supporting the development of a novel system for the isolation of a reference reflector in an absolute gravity

instrument that acts like an interferometer. This system, which uses electromechanical feedback to synthesize a very long period vertical mass-spring support, is being designed and built into a package that will be capable of directly supporting the reference reflector on a gravity instrument.

AFGL supported a six week visit by a team of Italian scientists who brought with them the transportable absolute gravity measurement system developed by the Istituto di Metrologia "G. Colonetti" of Turin, Italy, with the cooperation of the International Bureau of Weights and Measures. Gravity was measured at six sites: Hanscom AFB, Mass.; Denver, Colo.; Holloman AFB, N. Mex.; San Francisco, Calif.; Bismarck, N. Dak.; and Miami, Fla. The system had a mass of about 1500 kg when packaged for air transport. The work included a final remeasurement at Hanscom AFB. The uncertainty obtained was about one part in 10^8.

The AFGL instrumentation can quantitatively determine small effects on the measured acceleration of gravity. Effects caused by the gravity gradient and air resistance can be removed from the final value by using empirical determinations rather than theoretical corrections. Knowledge of the physics behind the measurement techniques will result in significant improvements in future instruments of this type.

AFGL is investigating new developments in electronics and other areas to solve some of the current problems with this kind of instrumentation. Several techniques for simplifying system operation are currently being employed at AFGL. The system is completely automated and data are analyzed and corrected for gravity tides in real time. Optical and mechanical alignments are simplified over previous systems, and self-checks on timing accuracy can be performed independently of a gravity measurement.

Measurements are currently being made with a system that incorporates the vacuum chamber from the first generation instrument and uses a control system and support base (with optics) built at AFGL. One reflector of a two-beam Michelson interferometer is dropped, and the distance traveled in known time intervals is determined by direct measurements of interference fringes.

The vacuum chamber allows a 60 cm free-fall path. A smaller vacuum pump is used than in the earlier system and the pump magnetic field is reduced considerably. An "old-fashioned," simple, free-fall technique is used. The system has a total mass of about 700 kg when packed for air transport in nine boxes that can be handled by one or two people.

The first field measurements were made in May 1978, approximately 6 months after the decision to convert the old vacuum chamber for use with the new system. At the time of that field trip, 150 time measurements were taken from 3 different positions in the free-fall path. This trip was very valuable in demonstrating the capabilities of the system, and in leading to an improved computational technique for data reduction.

In the new method, the time and distance data are fit with a least-squares technique to the formula for uniform acceleration. The following results are obtained from this least-squares fit: the acceleration of gravity, the initial velocity of the dropped reflector and the initial position of the dropped reflector, and a table of residuals for each drop. The residuals for each position in the path can be averaged and then plotted as a function of position. These residuals represent the deviation of the relative path difference between the reference reflector and the freely falling reflector from what it would be if the reference reflector were not accelerating at all, and the free-falling reflector were accelerating uniformly with the acceleration of gravity. The chamber was also placed on a separate vibration isola-

tion system to isolate it from the reference reflector and the rest of the optics.

The most recent value of gravity obtained at AFGL is: 980378.673 ± .007 milligal (one milligal = 10^{-3}cm/sec^2). This value is only 0.002 mgal different from the average of measurements obtained in 1968 and 1969 with the first generation AFCRL (Hammond-Faller) system. This demonstrates a remarkable stability in the value of gravity at the Haskell Observatory over a ten year period.

Satellite Altimetry: One of the major tasks of geodesy is the determination of the gravity field over the entire earth. Before the first satellites were launched, global representation of gravity was severely hampered by sparse or poorly distributed gravimetric measurements in the oceans. With the launching of the GEOS-3 satellite in 1976, and SEASAT in 1978, however, enormous improvements have been achieved in our knowledge of the ocean's gravity field. The radar altimeter readings from both satellites can be used to determine the shape of the ocean's surface with great accuracy, leading to important applications not only in geodesy, but also in geophysics and oceanography.

If the earth were all water, right to its center, mean sea level would be a simple spheroid that is closely approximated by an ellipsoid of revolution. However, the earth is largely solid and supports density variations in continental areas and under oceans. These density variations cause mean sea level to vary by scores of meters from an ideal or reference ellipsoid. The irregular, smooth surface, called the geoid, formed by the extension of mean sea level throughout the earth, is a fundamental reference surface in geodesy. Separations of the geoid above or below the reference are dependent on the variation of the earth's gravity field. This relationship has been a principal topic of investigation by geodesists, who have devised a means for determining the geoid separations from surface gravimetric measurements. Now, GEOS-3 and SEASAT satellite altimetry can also be used to derive geoid separations and, thus, the gravity field over the oceans with great accuracy.

The GEOS-3 and SEASAT radar altimeters are designed to measure the satellite's distance above sea level to a fraction of a meter. If the satellite's orbit can be independently established with 1 meter accuracy, the determination of the shape of the mean sea level is a straightforward procedure. However, standard global tracking nets cannot achieve 1 meter orbital accuracies, so that high precision requires denser nets or other advanced schemes.

At AFGL, the approach to satellite altimetry has been to assume that ground tracking is only good enough to achieve orbital accuracies of about 20 meters. If we knew the position and velocity of the satellite at any epoch and integrated the satellite motion over a short arc (less than one quarter of a revolution), we could recover the position of the satellite to within about 1 meter over the entire arc. Although the position and velocity of the satellite on the short arc are not known with adequate precision, we can refine our knowledge of these quantities by comparing altitudes from a number of independent, interlocking short arcs and improve our ability to determine the short arcs. Where two short arcs cross, the difference in measured altitudes to sea level is the vertical distance between the two arcs. The vertical interorbit ties provide a rather tight interlocking net of arcs, particularly in the important vertical direction. Subtracting the altimeter measurements from this net gives, finally, the shape of the ocean surface. To appreciate the magnitude of this computational task, one must remember that many thousands of GEOS-3 and SEASAT tracks are available, containing more than one million altimetric values.

Initial AFGL efforts to exploit GEOS-3 data produced the computer program "Short Arc Reduction of Radar Altimetry"

(SARRA). Because of the large number of measurements available, the North Atlantic and Indian Oceans received particular attention. With only a portion of the available data (416 tracks) used, the SARRA reduction showed that geoid heights could be determined from the altimeter data to an accuracy near the meter level. A final version of this program was delivered to the Defense Mapping Agency Aerospace Center for application in operational problems.

Further research led to the development of SAGG (Satellite Altimetry and Ground Gravity), which utilizes altimetry augmented by surface gravity measurements and leads to a more accurate global solution, especially over land areas where altimetry cannot be used.

The most recent research at AFGL has led to a further refinement in SAGG, the point-mass technique. Insertion of point masses in areas where detailed gravimetry or altimetry already exists can add fine detail to a geopotential model based on spherical harmonic coefficients. As a result, the short-wavelength variations in the geoid can be closely examined in a limited area without distorting the long wavelength features. Although comparable results might be attained by utilizing only harmonic coefficients, the point-mass approach offers a considerable advantage in economy and flexibility, an important consideration when large amounts of data must be processed.

A new satellite, SEASAT-1, with an improved altimeter accurate to 10 cm, was launched in 1978. SEASAT-1 permits extension of the altimetry measurements to 72 degrees north and south latitudes, denser global measurements, and increased accuracy. Although a power failure caused SEASAT-1 to cease transmitting after several months of operation, one global data set has been acquired.

Altimeter Data Reductions: The data in the spherical-harmonic global adjustment performed at AFGL consist of representative altimeter observations on essentially all the recorded SEASAT passes. The orbits have been divided into 9,645 short arcs used in the global adjustment. The input values of the state vector parameters at each mid-arc epoch have been supplied by the Naval Surface Weapons Center precise ephemeris. The standard deviations of these parameters in position

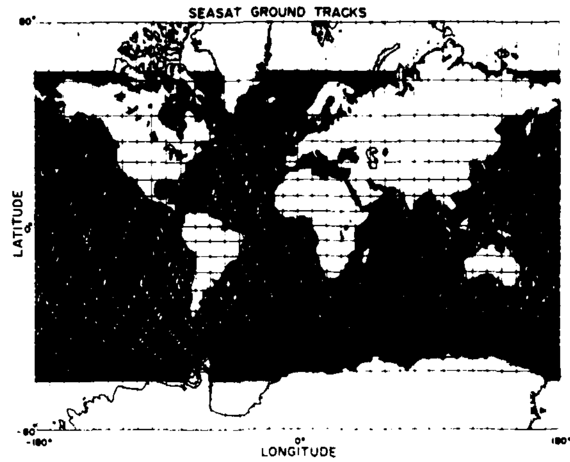

Ground Tracks of SEASAT Orbits.

(along-track, cross-track, radial) and in velocity (along-track, cross-track, radial) are 3.4 meters, 2.5 meters, 1.6 meters, 0.032 m/sec, 0.050 m/sec, 0.068 m/sec, respectively. The (weighted) state vector parameters for all arcs, together with a set of spherical harmonic potential coefficients, have been subjected to a simultaneous least-squares adjustment. A total of 582,400 SEASAT altimeter observations have been used in this process.

The (weighted) terrestrial parameters in this adjustment consist of the (14,14) subset of Goddard Earth Model GEM 10. This model contains gravity information together with a wealth of satellite information. Since the altimeter data are not included in GEM 10 the AFGL spherical harmonic adjustment obtains an improved geopotential model of degree and

order (14,14) through the combination of SEASAT altimeter data with the satellite and surface gravity data of GEM 10.

Present levels of observational accuracy make satellite altimetry much more sensitive to the shape of the earth than gravimetry; a 1 meter rms geoid height over an area of 1 square degree tells much more about the shape of the earth than the same square with a 3 mgal rms gravity anomaly. Because this relative information content applies to the description of the earth's gravity field as well, satellite altimetry has made significant contributions to gravity mapping.

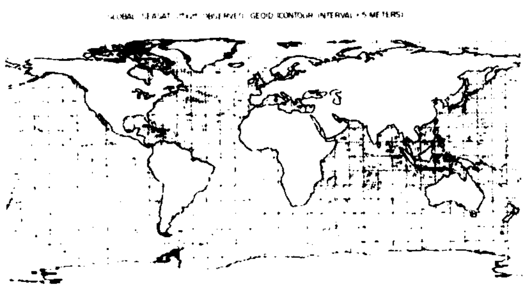

Global SEASAT 2° × 2° Observed Geoid (Contour Interval is 5 meters).

Geophysical Analysis of Short-Arc Altimetry Residuals: The AFGL short-arc technique produces an accurate model of the very long wavelength part of the geoid; i.e., wavelengths greater than a few thousand kilometers. Geoidal features at these wavelengths are primarily attributable to density variations at deep levels in the earth's crust or in the upper mantle. The short-arc adjustment, essentially a least-squares process, segregates all the short wavelength detail into the solution residuals. Thus the residuals contain geoid signals from such sources as the upper crust and sea-bottom topography, as well as sea-surface effects including waves, currents and tides. These signals are contaminated to some degree in SEASAT data by system noise.

The short wavelength residuals may be used, therefore, to study important geophysical problems, for example, the mechanism of sea-floor spreading, crustal subduction at trenches, and global tides. At AFGL, these residuals are being correlated with ocean-bottom topographic features, particularly sea mounts, conical volcanic mountains of various heights and diameters (less than 100 km) distributed widely over the ocean basins. Their sizes and positions must be known accurately for submarine navigation. Altimetric residuals are largely accounted for by variations in sea bottom topography. Major geologic features of the ocean: trenches, rises, mid-ocean ridges, shelves and fracture zones are resolved with remarkable fidelity. In fact, under favorable circumstances topographic features as small as 50 km may be detected.

Advanced Adjustment Techniques for Gravity Field Modeling: Geopotential models of regional and of global extent have been developed. The simplest approach is the standard linear least-squares method, which solves for an arbitrarily chosen set of parameters from a collection of measurements whose relative weights are assigned (for example, the coefficients of a truncated spherical harmonic expansion). Linear least-squares methods involving classical integral formulas are applicable when homogeneous, regularly distributed, and dense data coverage are available.

With the advent of modern techniques for gravity measurements—satellite orbital analyses, satellite altimetry, satellite-to-satellite tracking, and eventually, gravity gradiometry—an immense amount of information regarding the earth's gravity field at different levels is provided. These data are generally heterogeneous and irregularly distributed. Although the conventional least-squares collocation adjustment is a convenient

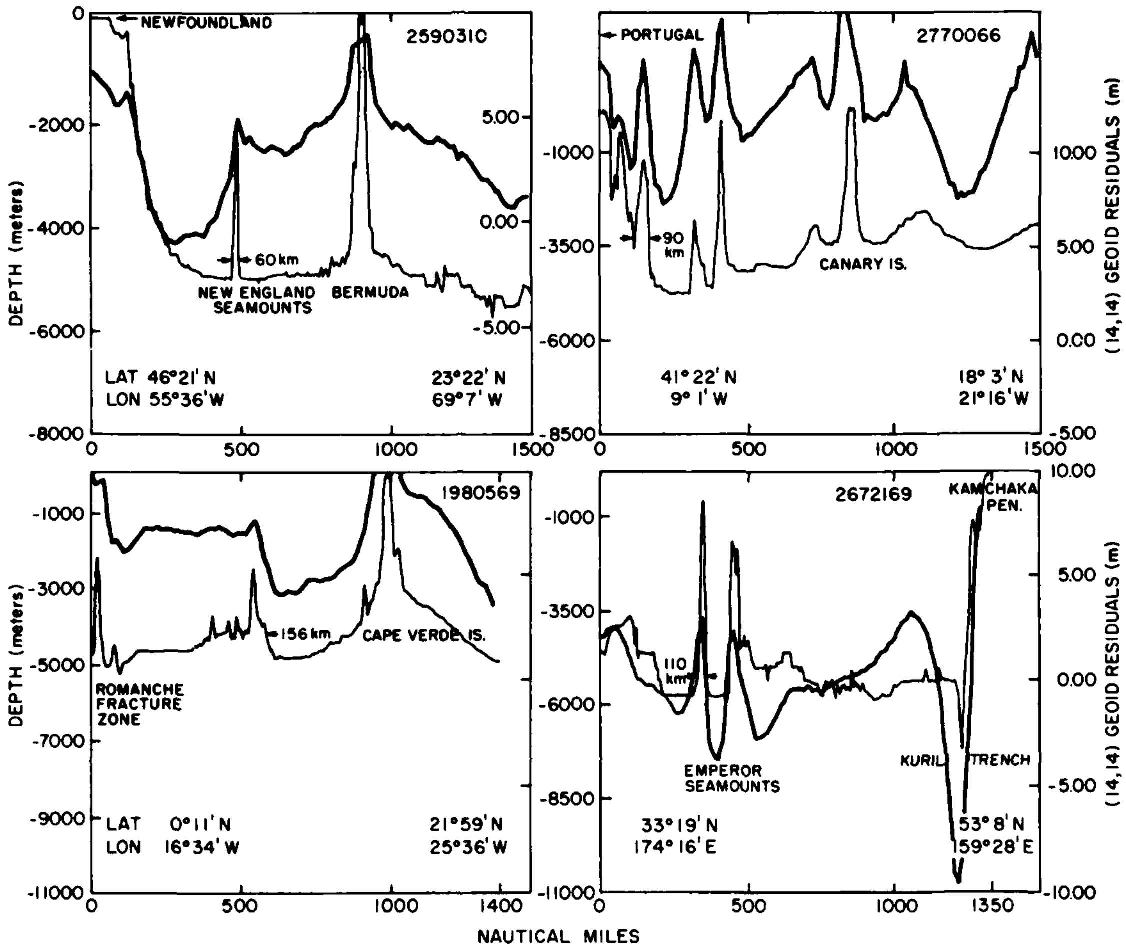

Along-Track Geoid Profiles from Satellite Altimeter and Coincident Bathymetry.

technique for the combination and/or processing of such data, it requires the inversion of a matrix of an order equal to the number of observations. Theoretically, all available data should be used to achieve results with the minimum variance; practically, this is neither possible nor is it necessary. Example: the predicted value of gravity at a point P depends primarily on the data in the neighborhood of P. Therefore, we take only a relatively small number of data for a single prediction into account. Other data which exceed a certain distance from the prediction point are not considered. Most cases, however, are much more complicated. For the determination of the gravity field of the earth, many types of data are used, all of them bearing information about the gravity field, all of them noisy. The problem is to optimally combine these data in such a way that the resulting gravity field deviates from the true one as little as possible.

Global models in use today were derived mainly from analyses of satellite orbits using tracking data, terrestrial data in the form of 5 × 5 degree mean anomalies, and satellite altimeter data.

Tests were conducted to gauge the effect of aliasing on the determination of potential coefficients from 5 × 5 degree mean

anomaly data. Results showed the effect to be significant, leading to the conclusion that, for highest accuracy, geodetic models to degree 36 should be determined from 1 × 1 degree mean anomaly data. However, because of the large amount of 1 × 1 degree data, a rigorous adjustment by least-squares or collocation techniques to solve for the potential coefficients is not feasible, as both computer time and storage requirements would be prohibitive.

The quality of results in the collocation adjustment depends on the covariance function introduced. This function is derived from a model covariance function that incorporates the general features of the gravity field. However, to minimize computation time, the covariance function must be approximated. In the network principle, exact covariances are calculated for the fixed points of a network, and the covariance function in a certain range is calculated by interpolation of finite elements, for example, using the bicubic spline function. Implementation of this procedure requires that the maximum range of covariances be known and prior storage of the network of covariances on a file.

Some numerical methods have been derived which efficiently use global data sets to estimate spherical harmonic coefficients. These methods exploit the relationship between spherical harmonic series and Fourier series coupled to the symmetries of spherical grids. The data may be either area means or point values and they may be free of errors or affected by measurement "noise." The summation of 90,000 terms of the harmonic series complete through degree 300 on a full 1 × 1 degree equal angular grid can be done in about 1 minute with a modern digital computer. Similar exploitation of specially gridded data leads to a tremendous increase in efficiency for the least-squares collocation technique by allowing the utilization of powerful matrix inversion algorithms.

GEOKINETICS

Improved technology in the design and construction of new Air Force systems has increased concern about the effects of earth motions (geokinetics) on system components. Inertial guidance instrumentation is a typical example. Each generation of gyros or accelerometers developed for use in guidance systems exceeds the sensitivity of the previous generation by an order of magnitude or more. Unfortunately, this enhancement in performance increases the sensitivity of such systems to geokinetic effects and increases the potential for errors caused by the motion environment in which the instrument must operate.

In other instances, the structural response of a facility to motion inputs may be the principal concern. If the facility must provide a relatively stable motion environment for the instrumentation or operational system housed in it, then the natural vibration frequencies of the structure must be well known outside the bandwidth of significant input motions to prevent amplification of those motions.

The apparent solution to problems caused by earth-motion effects is to develop more effective isolation or compensation techniques. However, complete knowledge of the characteristics of the motion environment and the manner in which this environment interacts with system or facility performance is needed to do this. The objective of the geokinetic research and exploratory development conducted by the Terrestrial Sciences Division is to develop this knowledge and provide it to system designers and engineers.

Missile Geophysics: In 1979 the Division conducted a follow-up vibro-acoustic study for the Space Division at Vandenberg AFB. This special study predicted expected vibro-acoustic levels for a Space Transportation System launch based on scaled measurements of a Titan III-D launch. The results are currently used to

update engineering models of vibration effects on new and existing facilities that will experience extreme acoustic and ground vibration levels during the initial Space Transportation System launch at Satellite Launch Complex 6, Vandenberg. Surface pressures, developed during the Titan III-D launch sequence, were characterized as functions of time, azimuth, and source distance; surface pressure-wave attributes were determined, including ground-coupling effects. Future follow-on studies will focus on source verification studies based on actual Space Transportation System launch data. The Division currently provides consultation services to the Space Division.

Support of the Ballistic Missile Office MX objectives continued in 1979. A program characterizing the ground motion attributes of alluvial basins in the American Southwest started with studies at the Nevada Test Site. This work complements the Division's Technological Base research, which studies and characterizes ambient ground-motion parameters and rheological properties of basin alluvial areas. Ground motion studies were also completed utilizing data collected in Steptoe Valley, Nevada, in 1980, which complements the work performed at the Nevada Test Site. The AFGL-developed Geokinetic Data Acquisition Stand-alone System was deployed for the first time in the field for these two efforts. This system is a portable, 16 channel digital system used for recording, displaying and processing geophysical field data. The system accepts data from a seismometer, a tiltmeter, and a pressure sensor, processes it, and stores it in a digital form. Alluvial basin studies in the American Southwest with the Geokinetic Data Acquisition Stand-alone System are continuing in Railroad Valley, Nevada. Additional valleys will be studied in FY82 and '83.

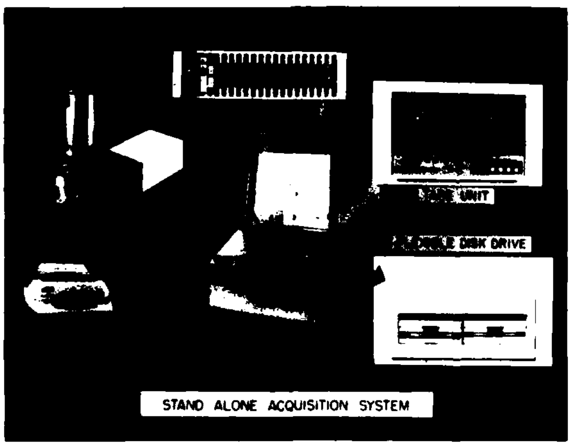

Stand Alone Acquisition System. An automated geokinetic data acquisition system utilizes three different sensors (pressure, tiltmeter and seismometer) to measure and evaluate horizontal and vertical earth motions.

A seismic hazard program was initiated in 1979. Three areas of special interest were studied. First, a theoretical method was developed for estimating strong ground-acceleration attenuation functions. This method is based on epicentral intensity and radius of the felt area as functions of earthquake magnitude. It is used in regions such as the central and eastern United States, where empirical data are insufficient to develop unique areal attenuation functions. Resulting equations can then be used empirically for a seismic risk analysis within subject regions. Next a study was undertaken to estimate the seismic hazard for the Space Transportation System Satellite Launch Complex 6 facility at Vandenberg AFB. Peak ground-motion curves covering the range of annual risks from 1.0 to 0.001 were estimated based on the seismic characteristics of a region within 500 km of Pt. Arguello on Vandenberg AFB. Contour maps of maximum credible ground motion in the vicinity of the base were generated as a function of location, faulting and estimated maximum credible earthquakes for neighboring faults. Resultant findings were presented in the form of horizontal

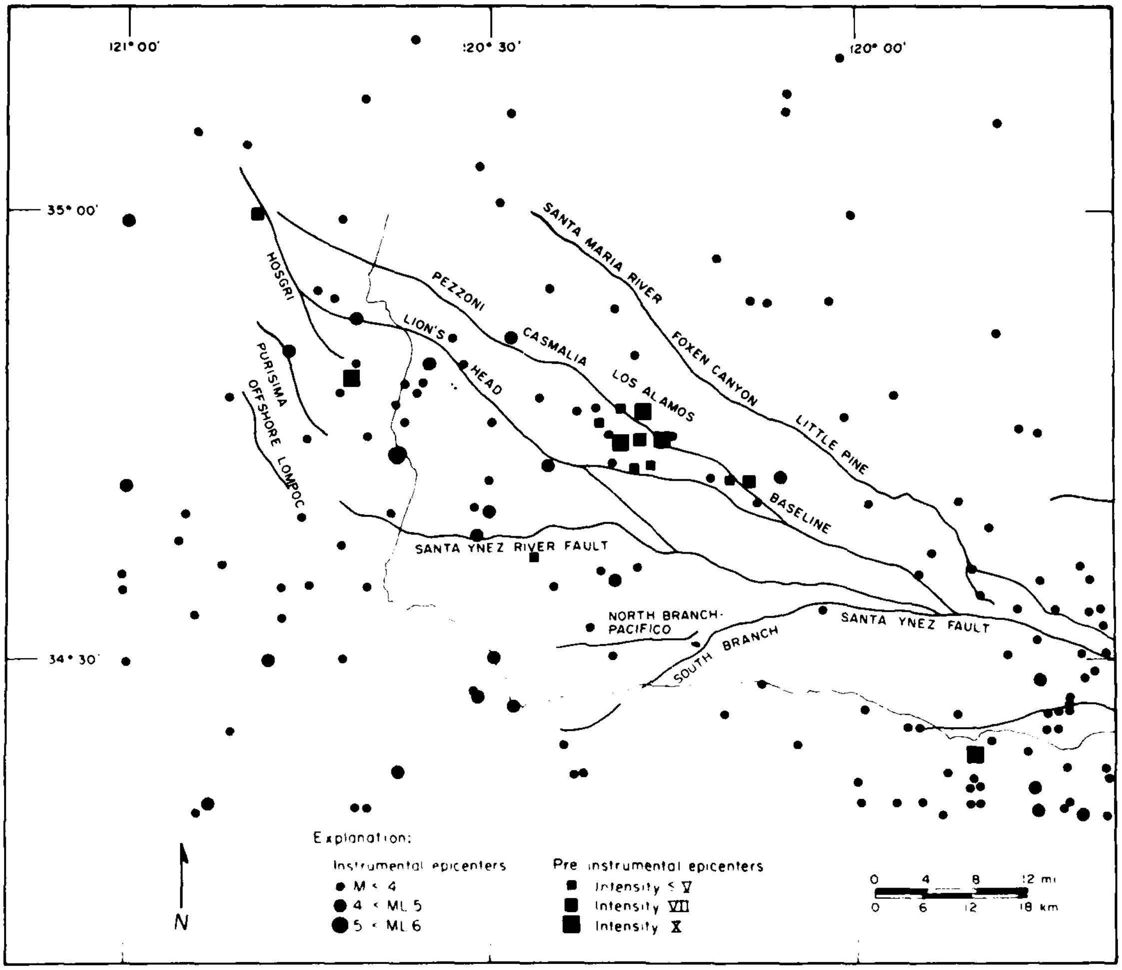

Example of Seismic Hazards Which Could Realistically Affect STS Launch Operation Planned for Vandenberg AFB, CA.

response spectra. The maximum credible ground motions estimated for the Pt. Arguello area are: peak acceleration, 700 cm/sec^2; velocity, 100 cm/sec; and displacement, 65 cm. Finally, recent strong motion events have shown that the influence of distant earthquake activity on Minuteman operations is more adverse than originally anticipated. Consequently, studies were begun to estimate ground motion for affected sites and to evaluate the seismic hazard for the six Minuteman Wings located within the continental United States. Modal determinations of expected dominant motions at siloed missile facilities were made with theoretical considerations. These determinations were supported by teleseismic observations of causal events. Annual risk curves for intensity and peak acceleration, velocity and displacement were generated for each Minuteman Wing, forecasting the recurrence expectation for like events.

Crustal Motion Research: Seismology, geology and geotectonics are studied to predict the spatial and temporal properties of motions of the earth's crust over a wide range of frequencies. Specific efforts include the measurement and interpretation of long-period deformations and the

realistic modeling of seismic motions of Air Force systems and structures.

The Applied Crustal Physics Branch continued the operation and evaluation of four groups of borehole tiltmeters: three

Borehole Tiltmeter Deployment Areas. Tiltmeters were deployed in different environmental and geological settings to determine effects on instrument measurement and repeatability capability. Distinct effects were identified, which were attributed to temperature, moisture, deployment depths, and other source factors.

instruments at a depth of 120 meters in bedrock at a site in Maynard, Mass., three at 3 meters in soil at Maynard, three at 20 meters in bedrock at Bedford, Mass., and two at 3 meters in bedrock at Bedford. Different installation techniques and meteorological effects were assessed in a study designed to determine the most effective method of measuring long-period earth motion over a large period range. In general, the greater the depth, the better the performance at all frequencies, and results from instruments in soils were much worse than those in bedrock.

Various types of tilt sensors are being tested for their response to static and slowly moving surface loads. The apparent elastic modulus for these two cases is considerably different and depends upon soil type. A new type of tilt sensor is being developed for near-surface installation to evaluate these and other phenomena. This long-base (5 meter) tiltmeter senses tilt through the change in height of two reservoirs partially filled with liquid and connected by a half-filled tube. Laser interferometers measure height changes. The long base should average out the short wavelength noise that plagues short-base

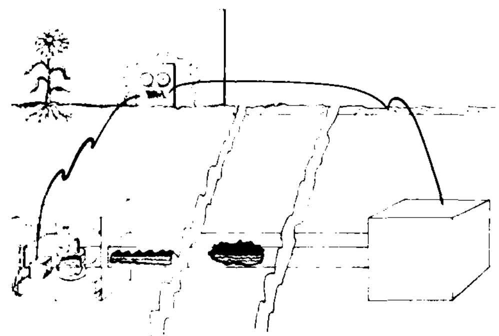

AFGL Long Baseline Tiltmeter. A laser-operated system which interferometrically determines relative fluid level differences between the two laser sources. The system is under development and will be compared with other instruments in a common deployment area.

instruments, particularly those emplaced in soils.

Several clusters of borehole tiltmeters have been deployed at sites in Colorado to assess instrumental performance and installation methods. The instruments will soon be moved to sites in Wyoming and Utah in a program to detect deep crustal anomalies and possible precursors to earthquakes for the area near Hill AFB. Another pair of tiltmeters has been emplaced in boreholes 50 meters deep in the Malbaie seismic region near Charlevoix, Quebec, to detect theoretically predicted changes in the local response to earth tides as rocks are stressed toward their fracture strength.

In a cooperative program with the U.S. Geological Survey, NASA, and a number of universities, AFGL recently installed a

biaxial tiltmeter at the University of California's Pinon Flat Geophysical Observatory in the San Andreas fault zone northeast of San Diego. The responses of a number of different types of strain-, tilt-, and stress-meters to a large tectonic signal, which should be present in this earthquake zone, will be compared.

The Applied Crustal Physics Branch is also supporting feasibility studies of the use of the Navstar Global Positioning System (GPS) in the measurement of earth strain. Correlation of the radio signals with Very Long Baseline Interferometry (VLBI) techniques yields baseline lengths with accuracies of about one centimeter over distances of hundreds of kilometers. Strain can be inferred from the apparent displacements from repeated measurements. Work is currently concentrated on receiver technology and water vapor corrections.

A program has been initiated to develop computer simulation models for seismic wave propagation through three-dimensional, inhomogeneous geologic media. The goal of this program is technology development to accurately predict explosion- and earthquake-induced ground motions in the alluvial basins of Nevada and Utah, designated deployment sites for the MX missile system. Previous work has shown that the complex geology of the region affects seismic wave propagation and surficial ground motions. These effects can not be adequately represented using simple assumptions such as plane layering, since the effects include such complications as focusing of seismic waves and resonant responses. Two contract research efforts have been started to develop the required computer codes. Three-dimensional finite-element methods will be used to study the long-period motions while dynamic ray-tracing techniques will be used for short-period propagation analysis. The geologic structure of the MX deployment region is also being investigated and will provide structural models for the initial computer simulation studies.

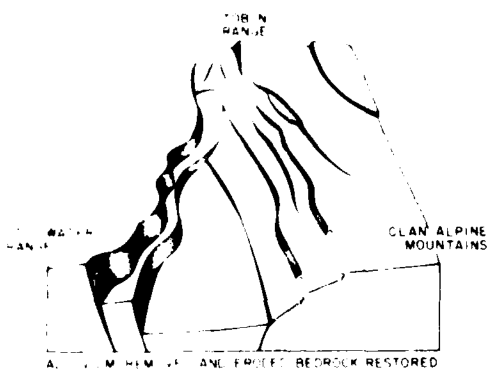

Complex Geology of MX Deployment Areas Which Influenced Seismic Modeling.

Accurate models of explosive and earthquake sources are required for inputs to these computer simulation codes. The induced ground motions from a near-surface nuclear explosion are complex because of the extreme temperatures and stresses resulting from the explosion. Cratering, material vaporization, and tensile crack formation result in non-linear ground deformation near the source. To simplify the modeling of nuclear explosions, a contractual work effort has been conducted to develop a linear equivalent to the nuclear surface burst. This work includes detailed calculations of the non-linear ground deformations with the effects propagated away from the source until simple elastic behavior is achieved. The linear elastic ground motions can then be related back to the source location to produce a linear source equivalent which represents the near-surface nuclear explosion.

Azimuth Studies: The determination of precise time-dependent azimuths is an important requirement for evaluation and maintenance of inertial navigation instrumentation. To accurately and continuously determine azimuthal motions, AFGL developed an Automated Azimuth Measuring System (AAMS) and has used it to measure the azimuthal motion environment at missile test silos (presented in the

Automated Azimuth Measuring System. A stand-alone automated azimuth measuring system capable of long-term continuous data acquisition. The system will be used to measure and model rotational earth motions.

Report on Research for the period July 1976-December 1978, p. 166).

In September 1979, the AAMS was used by AFGL at the Advanced Inertial Test Laboratory, Holloman AFB, N. Mex., to characterize the motions of several azimuth references. A Porro prism, an optical cube in the main gyro test table, and an astronomic azimuth transfer cube were continously monitored for several days.

Astronomic azimuths were also observed at the same time and after the AAMS measurements in the Advanced Inertial Test Laboratory through a newly constructed window that permitted direct observation of Polaris from within the building. These observations were directly transferred to the gyro test-table cube and the reference cube from the observation station. The accuracy of the AAMS and astronomic measurements was about 2 arc seconds and the closure of the quadrilateral formed by the test station and reference cubes and the AAMS and astronomic stations was 1.9 arc seconds, using mean values for the latter two stations.

An AFGL contractor has recently completed an error analysis with a projected accuracy evaluation of the AAMS. Performance and reliability assessments of the AAMS were first made using theoretical analyses and then estimated using data from various laboratory tests. Inver-

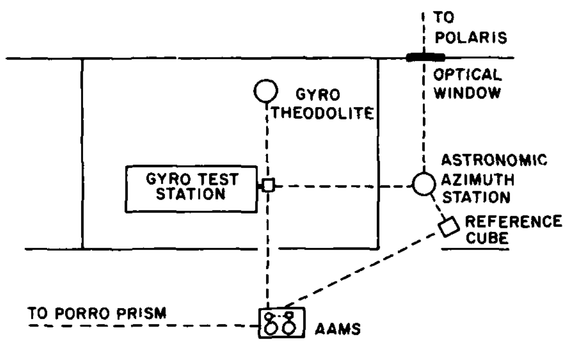

Azimuth Measurement Scheme, Advanced Inertial Test Laboratory.

sion-axis servo uncertainty, float-motion induced errors, and other significant error sources were found that could cause measurement errors of greater than 2 arc seconds. Work will begin next year on redesigning and reworking several AAMS components to correct this problem.

Currently the AAMS is controlled by a dedicated microprocessor which interfaces with each major component. The major components (Azimuth Laying System units, autocollimator, tiltmeters) are con-

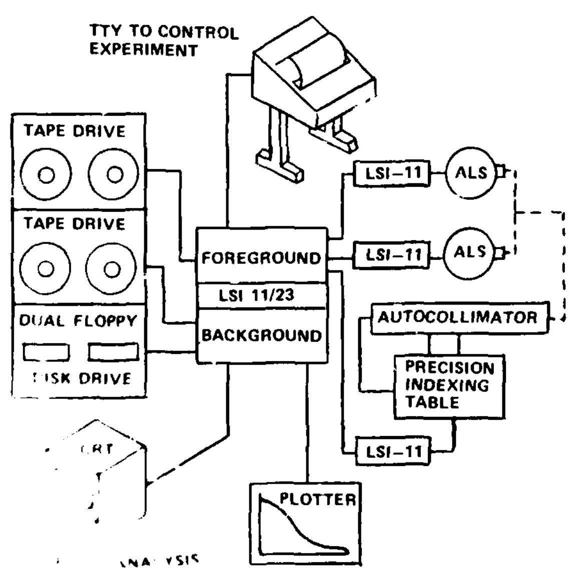

...d Data Processing System for ... Azimuth Measuring System.

trolled by their own unique discrete logic. In addition to controlling the experiment, this hardware acquires all experimental data, digitally filters analog data, and records all data on magnetic tape. The system is designed to be self-contained and to run unattended.

A second microprocessor is used to provide a quick field analysis of the experimental data. This microprocessor can provide real time multi-channel data plots and regression analyses of short data segments and other analyses at the discretion of the operator. Complete data reduction and analyses are done through post-processing on AFGL's general purpose computer.

However, the present AAMS is limited by the extensive amount of discrete logic and minimal field-data processing capability. To relieve these problems, a new distributed data processing system is now being developed. It consists of four microprocessors, three LSI-11s and one LSI-11/23, configured in a hierarchical network.

In this new configuration, each ALS and its associated sensors will be controlled by a dedicated microprocessor. A third microprocessor will be used to control the precision indexing table, autocollimator, and the remaining system sensors. These three microprocessors will transmit their pre-processed data to an LSI-11/23, which will record the data on tape. The LSI-11/23 uses a foreground/background operating system. While the data acquisition and recording program is running in the foreground, one of several data processing programs could also run in the background to analyze and plot experimental data. These data could be processed in real-time as they are recorded, or after data acquisition through the use of a second tape drive.

This new distributed configuration provides several advantages. Discrete logic will be replaced by software; local data-processing capability will be enhanced; and self-control will be incorporated through built-in data checks.

The replacement of discrete logic with software will greatly improve experimental flexibility. Data sample rates, filtering schemes, and timing and control functions can be quickly changed through a remote keyboard rather than by hardwiring at the test site.

The addition of a background data-processing capability will increase processing capacity and allow field processing before experiment teardown. This capability provides confirmation of data integrity before the system is disassembled for transport.

Finally, the system will monitor its own status and periodically print values for variable parameters. This will provide greater security against failure and ensure data integrity.

Traditionally, optical references have been used as azimuth holding devices, with an implied assumption that only long-term azimuth variations with periods of days or longer are significant. However, as accuracy demands increase, higher frequency, low-amplitude motions of these references become significant. The AAMS, which uses the technique of gyrocompassing to minimize systemic errors, is presently considered to be the most accurate means of tracking the azimuthal motions of these references. However, the accuracy needed for some Air Force systems has surpassed the capability of the AAMS.

To achieve these higher accuracies needed now, and to meet future requirements, AFGL has awarded two contracts. Under one, a contractor is studying the use of wheel speed modulation to eliminate the need for continuous multi-position gyrocompassing. Wheel-speed modulation is achieved by varying the wheel excitation frequency to vary wheel angular momentum. The resulting stable and repeatable wheel power and the reduced sensitivity of power to excitation frequency make wheel-speed modulation a more rapid and accurate approach to measuring azimuth.

Under the second contract, the feasibility of a latitude and azimuth determining system is being investigated to establish continuous north azimuth and astronomic latitude to sub-arc-second precision. Current design analysis and tradeoff studies will determine the feasibility of using an existing Laser Gyro Inertial Measuring Unit as a basic component of a latitude and azimuth determining system. Required modifications for the existing Inertial Measuring Unit hardware and software are now being defined.

JOURNAL ARTICLES JANUARY 1979 - DECEMBER 1980

CABANISS, G.H.
The Measurement of Long Period and Secular Deformation with Deep Borehole Tiltmeters
Proc. 9th GEOP Conf. (April 1979)

ECKHARDT, D.H.
Geodetic Theory
Rev. of Geophys. and Space Phys. 17, No.6 (September 1979)

PAPERS PRESENTED AT MEETINGS JANUARY 1979 - DECEMBER 1980

BATTIS, J.C.
Regional Modifications of Ground Motion Attenuation Functions
Am. Geophys. Un. Mtg. Fall, San Francisco, CA (3-7 December 1979)

CABANISS, G.H., and LEWKOWICZ, J.F.
(Space Data Analysis Lab., Boston College, MA)
A Reassessment of Meteorological Effects on Tiltmeters Emplaced in Soil
Am. Geophys. Un. Mtg., Fall, San Francisco, CA (3-7 December 1979)

ECKHARDT, D.H.
Correlations Between Global Features of Terrestrial Harmonic Fields
Int. Un. Geodesy and Geophys. 17th General Assbly., Canberra, Australia (2-15 December 1979)
The Global Positioning System - Current and Future Applications
The Hydrographic Soc., Symp. on Positioning Fixing at Sea, Southampton, England (April 1980)
Libration of the Moon, and Analytic Libration Theory and Its Comparison with Numerical Libration Theory
Analytic Methods and Ephemerides, Theory and Observations of the Moon and Planets, Namur, Belgium (July 1980)

HADGIGEORGE, G., and BLAHA, G. (Nova Univ. Ocean Sciences Ctr., Dania, FL)
Local Geoid and Gravity Anomaly Prediction Using Point Masses
Am. Geophys. Un. Mtg., Fall, San Francisco, CA (3-7 December 1979)

HADGIGEORGE, G., BLAHA, G., and ROONEY, T.P.
SEASAT Altimeter Reductions for Detailed Determinations of the Oceanic Geoid
The Space Geodesy and Its Applications Int. Symp., Cannes, France (18-21 November 1980); Am. Geophys. Un. Mtg., Fall, San Francisco, CA (8-12 December 1980)

HAMMOND, J.A.
Gravity Standards for Inertial Component Testing
AIAA Guidance and Control Symp., Boulder, CO (6-7 August 1979)

HERRING, T.A. (Mass. Inst. Tech., Cambridge, MA), et al.
Intercontinental Distance Measurement with Subdecimeter Precision Using Radio Interferometry
Int. Un. Geodesy and Geophys. 17th Gen. Assbly., Canberra, Australia (2-15 December 1979)

ROONEY, T.P., HADGIGEORGE, G., and BLAHA, G.
Analysis of Residuals from Short-Arc Adjustment of SEASAT Altimetry
Am. Geophys. Un. Mtg., Fall, San Francisco, CA (8-12 December 1980)

SHEARER, J.A., MIOLA, J.A., MUSAFF, H., ANTHONY, D., GAUTHIER, R.J., CAPT., and NOVAK, J.M.
Error Analysis and Performance Data from an Automated Azimuth Measuring System
AIAA Guidance and Control Conf., Danvers, MA (11-13 August 1980)

WIRTANEN, T.E., and MERTZ, B.M., CAPT.
Design of a Unique Azimuth Monitoring Device
AIAA Guidance and Control Conf., Danvers, MA (11-13 August 1980)

TECHNICAL REPORTS JANUARY 1979 - DECEMBER 1980

BATTIS, J.C.
Seismic Hazards Studies for Minuteman Missile Wings
AFGL-TR-80-0293 (9 September 1980), ADA096720
Seismic Hazards Estimation Study for Vandenberg AFB
AFGL-TR-79-0277 (14 November 1979), ADA082458

BLAHA, G., and HADGIGEORGE, G.
Local Geoid and Gravity Anomaly Predictions Using Point Masses
AFGL-TR-79-0124 (22 May 1979), ADA074524

CROWLEY, F.A., HARTNETT, E.B., and OSSING, H.A.
The Seismo-Acoustic Disturbance Produced by a Titan III-D with Application to the Space Transportation System Launch Environment at Vandenberg AFB
AFGL-TR-80-0358 (17 November 1980), ADA100209

LEWKOWICZ, J.F., and CABANISS, G.H.
Near Field Static Tilt from Surface Loads
AFGL-TR-80-0221 (8 July 1980), ADA094123

VON GLAHN, P.G., CAPT.
The Air Force Geophysics Laboratory Standalone Data Acquisition System: A Functional Description
AFGL-TR-80-0317 (9 October 1980), ADA100253

CONTRACTOR JOURNAL ARTICLES JANUARY 1979 - DECEMBER 1980

BACHE, T.C., LAMBERT, D.G., and BARKER, T.G. (Systems, Science and Software, La Jolla, CA)
A Source Model for the March 28, 1975 Pocatello Valley Earthquake from Time-Domain Modeling of Teleseismic P Waves
Bull. Seismological Soc. Am. 70, No.2 (April 1980)

SETTLE, M., and HEAD, J.W.
The Role of Rim Slumping in the Modification of Lunar Impact Craters
J. Geophys. Res. 84, No.B6 (June 1979)

CONTRACTOR TECHNICAL REPORTS JANUARY 1979 - DECEMBER 1980

BARKER, T.G. (Systems, Science and Software, La Jolla, CA)
Regional Ground Motions from a One Megaton Surface Burst
AFGL-TR-80-0377 (September 1980), ADA104189

BLAHA, G. (Nova Univ. Ocean Sciences Ctr., Dania, FL)
Extended Applicability of the Spherical-Harmonic and Point-Mass Modeling of the Gravity Field
AFGL-TR-80-0180 (February 1980), ADA089072
Improved Determinations of the Earth's Gravity Field
AFGL-TR-79-0058 (31 January 1979), ADA070186

COLOMBO, O.L. (Ohio St. Univ., Columbus, OH)
A World Vertical Network
AFGL-TR-80-0077 (February 1980), ADA086011
Optimal Estimation from Data Regularly Sampled on a Sphere with Applications in Geodesy
AFGL-TR-79-0227 (September 1979), ADA083034

DEBRA, D.B. (Stanford Univ., Stanford, CA)
Study to Develop Gradiometer Techniques
AFGL-TR-79-0063 (January 1979), ADA072821

HARRISON, J.C., and LEVINE, J. (Univ. of Colorado, Boulder, CO)
A Measurement of Long-Term Tilt in Colorado and Wyoming
AFGL-TR-80-0202 (1 June 1980), ADA091720

HARTNETT, E.B., and CARLEEN, E. (Boston Coll., Chestnut Hill, MA)
Characterization of Titan III-D Acoustic Pressure Spectra by Least Squares Fit to Theoretical Model
AFGL-TR-80-0004 (January 1980), ADA083021

HERBST, K.
Interpretation of Tilt Measurements in the Period Range Above That of the Tides
AFGL-TR-79-0093 (25 April 1979), ADA074525

MORITZ, H. (Ohio St. Univ., Columbus, OH)
Theories of Nutation and Polar Motion I
AFGL-TR-80-0363 (December 1980), ADA099015
Concepts in Geodetic Reference Frames
AFGL-TR-80-0052 (October 1979), ADA084099

RAPP, R.H. (Ohio St. Univ., Columbus, OH)
Potential Coefficient and Anomaly Degree Variance Modelling Revisited
AFGL-TR-79-0245 (September 1979), ADA082322
Comparison of Potential Coefficient Determinations with 5° and 1° Anomalies
AFGL-TR-80-0160 (April 1980), ADA089046

RAPP, R.H., and HEJELA, D.P. (Ohio St. Univ.)
Accuracy Estimates of 1° × 1° Mean Anomaly Determinations from a High-Low SST Mission
AFGL-TR-79-0269 (September 1979), ADA083035

REGAN, R.D. (Phoenix Corp., McLean, VA)
An Overview of Geomagnetic Field Models
AFGL-TR-80-0243 (15 August 1980), ADA102946

RIMER, N., HALDA, E., and CHERRY, T. (Systems, Science and Software, Los Angeles, CA)
Nonlinear Ground Motion from a Megaton Near Surface Nuclear Explosion
AFGL-TR-80-0167 (March 1980), ADA090019

RODI, W.L., BACHE, T.C., SWANGER, H.J., BARKER, T.G., and CHERRY, J.T. (Systems, Science and Software, La Jolla, CA)
Synthesis of Regional Ground Motion from Western U.S. Earthquakes
AFGL-TR-79-0080 (29 March 1979), ADA069727

ROUFOSSE, M.C. (Smithsonian Inst. Astrophys. Obs., Cambridge, MA)
Study of Oceanic Lithosphere Using GEOS-3 Radar Altimeter Data
AFGL-TR-79-0181 (July 1979), ADA077344
Perform a Gravity Correlation Study
AFGL-TR-80-0268 (August 1980), ADA097719

RUMMEL, R. (Ohio St. Univ., Columbus, OH)
Geoid Heights, Geoid Height Differences, and Mean Gravity Anomalies from "Low-Low" Satellite-to-Satellite Tracking — An Error Analysis
AFGL-TR-80-0294 (June 1980), ADA092707

SHAPIRO, I.I., COUNSELMAN, C.C., and HERRING, T.A. (MIT, Cambridge, MA)
Analysis of Laser Ranging and VLBI Observations for Geodetic Purposes
AFGL-TR-79-0196 (10 August 1979), ADA077294

SOLOMON, S.C. (MIT, Cambridge, MA)
The Relationship Between Marine Gravity and Bathymetry
AFGL-TR-80-0266 (2 September 1980), ADA092706

STEVENS, J.L., and BACHE, T.C. (Systems, Science and Software, La Jolla, CA)
Estimates of Ground Motion at Minuteman Missile Sites from Two Large 1979 Earthquakes
AFGL-TR-80-0327 (September 1980), ADA095365

SUNKEL, H. (Ohio St. Univ., Columbus, OH)
A Covariance Approximation Procedure
AFGL-TR-79-0075 (March 1979), ADA072853
A General Surface Representation Module Designed for Geodesy
AFGL-TR-80-0204 (June 1980), ADA092918

TAIT, K.S. (Analytic Sciences Corp., Reading, MA)
A Fast Estimation Algorithm for Two-Dimensional Gravity Data (GEOFAST)
AFGL-TR-80-0016 (15 November 1979), ADA086835

WEAVER, L.D. (Univ. of Utah, Salt Lake City, UT)
Geophysical Fiber Interferometer Gyroscope
AFGL-TR-79-0286 (November 1979), ADA092913

WHITE, J.V. (Analytic Sciences Corp., Reading, MA)
Error Models for Gravity Gradiometers in Airborne Surveys
AFGL-TR-80-0220 (January 1980), ADA097745

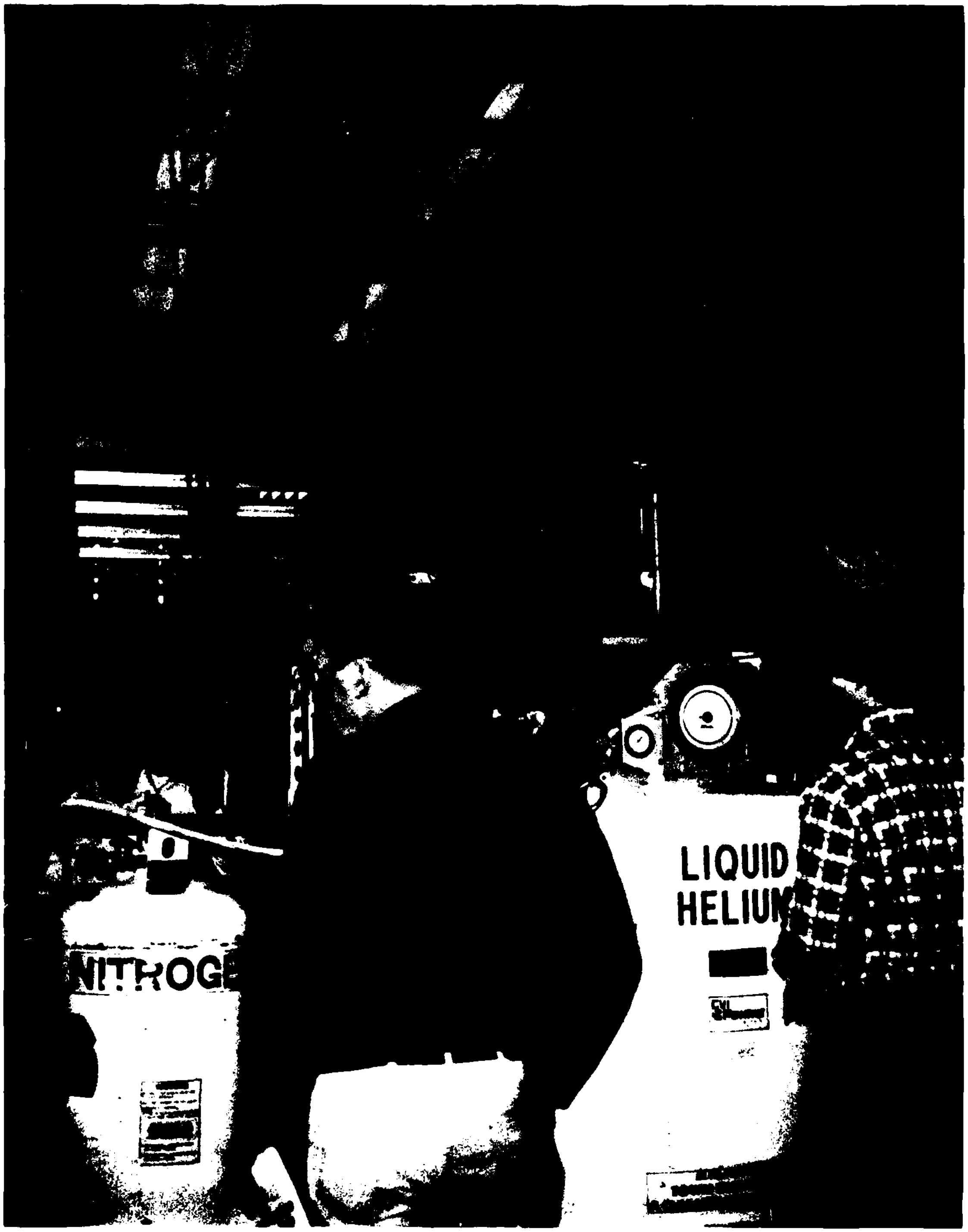

Preparing Cryogenic Sensor for Launch at White Sands Missile Range.

VII OPTICAL PHYSICS DIVISION

The Optical Physics Division conducts research on the optical and infrared properties of the natural and man-made environment and radiation sources. This includes atmospheric transmission, infrared backgrounds, target signatures, and the development of new optical and spectroscopic techniques. Infrared backgrounds comprise the earth, atmosphere, aurora, airglow, horizon or earthlimb, celestial sky, zodiacal emission, and such man-made backgrounds as nuclear weapon detonations. The research encompasses field measurements using aircraft, balloons, rockets, and satellites; laboratory studies on molecular spectroscopy and interactions, electron excitation, and high velocity collision phenomena; and theoretical studies and analyses.

The goal of the research program is to develop "tools" that can be used directly in the design and operation of Air Force and DOD systems. These tools include various data bases, models and computer codes such as the LOWTRAN atmospheric transmission and HITRAN laser transmission computer codes, the AFGL IR Star Atlas, and the LWIR Earth Limb Model.

The portion of the electromagnetic spectrum studied extends from 2,000 Å in the ultraviolet to 1 cm where the far infrared blends into the microwave radio spectrum.

The research in the Division is divided into studies of: the visible and near visible properties of the atmosphere, where aerosol and molecular scattering is the predominant mechanism of attenuation; the infrared properties of the lower atmos-

phere, where thermal equilibrium usually prevails; the optical and infrared properties of the upper atmosphere (including auroras and airglow), where individual molecular interactions must be considered; the infrared properties of exoatmospheric sources — stars, nebulae, zodiacal dust; measurements of the radiation from man-made sources such as missile or aircraft plumes; and development of improved techniques for spectroscopic measurements.

A major area of investigation by the Division concerns atmospheric attenuation or transmission of radiation by the atmosphere, including laser beams. Atmospheric molecules absorb optical and infrared radiation selectively at discrete wavelengths. Extensive computer programs have been developed which make use of the vast collection of spectroscopic data for molecules (AFCRL *Atmospheric Absorption Line Parameters Compilation*) and which permit the calculation of this transmission, both for laser beams and the emission and transmission of radiation from hot gases and plumes. Detailed atmospheric absorption curves and tables for high resolution and laser transmission are available. The well-known LOWTRAN atmospheric transmission computer code is used for determining the low-resolution (approximately 20 wavenumbers) transmission of the atmosphere for any path through the atmosphere for a wide range of tactical weapon delivery problems under various meteorological conditions. The codes have been designated as the standard atmospheric codes for the Department of Defense as part of the DOD transmission program and for the international research community as part of the Technical Coordination Program and the International Radiation Commission.

The measurement and use of atmospheric transmission and emission also provide a method for remotely sensing atmospheric composition and meteorological conditions such as temperature, humidity, and ozone content. The transmission codes have been extensively applied to the design and improvement of remote atmospheric sensing instrumentation on the Air Force meteorological satellites.

Scattering by aerosols and molecules in the atmosphere also contributes both to attenuation and to reduction in the contrast of a target seen through the atmosphere. A three-year program of surface and airborne measurements of the optical and infrared properties of the atmosphere in the Central European environment has been completed. A mobile facility to obtain aerosol and transmission data for the lower atmosphere at various locations especially under adverse weather conditions is being developed. The results of these measurements are applied to target acquisition and detection problems.

Similarly, infrared backgrounds against which a target must be located are a major concern of the Division efforts. Such emissions from the atmosphere or celestial sky represent interfering background noise superimposed on the optical/IR target signatures that a surveillance system may be trying to detect. The emission of the lower atmosphere can be calculated from computer programs similar to those discussed previously. However, the emission from the upper atmosphere (above about 70 km) requires a much more detailed knowledge of the interactions and collisions among the individual molecules, many of which will be in excited states with excess energy. The amount and wavelength of the radiation resulting from this non-equilibrium chemistry, and the effects of disturbances by protons and electrons during an aurora or a nuclear burst are also being studied. Therefore, a sizable laboratory and theoretical research program is conducted to study the physics and chemistry of the atmosphere, particularly those molecular interactions which lead to infrared emission, as well as an extensive measurements program. This has included both the use of the Divi-

sion's NKC-135 optical/infrared flying laboratory, and rockets, particularly in Alaska, where the infrared emission of the aurora is studied. Computer programs have been developed to predict and compute the IR emission of the earth limb and upper atmosphere, both for natural and disturbed conditions. Such background emission, particularly during disturbed conditions, such as auroras, could seriously impair the operation of surveillance, detection, tracking, or terminal guidance systems.

A satellite or rocket-borne infrared system looking away from the atmosphere will still see the celestial sky as a background. Consequently, the Division is carrying out a rocket program to map the celestial sky as well as zodiacal emission in the infrared. The first of two rocket flights to determine this zodiacal background has been successfully flown. Also, measurements of missile and aircraft plumes are being obtained from rockets and aircraft.

An inseparable part of these measurements and studies is the development and use of very sensitive advanced cryogenically cooled infrared sensors and spectrometers by the Division. Built and tested in the laboratory in this time period have been a cold telescope with an advanced off-axis, folded, doubly reimaging optical system for rocketborne infrared zodiacal emission measurements and several Michelson interferometers with automatic alignment features for use in the AFGL NKC-135 Flying Infrared Laboratory. In addition, novel optical techniques are being explored to discriminate targets from these backgrounds.

ATMOSPHERIC TRANSMISSION

The atmospheric transmission of electromagnetic radiation in the ultraviolet, visible, infrared and even in the millimeter wave region is affected by molecular absorption and scattering and by extinction from particulates (dust, haze, fog, rain) in the atmosphere. The relative importance of these different attenuation processes depends on the wavelength of the radiation and on the atmospheric conditions.

In general, molecular absorption dominates the infrared to millimeter region of the spectrum, whereas aerosol extinction dominates the visible part of the spectrum. This domination is not complete, however, and a full understanding of atmospheric propagation requires that we deal with the appropriate molecular and aerosol effects at all wavelengths. Molecular absorption is highly wavelength-dependent, whereas aerosol extinction varies much more slowly with wavelength. In the infrared, this rapid wavelength dependence tends to determine the "windows" within which atmospheric propagation is possible, whereas the transparency within these windows tends to be determined by more slowly varying molecular "continuum" and aerosol effects. As a result, aerosol and cloud attentuation can be the critical factor not only for visible wavelengths, but also for infrared radiation in the window regions.

Aerosol and cloud drop attenuation can affect radiation propagation in several ways. Particulate scattering and absorption along with molecular attenuation reduces the intensity of a beam of radiation as it travels along an atmospheric path and thereby becomes a factor in determining beam transmittance (e.g., in laser beam propagation). For many applications one is not only concerned with the extinction loss in a beam of radiation, but also with the intensity and angular distribution of the radiation scattered out of the direction of propagation of the direct (incident) beam. One of the most important effects of this scattered radiation is the reduction of contrast in imaging systems at visual and near IR wavelengths. The scattered light from the sun forms the background sky radiance against which

objects may have to be viewed and detected.

With some exceptions, which are discussed below, the attenuation processes by atmospheric molecules are sufficiently well understood to make accurate predictions of the attenuation effects when the basic atmospheric properties such as molecular concentrations, air temperature, and pressure are known.

It is much more difficult to predict accurately the optical properties of particulate matter in the atmosphere, especially those of haze and dust particles. Their optical effect is not only a function of particle concentration, but also of particle size, shape, chemical composition and physical structure. All these properties are highly variable with weather conditions and location and they are very difficult to measure. Because of the extreme variability of these properties, it is also very difficult to develop models for the optical/IR properties of aerosol particles or droplet clouds.

The final goal of this research in the Optical Physics Division has been the development of computer codes which allow an efficient and accurate calculation of these various atmospheric propagation properties.

Atmospheric Transmission Models: The atmospheric transmission modeling program includes the effects of extinction by both molecular and particulate (aerosol) constituents of the atmosphere. Two basically different models for predicting the transmission, thermal emission, and scattered radiative properties of the atmosphere have been developed for both high and moderate spectral resolution applications: LOWTRAN (Low Transmission) and FASCODE (Fast Atmospheric Signature Code). They use different transmission calculations to achieve high or low spectral resolution as required for application to specific atmospheric measurements.

The moderate resolution model, LOWTRAN 5 (AFGL-TR-80-0067), differs from previous LOWTRAN models in its inclusion of new altitude-dependent and relative-humidity-dependent aerosol models, as well as a complete restructuring of the computer code into subroutines. It maintains all the capabilities included in previous LOWTRAN models: contributions by molecular absorption using an empirical band model (20 cm^{-1} resolution), continuum absorption by water vapor and nitrogen, absorption and scattering by atmospheric aerosols, and the option of calculating background radiance as well as transmittance.

Measurements and theoretical studies have shown that the aerosol size distribution and refractive index both change significantly at high relative humidities. These humidity-dependent changes and resulting optical properties were incorporated into the optical/infrared aerosol models and into the LOWTRAN 5 code. At relative humidities above approximately 70 percent, and especially above 90 percent, aerosol particles begin to absorb water molecules and grow. The rate of growth is not the same for all particles. In general, the larger the particles and the more water they absorb, the faster the rate of growth. Consequently, the optical properties of aerosols change and the wavelength dependence of the extinction coefficient decreases.

Using data from the Optical Atmospheric Quantities in Europe (OPAQUE) program and other experimental data (AFGL-TR-80-0177) from various researchers, we are verifying the new aerosol models which have been developed and their optical and infrared extinction and scattering properties.

Work is continuing on laboratory measurements of the water vapor continuum absorption. A revised continuum model is planned for a forthcoming LOWTRAN model. Current LOWTRAN modeling efforts are centered on the development of a solar/lunar scattering model and

also a cirrus cloud transmittance model.

A second atmospheric transmission model, FASCODE (Fast Atmospheric Signature Code, AFGL-TR-78-0081), has been developed for the line-by-line calculation of radiance and transmittance with particular applicability to the earth's atmosphere. An algorithm for the accelerated convolution of line shape functions (Lorentz, Voigt and Doppler) with spectral line data is used. The contribution from continuum absorption is included in the model.

The present model and code, FASCOD1B, with its associated programs, comprises a computational package for the accelerated line-by-line calculation of spectral transmittance and radiance for atmospheric problems. The program is applicable to spectral regions from the microwave to the visible. A layered atmosphere is used, with each layer taken to be in local thermodynamic equilibrium (LTE). The spectral lines are optimally sampled at each layer. The Voigt line shape is utilized for all layers. The source of the spectral line information may be the *AFCRL Atmospheric Absorption Line Parameters Compilation* (AFCRL-73-0096), or equivalent data.

In conjunction with a program for modeling the atmosphere, FASCOD1B is applicable to atmospheric geometries including symmetrical and asymmetrical tangent paths. Spherical refractive geometry is utilized together with stored-model atmospheres or a user-defined atmosphere. The atmosphere is layered optimally to minimize computation for a desired precision for the radiance/transmittance calculations.

FASCOD1B calculations are performed starting at the lower altitudes and progressing to higher altitudes to reduce computation. A program called AERSOL (AFGL-TR-79-0253) is also included which characterizes the extinction due to clouds and rain in the 0-50 cm^{-1} spectral region. The effects of continuum absorption are treated for nitrogen, for self- and foreign-broadened water vapor, and carbon dioxide. Additional features include an option enabling execution of the program in the 0-50 cm^{-1} region without an external line file and a laser option for computation of radiance/transmittance for a specified monochromatic frequency.

The compilation of atmospheric absorption lines used as a basis for much of our work is described in the *AFCRL Atmospheric Absorption Line Parameters Compilation*. Since the publication of this report in early 1973, we have made five revisions to this compilation, which are available on magnetic tape. Articles have been published in *Applied Optics* to inform the scientific community of the modifications and additions to the data base. Detailed information on 160,000 spectral lines in the spectral region from 0.68 μm to the millimeter wave region are contained on this tape. Atmospheric species included in the compilation are H_2O, CO_2, O_3, N_2O, CO, CH_4 and O_2.

We are now improving the high resolution data base, both by correcting existing data and adding new material, such as weak absorption features of the major atmospheric absorbing gases. Absorption parameters for trace atmospheric and pollutant gases comprise a separate tape, which is also available to the scientific community. The gases included on this trace-gas tape are NO, SO_2, NO_2, NH_3, HNO_3, OH, HF, HCl, HBr, HI, ClO, OCS, and H_2CO. Work is underway to include other infrared active species which affect atmospheric tape problems. The AFGL Trace Gas Compilation tape now comprises some 37,000 transitions from 1 μm to the millimeter region.

Molecular Spectroscopy: Research in molecular spectroscopy seeks the capability of calculating parameters including transition frequencies, intensities, line widths, line shapes, and radiative lifetimes. Molecular constants are determined from available spectroscopic data

and used to predict spectral information at desired conditions of temperature, pressure, and abundance. Computer codes have been developed to calculate molecular constants that are difficult to measure, including those for high vibrational states populated at high temperatures and for isotopic species that are significant in weak absorption regions of the atmospheric spectrum.

To extend the available spectroscopic data, high-resolution measurements on CH_4, H_2O and CO_2 were made using an interferometer-spectrometer with a 2-meter path difference. A high-temperature cell was fabricated and coupled to the high-resolution interferometer. Data on CO_2 and H_2O at a resolution of approximately 0.006 wavenumber have been obtained at 600°K and 800°K and improved molecular parameters have been calculated. A cryogenic interferometer was flown for atmospheric emission measurements. The interferometer was cooled to 77°K and achieved a resolution of 0.1 wavenumber. The interferometer performed well throughout the flight. However, electronic or laser failure prevented obtaining data above 20,000 ft.

The Optical Physics Division also supported work to develop theoretical models and computer codes to calculate the effects of atmospheric turbulence on the propagation of light beams. This turbulence causes scintillation in light beams and is responsible for the blur in images. This effect not only occurs in visible light but also in infrared radiation. The theoretical model calculations show that significant short-time variations in infrared signal intensity around a mean value can occur, depending on atmospheric conditions, path length, and optical systems characteristics.

Applications: During the past several years, a great deal of the modeling effort has responded to specific application requirements. The development of the LOWTRAN code was spurred by such requirements. Both FASCODE and LOWTRAN have been applied to a wide variety of high resolution and broadband tactical system design and application problems.

Another application of transmittance modeling is the remote sensing of meteorological variables by satellites. *The Line Parameters Compilation* has been used as a data base for calculations to determine the spectral channels most suitable for use in remote sensing from satellites. In addition, transmittance calculations performed with these models are being used to develop software packages for determining the three-dimensional structure of temperature and moisture from satellite-measured radiances.

Tactical Decision Aid: A program was started to help the users of infrared sensors predict under which environmental conditions their sensors would discriminate targets. Early tests revealed situations where assumed hot targets were actually cold when compared to their backgrounds. The program is an effort of three Air Force laboratories. A target/background model from the Armament Test Laboratory combined with the LOWTRAN atmospheric transmission model from the Geophysics Laboratory is incorporated into a sensor performance model at the Avionics Laboratory. This performance model when combined with weather forecasting will become a generic infrared tactical decision aid.

Instrumentation Development: Detailed knowledge of the spectral characteristics of background radiation and of atmospheric emission and absorption is required to design high-sensitivity sensors for optimum performance. Concurrently, research on techniques to enhance the sensitivity of sensors is being performed. Multiplex high-throughput techniques can yield the required detailed spectral information and, at the same time, can be used to develop more sensitive sensors.

New techniques, such as the Spectrome-

ter Interferometer with Selective Modulation, are being studied. This technique obtains the spectrum directly without Fourier transformation, while still using a scanning interferometer of high throughput. The instrument was used to make OH measurements from the night sky for temperature determinations.

A background optical suppression scheme, conceived at AFGL, is being pursued for use in various applications. It has the potential of allowing the detection and spectral signature measurements of faint targets immersed in interfering background radiation. Laboratory and field data have been obtained which demonstrate a background suppression improvement of about two orders of magnitude.

Measurements: The Optical Physics Division completed a three-year program of surface and airborne measurements of optical and infrared properties of the atmosphere in the Central European environment. One objective of this program was to study the relationships between the optical infrared properties and the meteorological parameters. One very important atmospheric property for optical transmission effects is atmospheric humidity, or water vapor content. The effects of molecular water-vapor absorption on infrared radiation transmission have been long known and are predictable. However, there is also a correlation between visible-light transmission and humidity, which is most pronounced with relative humidity, i.e., percentage of water vapor saturation, rather than absolute water vapor content in grams per cubic meter. This effect is due to the growth of aerosol particles in an environment of high relative humidity, say above 90 percent. The relative humidity has a diurnal cycle which is more pronounced as the daily temperature cycle becomes stronger. Superimposed on this humidity effect are the changes in aerosol distribution and

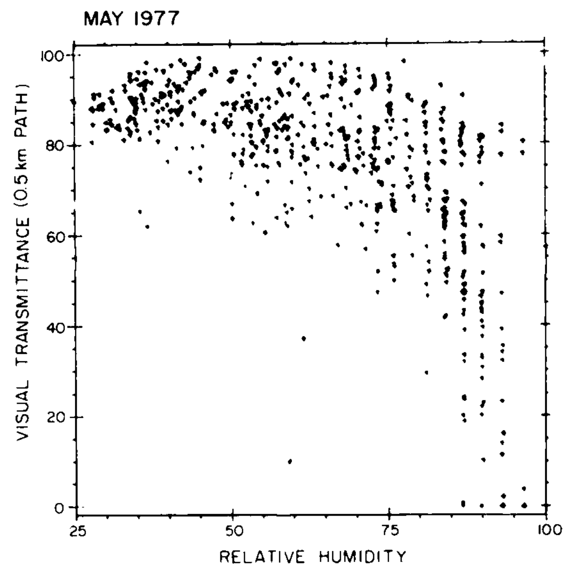

Relationship between Visual Transmittance and Relative Humidity for the Same Data Set as the Preceding Figure.

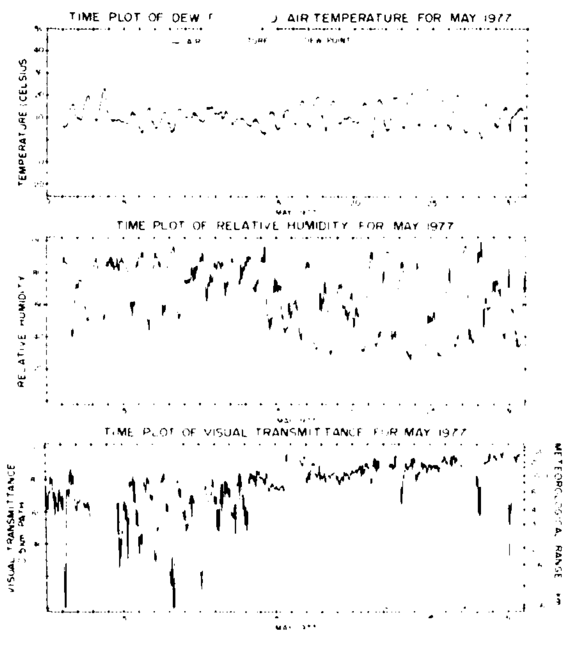

Comparison of Temporal Variability of Air Temperature, Humidity (dewpoint and relative humidity), and Visual Transmittance or Meteorological Range for a 30-day Period (location - Northern Germany)

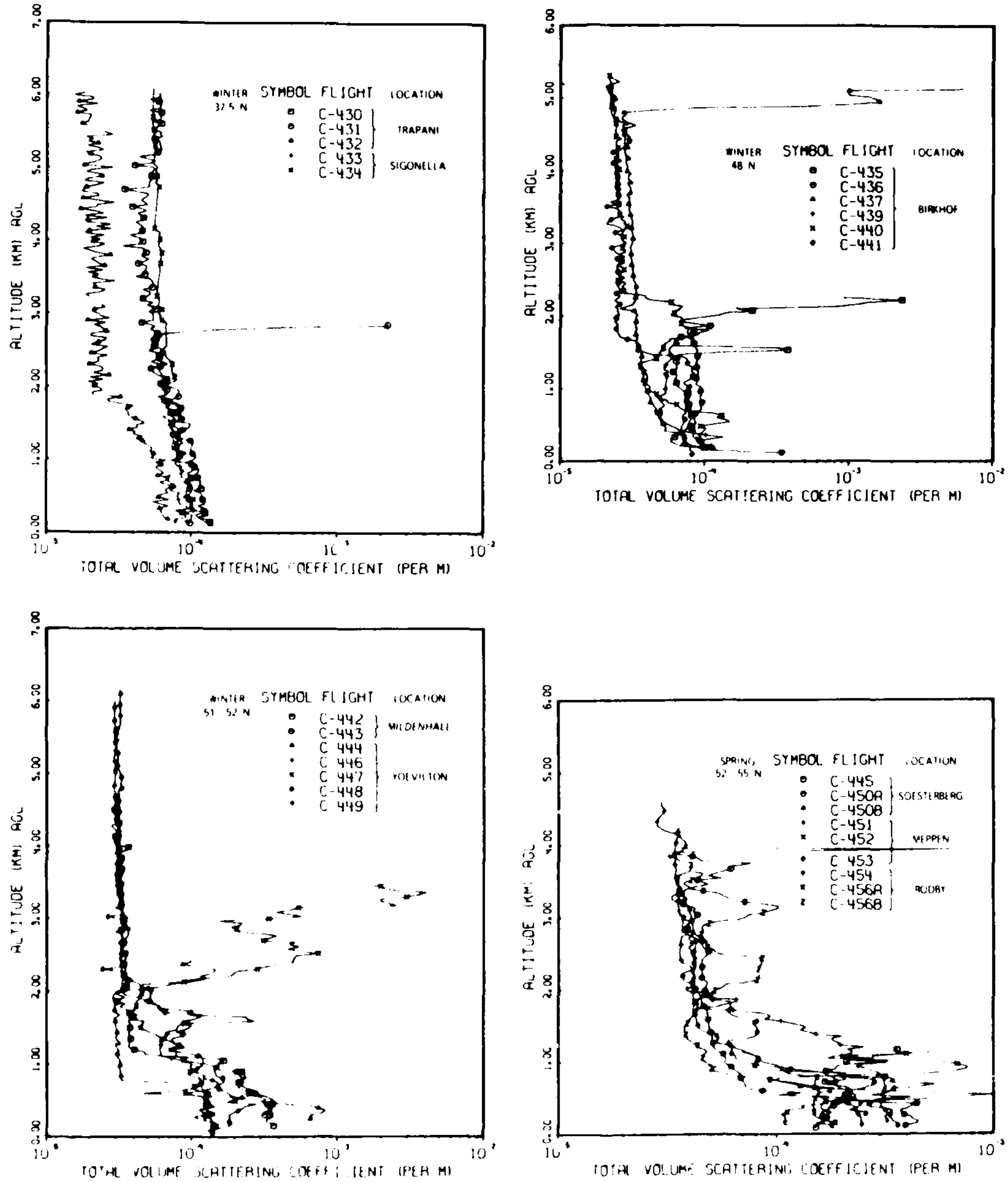

Vertical Profiles of Scattering Coefficient for Four Different Geographical Regions in Europe (a. Sicily, b. Southwest Germany, c. Southern England, d. Northern Germany-Netherlands-Denmark).

composition. Thus, this correlation holds in an exact physical sense only under laboratory conditions and not in the free atmosphere.

An aircraft measurement program conducted to supplement these surface measurements produced important results on the vertical variability of haze particles in the atmosphere. Under cloud-

AD-A126 004 REPORT ON RESEARCH AT AFGL JANUARY 1979-DECEMBER 1980 (U) AIR FORCE GEOPHYSICS LAB HANSCOM AFB MA A B MCGINTY APR 82 AFGL-TR-82-0132

3/3

UNCLASSIFIED F/G 5/1 NL

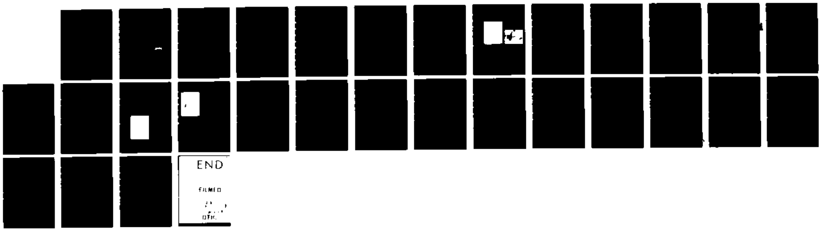

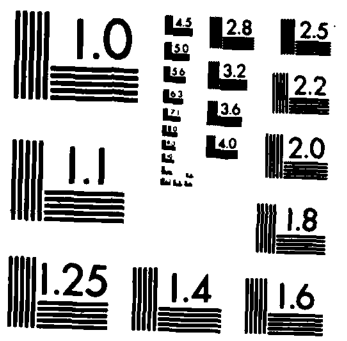

MICROCOPY RESOLUTION TEST CHART
NATIONAL BUREAU OF STANDARDS-1963-A

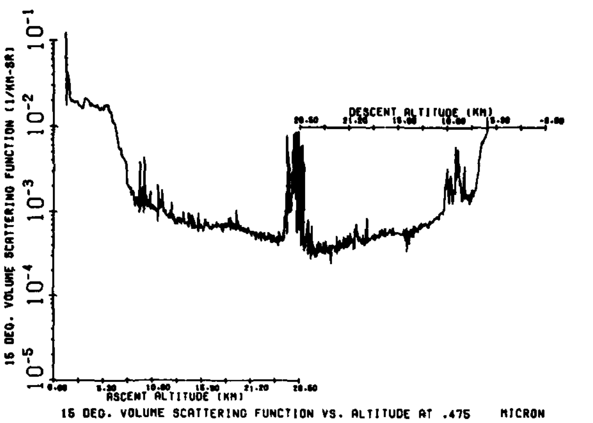

Balloon-borne Measurement of Absolute Scattering Intensity at 0.475 Micrometer Wavelength as Function of Altitude for the 15 degree Scattering Angle. Earlier flight showed nacreous cloud at 25 km.

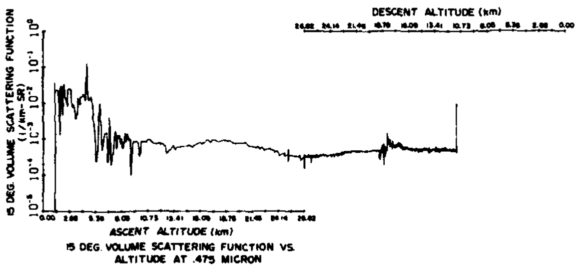

Absolute Scattering Intensity at 0.475 Micrometer Wavelength as Function of Altitude for the 15-degree Scattering Angle. Balloon flight conducted two years later than previous flight.

free conditions the number of aerosol particles generally decreases with altitude. In polluted urban industrial areas, however, a dense haze layer one to two thousand meters thick often forms. Under low level clouds the particle concentration may even increase with altitude, approaching the cloud base. These results have been the basis for models to calculate slant-path transmittance from an aircraft to a surface target.

A fixed-angle polar nephelometer was suspended from a high-altitude research balloon to provide information on optical scattering from atmospheric aerosols as a function of altitude. Comparative profiles of the absolute scattering intensity versus altitude at the 15-degree forward scattering angle are remarkably similar even though there was a two-year time separation between the experiments. Both flights were conducted during periods when the atmosphere was virtually free of

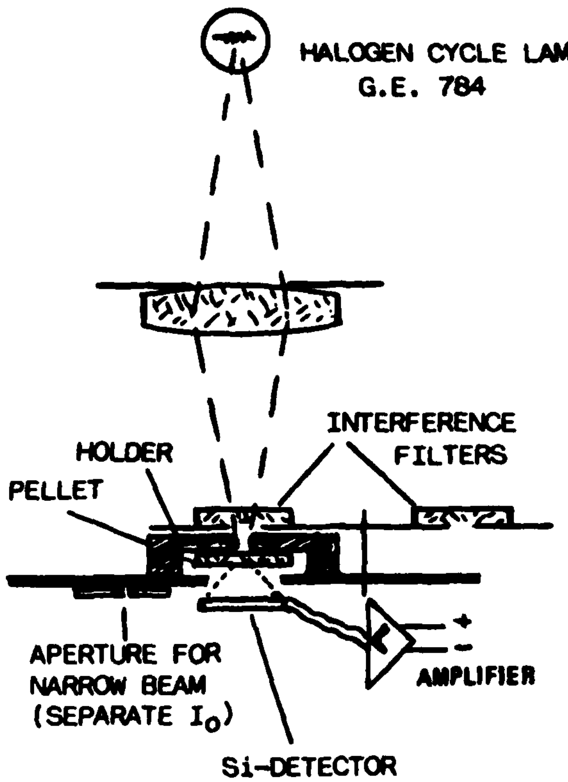

Photometer with Spot Illumination of Pressed Pellet and Wide Angle Receiver for Measurements of Aerosol Absorption Coefficients.

volcanic ash and dust and therefore are representative of quiescent background conditions. Of particular note is the enhanced scattering in the atmospheric region between 16-24 km, which identifies the well-known Junge layer of atmospheric aerosol particles.

Laboratory experiments were con-

ducted to determine the optical and infrared refractive indexes of atmospheric aerosol particles. In addition to particle size, particle refractive index is the most important aerosol property which determines the scattering and absorption effects of particles. The absorption part (n_i) of the refractive index can be measured by collecting a small amount (about 1 mg) of submicroscopic aerosol particles (several thousand particles). This aerosol material is then ground and mixed with an absorption-free supporting and diluting agent (potassium bromide powder). The mixture is then pressed into a glossy transparent disk for transmittance measurements.

In the infrared, these measurements can be performed with a double beam spectrograph. In the visible and near infrared, however, scattering effects by the particles (already much smaller than in air because the real part of their refractive index is closely matched to that of the supporting agent) have to be further reduced by illuminating only a small spot of the disk and placing a large area detector just behind the disk. With nonabsorbing test substances, scattering produced an apparent value of $n_i \approx 0.001$. For atmospheric aerosol collected in suburban environments, n_i is three to five times higher.

There is still a serious gap in our knowledge of aerosol properties in the planetary boundary layer, the well-mixed layer immediately adjacent to the ground, especially under marginal-to-poor weather conditions: heavy haze, fog and low clouds. To fill this data gap and, at the same time, provide for a flexible mechanism for responding to other data needs, a mobile optical/infrared laboratory is being developed. This laboratory, the Transportable Optical Atmospheric Data System (TOADS), will consist of two instrumented trailers housing numerous instruments controlled by a supervisory processor, and will be capable of deployment to remote locations. Spectral radiance and irradiance measurements in the visible and near infrared (0.35 - 1.2 mm) will be made from one trailer with four grating spectrometers controlled by a minicomputer. This trailer also has a set of standard meteorological sensors (wind, temperature, pressure and relative humidity). The second trailer will house two infrared transmissometers, a visible transmissometer, several aerosol probes and aerosol scattering sensors, additional meteorological sensors, and two systems for measuring over vertical paths: a dual frequency LIDAR and a slant path transmissometer. As new instrumentation is developed, it will be added to the system.

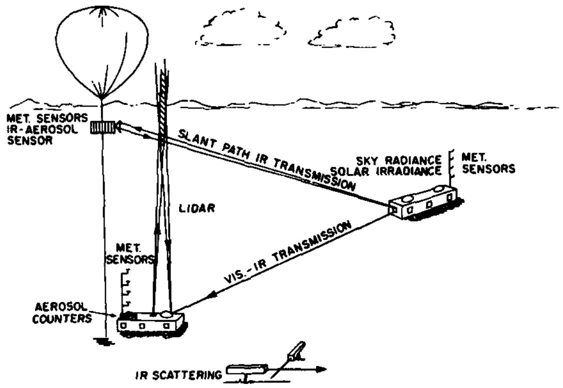

Schematic of the Transportable Optical Atmospheric Data System (TOADS) for Measuring Low Level Haze and Fog Profiles and Atmospheric Slant Path Propagation of Visible and Infrared Radiation.

The infrared transmissometers are standard units capable of measurements from about 2 to 14 μm over paths of up to 2 km. The aerosol probes are commercially available units which, taken together, will span a size range from 0.002 to 20 μm. Nephelometers for measuring the scattering properties of aerosols will include two instruments, one operating in the visible and a dual wavelength (1.06 and 10.6 μm) laser nephelometer.

The meteorological instrumentation in the second trailer will include the standard instruments for measuring wind,

temperature, and dewpoint; a very accurate cooled-mirror dewpoint sensor for studying high relative-humidity conditions; and two heated precipitation gauges for measuring the rate of rainfall and snowfall at a standard 0.01 inch resolution and an enhanced resolution of 0.001 inch for very light precipitation.

The LIDAR, a dual wavelength (1.06 and 0.53 μm) system, has been developed under contract and will be installed on the top of the trailer in a gimballed mount. It will provide relative profiles of aerosol backscattering with excellent time and

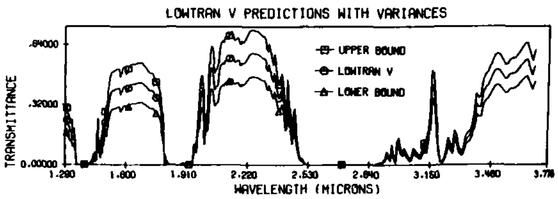

Atmospheric Transmittance Predicted by LOWTRAN 5. Upper and lower bound are due to turbulence fluctuations. 1962 US Standard Atmospheric Model is shown with rural aerosol model for a 5 km horizontal path at altitude 400 meter, and visual range 5 km for a point receiver (D = 0).

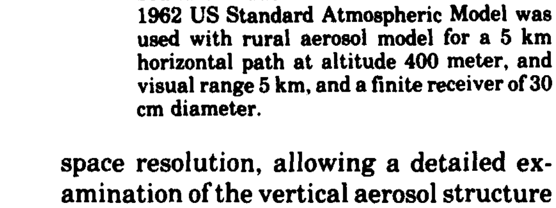

Atmospheric Transmittance Predicted by the Modified LOWTRAN 5. Upper and lower bound are due to turbulence fluctuations. 1962 US Standard Atmospheric Model was used with rural aerosol model for a 5 km horizontal path at altitude 400 meter, and visual range 5 km, and a finite receiver of 30 cm diameter.

space resolution, allowing a detailed examination of the vertical aerosol structure in the boundary layer. The slant path transmissometer will consist of one of the infrared transmissometers mentioned above and a retroreflector mounted on a tethered balloon or a tower. It will allow simultaneous determination of the total extinction along a slant path and is also being developed and tested under contract.

Data logging, instrument control and real-time data reduction will be accomplished with two microprocessor systems. One is dedicated to the LIDAR. The second, supervisory system will collect and sequence all data, control all other instruments according to operator specifications, and provide a quick-look data reduction capability so that experimental conditions can be changed as necessary based on near real-time analysis.

REMOTE SENSING

The first meteorological satellites were designed to transmit cloud pictures. It was soon realized that the spectral measurement of the satellite-viewed thermal emission made possible the remote temperature sounding of the atmosphere. Vertical temperature inferencing became operational in 1970 with the orbiting of the Vertical Temperature Profile Radiometer (VTPR) sounder aboard a NASA-NOAA meteorological satellite. Similar data observed by the Defense Meteorological Satellite Program (DMSP) became available in 1974. Later versions of these vertical sounding systems also contain spectral channels intended to sound the vertical distribution of water vapor, a parameter of substantial interest to the Air Force. In addition to the infrared sounders, microwave sounders were developed. AFGL was the technical leader in this field for DMSP.

Work in this Division has been concentrated in three areas: (1) forward problem discrepancy, (2) inversion procedure, (3) analysis of DMSP satellite radiance data. First, the transmittance modeling described earlier has been used to develop new design concepts and data analysis schemes employing both infrared and microwave techniques for remote sounding of

the vertical distributions of temperature and water vapor. Existing infrared sensors were modified and flown on DMSP. Water vapor and 15 μm carbon dioxide transmittances are being studied to aid in the understanding and interpretation of discrepancies found in comparisons of satellite-measured and computed atmospheric-radiance distributions (forward problem discrepancy). A study to determine if the microwave sounder orbited by DMSP in 1979 contained the same type of discrepancy as the infrared was initiated.

The ultimate utilization of the satellite-measured radiances in the thermal infrared and the microwave requires an inversion procedure, a mathematical device whereby either the vertical distribution of temperature (or water vapor), or the vertical distribution of the sources and sinks of radiation in the atmosphere are derived from a spectral scan of the upwelling radiance. This information can then be fed into dynamical models of atmospheric motion as a key element of weather forecasting on various scales.

DMSP satellite radiance data were analyzed and evaluated. DMSP water-vapor radiance data from the infrared sounder were compared with coincident ground truth data to determine the accuracy of inferred water vapor profiles. In determining the clear vs cloud-contaminated radiance data, an anomaly in the infrared temperature sounder channel E-2 (677 wavenumber) was identified. This anomaly was later related to a design problem in the sounder which has subsequently been corrected. The DMSP microwave temperature-sounder radiance data are being analyzed. Preliminary results indicate the microwave data do not exhibit the forward problem discrepancy.

Using the spectral scan to determine the temperature (or moisture) at each level in the atmosphere has proved to be very difficult. All levels of the atmosphere contribute at each particular frequency, so that the radiance sensed by the satellite is a mixture of thermal information from all levels. Probing different frequencies merely weights radiation according to height, depending on the transmittance of the atmosphere.

Mathematically, the radiation is expressible as an integral transform of the temperature-related Planck intensity summed over the atmosphere. Typically, the radiances are observed in six to eight different frequency channels. The vertical temperature distribution is then recoverable as an inverse transform of the radiance profile; hence, the name "inversion" given to this particular inference problem. The heart of the problem is that the vertical temperature distribution is deduced from intensity differences between neighboring frequency channels, a second-order effect. First the finite number of channels of observation means that many solutions for the temperature profiles are possible. Second, most inversion methods use some *a priori* algorithm in an attempt to smooth out the inevitable noise in the data and thus run the risk of discarding useful information. Techniques have been developed which recognize noise in the radiation measurement data and eliminate it from the data base, which is then used to infer temperature profiles. An operational technique implemented by the Air Force Ground Weather Center for the microwave sounder came out of this research.

The mismatch of satellite-observed radiances with those calculated using ground-truth data has brought into question the validity of all physical inversion methods. We believe this discrepancy results from a long-overlooked flaw in classical transfer theory. We are presently developing an eigentransform theory which will establish the correct linkage between satellite radiances and atmospheric thermal profiles and thus remove the observed discrepancy.

Snow-Cloud Discrimination: Near infrared spectra of snow, cirrus, and cumu-

lus backgrounds were measured by AFGL's KC-135 aircraft. The spectra were then analyzed to determine the spectral reflectance characteristics of snow, cirrus and cumulus. Specific snow/cloud discrimination design parameters were identified. This research led to the design of an optimum snow/cloud discriminator based on the measurement of the slope of the spectral radiance in this near infrared region. In 1979 DMSP orbited a single channel snow/cloud discriminator as a proof of concept.

INFRARED BACKGROUNDS

It is impossible for a sensor to observe or look in any direction without encountering the emission or radiation from some "background"—whether it is the celestial sky, the earth and clouds, the horizon or earth limb, the aurora or airglow, the atmosphere itself or even manmade backgrounds such as nuclear explosions or urban areas. Much of the research of the Division is devoted to obtaining direct measurements of these backgrounds, and developing data bases, models and codes to describe these backgrounds and the phenomenology related to them.

In particular, the optical/infrared properties of the upper atmosphere, both under normal conditions and when it is disturbed by auroras or nuclear backgrounds, is a major scientific area. At the altitudes considered, thermal equilibrium usually does not exist, and it is necessary to consider the collisions or interactions of individual pairs or triads of molecules, one or more of which may be an excited state (that is, with excess internal energy). Extensive laboratory and theoretical studies, as well as rocket and aircraft measurements of upper atmospheric optical/infrared phenomena, are carried out. The results of these laboratory studies and aircraft measurements also apply to missile or jet engine plume infrared radiation. The goal of the research is to generate both directly measured data and models and computer codes that permit the prediction of the optical/infrared emission of the upper atmosphere, particularly under disturbed conditions. Such data and codes are particularly applicable to surveillance and detection systems operating in space or near space.

Background Measurements in Space: The Air Force needs to detect infrared emitting targets in space at the greatest possible range. Because these targets are always viewed against background radiance, knowledge of this radiation is necessary to permit discrimination of the target from the background. These backgrounds include the celestial sky, zodiacal emission, and radiation from the earth limb, aurora and upper atmosphere.

First, the celestial background must be specified. We must be concerned not only with stars but with the effects of zodiacal radiation—thermal emission from particles distributed about the ecliptic plane which absorb solar radiation and then radiate in the infrared. To observe low-altitude satellites we must also determine the earth's upper atmospheric limb radiance.

The Division has conducted a series of experiments to obtain infrared survey data on the celestial background with state-of-the-art cryogenically cooled sensors flown on rocket probes. The thrust of the program has been threefold: to obtain the most complete sky coverage possible with as high a sensitivity as compatible with the need to cover a large area on each flight; to generate a background map from these data; and to apply these data to the model to extend statistically the empirical data base to faint irradiance levels.

To date, about 79 percent of the sky has been surveyed at an effective wavelength of 4.2 μm, 90 percent at 11 μm, 87 percent at 20 μm and 36 percent at 27 μm. The data have been published in *The AFGL Four Color Infrared Sky Survey: Catalog of Observations at 4.2, 11.0, 19.8 and 27.4* μm

(AFGL-TR-76-0208). A subsequent catalog (AFGL-TR-77-0160) extends the data to sources observed with low confidence. Many of these latter sources have been confirmed by ground-based observations. A diffuse component has also been observed to be centered on the galactic plane.

Present plans are to develop instrumentation to be flown on an ARIES compatible payload, which gimbals the cryogenic sensor. Two survey instruments are being built: the Survey Program Infrared Celestial Experiments (SPICE) sensor and the Far Infrared Sky Survey Experiment (FIRSSE) telescope, the latter with the Naval Research Laboratory. The instruments are mechanically similar. The telescopes and cryogens are both housed in a cylinder roughly 0.48 meter in diameter, 1.2 meters long with a mass of 70 kg. Both instruments use a doubly folded optical bench with a 36 cm diameter primary aperture. However, the sensors are fundamentally different in design and experimental requirements. The SPICE sensor is cooled with super-critical helium and covers the spectral region from 8 to 30 μm in three bands. The FIRSSE instrument includes these three bands and extends the measurements to 120 μm with two additional focal plane arrays. The longer wavelength detectors require colder operating temperatures, which are achieved with super-fluid helium. Each flight will survey approximately 35 percent of the sky. The optics will permit scanning to −55 degrees in declination from White Sands Missile Range with no degradation in sensitivity, permitting coverage of the important area south of the galactic center.

The zodiacal light is the limiting background for observations made from space platforms. In addition to an on-going modeling effort based on previous flight data, in August 1980 AFGL successfully launched and recovered a rocketborne experiment designed to measure the 2-30 μm infrared emission from this dust cloud. The cryogenically cooled telescope, built and tested at the Laboratory, is an advanced off-axis, folded, doubly reimaging optical system which represents the current state of the art. This experiment will be reflown during 1981, providing sufficient spatial coverage to model the interplanetary dust cloud and its appearance in the intermediate infrared.

Parallel efforts to develop computer codes which model the infrared radiance from the upper atmosphere have been under way for the past seven years. The atmospheric model incorporates photochemical and thermal emission mechanisms for the major infrared active molecular species. Radiance profiles can be generated in the 5 to 25 μm region up to 500 km altitude. The most recent version (AFGL-TR-77-0271) incorporates revisions including experimental data made available since the 1974 version.

A rocket probe program to measure infrared radiation from the upper atmosphere earth limb is currently being developed. The vertical distribution of the radiation in the 30-300 km region will be studied. Additionally, efforts are under way to incorporate measurements of the clutter components—that is, the spatial and temporal variations—into the program. The data, which will cover the 3-22 μm region, are intended to update the most recent limb model.

Balloon Measurements: The Balloon Altitude Mosaic Measurements (BAMM) Program obtained spectral, spatial, and temporal data of a variety of earth/atmosphere infrared backgrounds such as clouds, bodies of water, rural terrain, and densely populated areas to provide assessment and design data for future satellite-borne infrared surveillance systems. The requirements for this type of data were generated by an interest in the mosaic staring surveillance concept that utilizes a large array of detectors, each detector monitoring a specific earth surface area.

BAMM attempts to simulate this concept by taking measurements from a balloon-borne, inertially stabilized payload flown at an altitude of 100,000 feet. Platform instrumentation, controlled via ground command, includes a 4 × 4 mosaic radiometer and Michelson interferometer. The radiometer utilizes specific interchangeable band filters, while the interferometer covers the 2.5 to 5.5 micron spectral range with ten wavenumber resolution. Spectral measurements are recorded in the staring mode so as to obtain the background temporal changes within each spectral element. A real-time television camera system is boresighted to the interferometer and radiometer to provide a visual image of the earth's surface for data correlation. The payload is rigged with a Mid-Air Retrieval System (MARS) recovery parachute, which reduces payload structural damage by allowing a mid-air catch by a helicopter, rather than a ground impact. A MARS recovery is essential when launching over water or adverse terrain.

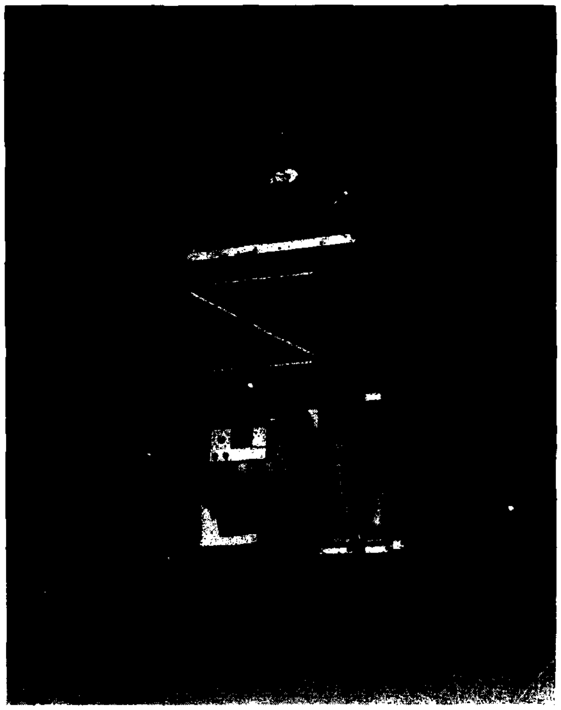

Balloon Altitude Mosaic Measurements (BAMM) Payload.

Data acquisition, payload telemetry, and balloon navigation are monitored from a ground base consisting of several mobile command stations. A PDP 1140 computer provides a fast Fourier transform capability to produce hard-copy spectra in near real-time.

Interior of BAMM Mobile Command Station.

Three highly succesful balloon flights and one refurbished payload test were conducted. Between September 1978 and October 1979, two flights were launched from Holloman AFB, NM, and one was flown from Keesler AFB, Miss. A test flight of an improved 3-axis stabilized platform was flown at Holloman AFB in May 1980. Several hours of data were gathered during these flights. A total of 39 scenes were selected for detailed analysis. These scenes catalog a wide variety of infrared background conditions in a staring, scanning, or dithering mode. Scenes selected for data reduction include backgrounds such as passive sea, mountains, desert, land/sea interface, and land with light cloud cover. Special interest scenes include scans, stares, and dithers over so-

lar specular reflection off water, clouds, and land. Additional missions are planned to study adverse weather conditions and terrain on long duration flights with a tricolor radiometer.

Aircraft Measurement Program: AFGL uses a modified NKC-135 aircraft as an Infrared Flying Laboratory. This aircraft has 55 viewing windows and ports behind which various radiometers, interferometers, spectrometers, and spatial mappers can be operated to collect basic infrared data. The range of this aircraft allows worldwide deployment and permits the infrared research scientists to study the environment well above obscuring clouds and atmospheric constituents. This NKC-135 has been serving as a reliable platform from which to study geographic and seasonal impacts upon infrared processes in the aurora and atmosphere. These studies are coordinated with balloon and rocket-borne measurements, and the data are subsequently used to test specific theoretical and laboratory-based modeling.

A variety of unique instrumentation is carried on board the Infrared Flying Laboratory. Five Michelson interferometers with automatic alignment features are utilized, at side-looking windows or at a down-looking window in the newly converted refueling "boomer's compartment." These instruments have been designed and built by a member of the scientific air crew, and the data obtained are widely acclaimed by the DOD infrared community. One of these interferometers is capable of producing data with 0.1 wavenumber spectral resolution. Two thermal scanners are operated simultaneously with the interferometers, providing infrared imagery in the 2 to 14 micron spectral region that serves a dual purpose in providing spatial imagery, enabling better interpretation of interferometric spectral data and by giving differential radiance with respect to the mean radiance of the scene. These instruments can be used with gold-coated periscopic mirrors that enable target aircraft to be observed flying in front or behind the infrared flying laboratory. With these mirrors a target aircraft can be observed at almost any aspect angle from nose-on to tail-on while in flight. Temporal data are obtained from a four-channel radiometer mounted at a side window. An array of 16 mm tracking cameras and a television camera provide visible region documentation of subjects being observed.

The data obtained with these various instruments are recorded on analog tape recorders and the tapes are returned to the laboratory for data reduction. From the interferometers come digital plots of infrared spectra in units of absolute spectral radiant intensity for targets, or absolute spectral radiance for backgrounds and extended sources. The infrared scanners provide imagery that gives differential radiance with respect to the mean radiance of the scene. The radiometer provides calibrated source radiances that can be compared with integrated spectral data, and if the source varies in intensity, curves may be obtained from computer plots showing the time history of the measured radiation.

Interferometric and spatial data products are generated in the laboratory by a powerful array of minicomputers. The interferometric data are transformed from raw analog interferograms into digitized spectra with a minicomputer and Fourier analyzer. The spatial imagery data are processed and converted to television images that can be calibrated in radiance units by the minicomputer analysis system. The images are displayed on a standard television monitor in a 16-step grey scale format by a video display unit.

The airborne infrared measurements program is collecting large amounts of data on a variety of backgrounds. Spectral and spatial data have been collected on desert, urban, rural, cultivated, mountain, snow and water backgrounds. Sky background data consist of several cloud

types viewed from above and below at several altitudes and at various solar azimuth and elevation angles. In addition, continuous urban data have been obtained for a period of approximately five hours, beginning before sunset and ending after sunset for three different seasons of the year. Forest fires have been measured on a number of occasions.

Design, construction and testing continue with follow-on generations of instrumentation. A large aperture trainable "eyeball" window system will enable telescopes with 7 inch apertures to be used with the interferometers and thermal mappers. Such telescopes will permit targets to be observed at much greater ranges, which will enable the absorption effects of the atmosphere and the influence of thin clouds on observations to be better understood. It is planned to eventually cool these telescopes and instruments to temperatures of -60°C, which will greatly increase their sensitivity over currently used systems. Such improvements will continue to provide the important data base necessary to support the design and development of advanced infrared sensing systems.

COCHISE: The Division has built and now operates a unique experimental facility to study specific atomic and molecular excitation processes which are important sources of atmospheric infrared radiation, and which may compromise the performance of DOD infrared-based systems. Detailed definitions of the microscopic processes which control the production and relaxation of energetically excited species are required, to make reliable predictions and assessments of atmospheric radiation perturbations resulting from natural and artificially induced atmospheric disturbances. The long radiative lifetimes associated with molecular vibrational transitions demand that experiments be operated at pressures low enough to simulate upper atmosphere densities and simultaneously not be perturbed by spurious surface effects such as wall collisions.

This AFGL cryogenic facility, called COCHISE (*CO*ld *CH*emi-excited *I*nfrared *S*imulation *E*xperiments), implements detection technology initially developed for space surveillance systems. It achieves infrared detection sensitivities up to six orders of magnitude better than those available in other laboratories, and concurrently provides a truly novel low-pressure, "wall-less" capability for simulation and study of high-altitude phenomena. Experiments are conducted entirely within a large cavity held at 20°K by a closed-cycle gaseous helium refrigeration system, part of whose capacity is also used to provide hyper-fast cryo-pumping of a temperature-controlled reaction chamber located inside the larger 20°K cavity. A grating spectrometer also stationed inside the 20°K environment measures infrared radiation produced by atmospheric phenomena being simulated in the reaction chamber. By reducing to a totally negligible level the thermal background radiation, a detectivity has been achieved which permits observation of emissions from excited species with number densities as low as 10^6 cm^{-3}. Operation of the facility is augmented by an unusually large and complex minicomputer system which executes a multitude of control, measurement, and analysis tasks. The computer is hard-wired to, and totally dedicated to, the support of COCHISE.

By experimentally defining the quantum details of the $N(^2D) + O_2$ reaction, through measurements made using the COCHISE facility, AFGL scientists were able to elucidate the role of this process as a source of fairly intense infrared radiation at high altitudes in the atmosphere. More recently, data have been collected on the COCHISE facility which also begin to define the extent to which the 10 to 12 μm atmospheric "window" can be degraded by ozone emission; in this case, it is the recombination of atomic oxygen (via the pro-

cess O + O_2 + M → O_3 + M, yielding vibrationally excited ozone) which is being subjected to scrutiny.

During 1980, new initiatives were established within the COCHISE program which will lead to extensive coupling of state-of-the-science lasers with the already formidable capabilities of the cryogenic simulation/spectroscopy system. A test-bed for such experiments has been built, and is known as FACELIF (Flowing Atmospheric Chemi-Excitation with Laser Induced Fluorescence). Lasers in use for these purposes include a Nd:YAG-pumped dye laser (with frequency doubler and Raman shifter), an excimer laser which can also be operated with CO, CO_2, and a color center laser. One of the major undertakings with these coupled capabilities is to be Laser Induced Nuclear Simulation (LINUS), wherein a laser-induced low-pressure point discharge will simulate the fireball plasma of a nuclear explosion, and will be probed by other lasers, as well as being examined by passive cryogenic infrared emission spectroscopy. The nature and scope of these activities make the AFGL COCHISE program one of the most advanced infrared emission spectroscopy activities in the country today.

LABCEDE: Electrons interacting with the atmosphere can cause many different physical effects, including the emission of infrared radiation. The Optical Physics Division has been working on this problem because it is related to the interpretation of data obtained by infrared target detection systems. The radiation from the targets is seen against the background of the earth and its atmosphere, and since this background is known to vary quite severely itself, the detection of the target radiation against this background requires a knowledge of these background fluctuations.

The two major short-term (time scale of a few seconds) influences are auroral excitation and nuclear explosions. Both are associated with the introduction into the atmosphere of energetic electrons. We have modeled this effect by directing a beam of electrons into both air and its molecular constituents. The infrared radiations are expected to be very weak and our instrumentation takes two principal forms, the Michelson interferometer with its multiplex and through-put advantages, and the circular variable filter which has an even larger throughput but lower spectral resolution. The wavelength region studied has spanned the region from 1 to 15 mm but most of the work has been in the short wavelength from 1 to 7 mm.

Two experimental facilities have been used. The first of these has already been described in the previous report on research. The techniques established for time-resolved studies of CO_2 gas mixtures led to an understanding of the kinetics of vibrationally excited CO. We have now extended these studies to the aeronomically more important molecule NO. In contrast to excited CO from CO_2, vibrationally excited NO is formed as part of a chain of atomic and molecular reactions. The electrons enter the chain in the first stage in which excited nitrogen atoms are formed from the molecules in the atmosphere, and these then react chemically with molecules of oxygen to form nitric oxide. The most probable excited nitrogen atom involved is the state known as ^2D, and this is capable of producing NO with as many as 18 vibrational quanta. These quanta cannot remain indefinitely long with the molecule. They must be removed either by collision with another molecule, a process called quenching, or by radiation, in which the quanta may be reradiated one at a time, giving rise to the "fundamental band," or reradiated two at a time, forming the "overtone band."

The process of radiation produces the infrared signature. The fundamental band of NO lies at 5.4 μm wavelength, and the overtone is at 2.7 μm. The various quanta are found to be unequal in energy and

their signatures thus occur at slightly different wavelengths, so that with sufficient spectral and temporal resolution it is possible to follow the precise details of the reactions.

Two major questions were asked and answered during this work: how intense is the radiation and how does it change with time? The probability of the molecule radiating in the fundamental region or in the overtone was well known from many previous studies, but experimental and theoretical studies failed to give adequate answers for higher vibrational quanta. The excited NO source obtained in the AFGL work has allowed this problem to be solved for vibrational excitation up to as

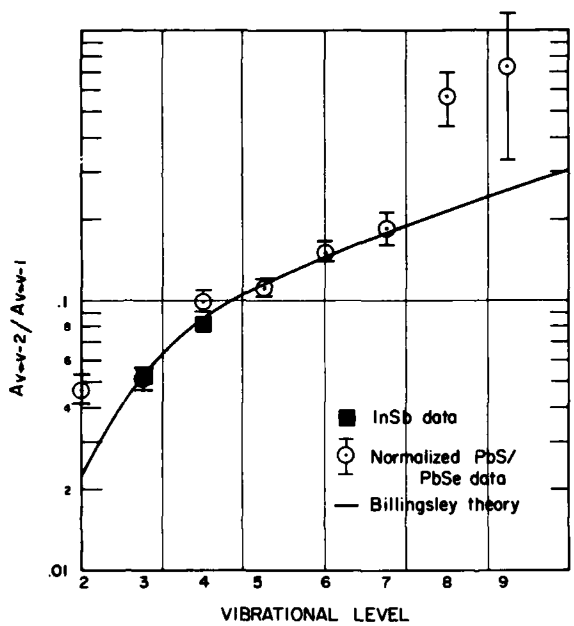

Experimental Einstein Coefficient Ratios for Overtone Fundamental Bands of NO and Theoretical Predictions.

high as the 9th level. The theoretical curve shown is one of several which have been developed and it fits the data far better than any other.

The other question concerned quenching, or energy lost, due to molecular collisions. This type of problem is usually tackled by the Stern Volmer technique. The addition of successively larger quantities of the quenching molecules caused the radiation from NO to last for a shorter time (and get much weaker) and from the slope of the curve the rate of quenching may be found. We have found that oxygen is a far more important quencher than nitrogen, even though there is less of it in the atmosphere.

The work just described was performed at moderate pressures, equivalent to around 20 km altitude in the atmosphere. Auroral electrons never reach this low; however, nuclear bursts can occur at any altitude. To better simulate the upper atmosphere, lower pressures are needed. This in itself is not difficult, but as the amount of gas is reduced, so is the signal, and this causes the infrared radiation, already quite weak, to become even weak-

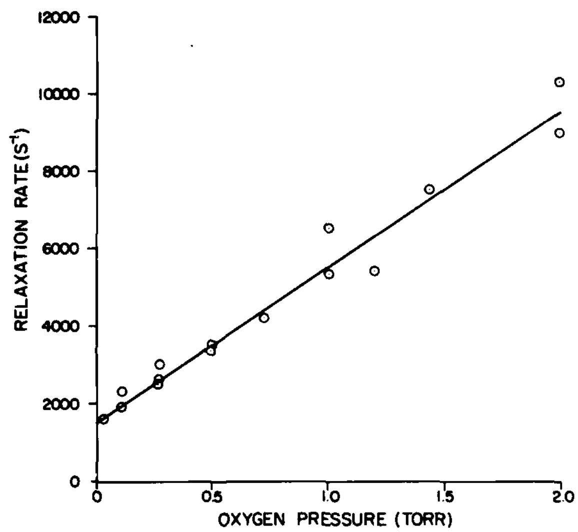

Relaxation Rates for Level 3 as Function of O_2 Pressure.

er. Some compensation can be made by increasing the beam current but a practical limit of about 20 ma occurs as the result of a number of practical trade-offs.

The low pressure facility is 1 meter in

diameter and can handle gas pressures down to an equivalent altitude of around 100 km. Besides increasing the beam current, which does not fully compensate for the lower signals, we cool the background to lower the noise against which the signal is observed. Surfaces at room temperature radiate with substantial intensity in the infrared, in fact, many thousands of times the expected signal intensity of the NO gas in the chamber at wavelengths in the NO fundamental region. Cooling the inner walls, against which the spectrometers "look," with liquid nitrogen is the solution used, and we have improved signal-to-noise ratios by several orders of magnitude.

With this apparatus we have succeeded in getting spectra both of nitrogen and air.

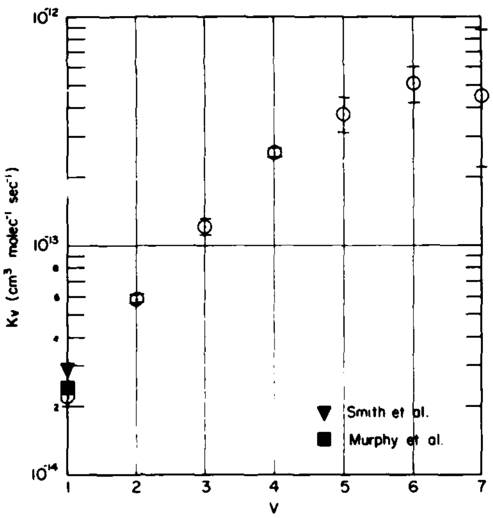

Preliminary Values of Relaxation Rate Constant for Relaxation of NO(v) by O_2. There is good agreement with values given in the literature for v = 1. The rate constants scale approximately as $v^{3/2}$- v^2.

In nitrogen we find a complex spectrum which shows a number of electronic band systems of the N_2 molecule. The intensity of the features in the 3 to 4 μm region was not expected and is still the subject of research. In air, the major intensity was not due to the predominant nitrogen molecule, but to NO formed as described earlier. The CO_2 identified is not actually due to the air, but to CO_2 freed from the chamber walls by the impact of the electron beam. The signals observed are typically a factor of 10,000 less than the background level of radiation observed before the tank is cooled.

Molecular Beam Studies: High velocity collisions occurring at high altitudes (above 300 km) between rocket plume and atmospheric gas species are investigated in the molecular beam facility. At these altitudes the main atmospheric species is atomic oxygen. At lower altitudes interac-

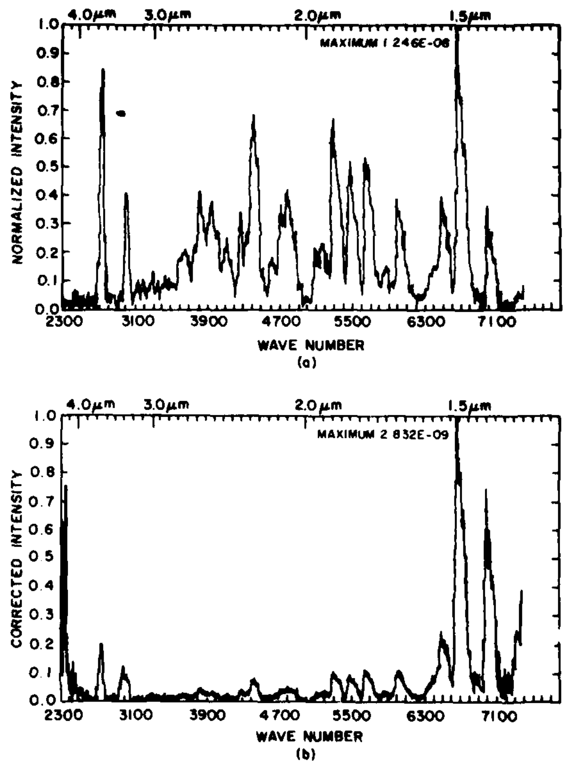

Interferometer Spectra of Nitrogen. N_2, P = 120 mTorr. (a) Direct output. (b) Intensity after correction by blackbody measurement.

tion with molecular nitrogen and oxygen becomes significant. Consequently, the experimental efforts are directed toward production of fast beams for the species O, N_2 and O_2. For the permanent gases N_2 and O_2, the beam production technique used is the well-established method of isentropic expansion of a gaseous mixture from a heated supersonic nozzle. Beam velocities and their speed distributions are studied by time-of-flight measurements. Beam intensities of 5×10^{18} particles per steradian per second are readily achieved.

In the early stages of this program, the plume particles (CO_2 and CO) were introduced into a collision chamber in the form of gaseous targets, where they interacted with fast beams of N_2 or O_2. The major improvements undertaken were design and construction of a new liquid-nitrogen-cooled collision chamber, design and construction of a 2.4 to 4.8 μm CVF-spectrometer, and introduction of the target gases CO_2 and others in the form of another molecular beam flowing opposite

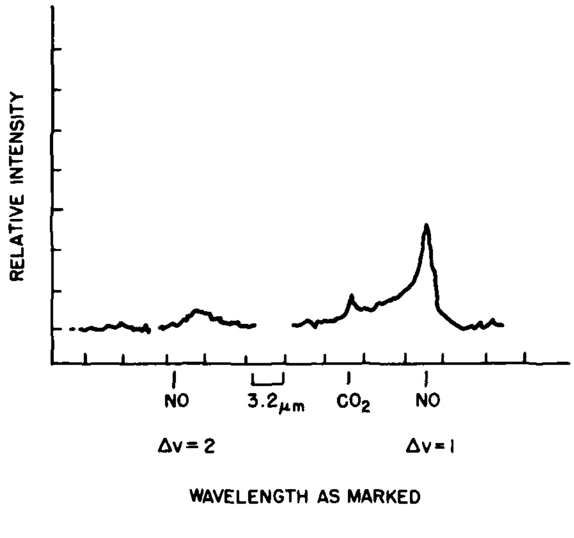

CVF Spectra: 1.6 to 5.6 μ.

to the fast beam of atmospheric species, in the so-called "180 degree geometry." These major improvements have finally been incorporated into the molecular beam facility and the apparatus is now operational and producing significant measurements.

Emission from CO_2 in the 4.3 μm band spectral region has been recorded following vibrational excitation of the asymmetric stretch mode of carbon dioxide by molecular nitrogen and oxygen over a velocity range of 2.2 km/sec to 4 km/sec. Excitation cross sections in both cases show very sharp dependence on collision velocity. The detailed study of the emission band shapes has shown that the carbon dioxide is also rotationally excited to very high rotational quantum members but the distribution cannot be described by a single temperature, indicating a non-Boltzmann distribution.

To study atomic oxygen collisions, a dc arc source was installed in the vacuum chamber and tested. Fifty to sixty percent dissociations of O_2 were observed, indicating very useful O-atom beam intensities. The source will be integrated into the double-beam collision chamber and vibrational excitation of plume species in collisions with oxygen atoms will be studied.

EXCEDE: EXCEDE is a Defense Nuclear Agency and AFGL program designed to study atmospheric radiative processes resulting from the controlled deposition of energetic electrons from rocketborne electron accelerators. On October 19, 1979, the 2600 kg EXCEDE SPECTRAL payload was succesfully launched from Poker Flat, Alaska, into a dark, clear and aurorally inactive night atmosphere. The stabilized payload contained: a 60 kW (3kV) electron accelerator; an array of ultraviolet, visible, and cryogenic infrared spectrometers; photometers; and both photographic film and video cameras. Atomic and molecular emissions induced in the atmosphere by the pulsed rocketborne electron accelerator and radiating in the 0.15 to 22 micron wavelength range were re-

corded at altitudes from 70 to 128 km. Observed emissions included: the N_2 Lyman-Birge-Hopfield system, the N_2 Wu Benesch infrared system, and the $N_2{}^+$ first negative and Meinel systems. In addition, the beam-induced emissions recorded by the cryogenic infrared instrumentation included CO_2 at 4.3 microns, NO at 5.4 microns, and a feature at 4.5 microns tentatively identified as NO^+. The comprehensive set of spectral measurements are volume emission rates and will be analyzed in terms of production and loss mechanisms.

The EXCEDE SPECTRAL experiment also used remote measurement platforms in an attempt to measure visible and infrared time-dependent pulse shapes and to record the spatial extent of the 3 kV electron beam with imaging systems. The AFGL KC-135 aircraft was instrumented with a 2.7 micron radiometer, a 3914 Å photometer and a low light-level television system. The Hilltop Optics Site at Poker Flat was instrumented with an array of film and video cameras and a dual-channel telephotometer, monitoring optical emissions at 3914 Å and 5577 Å.

The primary scientific interest of this

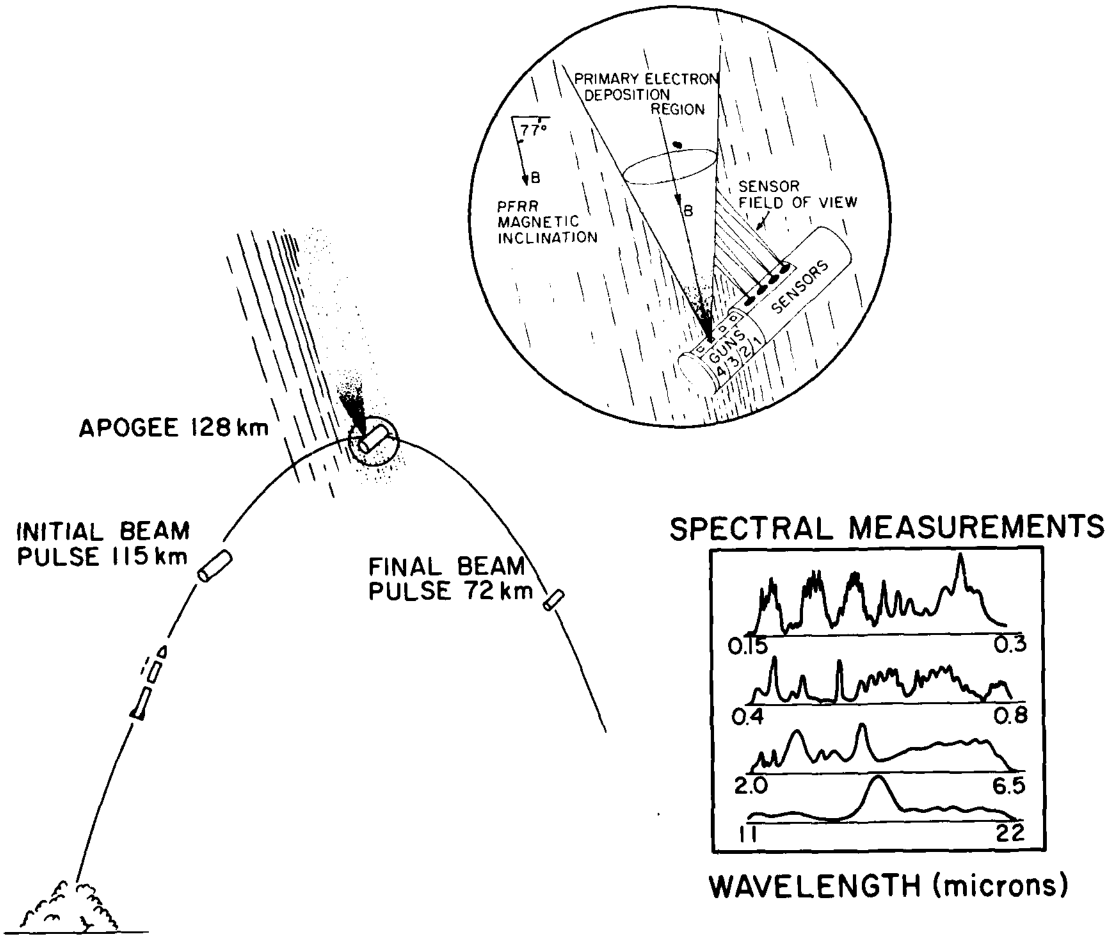

Flight Profile of the EXCEDE SPECTRAL Launch, Showing Payload Orientation, Electron Beam Geometry, and Wavelengths Monitored by Rocketborne Spectrometers.

experiment is the investigation of the detailed production and loss processes of various excited electronic and vibrational states that result in optical and infrared emission as energetic primary electrons, their secondaries, and all subsequent generation electrons are stopped in the atmosphere. In this artificial auroral experiment, the dosing conditions of electron energy and power, deposition volume, deposition altitude, and dosing duration are parameters that may be controlled and monitored. In natural aurora, these excitation conditions must be inferred and the observed atmospheric emissions typically are effects integrated over a range of conditions (electron energy, electron-flux density, altitude, and dosing time). Observations of these integral effects complicate the interpretation of auroral optical/infrared emissions in terms of basic production and loss processes.

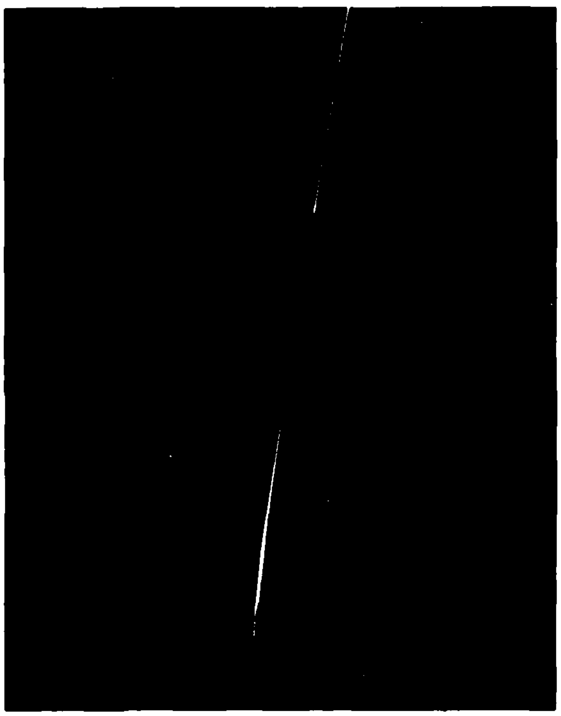

Launch of a Talos Castor Two-Stage Rocket From Poker Flat, Alaska. First-stage separation at second-stage ignition and subsequent trajectory are shown.

In the EXCEDE SPECTRAL experiment, the payload was despun and oriented such that the long dimension was elevated at an angle of approximately 43 degrees after nosecone and door ejection and payload separation. The proposed nominal electron-accelerator power was 100 kW (3kV, 32 A) using 4 electron-gun modules, each of which provided an 8 A beam. The electron accelerators initiated a pulse sequence at approximately 120 km on payload ascent, which continued through apogee, 128 km, and on to approximately 70 km on payload descent, providing a total experiment duration of 180 sec.

The payload orientation during the experiment positioned the electron accelerator and instruments so that: (1) the electron-beam injection angle was canted 30 degrees from the normal to the payload; (2) the fields of view of the optical sensors were normal to the payload, intersected the magnetic field (and the electron-beam axis) at 30 degrees, a few meters from the accelerator port, and were aligned with the plane of the vehicle trajectory to observe both the prompt emissions in the primary electron deposition region and slower emissions in the electron-beam afterglow.

The comprehensive set of spectra measured in this experiment will be analyzed to determine production mechanisms for each excited state, to determine electron-induced luminous efficiencies, and to determine collisional deactivation rate coefficients in the 72 to 128 km altitude range. The spectra also serve as a diagnostic measure of the electron energy distribution within the plasma produced by the electron beam based on known cross sections for the production of excited states as a function of electron energy.

The N_2 Wu Benesch system is the dominant electronic transition measured at infrared wavelengths greater than 2 microns. The electron-induced luminous effi-

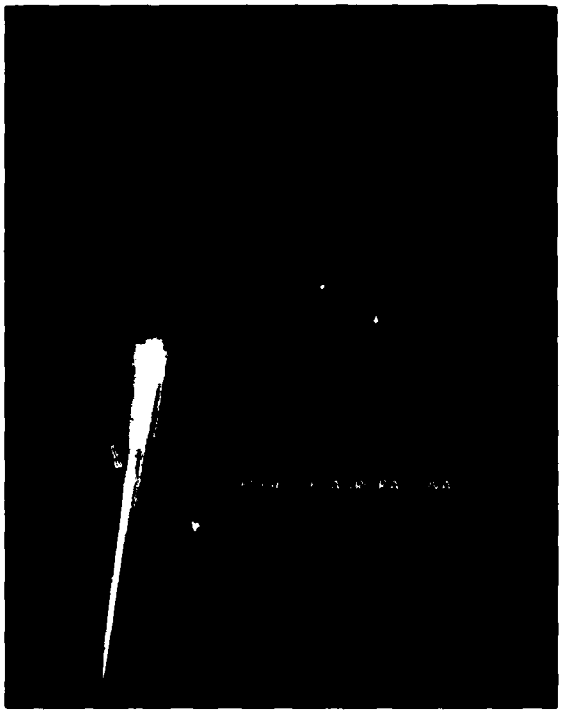

First Stage Burnout of a Two-Stage Rocket Carrying a Payload of Instruments Designed to Study Infrared Auroral Processes. An auroral arc can be seen in the background.

ciencies for the N_2 Wu Benesch (2-0) and (3-1) transitions at 3.3 and 3.6 microns have been assigned a preliminary value in the range of $2\text{-}5 \times 10^{-4}$. The data indicate this band system is collisionally deactivated at lower descent altitudes (90 to 70 km).

Excited states with Einstein coefficients of 10^5 s^{-1} or less are vulnerable to collisional deactivation at the lower altitude range (70 to 80 km) of the EXCEDE SPECTRAL measurements. Electronic states susceptible to collisions at these altitudes prior to spontaneous relaxation to a lower state include the parent states of the Wu Benesch, the Herman Kaplan, the Lyman Birge Hopfield, the Vegard Kaplan, and the first positive systems of N_2 and the Meinel system of N_2^+. The electron-induced luminous efficiencies for these and other band systems will be determined in the complete interpretation of the EXCEDE SPECTRAL data. In addition, these systems will be analyzed to determine either a definitive value or upper bound for the collisional deactivation rate coefficient of an air-like gas mixture for each observed vibrational level.

Infrared Background Modeling: Computer code modeling describing the optical/infrared characteristics of natural and high energy sources in the atmosphere has been developed. The capability for describing the space-time behavior of optical/infrared radiation from nuclear bursts in the atmosphere has been developed. Models of the infrared time history of beta patches, x-ray deposition regions and fireballs were included with appropriate space and time resolution. Scaling laws were developed for representing fireball optical/infrared radiation from bursts detonated from 0-150 km. The modeling builds heavily upon the earlier AFGL OPTIR code.

JOURNAL ARTICLES JANUARY 1979 - DECEMBER 1980

CALEDONIA, G.E., and GREEN, B.D., MURPHY, R.E.
A Study of the Vibrational Level Dependent Quenching of CO (v = 1-16) by CO_2
J. Chem. Phys. 71, Number 11 (December 1979)

CLOUGH, S.A., and KNEIZYS, F.X.
Convolution Algorithm for the Lorentz Function
Appl. Opt. 18 (July 1979)

CLOUGH, S.A., KNEIZYS, F.X., DAVIES, R.W., GAMACHE, R., and TIPPING, R.
Theoretical Line Shape for H_2O Vapor; Application to the Continuum, Atmospheric Water Vapor
Ed. by A. Deepak, T.D. Wilkerson, and L.H. Ruhnke, Academic Press NY (1980)

FALCONE, V.J., and ABREU, L.W.
Atmospheric Attenuation of Millimeter and Submillimeter Waves
EASCON '79 Record (October 1979)

FLAUD, J.M., CAMY-PEYRET, C., and ROTHMAN, L.S.
Improved Ozone Line Parameters in the 10- and 4.8- μm Regions
Appl. Opt. 19 (March 1980)

McClatchey, R.A.
An Atmospheric Temperature Profile Measured with an In-Situ Infrared Radiometer
Proc. of the International Radiation Symposium, Colorado State Univ., Fort Collins, CO (11-16 August 1980)

McClatchey, R.A., and Kneizys, F.X.
Long-Path High-Resolution Atmospheric Transmission Measurements: Comparison with LOWTRAN 3B Predictions
Appl. Opt. 18(March 1979)

Murphy, R.E., Andrada, T., Cook, F., Billingsley, F., Grieder, W.F., and Yap, B.K.
Staring Infrared Mosaic Observation of an F-15 Aircraft
SPIE Vol. 253
Modern Utilization of Infrared Technology VI (1980)

Price, S.D., Murdock, T.L., and Marcotte, L.P.
Infrared Observation of the Zodiacal Dust Cloud
Astron. J. 85, No.6 (June 1980)

O'Neil, R.R., Lee, E.T.P., and Huppi, E.R.
Auroral O(1S) Production and Loss Processes: Ground-Based Measurements of the Artificial Auroral Experiment Precede
J. Geophys. Res. 84, No. A3 (March 1979)

Rothman, L.S.
Update of the AFGL Atmospheric Absorption Line Parameters Compilation
Appl. Opt. 17 (November 1978)

Schummers, J.
Interferometer Design and Data Handling in a High-Vibration Environment - Part II: Data Handling
SPIE 191
Multiplex and/or High-Throughput Spectroscopy (1979)

Shettle, E.P.
Non-Spherical Particle Scattering: Air Force Applications, Light Scattering by Irregularly Shaped Particles
Ed. by D.W. Schuerman, Plenum Pub., NY (1980)

Shettle, E.P., Kneizys, F.X., and Gallery, W.O.
Suggested Modification to the Total Volume Molecular Scattering Coefficient in LOWTRAN
Appl. Opt. 19 (September 1980)

Vanasse, G.A., Esplin, R.W., and Huppi, R.J.
Selective Modulation Interferometric Spectrometer (SIMS) Technique Applied to Background Suppression
Optical Engineering 18, No. 4 (July-August 1979)

Volz, F.E.
Sulfuric Acid in KBr Pellet Spectroscopy
Appl. Opt. 18 (July 1979)

Walker, R.P., and Rex, J.D.
Interferometer Design and Data Handling in a High-Vibration Environment - Part I: Interferometer Design
SPIE 191
Multiplex and/or High-Throughput Spectroscopy (1979)

Zehnpfennig, T.F., Shepherd, O., Rappaport, S., Reidy, W.P., and Vanasse, G.
Background Suppression in Double-Beam Interferometry
Appl. Opt. 18 (June 1979)

PAPERS PRESENTED AT MEETINGS JANUARY 1979 - DECEMBER 1980

Baker, D.J., and Frodsham, G.D. (Utah St. Univ., Logan, UT), Kumer, J. (Lockheed Palo Alto Res. Lab., Palo Alto, CA), Stair, A.T., and Ulwick, J.C.
Rocketborne Measurements of Infrared Aurora and Airglow Emissions at 4.3 μm
Am. Geophys. Un. Mtg., Washington, DC (28 May - 1 June 1979

Baker, D.J., Steed, A.J. (Utah St. Univ., Logan, UT), and Stair, A.T.
Upper Atmospheric Studies Using Remote Infrared Cryogenically Cooled Sensors, Upper Atmospheric Studies Using Remote Infrared Sensing
8th Annual Mtg. Upper Atmos. Studies by Optical Methods, Dublin, Ireland (8-11 September 1980)

Bien, F. (Aerodyne Res., Inc., Bedford, MA), O'Neil, R.R., Fitzgerald, T.J. (E.G.& G., Inc., Los Alamos, NM), and Boquist, W.P. (Technology Int'l., Bedford, MA)
Observations of the Chemiluminescent Reaction of an Aluminized Rocket Propellant and Atmospheric Atomic Oxygen
Am. Geophys. Un. Mtg., Spring, Washington, DC (28 May - 1 June 1979)

Clough, S.A., Kneizys, F.X.; Davies, R.W., and Gamache, R. (Univ. of Lowell, Lowell, MA), and Tipping, R. (Univ. of Nebraska, NB)
Theoretical Line Shape for H_2O Vapor; Application to the Continuum
Course on Application of Molecular Physics to the Atmosphere and the Environment, Montfoulon, France (1 December 1980)

Cress, T.S., Maj.
Altitudinal Variation of Aerosol Size Distributions over Northern Europe
Wkshp. on Atmospheric Aerosols, Baltimore, MD (6-8 November 1979)

DEGGES, T.C. (Visidyne, Inc., Burlington, MA), STAIR, A.T., NADILE, R.M., and HEGBLOM, E.R. (Boston College, Boston, MA)
Altitude Dependence and Spectral Character of Atmospheric Ozone Long Wavelength Infrared Emission
Am. Geophys. Un. Mtg., Washington, DC (28 May-1 June 1979)

FALCONE, V.J., and ABREU, L.W.
Atmospheric Attenuation of Millimeter and Submillimeter Waves
EASCON 79, Washington, DC (8-11 October 1979)
Millimeter Wave Propagation Modelling,
SPIE Huntsville Electro-Optical Tech. Symp., Huntsville, AL (29 September - 2 October 1980)

FENN, R.W., SHETTLE, E.P., HERING, W.I., and JOHNSON, R.W. (Univ. of California, San Diego, CA)
Atmospheric Optics and Meteorology
Symp. on Plumes and Visibility, CAPITA, Washington Univ. at St. Louis, MO (10-14 November 1980)

FILIPPELLI, A.R., SHARPTON, F.A., and LIN, C.C. (of Univ. of Wisconsin, Madison, WI), and LEE, E.T.P.
Production of Excited Nitrogen Atoms by Electron-Impact Dissociation of N_2
33rd Gaseous Electronics Conf., Norman, OK (7-10 October 1980)

GORDON, J.I., and JOHNSON, R.W. (of Univ. of California, San Diego, CA)
Daytime Visibility and Nephelometer Measurements Related to Its Determination
Symp. on Plume and Visibility, CAPITA, Washington Univ. at St. Louis, MO (10-14 November 1980)

HOLLEY, T.K., CHUNG, S., and LIN, C.C. (Univ. of Wisconsin, Madison, WI), and LEE, E.T.P.
Close-Coupling Calculation of the $X^1 \Sigma_g^+ \rightarrow B^3 \pi g$ Excitation Cross Section of N_2 by Electron Impact
33rd Gaseous Electronics Conf., Norman, OK (7-10 October 1980)

KELLEY, M.C. (Cornell Univ., Ithaca, NY), BAKER, K.D. (Utah St. Univ., Logan, UT), and ULWICK, J.C.
A. C. Electric Field Measurements in the Equatorial Electrojet
Am. Geophys. Un. Mtg., Washington, DC (28 May - 1 June 1979)

KENNEALY, J.P., RAWLINS, W.T., and CALEDONIA, G.E. (Physical Sciences, Inc., Woburn, MA)
Cryo-Spectroscopic Measurements of Ozone IR Chemiluminescence
Am. Geophys. Un. Mtg., Spring, Toronto, Canada (22-27 May 1980)

KENNEALY, J.P., and CALEDONIA, G.E.
A Model of Upper Atmospheric Nitric Oxide IR Radiation
Am. Geophys. Un. Mtg., Washington, DC (28 May - 1 June 1979)

KING, J.I.F.
The Forward Problem Discrepancy and Temperature Profile Inversion, ILL-Posed Problems: Theory and Practice
Univ. of Delaware, Newark, DE (2-6 October 1979)

LEE, E.T.P., O'NEIL, R.R., and STAIR, A.T.
Auroral $O(^1S)$ Emission
Am. Geophys. Un. Mtg., Washington, DC (28 May - 1 June 1979)

MCCLATCHEY, R.A.
Atmospheric Transmission Models and Measurements
SPIE, San Diego, CA (27-30 August 1979)
An Atmospheric Temperature Profile Measured with an In-Situ Infrared Radiometer
Int. Radiation Symp., Colorado St. Univ., Fort Collins, CO (11-16 August 1980)

MURDOCK, T.L., TANDY, P.C., WALTERS, R., and WANG, D. (Sensor Sys. Group, Waltham, MA)
An Infrared Sensor Designed to Measure the Diffuse Zodiacal Light
SPIE, San Diego, CA (28 July - 1 August 1980)

MURPHY, R.E.
The BAMM System and Recent Measurements
IR Data Symposium, IDA, Washington, DC (1-3 April 1980)

MURPHY, R.E., and FAIRBAIRN, ALASTAIR
LABCEDE Studies
DNA Symposium at NRL, Washington, DC (January 1980)

MURPHY, R.E., and GREEN, B.D., and CALEDONIA, G. (Physical Sciences, Inc., Woburn, MA)
Vibrational Relaxation of NO ($v = 1$-8) Created in Electron Irradiated N_2/O_2 Mixtures
33rd Gaseous Electronics Conf., Norman OK (7-10 October 1980)

NADILE, R.M., GIBSON, J.J., WHEELER, N.B., and STAIR, A.T.
Altitude Dependence and Spectral Character of Atmospheric Hydroxyl IR Emission
Am. Geophys. Un. Mtg., Washington, DC (28 May - 1 June 1979)

NADILE, R.M., STAIR, A.T., SMITH, H.J.P., and DEGGES, T.C. (Visidyne, Inc., Burlington, MA)
Spire Water Vapor Results Using the AFGL FASCODE Computer Code
Am. Geophys. Un. Mtg., Toronto, Canada (22-27 May 1980)

O'NEIL, R.R., STAIR, A.T., BIEN, F., and CHENG, W. (Aerodyne Res., Inc., Bedford, MA), GRIEDER, W. (Boston Coll., Boston, MA), and BURT, D. (Utah St. Univ., Logan, UT)
Infrared Emission Between 4.5 and 5.0 μm in EXCEDE:SPECTRAL
Am. Geophys. Un. Mtg., San Francisco, CA (8-12 December 1980)

O'NEIL, R.R., STAIR, A.T., LEE, E.T.P., BURT, D., and FRODSHAM, G. (Utah St. Univ., Logan, UT)
Artificial Auroral Experiments
8th Annual Mtg on Upper Atmos. Studies by Optical Methods, Dublin, Ireland (8-11 September 1980)

O'NEIL, R.R., STAIR, A.T., BURT, D., FRODSHAM, G., and KEMP, J. (Utah St. Univ., Logan, UT)
EXCEDE SPECTRAL: An Artificial Auroral Experiment
Am. Geophys. Un. Mtg., Toronto, Canada (22-27 May 1980

PLONUS, M.A. (Northwestern Univ., Evanston, IL)
Intensity Propagation of Partially Coherent Optical Radiation in Atmospheric Turbulence
Int. URSI Symp. on Electromagnetic Waves, Munich, Federal Republic of Germany (26-29 August 1980)

PRICE, S.D.
Large Scale Infrared Structure of the Galaxy
IAU Symp. No. 96 on Infrared Astron., Inst. for Astron., Honolulu, Hawaii (23-27 June 1980)
Medium Resolution IR-Maps of the Cygnus X Region
156th Mtg. of the Am. Astronom. Soc., Univ. of Maryland, MD (15-18 June 1980)
Deconvolution of Low Frequency Information from Signals Obtained with AC Coupled Sensors
Conf. on Applications of Digital Image Processing to Astron., CAL Tech., Pasadena, CA (20-22 August 1980)
An Infrared Map of the Galactic Plane
155th Mtg. Am. Astron. Soc., San Francisco, CA (13-16 January 1980)

RAHBEE, A., GIBSON, J.J., and DOLAN, C.P.
Spectral Observation of SWIR in High Velocity Collisions of Plume and Atmospheric Species
Joint AFOSR/AFRPL Rocket Propulsion Res. Mtg., Lancaster, CA (20-22 March 1979)

RANSOM, M.J., MURPHY, R.E., and COOK, R.A. (AFGL), YAP, B.K. (SSG, INC.), MORSE, D.E. (Electrodynamics Lab., Logan, UT)
Balloon Altitude Mosaic Measurements of the Earth Infrared Background
IRIS Mtg. (8 May 1979)

RAWLINS, W.T., and CALEDONIA, G.E. (Physical Sciences, Inc., Woburn MA), KENNEALY, J.P., and DELGRECO, F.P.
Observations of IR Emission from Chemi-Excited O_3
Am. Geophys. Un. Mtg. Washington, DC (28 May - 1 June 1979)

RAWLINS, W.T., CALEDONIA, G.E., STAIR, A.T., and GIBSON, J.J.
Infrared Emission from NO ($\Delta v = 1$) in an Aurora: HIRIS Measurements
Am. Geophys. Un. Mtg., Toronto, Canada (22-27 May 1980)

REIDY, W.P., DEGGES, T.C., and HURD, A.G. (Visidyne, Inc., Burlington, MA), and ULWICK, J.C.
Rocketborne Measurements of Auroral NO Emission
Am. Geophys. Un. Mtg., Washington, DC (28 May - 1 June 1979)

SHARMA, R.D. (Stewart Radiance Lab., Bedford, MA), and NADILE, R.M.
Carbon Dioxide (v_2) Radiance Results Using a New Non Equilibrium Model
Am. Geophys. Un. Mtg., Toronto, Canada (22-27 May 1980)

SHETTLE, E.P.
Nonspherical Particle Scattering, Air Force Applications
Int. Wkshp. on Light Scattering by Irregularly Shaped Particles, St. Univ. of New York, Albany, NY (5-7 June 1979)

SHETTLE, E.P., and FENN, R.W.
Relative Humidity Dependent Aerosol Models
Wkshp. on Atmospheric Aerosols, Baltimore, MD (6-8 November 1979)

SILVERMAN, S.M.
On the Literature of the Aurora in Nordic Countries
NATO Summer Study Inst. on Polar Geophys. Mtg. (May 1980)

SILVERMAN, S.M., and FEYNMAN, J. (Boston Coll., Boston, MA)
The Changing Aurora of the Past Three Centuries
NATO Summer Study Inst. on Polar Geophys. Mtg. (May 1980)

STAIR, A.T., NADILE, R.M., GIBSON, J.J., BAKER, D.J., and FRODSHAM, G.D. (Utah St. Univ., Logan, UT)
Atmospheric Measurements of CO_2, NO, O_3 and OH from the Earth Limb (Project SPIRE)
Am. Geophys. Un. Mtg., Spring, Washington, DC (28 May - 1 June 1979)

STAIR, A.T., NADILE, R., ULWICK, J.C., and BAKER, D.J. (Utah St. Univ., Logan, UT)
Infrared Measurements of Aurora, Airglow and the Upper Atmosphere
8th Mtg. on Upper Atmosphere Studies by Optical Methods, Dublin, Ireland (8-11 September 1980)

ULWICK, J.C., O'NEIL, R.R., LEE, E.T.P., STAIR, A.T., BAKER, K.D., and BAKER, D.J. (Utah St. Univ., Logan, UT)
Auroral Probe Measurement of NO Emission at 2.7 Microns
Am. Geophys. Un. Mtg., Washington, DC (28 May - 1 June 1979)

VOLZ, F.E.
Some Basic Investigations on IR Optical Constants of Aerosol Substances
Int. Radiation Symp., Colorado St. Univ., Fort Collins, CO (11-16 August 1980)
Derivation of IR Optical Constants of Aerosols and Polycrystalline Surfaces [Specular Reflection by Pressed Crystal Powders]
Topical Mtg. Optical Phenomena Peculiar to Matter of Small Dimensions, Optical Sciences Ctr., Univ. of Arizona, Tucson, AZ (18-20 March 1980)

TECHNICAL REPORTS JANUARY 1979 - DECEMBER 1980

CRESS, T.S., LT. COL.
Airborne Measurement of Aerosol Size Distributions Over Northern Europe Vol. I: Spring and Fall 1976, Summer 1977
AFGL-TR-80-0178 (29 May 1980), ADA097090

FAIRBAIRN, A.R., GIRNIUS, R., and WOLNIK, S.J.
SWIR Studies in LABCEDE Facility: Initial Findings
AFGL-TR-80-0054 (8 February 1980), ADA090503

FALCONE, V.J., ABREU, L.W., and SHETTLE, E.P.
Atmospheric Attenuation of Millimeter and Submillimeter Waves: Models and Computer Code
AFGL-TR-79-0253 (15 October 1979), ADA084485

GALLERY, W.O.
Comparison of EMI Long Sea Path Transmittance Measurements with LOWTRAN 5 Calculations
AFGL-TR-80-0177 (28 May 1980), ADA092593

KNEIZYS, F.X., SHETTLE, W.P., GALLERY, W.O., CHETWYND, J.H., ABREU, L.W., SELBY, J.E.A., FENN, R.W., and MCCLATCHEY, R.A.
Atmospheric Transmittance/Radiance: Computer Code LOWTRAN 5
AFGL-TR-80-0067 (21 February 1980), ADA088215

MCCLATCHEY, R.A., and D'AGATI, A.P.
An Atmospheric Temperature Profile Measured With an In-Situ Infrared Radiometer
AFGL-TR-79-0100 (3 May 1979), ADA074471

PRICE, S.D., and MARCOTTE, L.P.
An Infrared Survey of the Diffuse Emission within 5° of the Galactic Plane
AFGL-TR-80-0182 (5 June 1980), ADA100289

PRICE, S.D., MURDOCK, T.L., MCINTYRE, A., HUFFMAN, R.E., and PAULSEN, D.E.
On the Diffuse Cosmic Ultraviolet Background Measured from Aries A-8
AFGL-TR-80-0325 (24 November 1980), ADA092491

ROTHMAN, L.S.
COMMUTE - A Computer Code for Non-Commutative Algebra
AFGL-TR-79-0152 (5 July 1979), ADA077360

SAKAI, H., ESPLIN, M., DALTON, W., and VANASSE, G.A.
High-Temperature, High-Resolution Measurements of CO_2 in the Region of 2200 to 2400 cm^{-1}
AFGL-TR-80-0068 (27 February 1980), ADA087234

SCHUMMERS, J.H., and HUPPI, R.J.
Analysis of NO and OH Emissions Relative to Ice-cap 1976 Aircraft Borne Measurements
AFGL-TR-79-0027 (1 January 1979), ADA073898

SHETTLE, E.P.
Non-Spherical Particle Scattering: Air Force Applications
AFGL-TR-80-0146 (1 May 1980), ADA084295

SHETTLE, E.P., and FENN, R.W.
Models for the Aerosols of the Lower Atmosphere and the Effects of Humidity Variations on Their Optical Properties
AFGL-TR-79-0214 (20 September 1979), ADA085951

VALOVCIN, F.R.
DMSP Water Vapor Radiances, A Preliminary Evaluation
AFGL-TR-80-0313 (6 October 1980), ADA099305

CONTRACTOR JOURNAL ARTICLES JANUARY 1979 - DECEMBER 1980

BAYKAL, Y., and PLONUS, M.A. (Northwestern Univ., Evanston, IL)
Two-Source, Two-Frequency Spherical Wave Structure Functions in Atmospheric Turbulence
J. Opt. Soc. Am. 70, No. 10 (October 1980)

BERNSTEIN, L.S., ROBERTSON, D.C., CONANT, J.A. (Aerodyne Res. Inc., Bedford, MA), and SANDFORD, B.P.
Measured and Predicted Atmospheric Transmission in the 4.0 - 5.3 μm Region, and the Contribution of Continuum Absorption by CO_2 and N_2
Appl. Opt. 18 (July 1979)

BLYTH, A.M., CHOULARTON, T.W., FULLARTON, G., LATHAM, J., MILL, C.S., SMITH, M.H., and STROMBERG, I.M. (Univ. of Manchester, Manchester, England)
The Influence of Entrainment on the Evolution of Cloud Droplet Spectra: II. Field Experiments at Great Dun Fell
Qtly. J. Royal Meteor. Soc. 106, No. 450 (October 1980)

PHELPS, J.O., SOLOMON, J.E., KORFF, D.F., LIN, C.C. (Univ. of Wisconsin, Madison, WI), and LEE, E.T.P.
Electron-Impact Excitation of the Potassium Atom
Phys. Rev. A. 20, No. 4 (October 1979)

PLONUS, M.A., OUYANG, C.F., and WANG, S.C.H. (Northwestern Univ., Evanston, IL)
Intensity Properties of Partially Coherent Beam Waves
Appl. Opt. 19, No. 18 (September 1980)

WANG, S.C.H., PLONUS, M.A., and OUYANG, C.F.
Irradiance Scintillations of a Partially Coherent Source in Extremely Strong Turbulence
Appl. Opt. 18 (April 1979)

WANG, S.C.H., and PLONUS, M.A.
Optical Beam Propagation for a Partially Coherent Source in the Turbulent Atmosphere
J. Opt. Soc. Am. 69, No. 9 (September 1979)

CONTRACTOR TECHNICAL REPORTS JANUARY 1979 - DECEMBER 1980

BURCH, D.E., and GRYVNAK, D.A. (Ford Aerospace & Communications Corp., Newport Beach, CA)
Method of Calculating H_2O Transmission Between 333 and 633 cm^{-1}
AFGL-TR-79-0054 (April 1979), ADA072850

BURT, D.A., and ALLRED, G.D. (Utah St. Univ., Logan, UT)
Rocketborne Ionospheric Studies: 1976-1979
AFGL-TR-79-0179 (6 August 1979), ADA078799

CARPENTER, J.W., HUMPHREY, C.H., HURD, A.G., REIDY, W.P., SHEPARD, O., SMITH, H.J.P., ZEHNPFENNIG, T.F. (Visidyne, Inc., Burlington, MA)
Evaluation and Development of Advanced High Altitude Experiments and Systems
AFGL-TR-79-0043, VI 465 (1 December 1979), ADA087579

DAVIES, R.W. (Univ. of Lowell, Lowell, MA)
Computation of H_2O Quadrupole Moment Matrix Elements for Pressure Broadening Calculations
AFGL-TR-79-0035 (January 1979), ADA068569

DAVIES, R.W., GAMACHE, R.R., and OLI, B.A. (Univ. of Lowell)
Near and Far Wing Pressure Broadening Theory for Application to Atmospheric Absorption
AFGL-TR-80-0062 (February 1980), ADA084116

ENG, R.S., MANTZ, A.W., and VENKATESH, C.C. (Laser Analytics, Inc., Bedford, MA)
High Resolution Tunable Diode Laser Measurements of Water Vapor Continuum Absorption and Theoretical Feasibility Study of Water Vapor Lineshape by Double Resonance Spectroscopy
AFGL-TR-79-0239 (15 October 1979), ADA089071

FAIST, M.B. (Aerodyne Res., Inc., Bedford, MA)
A Qualitative Theoretical Characterization of High Energy Excitation Cross Sections
AFGL-TR-80-0049 (May 1980), ADA092061

FITCH, B.W. (Univ. of California, San Diego, CA), and CRESS, T.S.
Measurements of Aerosol Size Distributions in the Lower Troposphere Over Northern Europe
AFGL-TR-80-0192 (June 1981), ADA104272

GEHRZ, R.D., HACKWELL, J.A., and GRASDALEN, G.L. (Univ. of Wyoming, Laramie, WY)
Infrared Studies of AFGL Sources
AFGL-TR-79-0274 (14 April 1980), ADA084713

GORDON, J.I. (Univ. of California, La Jolla, CA)
A Conceptual Review
AFGL-TR-79-0257 (November 1979), ADA085451

GREEN, B.D., and CALEDONIA, G.E. (Physical Services, Inc., Woburn, MA)
LABCEDE and COCHISE Analysis II, Vol. II
AFGL-TR-80-0063 (II) (February 1980), ADA112253

HANSEN, D.F., STEWART, H.S., PETTY, C.C., and WOOLAVER, L.B. (HSS Inc., Bedford, MA)
Evaluation, Feasibility, and Design of a Three-Wavelength Infrared Atmospheric Aerosol Extinctiometer
AFGL-TR-80-0323 (September 1980), ADA099306

HANSEN, P., and SAKAI, H. (Univ. of Massachusetts, Amherst, MA)
Infrared Emission Spectroscopy of Low Pressure Gaseous Discharges, II
AFGL-TR-79-0150 (10 July 1979), ADA078796

JOHNSON, R.W., and GORDON, J.I. (Univ. of California, San Diego, CA)
Airborne Measurements of Atmospheric Volume Scattering Coefficients in Northern Europe, Winter 1978
AFGL-TR-79-0159 (June 1979), ADA082044
Airborne Measurements of Atmospheric Volume Scattering Coefficients in Northern Europe, Summer 1978
AFGL-TR-80-0207 (June 1980), ADA097134

KUMER, J.B. (Lockheed Palo Alto Res. Lab., Palo Alto, CA)
Multidimensional Time Dependent Structure and Mechanisms for Non-LTE CO_2 Infrared Emissions and 4.3 μm Aurora
AFGL-TR-79-0224 (31 August 1979), ADA084940

LIOU, K-N, AUFDERHAAR, G.C., HUTCHISON, K., and YEH, H-Y (Univ. of Utah, Logan, UT)
Investigation of the Forward Radiative Transfer Problem Utilizing DMSP and NIMBUS 6 Data
AFGL-TR-80-0339 (30 September 1980), ADA109874
Development of the Microwave Radiative Transfer Program for Cloudy Atmospheres: Applications to DMSP SSM T Channels
AFGL-TR-80-0051 (30 December 1979), ADA087434

NEY, E.P. (Univ. of Minnesota, Minneapolis, MN)
Study of Sources in AFGL Rocket Infrared Study
AFGL-TR-80-0050 (7 February 1980), ADA084098

OUYANG, C.F., WANG, S-J, and PLONUS, M.A. (Northwestern Univ., Evanston, IL)
LOWTRAN V Subroutine for the Calculation of Intensity Deviation for Point and Finite Aperture Receivers
AFGL-TR-80-0297 (September 1980), ADA094018

PENDLETON, W.R., and HOWLETT, L.C. (Utah St. Univ., Logan, UT)
Thermospheric Diagnostics Using In-Situ Probing by Electron-Beam-Induced Luminescence
AFGL-TR-80-0047 (30 January 1980), ADA092942

RAWLINS, W.T., PIPER, L.G., GREEN, B.D., WILEMSKI, G., GOELA, J.S., and CALEDONIA, G.E. (Physical Sciences Inc., Woburn, MA)
LABCEDE and COCHISE Analysis II, Vol. I
AFGL-TR-80-0063 (I) (February 1980), ADA111827

RIDGWAY, W.L., MOOSE, R.A., and COGLEY, A.C. (Sonicraft, Inc., Chicago, IL)
Atmospheric Transmittance/Radiance Computer Code FASCODE 2
AFGL-TR-80-0250 (8 August 1980), ADA097593

RUDY, R.J., GOSNELL, T.R., and WILLNER, S.P. (Univ. of California, San Diego, CA)
Ground-Based Measurements of Sources in the AFGL Infrared Sky Survey
AFGL-TR-79-0172 (27 July 1979), ADA081381

SAKAI, H. (Univ. of Massachusetts, Amherst, MA)
Infrared Emission Spectroscopy of Low Pressure Gaseous Discharges IV
AFGL-TR-80-0355 (November 1980), ADA104123
Infrared Emission Spectroscopy of Low Pressure Gaseous Discharges, III
AFGL-TR-80-0157 (May 1980), ADA091744
Study of Background Radiance in Upper Atmosphere
AFGL-TR-80-0048 (January 1980), ADA092927

SHEPHERD, O., ZEHNPFENNIG, T.F., RAPPAPORT, S.A., REIDY, W.P., and VANASSE, G. (Visidyne, Inc., Burlington, MA)
Background Optical Suppression System (BOSS)
AFGL-TR-79-0243 (October 1979), ADA077871

SLUDER, R.B., ANDRUS, W.S., and KOFSKY, I.L. (PhotoMetrics, Inc., Lexington, MA)
Aircraft Program for Target, Background, and Sky Radiance Measurements
AFGL-TR-79-0139 (15 June 1979), ADA076959

SLUDER, R.B., VILLANUCCI, D.P., ANDRUS, W.S., and KOFSKY, I.L. (PhotoMetrics, Inc., Lexington, MA)
Aircraft Program for Target, Background, and Sky Radiance Measurements
AFGL-TR-80-0165 (17 May 1980), ADA095363

SMITH, H.J.P., GARDNER, M.E., and DUBE, D.J. (Visidyne, Inc., Burlington, MA)
FASCODE Computer Program Predictions of Typical NO_2 Stack Plume Spectral Radiative Properties as Viewed from Space
AFGL-TR-79-0014 (January 1979), ADA067942

SULLIVAN, R. (Honeywell Radiation Center, Lexington, MA)
Spatial Radiometer, Vol. I
AFGL-TR-80-0061 (I) (March 1979), ADA081584

TUAN, T-F. (Univ. of Cincinnati, Cincinnati, OH)
Theoretical Investigation of the Effects of Atmospheric Gravity Waves on the Hydroxyl Emissions of the Atmosphere
AFGL-TR-80-0007 (31 December 1979), ADA083025

ZACHOR, A.S. (Atmospheric Radiation Consultants, Inc., Acton, MA)
Down-Looking Interferometer Study II Volume I
AFGL-TR-80-0236 (March 1980), ADA108299
Down-Looking Interferometer Study II Volume II: Handbook of Results
AFGL-TR-80-0237 (March 1980), ADA108235

ZANDER, R. (Inst. of Astrophysics, Univ. of Liege, Liege-Ougree, Belgium)
High Resolution Transmission Measurements of the Atmosphere in the Infrared
AFGL-TR-79-0119 (27 April 1979), ADA070182

APPENDIX A

AFGL PROJECTS BY PROGRAM ELEMENT
FY 1980

Program	Project Number and Title	
61101F	ILIR	Laboratory Director's Fund
61102F	*DEFENSE RESEARCH SCIENCES*	
	2303G1	Upper Atmosphere Chemistry
	2303G2	Plume/Atmosphere Interactions
	2309G1	Earth Sciences and Technologies
	2309G2	Crustal Motion Studies
	2310G1	Infrared and Optical Techniques
	2310G2	Atmospheric Dynamics
	2310G3	Upper Atmosphere Composition
	2310G4	Infrared Non-Equilibrium Radiation Mechanisms
	2310G5	Cloud Physics
	2311G1	Energetic Particles in Space
	2311G2	Magnetospheric Plasmas and Fields
	2311G3	Solar Environmental Disturbances
62101F	*GEOPHYSICS*	
	4643	Aerospace Radio Propagation
	6670	Meteorological Development
	6687	Stratospheric Environment
	6690	Upper Atmosphere Technology
	7600	Terrestrial Sciences
	7601	Magnetospheric Effects on Space Systems
	7659	Aerospace Probe Technology
	7661	Spacecraft Charging Technology
	7670	Optical/IR Properties of the Environment

In addition to the continuing Air Force funded projects cited above, AFGL participates in joint programs supported by the following agencies:

1) U.S. Air Force
   - Air Force Tactical Applications Center
   - Air Force Weapons Laboratory
   - Air Weather Service
   - Electronic Systems Division
   - Space Division
   - Ballistic Missile Office
   - Ogden Air Logistics Center
2) Army
3) Advanced Research Projects Agency
4) Defense Mapping Agency
5) Defense Nuclear Agency
6) Department of Energy
7) National Aeronautics and Space Administration

AFGL PROJECTS BY PROGRAM ELEMENT
FY 1981

Program	Project Number and Title	
61101F	ILIR	Laboratory Director's Fund
61102F	*DEFENSE RESEARCH SCIENCES*	
	2303G1	Upper Atmosphere Chemistry
	2303G2	Plume/Atmosphere Interactions
	2309G1	Earth Sciences and Technologies
	2309G2	Crustal Motion Studies
	2310G1	Infrared and Optical Techniques
	2310G3	Upper Atmosphere Composition
	2310G4	Infrared Atmospheric Processes
	2310G5	Cloud Physics
	2310G6	Remote Ionospheric Mapping
	2310G7	Atmospheric Dynamic Models
	2311G1	Energetic Particles in Space
	2311G2	Magnetospheric Plasmas and Fields
	2311G3	Solar Environmental Disturbances
62101F	*GEOPHYSICS*	
	4643	Aerospace Radio Propagation
	6670	Meteorological Development
	6687	Stratospheric Environment
	6690	Upper Atmosphere Technology
	7600	Terrestrial Geophysics
	7601	Magnetospheric Effects on Space Systems
	7659	Aerospace Probe Technology
	7661	Spacecraft Charging Technology
	7670	Optical/IR Properties of the Environment
63707F	*WEATHER SYSTEMS (Advanced Development)*	

In addition to the continuing Air Force funded projects cited above, AFGL participates in joint programs supported by the following agencies:

1) U.S. Air Force
    - Space Division
    - Armament Division
    - Ballistic Missile Office
    - Air Force Tactical Applications Center
    - Air Force Weapons Laboratory
    - Air Weather Service
    - Electronic Systems Division
    - Air Force Flight Test Center
2) Army
3) Advanced Research Projects Agency
4) Defense Mapping Agency
5) Defense Nuclear Agency
6) Department of Energy
7) National Aeronautics and Space Administration

Appendix B

AFGL ROCKET PROGRAM: January 1979 - December 1980

Date	Launch Site	Vehicle	Experiment	Scientist	Results
28 Jan 79	WSMR	Aries	Survey Probe Infrared Celestial Exp. (SPICE)	Price	Success
26 Feb 79	Red Lake	Nike Orion	Solar Eclipse Program	Philbrick	Success
26 Feb 79	Red Lake	Nike Orion	Solar Eclipse Program	Ulwick	Success
26 Feb 79	Red Lake	Paiute Tomahawk	Solar Eclipse Program	Narcisi	Success
26 Feb 79	Red Lake	Paiute Tomahawk	Solar Eclipse Program	Narcisi	Success
26 Feb 79	Red Lake	Niro	Solar Eclipse Program	Faire	Success
3 Aug 79	WSMR	Astrobee F	IR Spectra	Ulwick	Success
7 Aug 79	WSMR	Black Br. VC	Post Burnout Thrust	McKenna	Success
14 Aug 79	WSMR	Nike-Tomahawk	Composition - DMSP Cal.	Philbrick	Success
14 Aug 79	WSMR	Nike-Tomahawk	Density for DMSP	Philbrick	Failure
14 Aug 79	WSMR	Aerobee-170R	UV Measurements for DMSP	Heroux	Success
19 Oct 79	PFRR	Talos Castor	Excede II	O'Neil	Success
23 Oct 79	Punta Lobos, Peru	Nike-Nike	Equatorial Smoke	Quesada	Success
21 May 80	WSMR	Aries	Multi Spectral Measurements	McIntyre	Success
18 Aug 80	WSMR	Aries	Zodiacal Infrared Program	Murdock	Success
18 Sep 80	WSMR	Aerobee-170	Solar Max UV Experiment	Bedo	Success
22 Oct 80	PFRR	Paiute Tomahawk	Solar Proton Event	Narcisi	Success
22 Oct 80	PFRR	Superarcas	Solar Proton Event	Narcisi	Success
16 Nov 80	Andoya, Norway	TAURUS-Orion	Energy Budget Campaign	Wheeler	Success

WSMR —White Sands Missile Range, New Mexico
PFRR —Poker Flat Rocket Range, Alaska

Air Force Geophysics Laboratory

HANSCOM AIR FORCE BASE, BEDFORD, MASS.

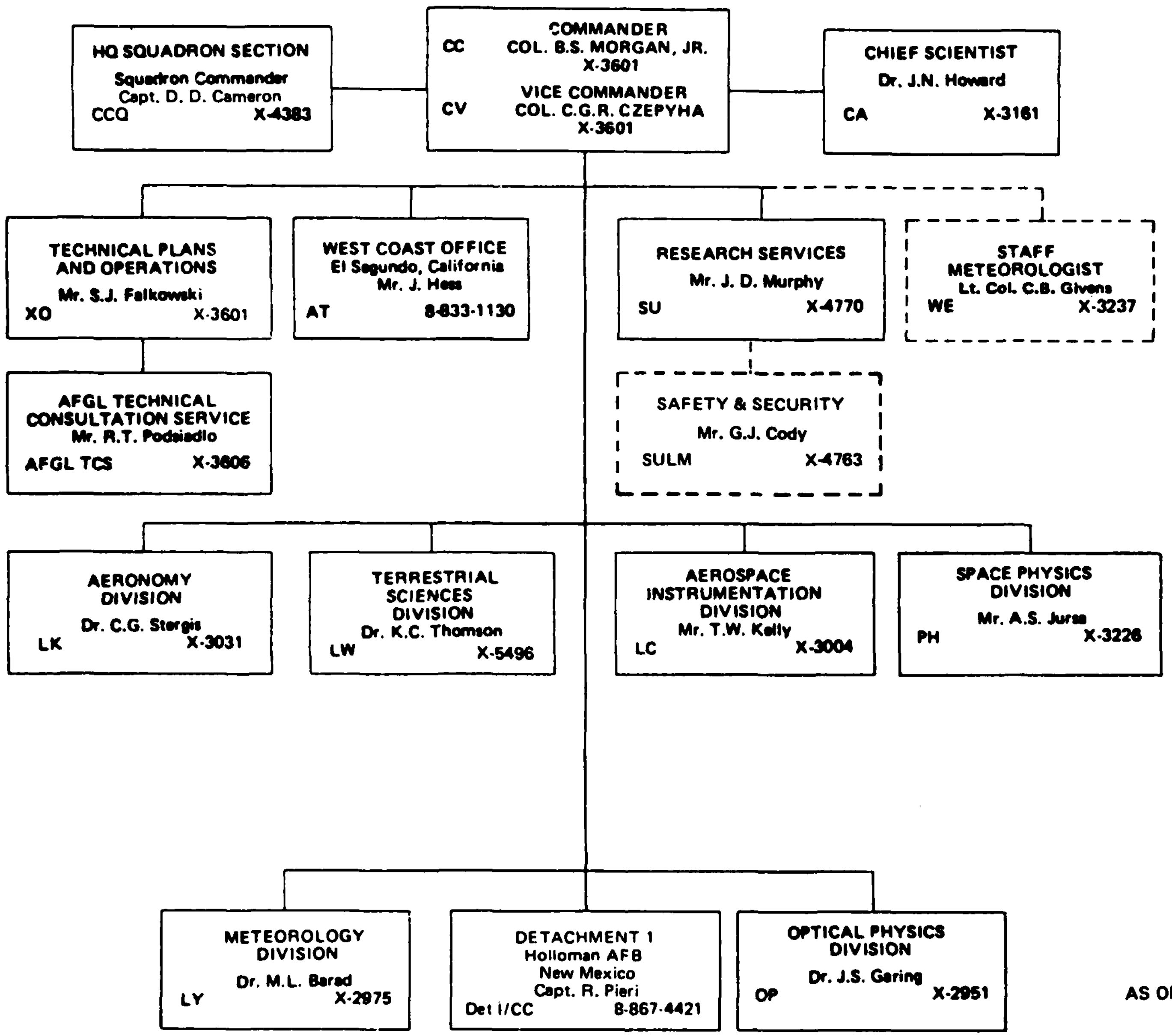

AS OF 1 MARCH 1979
*ACTING

CC COMMANDER
COL. B.S. MORGAN, JR.

CV VICE COMMANDER
COL. C.G.R. CZEPYHA

XO TECHNICAL PLANS & OPERATIONS
Director — S.J. Falkowski

AFGL TECHNICAL CONSULTATION SERVICE
Technical Consultation Services Officer
R. T. Podsiadlo

AFGL Staff Meteorologists

Col. J. W. Hall	AFSC
Lt. Col. R. F. Wachtmann	SAMTEC
Lt. Col. W. E. Buchan	ETR
Lt. Col. J. Sartor	ADTC
Lt. Col. C. H. Bush	AFFTC
Lt. Col. F. Fowler	SAMSO
Lt. Col. J. Lasley	ASD
Maj. D. A. Morss	FTD
Maj. S. Y. Strader	6585 TG
Capt. D. E. Bielicki	AFRPL
Maj. D. B. Johnson	RADC
Maj. G. J. Thompson	AFWL
Maj. P. Soliz	AFAL
Capt. G. Jackson	AFFDL
Capt. J. A. Phillips	AFESC
Lt. Col. C. B. Givens	ESD
Lt. Col. H. J. E. Fischer	AFSCF

XOP TECHNICAL PROGRAMS BRANCH
Chief — R.A. Skrivanek

XOR RESOURCES BRANCH
Chief — J.I. Haley, Jr.

AT WEST COAST OFFICE
El Segundo, California
Chief — J. Hess

SU RESEARCH SERVICES
Director — J.D. Murphy

SUO OPERATIONAL SERVICES BRANCH

Chief	J. P. Cushman
SUOC LMCA	J. C. Larkin
SUOF Technical Facilities	W. K. Foss
SUOR Field Requirements	R. F. Carnevale
SUOS R&D Fabrication	R. J. Campbell

SUW AFGL COMPUTATION BRANCH

Chief	J. D. Murphy*
SUWA Analysis & Simulation	E. C. Cronin
SUWR Decommutation	R. C. Penney
SUWD Data Processing	R. G. Gosselin
SUWDS Systems Programming	S. Smith
SUWDO Computer Operations	
1st Shift	D. J. LaChance
2nd Shift	R. R. DaPolito
3rd Shift	J. R. DeVito

SUL MANAGEMENT & ADMINISTRATIVE SERVICES BRANCH

Chief	E.G. Corliss
DA Administrative Services	SSgt R. Plamondon
SULL Research Library	E.L. Cunha
SULR Research Publications	A.G. Mueller
SULM Management Services	E.G. Corliss*

SUP TECHNICAL PHOTOGRAPHY BRANCH
(Special mission photographic laboratory)
Chief — C. Rodberg

SUM MECHANICAL ENGINEERING BRANCH
Chief — S. Rosenthal

AS OF 1 MARCH 1979
*ACTING

COMMANDER
CC COL. B.S. MORGAN, JR

CV **VICE COMMANDER**
COL. C.G.R. CZEPYHA

LK AERONOMY DIVISION

Director	C.G. Stergis
Senior Scientist - Solar Ultraviolet	H. Hinteregger
LKB Atmospheric Structure	K.S.W. Champion
LKO Ultraviolet Radiation	*L.J. Heroux
LKD Composition	R.S. Narcisi

LY METEOROLOGY DIVISION

Director	M.L. Barad
Senior Scientist - Heat Transfer	C.N. Touart
Senior Scientist - Cloud Physics	R.M. Cunningham
LYW Weather Radar	K. M. Glover
Weather Radar Facility Maynard, MA	K. M. Glover
LYC Cloud Physics	A. A. Barnes
LYD Climatology & Dynamics	R. Shapiro
LYU Mesoscale Forecasting	D. A. Chisholm

LW TERRESTRIAL SCIENCES DIVISION

Director	K.C. Thomson
Senior Scientist - Gravity	B. Szabo
LWG Geodesy and Gravity	D. H. Eckhardt
LWH Applied Crustal Physics	Capt. J.A. Shearer*

OP OPTICAL PHYSICS DIVISION

Director	J.S. Garing
OPA Atmospheric Optics	R.W. Fenn
OPI Infrared Physics	R.A. McClatchey
OPR Radiation Effects	A.T. Stair

LC AEROSPACE INSTRUMENTATION DIVISION

Director	T.W. Kelly
LCA Balloon Flight Requirements Analysis	T.J. Danaher
LCB Balloon Research	J.C. Payne
LCC Balloon Instrumentation	R. J. Cowie
LCR Sounding Rocket	C. N. Stark

DET 1/CC
DETACHMENT 1
HOLLOMAN AFB
NEW MEXICO

Detachment Commander	Capt. R. Pieri

PH SPACE PHYSICS DIVISION

Director	A. S. Jursa
Senior Scientist - Radio Astronomy	J. Aarons
Senior Scientist - Magnetospheric Physics	J. McClay
PHS Solar Research	G. Simon
PHP Trans-Ionospheric Propagation	J. Aarons
PHI Ionospheric Dynamics	Lt. Col. A. L. Snyder
PHG Plasmas, Particles & Fields	R. C. Sagalyn

AS OF 1 MARCH 1979
*ACTING

4-8

DT